Synthesis of Functional Core-Corona Polymer Microsphere and Its Application to Asymmetric Organocatalysis

(機能性コア-コロナ高分子微粒子の合成とキラル有機分子触媒への応用)

September, 2019

Doctor of Philosophy (Engineering)

MD. WALI ULLAH

エムディ ワリ ウッラ

Toyohashi University of Technology

Date of Submission: September 24, 2019

Department of Applied Chemistry and Life Science	Student ID Number	169402
Applicant's name	MD. WALI ULLAH	

Supervisor	Assoc. Prof. Dr. Naoki Haraguchi

Abstract（Doctor）

Title of Thesis	Synthesis of Functional Core-Corona Polymer Microsphere and Its Application to Asymmetric Organocatalysis

Approx. 800 words

Chiral organocatalysts have been received considerable attention in asymmetric synthesis because of their advantages of being cost effective, readily available, non-toxic and environmental friendly. Among a variety of chiral organocatalysts, *Cinchona* alkaloids are one of the efficient organocatalysts in the asymmetric organocatalysis which are available in pseudoenantiomeric forms, due to their commercial availability at low prices, stability and easy handling in laboratory, as well as their convenient modifications by simple reactions. *Cinchona* derived quaternary ammonium salts are one of the most popular organocatalysts in the field of asymmetric catalysis especially for the synthesis of unnatural α-amino acids. Chiral imidazolidin-4-ones and their salts, originally developed by MacMillan and co-workers, are also one of the most important classes of chiral organocatalysts.

Immobilization of a chiral organocatalyst onto a heterogeneous support represents an attractive approach for catalytic asymmetric reactions from a viewpoint of its sustainability. Although there have been numerous reports on covalently bonded both polymer-immobilized chiral quaternary ammonium salt and MacMillan catalyst for asymmetric alkylation and the Diels-Alder reaction, respectively, these heterogeneous catalysts sometimes offer inherent disadvantages, such as low selectivity and low catalytic activity. These can be interpreted in terms of direct covalent-bonding of organocatalysts to the support material, decreasing the intrinsic properties of steric sensitivity of organocatalyst on asymmetric synthesis.

To solve the above problem, an alternative strategy involving the ionic immobilization of an organocatalyst on a support using an ion-exchange reaction has been reported. This method is a facile and general technique for the immobilization of ammonium onto sulfonated polymers regardless of kinds of ammonium and sulfonated polymer, which can be employed in mild conditions. In some cases, these ionically immobilized organocatalysts also showed low catalytic activity.

Nevertheless of the efficiency of polymer microsphere as polymer support, there is no report on the immobilization of chiral cinchonidinium salt or MacMillan catalyst onto polymer microsphere. Monodisperse sulfonated core-corona polymer microspheres seem to be suitable solid-supports for the ionic immobilization of chiral organocatalysts because of their high surface area, facile dispersibility, and high mechanical and thermal stability. In addition, an advantage of polymer microspheres is the ability to control their hydrophilic-hydrophobic balance, which offers suitable microenvironments for catalytic asymmetric reactions. Therefore, synthesis of well-defined core-corona polymer microsphere-supported

chiral organcatalyst is a new idea in asymmetric catalysis for obtaining optically active compounds. To investigate the effect of these polymeric organocatalysts in asymmetric catalysis, we have developed both core-corona polymer microsphere-supported chiral cinchonidinium salt and MacMillan catalyst and applied them as heterogeneous catalysts in the asymmetric alkylation and the Diels-Alder reaction, respectively.

Chapter **I** describes the general introduction and background of the thesis work.

Chapter **II** describes the synthesis of narrowly dispersed functional polymer microspheres having benzyl halide moiety by precipitation polymerization of various comonomers (styrene (St), methyl methacrylate (MMA), or 2-hydroxyethyl methacrylate (HEMA)), divinylbenzene (DVB) with 4-vinylbenzyl chloride (VBC). We have also successfully synthesized low crosslinked polymer microspheres using 10 mol% of crosslinker (DVB and a divinyl crosslinker) by precipitation polymerization and transformation reaction. The nature of comonomer and the molar ratio of monomers affected the yield and diameter of polymer particles.

Chapter **III** provides a novel strategy for the synthesis of well-defined hairy polymer or core corona polymer microspheres by precipitation polymerization and surface-initiated atom transfer radical polymerization (SI-ATRP). The M_n of grafted polymer can be controlled up to 15,000 g mol^{-1} by changing the M/I, and the M_w/M_n was lower than 1.30 when M/I $\leq$ 150. In this Chapter, monodisperse sulfonated core-corona polymer microsphere was also successfully synthesized from the graft copolymerization of an achiral monomer and phenyl *p*-styrenesulfonate with polymer microsphere having benzyl chloride moiety as a macroinitiator by SI-ATRP, followed by the treatment NaOH. The graft copolymerization of styrene and phenyl *p*-styrenesulfonate proceeded in a controlled manner to afford well-defined core-corona polymer microsphere when poly(DVB-HEMA-VBC) or poly(DVB-St-VBC) microsphere was used as a macroinitiator.

Chapter **IV** describes the synthesis of core-corona polymer microsphere-supported chiral cinchonidinium salt by the ion exchange reaction of sodium sulfonate moiety at the side chain of corona with chiral cinchonidinium salt, which was applied as chiral heterogeneous organocatalyst in the asymmetric alkylation of a glycine derivative to give high yields (up to 99%) and enantioselectivites (up to >99% ee). The effect of nature and size of core, nature and length of corona, grafting density, as well as the degree of crosslinking on the catalytic reactivity was investigated in detail in this chapter. The heterogeneous catalyst could be easily and quantitatively recovered from reaction mixture and reused several times without loss of the enantioselectivity. To our knowledge, this is the first report of core-corona polymer microsphere-supported cinchonidinium salt in the asymmetric alkylation.

Chapter **V** describes the synthesis of core-corona polymer microsphere-supported MacMillan catalyst by the neutralization reaction of sulfonic acid moiety at the side chain of corona with MacMillan catalyst precursor. We evaluated their catalytic efficiency in the asymmetric Diels-Alder reaction of *trans*-cinnamaldehyde and cyclopentadiene. The desired Diels-Alder adducts were obtained in good yield (up to 99%) with excellent ee value (up to 99% ee (*exo*) and >99% ee (*endo*)). The core and corona (kinds of monomer, diameter, and length of corona) significantly affected on the catalytic activity. The catalyst could be reused several times without loss of the enantioselectivity.

Chapter **VI** describes the general summary of the thesis work.

TABLE OF CONTENTS

LIST OF SCHEMES, TABLES AND FIGURES

CHAPTER I

CHAPTER II

CHAPTER III

CHAPTER IV

CHAPTER V

CHAPTER VI

CHAPTER I

Introduction

1.1 Asymmetric Synthesis

Enantiomerically pure compounds are extremely important in different fields such as medicine and pharmacy, nutrition, or materials sciences. Among the different methods to obtain enantiomerically pure compounds (Figure 1.1), asymmetric synthesis is one of the most interesting and challenging, which can be achieved in several ways: (a) from chiral natural products ("chiral pool" approach);[1-3] (b) use of a chiral auxiliary;[4] (c) use of a chiral catalyst.[5] Several criteria are useful for judging an asymmetric synthesis: (i) The synthesis should be highly stereoselective; (ii) If a chiral catalyst is employed, low catalyst loadings are preferable, and the catalyst must be easily separable from the product; (ii) If a chiral auxiliary is used, it must be removable without compromising the new stereocenter, and should be recoverable in good yield and without racemization; (iv) The chiral auxiliary or catalyst should be readily and inexpensively available, preferably as either enantiomer.

The chiral pool method is limited to natural-occurring chiral compounds, and often only one of the enantiomers is available, e.g. *D*-sugars, α-amino acids. The major disadvantage of optical resolution is that half of the product is the undesired enantiomer, although, via racemization of the undesired enantiomer, the yield can be improved. The chiral auxiliary in method (c) has to be used in stoichiometric amounts. After reaction, removing the chiral auxiliary requires additional steps. By contrast, an asymmetric catalytic reaction with a turnover number of 1000 means that 1000 new chiral molecules can be generated with one molecule of a chiral catalyst (Scheme 1.1), which leads to higher economy, efficiency, and environmentally friendly. The work-up is often relatively simple, as only a small amount of the catalyst is used. The relationship between the chiral catalyst and the reaction system is just like the relationship between the lock and the key, which is highly selective. In the past 20 years, asymmetric catalysis has become one of the most important areas of research, and major breakthroughs have been achieved.[2-6] Some of the catalytic methods (e.g., organometallic catalysis, enzyme catalysis, organocatalysis) developed have been successfully applied in the synthesis of enantiopure drugs on an industrial scale. William. S. Knowles, Ryoji Noyori, and K. Barry Sharpless received the Nobel Prize for Chemistry in 2001 for their achievements in the field of homogeneous catalysis, which contributed to the development of industrial syntheses of pharmaceutical products and other biologically active substances.[7] The pioneering work of these three Nobel laureates paved the way for the further development of asymmetric catalysis.

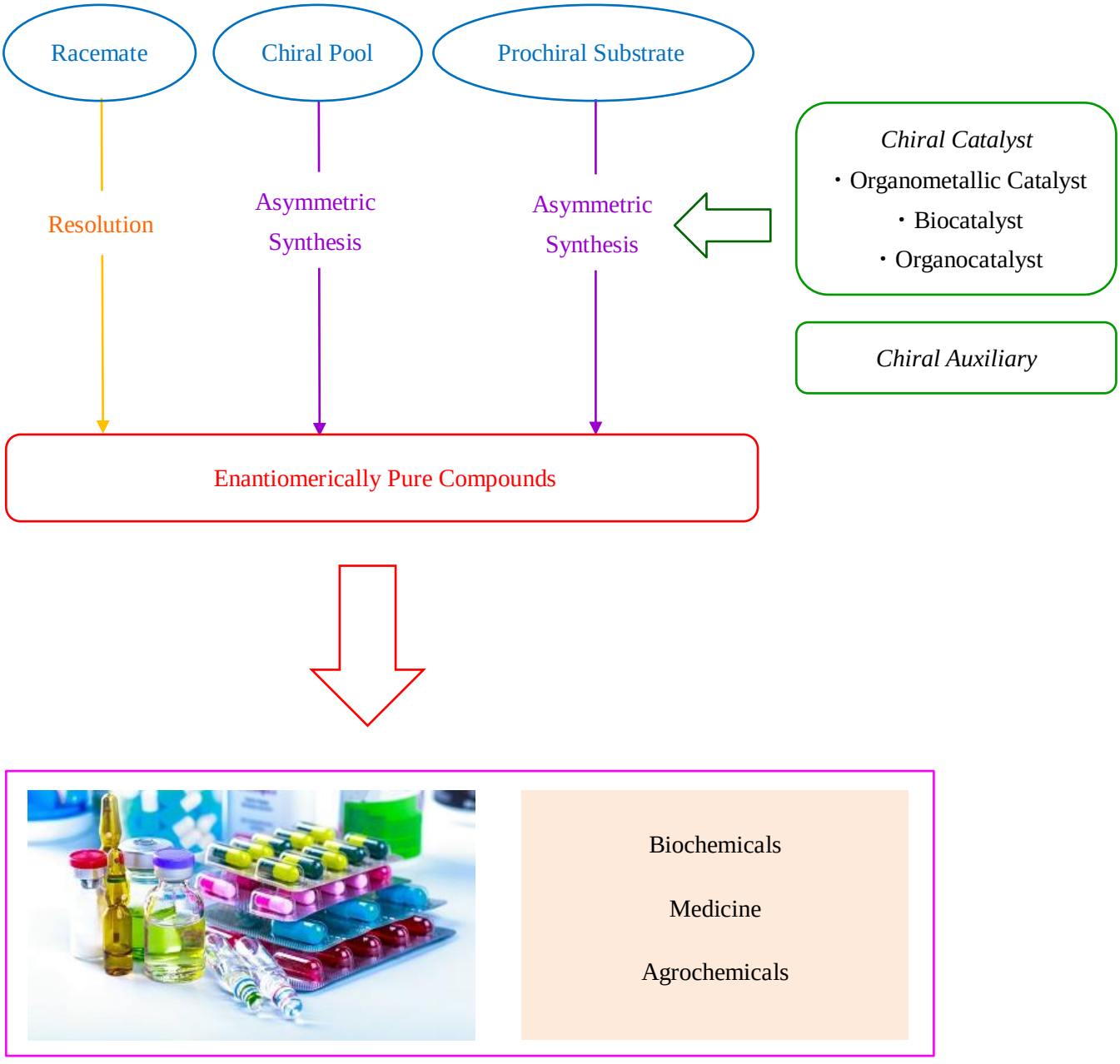

Figure 1.1 Strategies for the synthesis of enantiopure compounds.

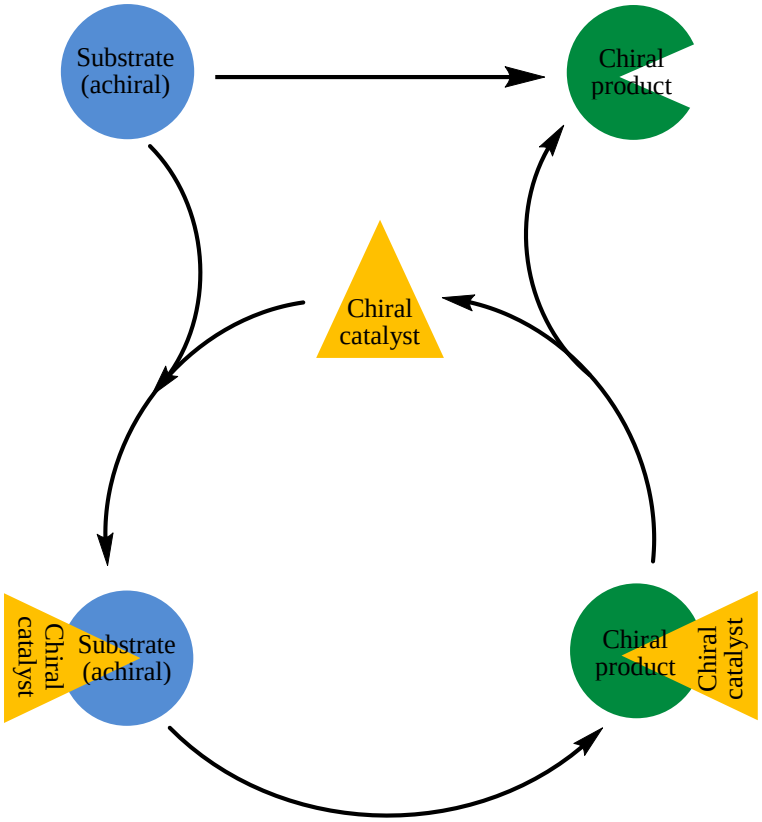

Scheme 1.1 Strategy for the synthesis of enantiopure compound using chiral catalyst.

1.2 Organocatalyst

Organocatalysts are small organic molecules that do not contain a metal element as the catalytic center in their structures, and they are able, in substoichiometric amounts, to promote an acceleration in chemical reactions.[8] The organocatalyst is generally composed of C, H, N, S, and P, and could be achiral or chiral. Organocatalysts can be Lewis acids, Lewis bases, Brønsted acids, and Brønsted bases. The absence of metal in organocatalysts brings an unquestionable advantage considering both the principles of “green chemistry" and the economic point of view. In addition, organocatalysts are generally robust and low-cost compounds, non-toxic with high resistance to air and moisture. They are usually stable under aerobic conditions, and the reactions do not require extremely dry conditions. Thus, inert equipment such as vacuum lines or gloveboxes is not necessary. All these advantages are in striking contrast with enzymes, which are very expensive, rather unstable and condition-dependent, or with metal complexes which are often moisture and oxygen sensitive and requires demanding reaction conditions such as absolute solvents, low temperature, inert atmosphere etc.

Nowadays, organocatalysis has been one of the hot research topics in advanced organic chemistry.

It is a novel synthetic philosophy and mostly an alternative to the prevalent transition metal catalysis. It can be greener than traditional catalysis because: (i) The use of catalysts is, itself, a green chemistry principle; (ii) It employs mild conditions, consequently saving energy; (iii) It uses, in general, oxygen-stable reagents and does not require anhydrous conditions, reducing the cost of the synthesis; (iv) It is compatible with several functional groups that could be sensitive to other processes, and this reduces the need for protection groups, lowering the total number of reaction steps; (v) It uses less toxic and safer substances; (vi) It prevents the formation of metallic waste and avoids traces of metals in the products, which is an essential feature for applications in medicinal chemistry.

Liebig's synthesis of oxamide from cyanogen and water with acetaldehyde as an organocatalyst is the first organocatalytic reaction reported.[9] Acetaldehyde was further identified to behave as the then-named "ferment," now called as enzyme. Dakin in 1909 demonstrated that in a Knoevenagel type condensation between aldehydes and carboxylic acids or esters with active methylene groups, the basic amines (organocatalysts) could be mediated by amino acids.[10] Natural products, in particular, strychnine, brucine, and *Cinchona* alkaloids and amino acids (including short oligopeptides), were among the first chiral organocatalysts tested.[11,12]

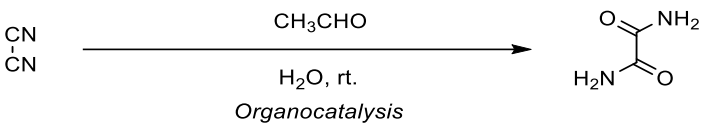

Scheme 1.2 First example of organocatalysis.[9]

1.2.1 Chiral Organocatalyst

Chiral organocatalysts are one of the organocatalysts which have been developed considering the following two tasks: (1) They are responsible for the activation of the electrophile or nucleophile of the reaction (or both of them in the case bifunctional catalysts) and (2) They are liable for the induction of the enantioselectivity of the reaction. The chiral organocatalyst behaves as a shield by preferentially blocking one of the two prochiral faces of the substrate (which usually has a prochiral Csp^2 center, at least in the transition state), making possible the reaction with the corresponding electrophile or nucleophile takes place from the unshielded side. The substrate may be activated by the organocatalyst either by covalent linking or noncovalent interactions. Enantioselective synthesis can be achieved when a chiral organocatalyst is used. It has emerged as a powerful synthetic method complementary to the metal- and enzyme-catalyzed reactions. Chiral organocatalysts have special reactivity in asymmetric synthesis, and they can be applied in various asymmetric reactions, e.g.,

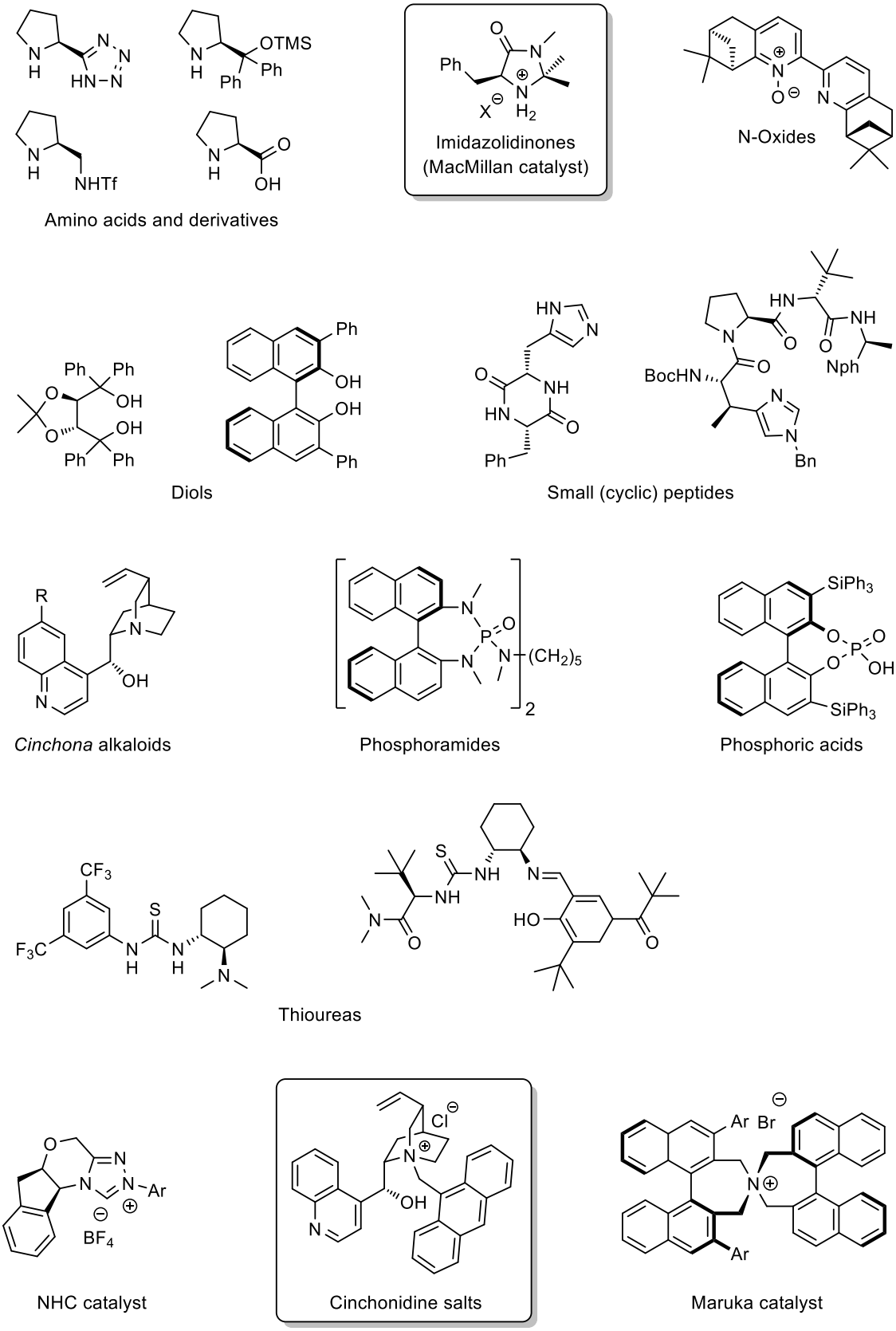

Figure 1.2 Chemical structures of chiral organocatalysts.

alkylation, Diels-Alder reaction, asymmetric reduction, hydroformylation, epoxidation, dihydroxylation, etc. Since the mid-1990s, chiral organocatalysts have received considerable attention

in asymmetric synthesis over metal-based catalysts because they have several advantages like organocatalysts that have discussed in section **1.2**. Figure 1.2 shows examples of chiral organocatalysts.

In 1912, Bredig and Fiske reported the addition of HCN to aldehyde in the presence of chiral cinchona alkaloids **1** with low enantioselectivities.[13] Later in 1960, Pracejus investigated the addition of methanol to ketenes with ee's up to 74%.[14,15] Pioneering work in the enantioselective synthesis dates back to the 1970s in which Eder et al. and Hajos et al. separately reported an intramolecular asymmetric aldol reaction which employed *L*-proline **2** as catalyst.[16,17] This reaction was considered to be a special case at that time. Later in 2000, List et al. reported an *L*-proline-catalyzed intermolecular asymmetric aldol reaction.[18] The same year, MacMillan et al. documented the first highly enantioselective amine-catalyzed Diels-Alder reaction.[19-21] These reports received a great deal of attention, and the research in the area of asymmetric organocatalysts has since thrived.[22]

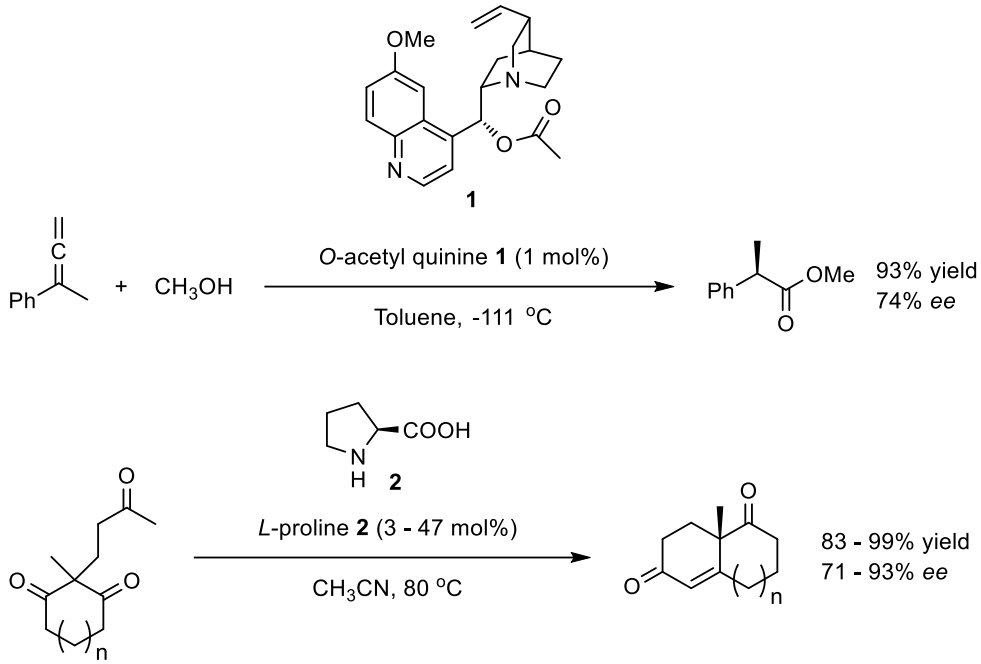

Scheme 1.3 Two pioneering examples of asymmetric organocatalysis.

1.2.2 Chiral *Cinchona* Derived Organocatalyst

Cinchona alkaloids have a venerable history as organocatalysts in the development of enantioselective reaction. *Cinchona* alkaloids have a unique structural nature (Figure 1.3). The alkaloids of *Cinchona* species, which were once known for the popular antimalarial drug quinine, have emerged as the most powerful class of compounds in the realm of asymmetric organocatalysis during the last two decades.[23,24] Apart from natural *Cinchona* alkaloids, many derivatives, such as those containing hydroxyl groups, amines, ureas, and thiourea functionalities, especially at the C9 position,

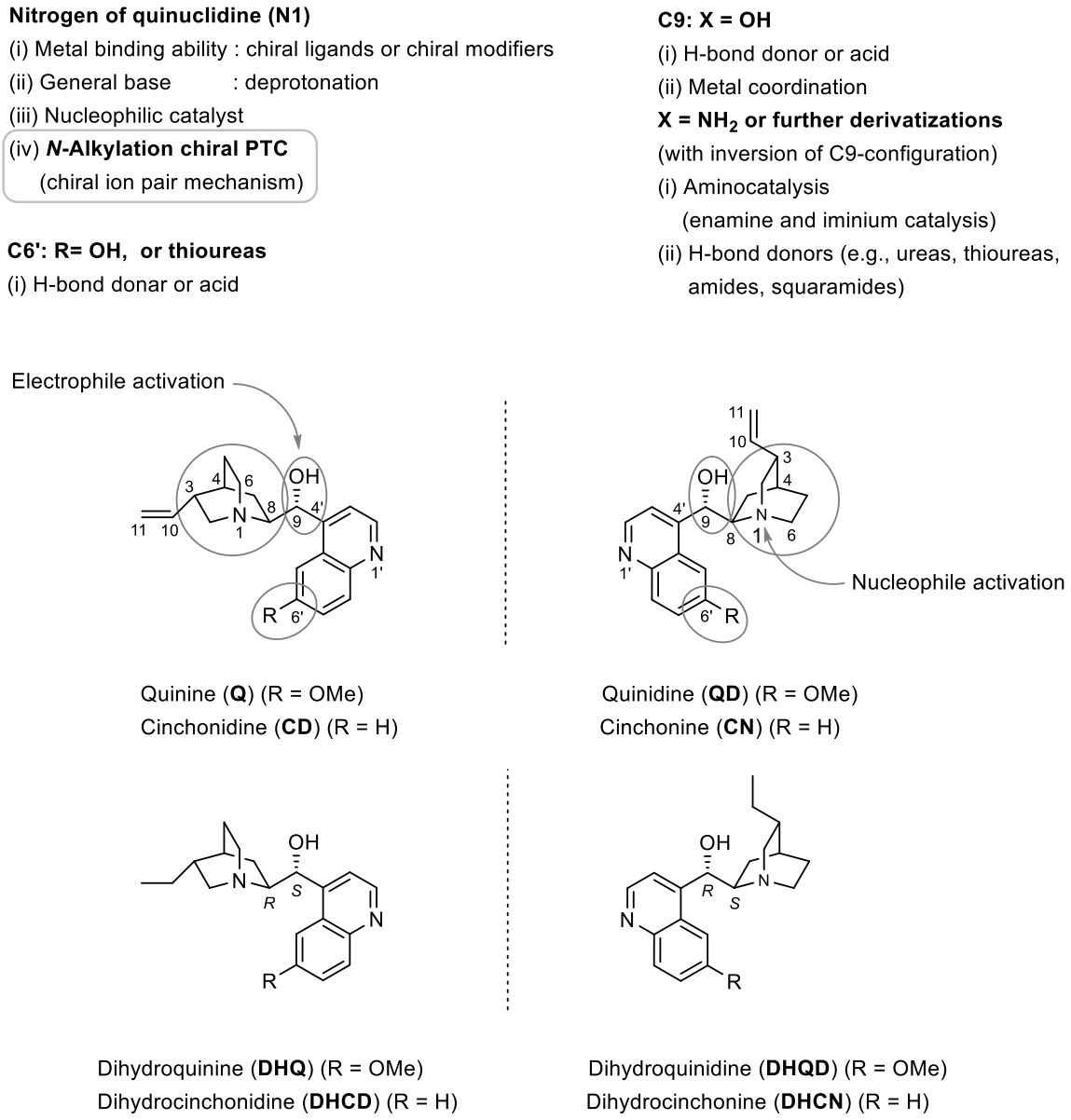

Figure 1.3 Active sites in *Cinchona* alkaloids and their structures.

either alone or in the presence of an additional catalyst that might be a simple achiral compound or metal salt, have been employed in diverse types of enantioselective syntheses by asymmetric catalysis. This can be attributed to the abundance of *Cinchona* alkaloids in nature: their commercial availability at reasonable prices, stability and easy handling in a laboratory, and their convenient modification by simple reactions.

The *Cinchona* skeleton consists of two rigid rings: an aliphatic quinuclidine and an aromatic quinoline ring joined together by two carbon-carbon single bonds. The relative orientation of the two rings quinoline and quinuclidine creates a “chiral pocket” around the reactive site, forcing a particular approach of the substrates, resulting in enantioselective product formation. There are five stereocenters (N1, C3, C4, C8, and C9) in the molecule. The *Cinchona* alkaloids occur in pairs, which differ in

configuration at C8, C9, and N1 positions. The eight major *Cinchona* alkaloids (Figure 1.3) are diastereomers, usually referred to as pseudoenantiomers, because they offer enantiomeric products when used as catalysts. The structural features of *Cinchona* alkaloids and their derivatives responsible for their catalytic activity in terms of yields and diastereoselectivity and enantioselectivity of products have been reported.[25] The key features responsible for their successful utility in asymmetric catalysis is that they possess several chiral skeletons and are readily tunable for various types of reactions.

Several studies have shown that *Cinchona* compounds work as bifunctional catalysts. The quinuclidine ring, bearing a tertiary nitrogen atom (N1), is 10^3 times more basic in comparison to quinoline nitrogen (N1´). The presence of the quinuclidine base functionality (N1) makes them effective ligands for a variety of metal-catalyzed processes. The most representative example is the osmium-catalyzed asymmetric dihydroxylation of olefins.[26] The metal-binding properties of the quinuclidine nitrogen also allow using cinchona alkaloids as metal surface modifiers, for example, in the highly enantioselective heterogeneous asymmetric hydrogenation of α-keto esters. Both reactions are classified as ligand-accelerated catalysis (LAC).[27] In addition to its ability for metal-binding, the quinuclidine nitrogen can be used as a chiral base or chiral nucleophilic catalyst promoting the vast majority of organocatalytic reactions.

The tertiary amine in the quinuclidine ring can be derivatized to provide a variety of quaternary ammonium salts, which are called phase transfer catalysts (PTCs). PTC has proved to catalyze a variety of reactions under phase-transfer conditions, where asymmetric inductions occur through a chiral ion-pairing mechanism between the cationic ammonium and an anionic species.[28] One of the most complex applications of PTCs involves asymmetric α-alkylation of carbonyl compounds, Michael addition, and epoxidation of enones, which are catalyzed by PTCs. PTCs are prepared by a simple and easy chemical transformation of the bridgehead tertiary nitrogen with a variety of active halides (Figure 1.4).[29]

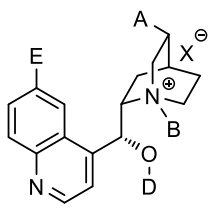

A: vinyl, ethyl, etc.
B: methyl, benzyl, substituted benzyl
anthracenylcemethyl, etc.
D: hydrogen, allyl, benzyl, etc.
E: hydrogen, methoxy, etc.
X: halogens

Figure 1.4 Quaternary ammonium salts (PTCs) derived from *Cinchona* alkaloids.

In addition to the bridgehead tertiary amine, *Cinchona* alkaloids have versatile functional groups such as the 9-hydroxy group, the 6´-methoxy group in quinoline, and the 10,11-vinyl group in the quinuclidine, all of which sometimes play critical roles in chirality creating steps, either themselves or

in chemically modified forms. The H-bonding groups, such as the hydroxyl group, urea, and thiourea at the C9 position, activate the electrophile by hydrogen bonding. The C6´ methoxy group of quinine and quinidine is readily derivatized as an effective H-bond donor. The modification of these moieties in *Cinchona* alkaloids (the 9-hydroxy, the 6´-methoxy, or the 10, 11-vinyl) enhance both chemical and optical yields in the asymmetric synthesis. In general, these active sites in *Cinchona* alkaloids and their derivatives act in catalysis not independently but cooperatively; that is, they activate the reacting molecules simultaneously. Furthermore, in many cases, the catalysis is also supported by a π-π interaction with the aromatic quinoline ring or by its steric hindrance.

Shi. M and coworkers have first reported the highly efficient asymmetric Michael addition of anthrone to nitroalkenes using *Cinchona* organocatalysts.[30] The Michael acceptors could exclusively produce the corresponding Michael adducts in good yields with moderate to high ee values in the presence of bifunctional *Cinchona* organocatalysts (Scheme 1.4).

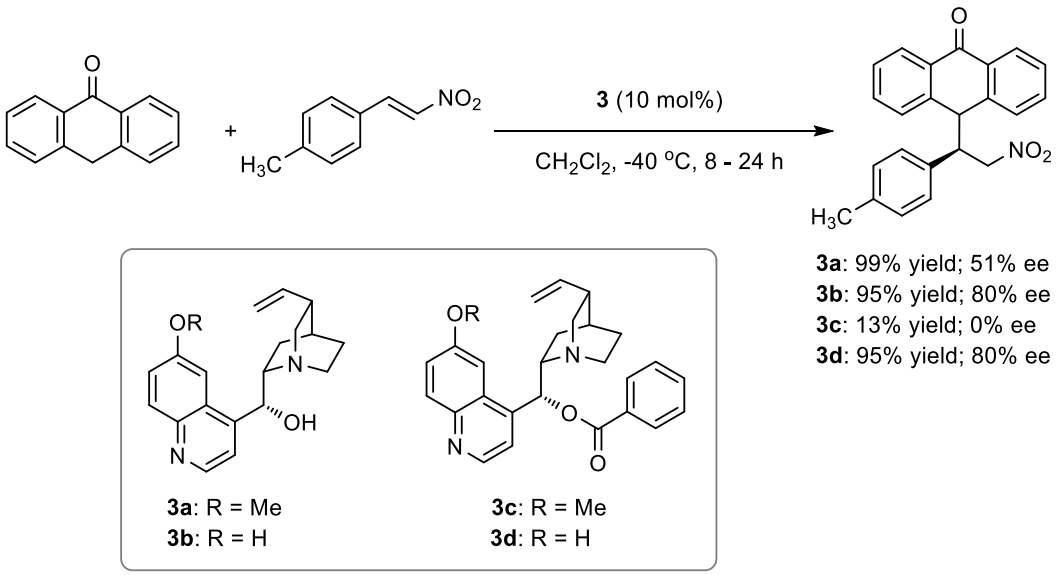

Scheme 1.4 Asymmetric Michael addition using *Cinchona*-derived organocatalyst.[30]

Since the first *Cinchona* alkaloid-derived phase-transfer catalyst was disclosed in 1981, diverse generations of *Cinchona*-derived phase-transfer catalysts have been developed and successfully applied to various asymmetric syntheses. The first significant utilization of *Cinchona* alkaloids as a catalyst scaffold for a PTC (What is APTC?-Asymmetric PTC) was carried out by Dolling and coworkers of the Merck research group in 1984 for the alkylation of α-substituted indanone substrate (Scheme 1.5).[31] Prior to this work, only moderate levels of enantioselectivity had been reported for PTC alkylations. Later in 1989, O'Donnell *et al.* demonstrated that the PTC alkylation of *N*-(diphenylmethylene)glycine *tert*-butyl ester **5** with 1st generation PTCs afforded good levels of enantioselectivity (Scheme 1.6).[32] Among the *Cinchona* alkaloids examined, cinchonine **6** and

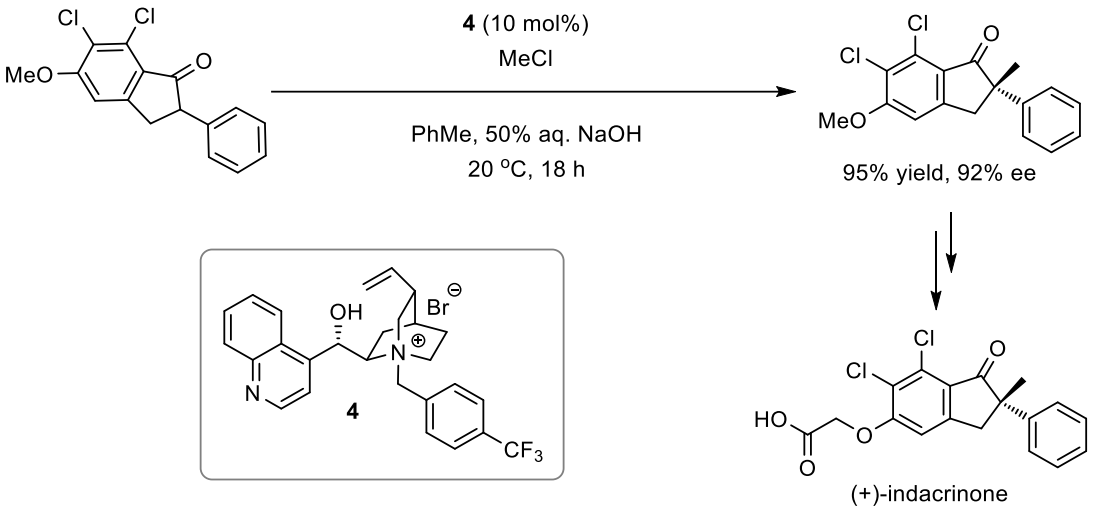

Scheme 1.5 Asymmetric alkylation reaction of α-substituted indanone.[31]

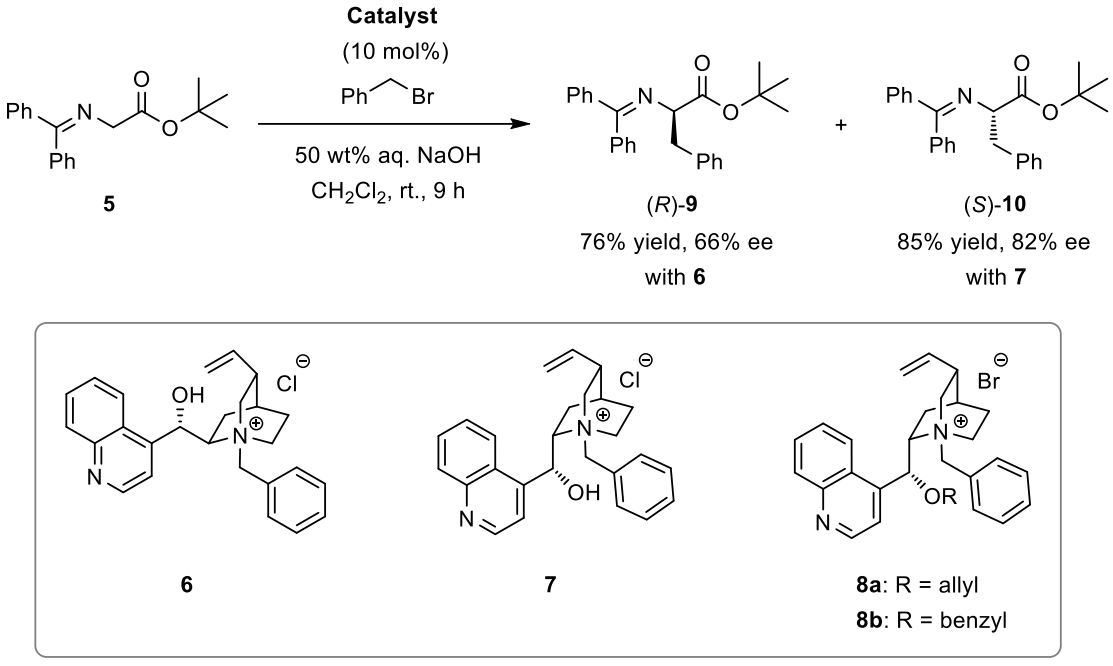

Scheme 1.6 Asymmetric benzylation reaction of a glycine derivative.[32]

cinchonidine **7** derived catalysts afforded the *R* and *S* configurations of the alkylation product as the major enantiomer, respectively. It was also observed that the cinchonidine based catalyst was more selective than the corresponding quinine-derived catalyst (er 78:22 compared to er 60:40, respectively). In 1994, the same group prepared corresponding *O*(9)- alkylated *Cinchona* PTCs **8a**, **8b** by using allyl or benzyl bromide. The modified C*inchona* PTCs catalyst **8a**, **8b** showed considerable enhancement of the catalytic activity in terms of enantioselectivity.

1.2.3 Chiral Imidazolidinone (MacMillan Catalyst) Organocatalyst

Chiral imidazolidin-4-ones (chiral secondary amines) and their salts developed by MacMillan and co-workers are one of the most important classes of chiral organocatalysts. They can be easily prepared from inexpensive natural amino acids.[19] These are good alternatives to toxic, hazardous, and expensive metals. The ability to activate both carbonyl compounds by enamine formation as well α, β-unsaturated carbonyl compounds by intermediate formation of iminium ions makes imidazolidin-4-ones a valuable class of organocatalysts in both series. A major focus of research in the MacMillan group has become the study of a broadly applicable reaction manifold based upon iminium activation using chiral imidazolidinones. The advantage of this approach is that the iminium generated *in situ* by the equilibrium between an α, β- unsaturated carbonyl compound (ketone or aldehyde) and a secondary amine salt can replace the traditional use of Lewis acid to lower the LUMO of the electrophile.[33] Iminium catalysis is comparable to Brønsted- or Lewis acid activation of carbonyl compounds. The LUMO energy is lowered, the α-CH-acidity increases and nucleophilic additions including conjugate additions as well as pericyclic reactions are facilitated. The mode of iminium activation of carbonyl compounds is the domain of many and various cycloadditions and conjugate additions. The ability to form iminium salts was utilized in several important C–C bond formation processes, such as Diels-Alder reactions. The first generation of MacMillan catalyst has been employed in a variety of organocatalytic enantioselective reactions, including the Diels-Alder reaction,[19] nitrone cycloaddition,[34] pyrrole Friedel-Crafts reaction,[35] indole addition,[36] vinylogous Michael addition,[37] α-chlorination,[38] hydride addition,[39] cyclopropanation,[40] α-fluorination.[41]

In 2000, MacMillan et al. reported the first enantioselective organocatalytic Diels-Alder cycloaddition using catalyst **12** under mild conditions with excellent enantioselectivities for both stereoisomers (*exo* and *endo*) (Scheme 1.7.[19] In addition, imidazolidin-4-one catalyzed **12** cycloadditions have been used in several total syntheses of natural products. Intramolecular Diels–Alder reactions (IMDA) were reported as key steps in the synthesis of bicyclo-undecenes,[23a]

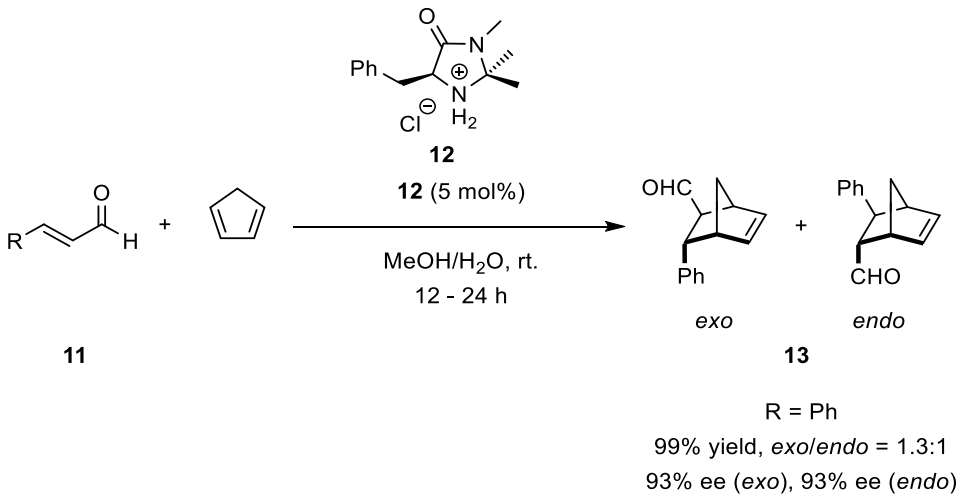

Scheme 1.7 Imidazolidinone-catalyzed Diels-Alder reaction.[19]

amaminols,[42c-d] solanapyrones,[21] telomerase inhibitor UCS1025A,[42e] englerin A,[42f] (–)-nor-platencin,[42g] and muironolide A.[42h] In addition, asymmetric [3 +2]-cycloadditions of azomethines were accomplished in the presence of chiral imidazolidinones.[42i]

1.3 Immobilized Organocatalyst

There are several advantages of organocatalysts over organometallic and biocatalysts considering both the principles of "green chemistry" and the economic point of view that were discussed in section **1.2**. When an organocatalyst is employed under a homogeneous condition, a tedious workup procedure is often required to isolate and purify the product form a reaction mixture. Therefore, organocatalysts are generally not reused. The recyclability of catalytic materials is one of the central principles of green chemistry regarding save resources and limit waste. Researchers have addressed these issues by immobilized organocatalysts that can be easily recovered from the reaction mixture and reused many times. A convenient strategy to render organocatalysts ''greener'' consists in their immobilization on a support with the purpose of facilitating catalyst recovery and reuse by simple work-up protocols. The range of supports expanded from silica to polymer particles and soluble polymers.[43]

Immobilization would be clearly convenient, especially when sophisticated and synthetically time-consuming catalysts in up to 20-30 mol% are used. Moreover, since the catalyst recovery is usually carried out by mean of simple methods like solvent extraction or, more likely, by simple filtration, the immobilization results in a simpler work-up of the reactions with beneficial effects under the process sustainability point of view. Finally, immobilization gives the possibility of exploring modifications of the properties of the supported catalysts by employing the specific characteristics of the support material. Additionally, in some cases, immobilization processes allow the use of low amounts of the catalyst, because the active molecules are better distributed in the supporting material relative to a non-immobilized catalyst. Generally, immobilization of an organocatalyst is more expensive than the use of a non-immobilized organocatalyst, because several synthetic steps may be necessary for the immobilization procedure. To counterbalance this point, the immobilized organocatalyst should be: (i) easily separated from reaction mixture; (ii) reused for several times without loss of reactivity and selectivity (in case of chiral organocatalyst); (iii) adaptable to continuous flow processes; (iv) less toxic and odorful; and (v) clean and safe for products.

Immobilized organocatalysts can be divided into the following (Scheme 1.8): (a) organocatalysts linked to a polymer support (covalently linked or not covalently linked, insoluble or soluble); (b) tagged organocatalysts with ionic liquid moieties, fluorous moieties, etc. There are three general strategies for immobilization of organocatalysts (both chiral and achiral) depending on the nature of both the catalyst to be anchored and the support (Scheme 1.8):

(A) ***Covalently supported catalysts***. The organocatalyst is covalently linked or anchored to a soluble (e.g., PEG, dendrimer) or insoluble (e.g., MCM-41, polystyrene, magnetite) support. The immobilization process involves either reaction of a functional resin or polymer with a suitably functionalized organocatalyst or copolymerization of a derivative of the functionalized catalyst with other monomers. The covalent bonding of catalyst to support implies, in general, a more stable of interactions and, therefore, a broader applicability of the immobilized organocatalyst. However, it usually requires higher synthetic effort due to the chemical modifications of the catalyst typically needed for linking it to the support.

(B) ***Non-covalently supported catalysts***. In this case, the catalyst is immobilized through adsorption (e.g., onto ionic liquids-modified SiO_2), hydrogen bonding on a polar support (e.g., SiO_2, stability is improved), entrapment (e.g., on a polydimethylsiloxane (PDMS) film.), dissolving (e.g., polyelectrolytes), included (e.g., β-CD, zeolites, clays) or linked by electrostatic interactions (e.g., PS-SO_3H, Layered Double Hydroxides) in the support. This approach is facile and straightforward because the modifications of the catalyst is not required. Sometimes, depending on the nature of the catalyst, the weak interactions making the supported catalysts less robust.

(C) ***Biphasic catalysts***. The organocatalyst is dissolved and remains into ionic liquids (ILs). After the reaction, the product is separated by distillation, extraction, or any other physical mean. Ionic

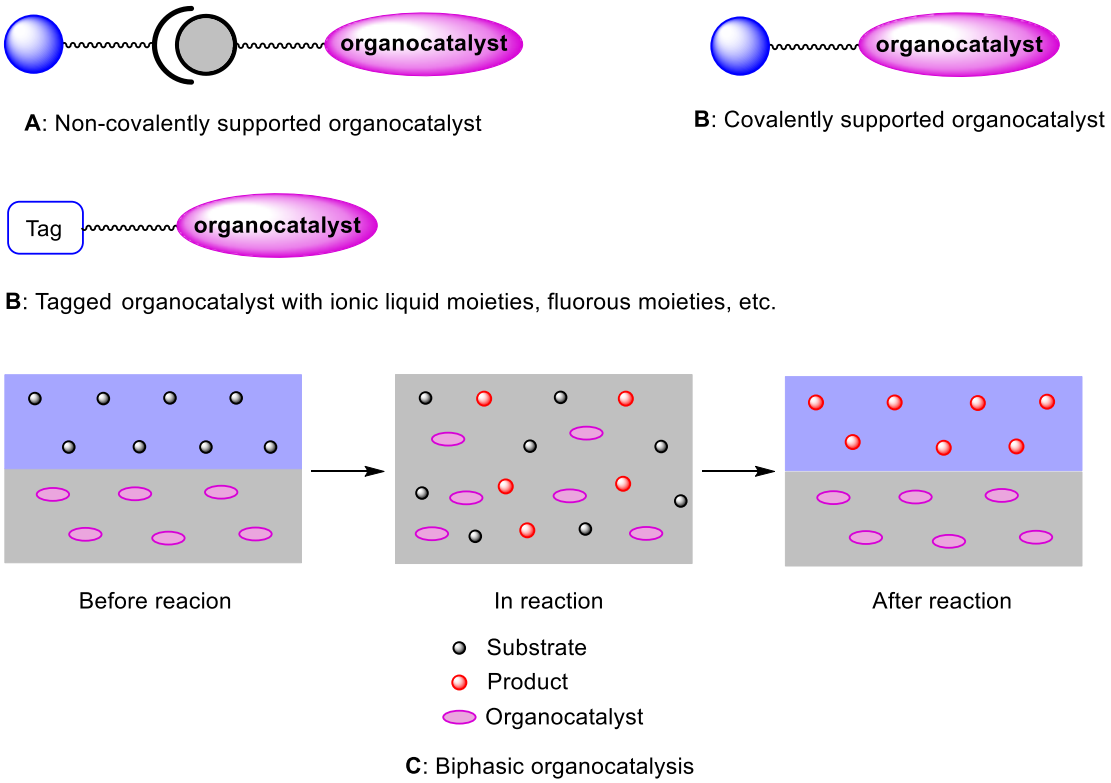

Scheme 1.8 Different approaches for organocatalyst immobilization

liquid-anchored organocatalysts can be considered as an advanced development of this approach since this simplifies the work-up and avoid extraction and phase separation.

A great deal of work has been reported on polymer supported-achiral organocatalysts that have been used as heterogeneous catalysts in organic synthesis.[43] Typical examples of polymer-supported organocatalysts used in organic synthesis involve poly(4-vinylpyridine) **15** in its basic form and sulfonated polystyrene **16** in its acid form, which act as catalysts in some base- and acid-catalyzed reactions, respectively. Regen was the first to report the immobilization of quaternary ammonim salts on polystyrene crosslinked with 2% divinylbenzene (DVB), and the immobilized catalyst **14** was used to catalyze the 1-bromooctane to nonanitrile conversion (Scheme 1.9).[44a] The simultaneous presence of an insoluble catalyst and of immiscible aqueous and organic phases led the author to dub the process "triphase catalysis".[44b,44c] Recently, our research group has successfully synthesized polymer microsphere-sulfonic acid catalysts and applied them as heterogeneous catalysts in organic synthesis. These catalysts showed better reactivity in both batch and continuous flow processes. They could be reused without loss of reactivity.

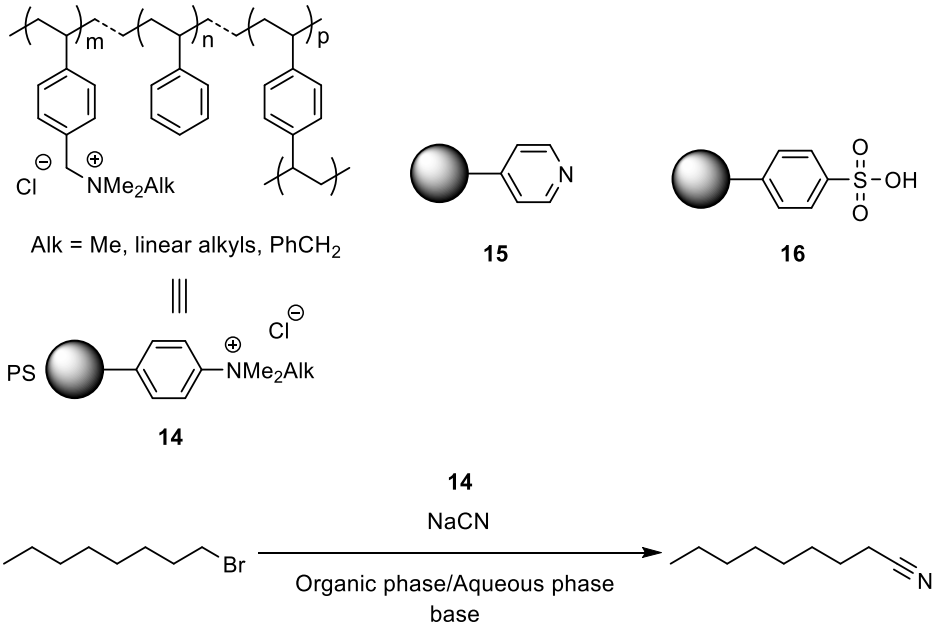

Scheme 1.9 Typical examples of polymer-supported organocatalysts in organic synthesis.

1.3.1 Support Material for Immobilization of Organocatalyst

The choice of a suitable support for the immobilization of an organocatalyst plays an important, although not fully understanding, role.

Possible problems can diminish the performance of a catalyst:

(i) Undesired interactions between the support and the catalyst (in case of chiral catalyst)

→ low enantioinduction;

(ii) Instability of the linkage between the catalyst and support or the catalyst itself

→ metal leaching (in case of organometallic catalyst);

(iii) Limited accessibility of the active site from substrate → low reactivity.

The following materials are used as supports for immobilization of organocatalysts:

(1) Organic polymer supports:

(i) Polymeric resins:

- Merrifield resins: poly(styrene-divinylbenzene) polymers
- JandaJel : polystyrene polymers containing a tetrahydrofuran-derived crosslinker
- TentaGel : polystyrene-polyethyleneglycol-OC_2H_4-$NHCOC_2H_5$
- PS-PEG : polystyrene-polyethyleneglycol resins

(ii) Soluble polymers: PEG, PS, etc.

(2) Inorganic supports:

(i) Zeolites, Alumina, Zinc oxides, Clays, Amorphous silica gel

(ii) Mesoporous silica (2~50 nm pore size):

MCM-41 "mobile crystalline material", ordered hexagonal, 3~4 nm pore diameter)

SBA-15 (ordered hexagonal, 1.2~3 nm pore diameter)

(iii) Crystalline nanoparticles: Gold NPs

(iv) Magnetite

(v) Polyoxometalates

(3) Biomolecules (e.g., DNA, RNA)

(4) Dendrimeric supports

(5) Cyclodextrins (CDs)

(6) Ionic liquids (ILs)

1.3.2 Immobilized Chiral Organocatalyst

Chiral organocatalysts have been highly effective over the last decade for the synthesis of optically active compounds for medical and pharmaceutical applications. They have been developed considering their two main functions that have discussed in section **1.2.1**. A complex work-up procedure (e.g., silica-gel column chromatography) is often necessary to purify the asymmetric products form a reaction mixture when a chiral organocatalyst is used under a homogeneous condition. Regarding the production of fine chemicals without contamination of catalysts, recovery of chiral organocatalysts is essential considering the principles of sustainable development.

To overcome the separation problem of molecular catalyst, heterogenization of a chiral organocatalyst by immobilization onto a support is a potential solution.[45] From the viewpoint of green chemistry, the method of asymmetric processes by using immobilized chiral organocatalyst provides a clean and safe alternative to conventional ones. In addition, the unique microenvironment formed between the reactants and the support material is of significance. It is possible to heterogenize all the existing chiral organocatalysts, however, the immobilization of highly versatile and efficient catalysts which is able to promote several organic processes with high levels of activity and stereoselectivity should be developed preferentially. The additional morphological properties of heterogeneous supports (polystyrene, silica, or polymer microspheres) and the choice of the linker between support and catalyst may have a great influence on the performance of the reactions due to electronic and steric effects against the reaction environment. As a consequence, these materials can be modulated in such a way that high stereoselectivities can be achieved.

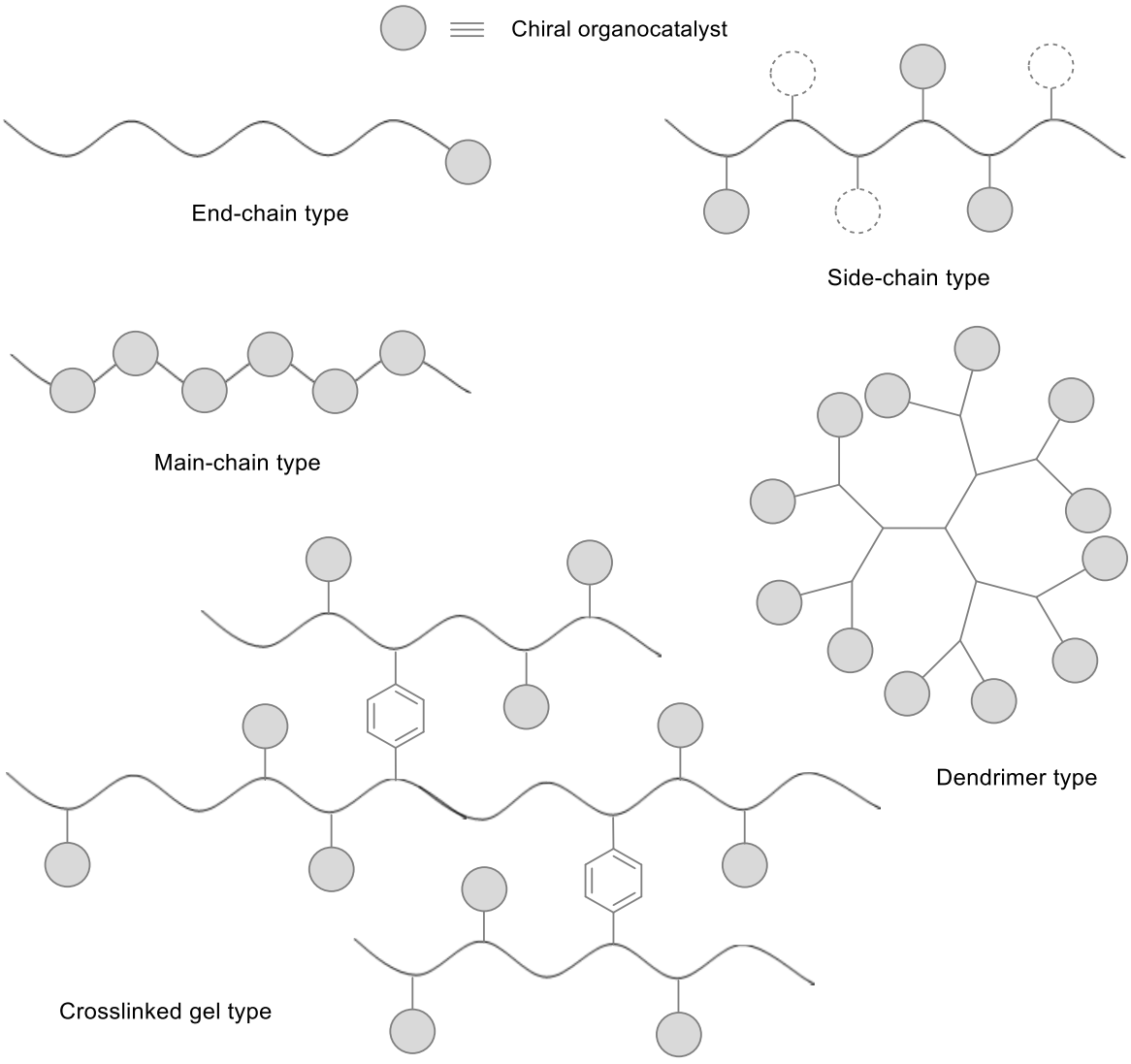

Figure 1.5 Structures of polymer-supported chiral organocatalyst.

1.3.3 Polymer-supported Chiral Organocatalyst

The use of polymer-supported chiral organocatalysts has become an essential technique in the green chemistry process of organic asymmetric synthesis. They can be easily separated from the

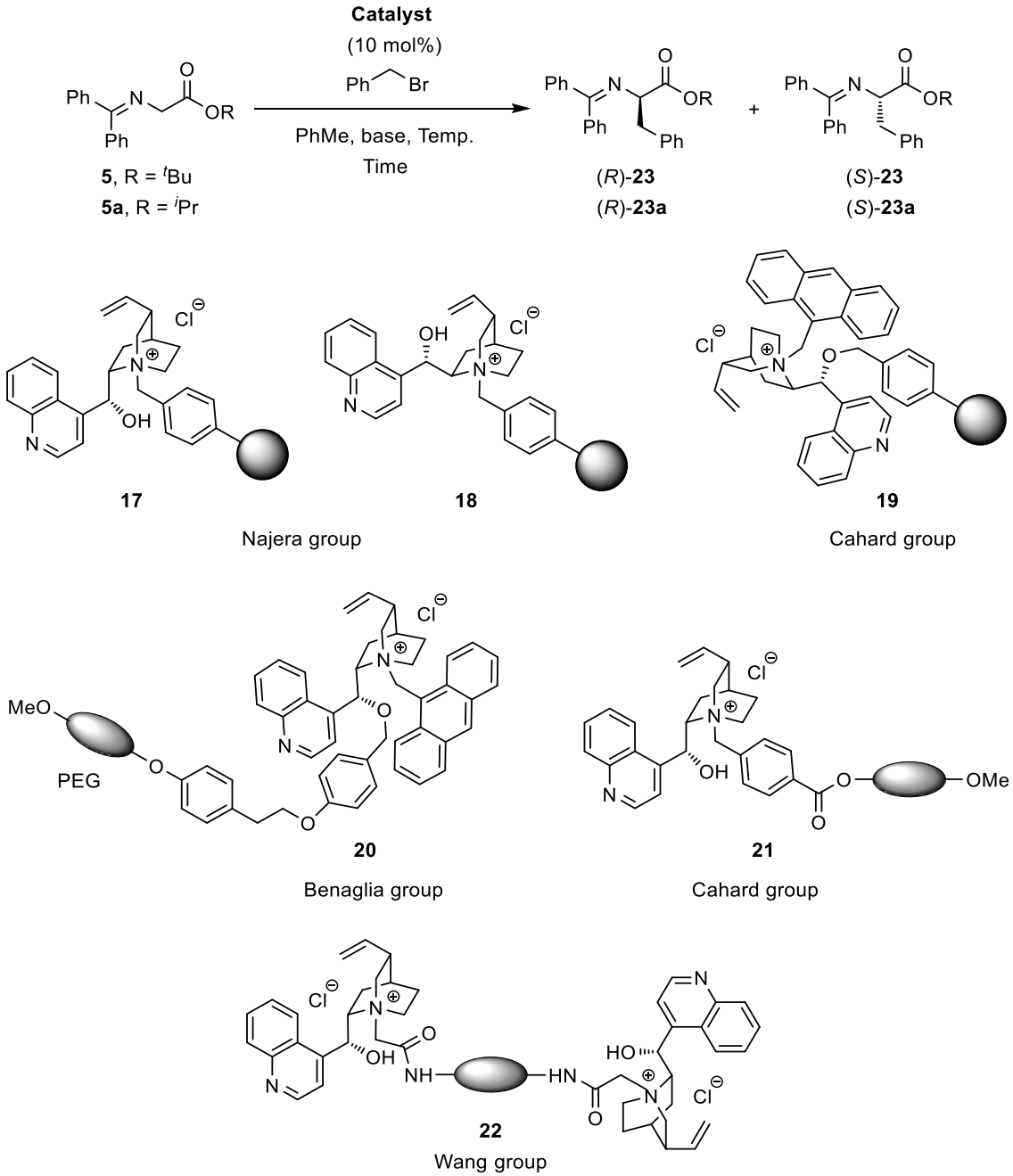

With **17**, 25 wt% aq. NaOH, 0 °C, 17 h; 90% yield, 90% ee, (*S*)-**23a**
With **18**, 25 wt% aq. NaOH, 0 °C, 17 h; 80% yield, 40% ee, (*R*)-**23a**
With **19**, $CsOH.H_2O$, -50 °C, 30 h; 67% yield, 94% ee, (*S*)-**23**
With **20**, $CsOH.H_2O$, CH_2Cl_2, -78 °C, 60 h; 75% yield, 64% ee, (*S*)-**23**
With **21**, 50 wt% aq. KOH, PhMe, 0 °C, 15 h; 84% yield, 81% ee, (*S*)-**23**
With **22**, 1M KOH, rt., 6 h; 98% yield, 83% ee, (*S*)-**23**

Scheme 1.10 Asymmetric benzylation reaction of a glycine derivative catalyzed by polymer-supported catalyst.

reaction mixture by simple filtration or centrifugation and reused many times. They can also be applied to the continuous flow system. Mostly polymer-supported chiral organocatalysts are synthesized using crosslinked polystyrene derivatives as support materials. There is the following type of polymer-supported chiral organocatalysts that are used in asymmetric organocatalysis (Figure 1.5).

In 2000, Najera group anchored both cinchonidine and cinchonine onto cross-linked polystyrenes (**17, 18**) for the asymmetric alkylation of glycine Schiff base (Scheme 1.10).[46] These polymer-supported PTCs were found to be more effective in the asymmetric alkylation reaction. The recovered catalysts showed almost identical reactivity and enantioselectivity at its second cycle in the alkylation. Cahard and co-workers also reported the modified Lygo-Corey analog **19** prepared by the attachment of Merrifield resin on the C(9)-OH position (Scheme 1.10). With this PTC, the asymmetric product (***S***)-**23** was obtained in the enhanced enantioselectivity of 94% ee using $CsOH.H_2O$ at -50 ^oC. Poly (ethylene glycol) (PEG) supported *Cinchona* PTCs were developed for the asymmetric alkylation by several groups (Scheme 1.10).[47,48] The beneficial aspects of PEG include that PEG is soluble in water, inexpensive, readily functionalized, and commercially available in different molecular weights. All these covalently bonded end-chain type polymer-immobilized chiral quaternary ammonium salts showed moderate to good enantioselectivities. In some cases, these exhibited low catalytic reactivity.

The chiral imidazolidinone was also immobilized onto a support such as PEG (**24**),[49] JandaJel (**25**),[50] poly(alkyl methacrylate), silica (**27**),[50] siliceous mesocellular foam (MCF) (**28**)[51] and polymer-coated MCF (**29**)[51] (Figure 1.6). Benaglia et al. were the first to immobilize a MacMillan catalyst on PEG_{5000} support.[49] The PEG immobilized MacMillan catalyst **24** was used for the asymmetric Diels–Alder reaction of acrolein with 1,3-cyclohexadiene to obtain the corresponding Diels–Alder adduct in moderate yield (67%) and with high enantioselectivity (92% ee).[49] The same catalyst effectively catalyzed asymmetric 1,3-dipolar cycloadditions.[52] At the same time, Pihko and co-workers also reported both JandaJel- and silica-supported MacMillan catalysts (**25** and **27** which were used as heterogeneous catalysts for Diels–Alder reactions.[50] The catalyst **25** performed better not only than **24** but also **27**. Another polymer-immobilized MacMillan catalyst **26** was obtained by polymerization of a methacrylated MacMillan monomer.[53] The catalyst **28** and **29** were tested in the cinnamaldehyde cycloaddition with cyclopentadiene, which showed lower enantioselectivities than the non-supported catalyst (83% ee Vs. 93% ee). Recovery of the soluble PEG-supported catalyst was not quantitative (70% - 80%). In contrast, the insoluble catalysts were recovered by filtration and can be reused many times.

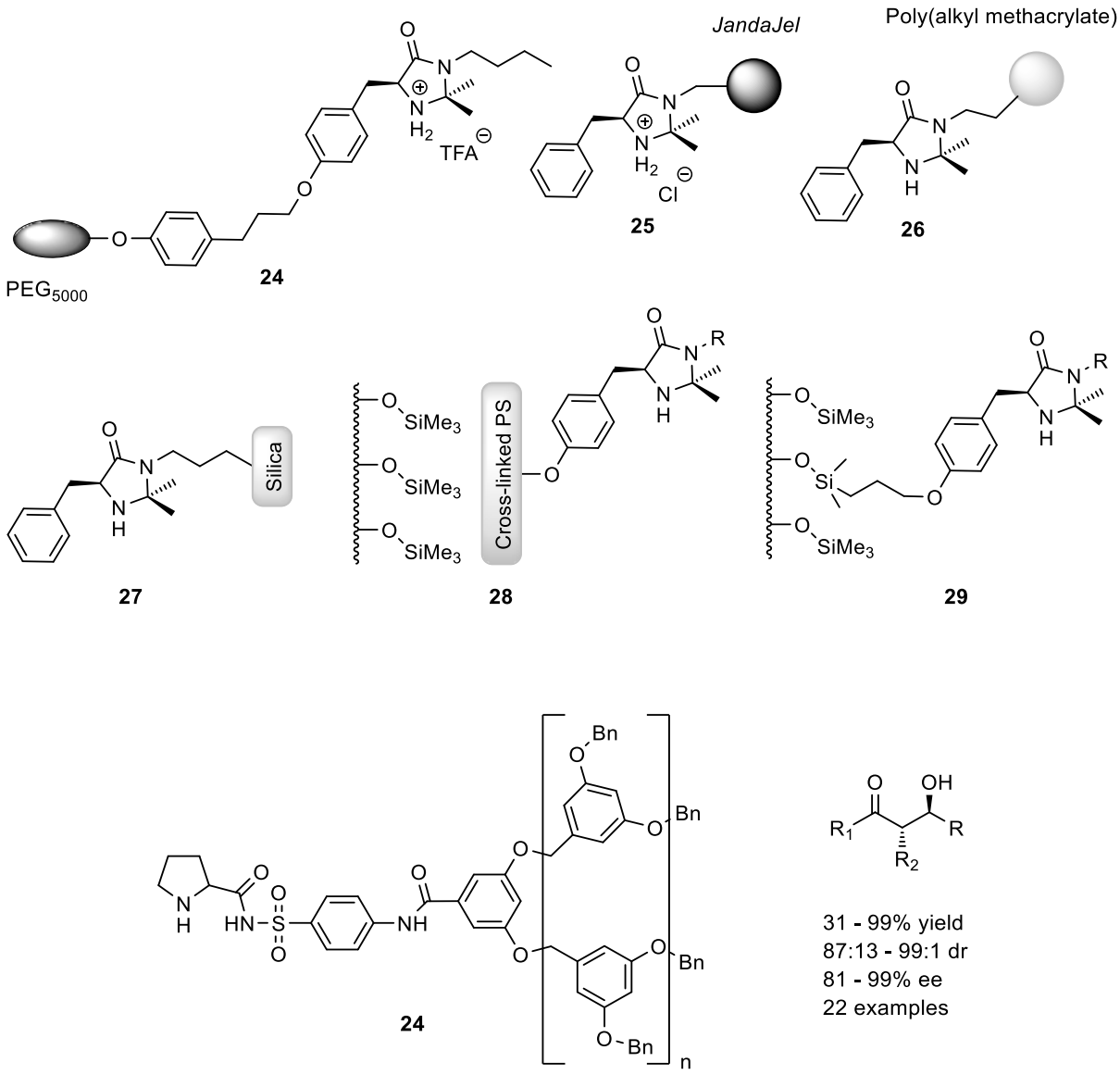

Scheme 1.11 Examples of covalently immobilized MacMillan catalyst.[54]

In 2006, Wang et al. reported the synthesis of chiral dendritic catalyst derived from proline-*N*-sulfonamide that was as a heterogeneous catalyst in the aldol reaction between cyclohexanone and 4-nitrobenzaldehyde in the presence of water (Scheme 1.11).[54] This catalyst exhibited good reactivity (up to 99% yield) with excellent enantioselectivity (up to 99% ee). The recovery of the dendritic catalyst was not also quantitative because it cannot be recovered by either precipitation or filtration.

In all the above polymer catalysts (Figure 1.6), the MacMillan catalyst was covalently bonded to the polymer support. The covalently bonded polymer-supported organocatalysts have disadvantages, including multi-step preparations and deactivation of the inherent catalysis due to the modification necessary to anchor the organocatalysts to supports. It can be interpreted in terms of direct

covalent-bonding of organocatalysts to the support material, decreasing the intrinsic properties of the steric sensitivity of organocatalyst on asymmetric synthesis.

To solve these problems, an alternative strategy involving the immobilization of organocatalysts on support materials using an ion-exchange reaction has been reported.[55] This method can be expected to allow for simple and facile preparation, easily separation from the reaction mixture, reusability of the immobilized catalyst, and higher enantioselectivity due to increased steric steering by the support material. Recently, some examples of ionically immobilized MacMillan catalysts have been reported. Montmorillonite clay was found to entrap MacMillan catalysts readily, and the resulting heterogeneous chiral organocatalyst **30** was utilized in Diels–Alder reactions (Scheme 1.12).[56] In another case, silica gel soaked in an ionic liquid such as a medium containing 1-butyl-3-methylimidazolium salt was used for the immobilization of MacMillan catalysts (Scheme 1.12).[57] In 2008, Itsuno et al. have developed two methods for the ionically immobilization of chiral

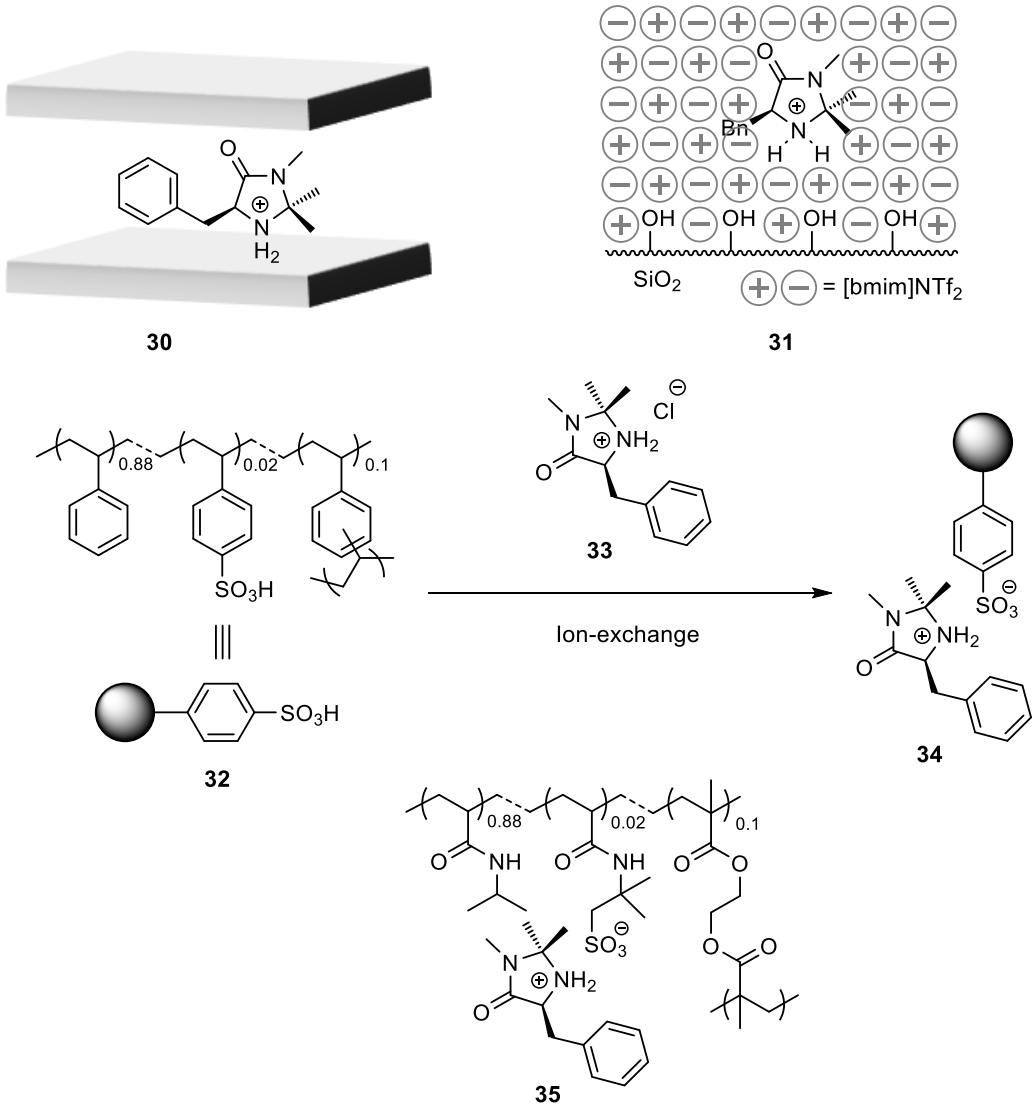

Scheme 1.12 Examples of ionically immobilized MacMillan catalyst.

quaternary ammonium salts onto polymer supports.[58] The first method involves the polymerization of a chiral quaternary ammonium sulfonate monomer, and the second one is the immobilization of a chiral quaternary ammonium salt onto a sulfonated polymer through an ion exchange reaction. The latter is a facile and general technique for the immobilization of ammonium onto sulfonated polymers regardless of kinds of ammonium and sulfonated polymer. These supported chiral quaternary ammonium salts obtained from the two methods showed similar performance in the asymmetric PTC alkylation of glycine derivatives. The supported catalysts synthesized by the latter one exhibited significantly improved enantioselectivity compared with the unsupported catalyst. They are quite stable and can be quantitatively recovered and reused twice without any loss of activity and enantioselectivity.

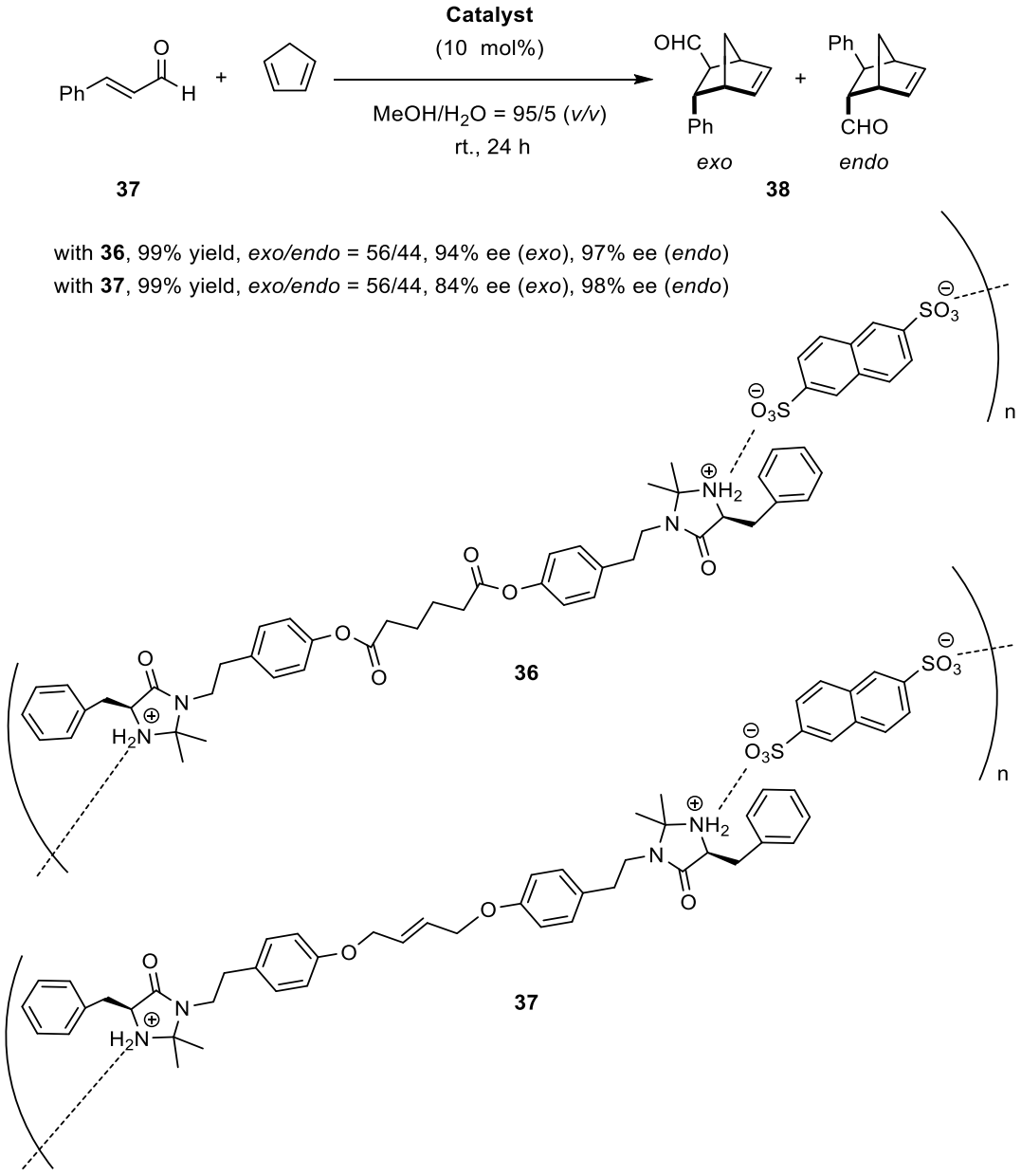

Scheme 1.13 Asymmetric Diels-Alder reaction catalyzed by main-chain polymer-supported MacMillan catalyst.

Haraguchi et al. applied this strategy for the ionic immobilization of a MacMillan catalyst on a gel-type polymer (Scheme 1.12).[59] The polymer-immobilized MacMillan catalyst **34** was easily obtained by the polymerization of the MacMillan monomer or by the ion exchange reaction between MacMillan hydrochloride **33** and the sulfonated polymer **32**. The MacMillan catalyst was successfully linked to the polymer through the formation of an ionic bond, which was stable under the asymmetric Diels–Alder reaction conditions. The reaction between cinnamaldehyde and cyclopentadiene proceeded smoothly in the presence of **34** to afford the Diels–Alder adduct in quantitative yield with high enantioselectivity (up to 91% ee for endo isomer). The hydrophilic–hydrophobic balance of the polymer structure was found to be important for the catalyst performance in an asymmetric reaction. The poly(*N*-isopropyl acrylamide)-immobilized catalyst **35** showed the best performance in the Diels–Alder reaction between cinnamaldehyde and cyclopentadiene. This catalyst could be reused without significant loss of its activity. They have also developed several main-chain chiral polymers containing imidazolidinone repeating units by ionic bond formation between imidazolidinones and sulfonates.[60-63] These main-chain chiral ionic polyesters **36** and polyethers **37** containing imidazolidinone units were synthesized by ion-exchange polymerization and used as heterogeneous catalysts in the asymmetric Diels-Alder reactions (Scheme 1.13). Both catalysts gave the Diels-Alder adducts with quantitative yield and excellent enantioselectivity of up to 97% and 98% ee for the *endo* isomer, respectively, that were higher than that obtained by the corresponding monomeric chiral imidazolidinone salts.

To date, there have been little reports about microsphere-supported chiral organocatalyst which was used in asymmetric synthesis.[64a] Recently, X. Li et al. have been reported micron-/nano-sized hairy microsphere-supported MacMillan catalyst in the asymmetric Diels–Alder reaction in water.[65a] The results in their investigations showed that the chiral polymer grafted on the nanoparticles had better dispersion in the reaction media than those grafted on the microspheres and exhibited better catalytic activity and selectivity in the asymmetric Diels–Alder reaction between *trans*-cinnamaldehyde and 1,3-cyclopentadiene. As a result, the obtained catalyst can be easily recovered in quantitative and recycled without losing significant activity and selectivity after 5 cycles. Our research group was developed uniform-, core-shell-, and core-corona-type polymer microsphere-supported chiral ligands in asymmetric transfer hydrogenation.[64b] The introduction position of the chiral catalyst onto the polymer microsphere and the degree of crosslinking as well as structure and hydrophobicity of polymer microsphere affected on the catalytic performance.

1.4 Polymer Microspheres

Polymer microspheres refer to particles containing polymer components with a diameter in the order of sub-micron to several microns with spherical shape. Colloid science deals with the formation and properties of many types of small particles, including polymer microspheres. These nano- or microspheres have many unique characteristics: (i) small size and volume; (ii) large specific surface area; (iii) high diffusibility; (iv) stable dispersions due to the following forces, electrostatic repulsive forces, van der Waal's attractive forces, and steric repulsive forces among the particles; (v) uniformity of the size distribution; and (vi) variation of diameter, surface chemistry, composition, surface texture, and morphology easily possible.

Polymer microspheres were widely used in different fields, including separation resins, drug delivery systems, and microreactors. Porous PDVB microspheres can be packed into columns for size exclusion chromatography.[65] In another research, chlorobenzyl particles were used as a stationary phase in high-performance liquid chromatography.[66]

1.4.1 Functional Polymer Microspheres and Hierarchical Polymer Microspheres

Functional polymer microspheres are one of the polymer microspheres containing one or more than one functional group. Functional polymer microspheres have been attracted considerable attention for their potential applications in a variety of fields such as coatings, electronics, biomedical engineering, and polymeric support materials in organic synthesis. Functional polymer microspheres can be prepared directly using functional monomers by a range of heterogeneous polymerization techniques, including emulsion polymerization, soap-free emulsion polymerization, dispersion polymerization, suspension polymerization, and precipitation polymerization. They can also be obtained by another method where the surface modification of existing polymer microspheres is required.

For the synthesis of polymer microsphere, precipitation polymerization has received much attention because of its easy operation and unnecessity of surfactant or stabilizer. In this technique, steric stabilization through a self-renewing surface gel layer can prevent coagulation of particles and can lead to stabilizer-free, narrowly dispersed functional polymer microspheres with controllable surface chemistry. These particles may be colloidally stabilized by electrostatic, steric, and electrostatic forces in all other traditional techniques. Initially, this technique did not attract much attention due to the difficulty in controlling the polymer particle uniformly. Recently, Stöver et al. reported the precipitation polymerization for the synthesis of monodisperse cross-linked polydivinylbenzene (PDVB) microspheres[67] and core-shell polymer microspheres.[68]

Hierarchical or core-corona polymer microsphere is one of the functional polymer microspheres where linear polymer chains are grafted onto the surface. These hierarchical polymer microspheres

allow more flexible, high dispersity, and reactive functional site. Stöver et al. were also first to report the synthesis of hierarchical polymer microspheres by grafting of polystyrene [69a] and poly(alkyl(meth)acrylates)[69b] from polymer microspheres having initiator moiety by surface-initiated atom transfer radical polymerization (SI-ATRP). The 'grafting from' technique allows precise control of particle growth and surface modification.

1.5 Synthesis of Well-defined Polymer Microspheres

1.5.1 Synthesis of Well-defined Functional Polymer Microspheres

Well-defined functional polymer microspheres are one of the polymer microspheres where the polymer chains are well-defined. Conventional free radical polymerization has been the most widely used polymerization approach for both the commercial and lab-scale production of high-molecular-weight polymer particles due to its applicability to a large number of monomers, mild polymerization conditions, and tolerance to many different solvents (such as water) and impurities. The difficulty of the free radical polymerization is that this is an uncontrolled polymerization process with the occurrence of significant chain-breaking reactions because of the continuous initiation, growth, and termination of polymer chains. As a result, polymers particles with high molecular weights and large dispersities (*Đ* values) are generally produced, which are inappropriate for applications where good control over the polymer structures is required. In this sense, the polymerization methods allowing the precise synthesis of polymer particles with well-defined polymer chains are highly desirable.

The polymer microspheres prepared by traditional polymerization techniques, however, normally do not have such "living" groups, which makes their further surface modification necessary to introduce the required "living" groups prior to their surface functionalization.[69,70] Controlled/"living" radical polymerization techniques (CRPs) (e.g., nitroxide-mediated radical polymerization atom transfer radical polymerization (ATRP), and reversible addition-fragmentation chain transfer (RAFT) polymerization) can provide well-defined polymers with end-capped "living" groups. When the CRP mechanism is introduced into the traditional heterogeneous polymerization approaches, it should be allowed the synthesis of well-defined polymer microspheres with "living" groups on their surfaces. Although the precision synthesis of polymer particles on the basis of the above principle by applying various CRPs in dispersion polymerization system has been reported, it seems to be insufficient for the preparation of well-defined polymer microspheres consisting of regulated polymer chains, presumably because the concentration of the growing species in the polymer microspheres is too high to suppress side reactions.[71]

To overcome the above problem, some controlled/‘‘living’’ radical precipitation polymerization (CRPP) approaches have recently been developed by the introduction of CRP mechanism into the precipitation polymerization system, including atom transfer radical precipitation polymerization (ATRPP),[72] iniferter-induced ‘‘living’’ radical precipitation polymerization (ILRPP),[73] and RAFT precipitation polymerization (RAFTPP).[74] Among them, ATRPP and ILRPP have proven to be more facile, general, and highly efficient approaches over RAFTPP for preparing narrowly or monodispersed highly crosslinked living’’ functional polymer microspheres with well-defined polymer chains. In addition, they have also been demonstrated to be highly versatile for the synthesis of advanced synthetic receptors with tailor-made recognition sites (i.e., molecularly imprinted polymers). In this thesis, low cross-linked functional polymer microspheres having sulfonic acid moiety with well-defined polymer chains have first synthesized using atom transfer radical precipitation polymerization (ATRPP). To find optimal conditions for the synthesis of such functional polymer microspheres by ATRPP is now under investigation.

1.5.2 Synthesis of Well-defined Hierarchical Polymer Microspheres

Well-defined hierarchical or core-corona polymer microspheres are a kind of core-shell type polymer microspheres whose shell is composed of well-defined linear polymer chains having a high affinity to the dispersion medium. They have on chemical crosslinking among polymer chains. The rigidity and stability of the core, as well as flexibility, processability, functionality of corona, enlarge the potential applications of core-corona (CC) polymer microspheres. They can be synthesized by a “grafting onto”[75], a “grafting from”[76], or a “grafting through”[77] approaches. The ‘‘grafting from” approach corresponds to surface-initiated graft polymerization from the surface of core particles. This technique allows linear polymer chains to initiate from every initiator site on the surface of particles, giving high grafting densities and layer thicknesses because monomers can easily diffuse to the propagating sites[78]. In contrast, the other techniques give low grafting densities and layer thicknesses due to steric hindrance of polymer chains.

Among the above three approaches, we have used controlled “grafting from” approach to synthesize hierarchical polymer microspheres in this thesis considering the possible designing of coronas. Because in this approach, the density of coronas s should be constant, but the length of coronas would be increased with increasing conversion. The controlled ‘‘grafting from’’ method by various surface-initiated controlled/‘‘living’’ radical polymerizations (CRPs) such as iniferter-induced living radical polymerization(ILRP),[79] nitroxide-mediated radical polymerization (NMP),[80] atom transfer radical polymerization (ATRP),[81] and reversible addition-fragmentation chain transfer (RAFT)[82] polymerization from the surface of functional polymer microsphere provides highly grafted

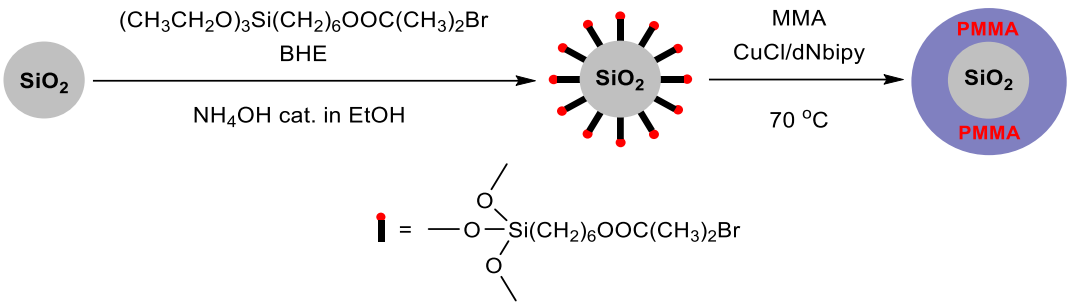

Scheme 1.14 Synthesis of PMMA-grafted silica particles by SI-ATRP.[85d]

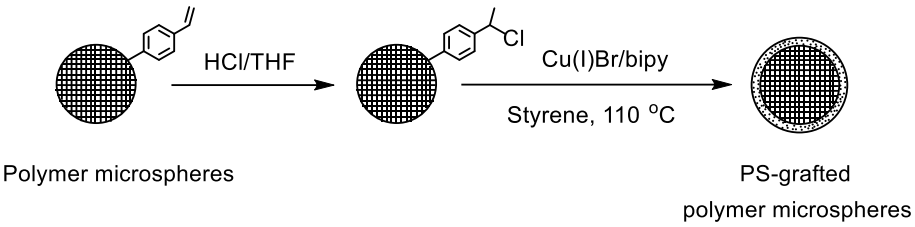

Scheme 1.15 Synthesis of PS-grafted polymer microspheres by SI-ATRP.[69a]

and well-defined hierarchical or core-corona polymer microspheres. In comparison with other CRP techniques, ATRP has been particularly attractive because this polymerization process can be easily controlled, enabling the achievement of a low polydispersity index, a high degree of chain-end functionalities, and high living nature.

Surface-initiated atom transfer radical polymerization (SI-ATRP) was first reported in 1997 by Huang and Wirth, who successfully grafted poly(acrylamide) (PAm) chains from benzyl chloride-functionalized silica particles.[83] Later, Ejaz et al. described the preparation of poly(methyl methacrylate) (PMMA) brushes hat were grown from 2-(4-chlorosulfonylphenyl)ethyl silane self-assembled monolayers (SAMs).[84] There have been several reports on polymer grafted-SNPs synthesized by SI-ATRP using surface-modified SNPs as core considering their potential applications in various areas such as colloid chemistry, catalysis, nanopatterning, photonics, drug delivery, and biosensing (Scheme 1.13).[85] Stöver et al. and other few groups were used polymer microspheres synthesized via heterogeneous polymerizations prior to introducing ATRP initiator moiety onto their surfaces as macroinitiators to synthesize hierarchical polymer microspheres by SI-ATRP (Scheme 1.14).[69,70]

In this thesis, monodispersed polymer microspheres having ATRP initiator moiety were directly synthesized using 4-vinylbenzyl chloride as comonomer by precipitation polymerization, which was used as macroinitiators to synthesize hierarchical or core-corona polymer microspheres by SI-ATRP. In this case, surface modification of polymer microspheres is not required to introduce ATRP initiator moiety that was an advantage over-reported.

1.6 Research Objectives

In spite of the efficiency of polymer microsphere as polymer support, there is no report on the immobilization of chiral organocatalyst onto polymer microspheres or core-corona polymer microspheres. Monodisperse sulfonated uniform microspheres or sulfonated core-corona polymer microspheres seem to be suitable solid-supports for the ionic immobilization of chiral organocatalysts because of their large surface area, facile dispersibility, and high thermal and mechanical strength compared to inorganic (e.g., silica, magnetite, or other metal oxides) and linear polymer supports. In addition, an advantage of polymer microspheres is the ability to control their hydrophilic-hydrophobic balance, which offers suitable microenvironments for catalytic asymmetric reactions. It can be expected to allow high catalytic reactivity and enantioselectivity in asymmetric organocatalysis due to these advantages of polymer microsphere supports. Considering these advantages of polymer microspheres, the main objective of this research is to design and synthesize of core-corona polymer microspheres and their applications as heterogeneous catalysts to asymmetric organocatalysis.

In this research, monodispersed polymer microspheres having benzyl halide moiety (ATRP initiator moiety) were successfully synthesized by precipitation polymerization of various comonomers and crosslinkers with 4-vinylbenzyl chloride (VBC) as dual functional comonomer that was discussed details in Chapter **II**. In Chapter **III**, well-defined hairy polymer microspheres were synthesized by the surface-initiated atom transfer radical polymerization (SI-ATRP) of various monomers using polymer microspheres having ATRP initiator moiety prepared via precipitation polymerization as a macroinitiator. Sulfonated core-corona polymer microspheres were synthesized by the surface-initiated ATRP of an achiral vinyl monomer and phenylsulfonated styrene with monodispersed polymer microspheres having benzyl halide moiety synthesized via precipitation polymerization as a macroinitiator, followed by the treatment of NaOH. *N*-(9-Anthracenemethyl)-cinchonidinium chloride was successfully immobilized onto the side chain of the corona by the ion exchange reaction to afford core-corona polymer microsphere-supported chiral cinchonidinium salt. These immobilized chiral catalysts were used heterogeneous catalysts in the asymmetric alkylation of a glycine derivative that was briefly investigated in Chapter **IV**. Core-corona polymer microspheres having sulfonic acid were also synthesized by the surface-initiated ATRP of an achiral vinyl monomer and phenylsulfonated styrene with monodispersed low cross-linked polymer microspheres having benzyl halide moiety prepared *via* precipitation polymerization as a macroinitiator, followed by the treatment of NaOH and H_2SO_4. Chiral Imidazolidinone (MacMillan catalyst) was also successfully immobilized onto the side chain of the corona by neutralization reaction to provide core-corona polymer microsphere-supported MacMillan catalyst which was as a heterogeneous catalyst in the Diels-Alder reaction that was shortly described in Chapter **V**.

References

[1] Eliel, E. L.; Wilen, S. H.; Mander, L. N. Eds., *Stereochemistry of Organic Compounds*, Wiley, New York, 1994.

[2] (a) Ojima, I. Ed., *Catalytic Asymmetric Synthesis*, Wiley-VCH, New York, 2000. (b) Noyori, R. Eid., *Asymmetric Catalysis in Organic Synthesis*, Wiley-Interscience, New York, 1994. (c) Jacobsen, E. N.; Pfaltz, A.; Yamamoto, H. Eds., *Comprehensive Asymmetric Catalysis, Springer*, Berlin, 1999.

[3] (a) Collins, A. N.; Sheldrake, G. N.; Crosby, J. Eds., *Chirality in Industry*, 1992; *Chirality in Industry II: Developments in the Commercial Manufacture of Optically- Active Compounds*, Wiley, Chichester, 1996 and 1997. (b) Aronson, J. K. Eds., *Side Effects of Drugs*, Elsevier, Amsterdam, 1997. (c) Makins, R.; Ballingger, A. *Expert Opinion on Drug Safety* **2003**, *2*, 421 - 429. (d) Keller, T. H.; Bray-French, K.; Demnitz, F. W. J.; Muller, T.; Pombo-villar, E.; Walker, C. *Chem. Pharm. Bull.* **2001**, *49*, 1009 - 1017. (e) Eriksen, J. L.; Sagi, S. A.; Smith, T. E.; Weggen, S.; Das, P.; McLendon, D. C.; Ozolos, V. V.; Jessing, K. W.; Golde, T. E. *J. Clini. Invest.* **2003**, *112*, 440-449. (f) Patent, Li, Z.; Lu, X.; Liao, C.; Shi, L.; Liu, Z.; Ma, B.; Ning, Z.; Shan, S.; Deng, T. WO2004048333 A1, **2004**.

[4] (a) Nogradi, M. Ed., *Stereoselective Synthesis, A Practical Approach*, 2nd Edition, VCH, 1995. (b) Finn, M. G.; Sharpless, K. B. Eds., *Asymmetric Synthesis*, Academic Press, New York, 1985. (c) Coppola, G. M.; Schuster, H. F. Eds., *Asymmetric Synthesis (Construction of Chiral Molecules using Amino Acids)*, Wiley, 1987.

[5] (a) Atiken, R. A.; Kilenyi, S. N. Eds., *Asymmetric Synthesis*, Blackie Academic & Professional, Chapman & Hall, 1992. (b) Morrison, J. D.; Mosher, H. S. Eds., *Asymmetric Organic Reactions*, Prentice-Hall, Inc., Englewood Cliffs, New Jersey, 1971.

[6] (a) Helmchen, G.; Hoffmann, R. W.; Mulzer, J.; Schaumann, E. Eds., *Methods of Organic Chemistry*, Volume E 21a, *Stereoselective Synthesis*, Thieme, Stuttgart, 1995, p 75. (b) Morrison, J. D. Ed., *Asymmetric Synthesis*, 5 volumes, Academic Press, Orlando, 1983 -1985.

[7] Yeboah, Elizabeth M. O.; Yeboah, Samuel O.; Singh, Girija S. *Tetrahedron* **2011**, 67, 1725 - 1762.

[8] (a) Berkessel, A.; Gröger, H.; Eds., *Asymmetric organocatalysis: from biomimetic concepts to applications in asymmetric synthesis*, Wiley-VCH, Weinheim, 2005. (b) Dalko, P.I.; Ed., *Enantioselective Organocatalysis*, Wiley-VCH, Weinheim, 2007.

[9] von Liebig, J. *Annalen der Chemie und Pharmacie* **1860**, *113*, 246 - 247.

[10] Dakin, H. D. *J. BioChem.* **1909**, *7*, 49 - 55.

[11] Vavon, M. M.; Peignier, P. *Bulletin de la Soci´et´eChimique deFrance* **1929**, *45*, 293-298.

[12] Wegler, R. *Justus Liebigs Annalen der Chemie* **1932**, *498*, 62 - 73.

[13] Bredig, G.; Fiske, W. S. *Biochem. Z.* **1912**, 7 - 23.

[14] Pracejus, H.; Justus Liebigs *Ann. Chem. Pharm.* **1960**, *634*, 9 - 22.

[15] Pracejus, H.; Mätje, H.; Prakt, J. *Chem./Chem.-Ztg.* **1964**, *24*, 195 - 205.

[16] Eder, U.; Sauer, G.; Wiechert, R. *Angew. Chem. Int. Ed.* **1971**, *10*, 496 - 497.

[17] Hajos, Z. G.; Parrish, D. R. *J. Org. Chem.* **1974**, *39*, 1615 - 1621.

[18] List, B.; Lerner, R. A.; Barbas III, C. F. *J. Am. Chem. Soc.* **2000**, *122*, 2395 - 2396.

[19] Ahrendt, K. A.; Borths, C. J.; MacMillan D. W. C. *J. Am. Chem. Soc.* **2000**, *122*, 4243 - 4244.

[20] Northrup, A. B.; MacMillan, D. W. C. *J. Am. Chem. Soc.* **2002**, *124*, 2458 - 2460.

[21] Wilson, R. M.; Jen, W. S.; MacMillan, D. W. C. *J. Am. Chem. Soc.* **2005**, *127*, 11616 - 11617.

[22] Mukherjee, S.; Yang, J. W.; Hoffman, S.; List, B. *Chem. Rev.* **2007**, *107*, 5471 - 5569.

[23] Kacprzak, K.; Gawronski, J. *Synthesis (Stuttg)*. **2001**, *7*, 961 - 998.

[24] Marcelli, T.; Hiemstra, H. *Synthesis (Stuttg)*. **2010**, *8*, 1229 - 1279.

[25] Yeboah, E. M.; Yeboah, S. O.; Singh, G.S. *Tetrahedron* **2011**, *67*, 1725 - 1762.

[26] Kolb, H. C.;VanNieuwenhze, M. S.; Sharpless, K.B. *Chem. Rev.* **1994**, *94*, 2483 - 2547.

[27] Berrisford, D. J.; Bolm, C.; Sharpless, K. B. *Angew. Chem. Int. Ed.* **1995**, *34*, 1059 - 1070.

[28] (a) Maruoka, K. Ed., *Asymmetric Phase Transfer Catalysis*, Wiley-VCH Verlag-GmbH, Weinheim, **2008**. (b) Hashimoto, T.; Maruoka, K. *Chem. Rev.* **2007**, *107*, 5656 - 5682.

[29] Song, C. E. Ed., *Cinchona Alkaloids in Synthesis & Catalysis*, Wiley-VCH Verlag GmbH, Weinheim **2009**, ISBN 978-3-527-32416-3.

[30] Shi, M.; Lei, Z. -Y.; Zhao, M. -X.; Shi, J. -W. *Tetrahedron Lett.* **2007**, *48*, 5743 - 5746.

[31] Dolling, U.-H.; Davis, P.; Grabowski, E. J. J. *J. Am. Chem. Soc.* **1984**, *106*, 446 - 447.

[32] O'Donnell, M. J.; Bennett, W. D.; Wu, S. *J. Am. Chem. Soc.* **1989**, *111*, 2353 - 2355.

[33] Kagan, H. B.; Riant, O. *Chem. Rev.* **1992**, *92*, 1007 - 1019.

[34] Jen, W.; Wiener, J.; MacMillan, D. W. C. *J. Am. Chem. Soc.* **2000**, *122*, 9874 - 9875.

[35] Paras, N.; MacMillan, D. W. C. *J. Am. Chem. Soc.* **2001**, *123*, 4370 - 4371.

[36] Austin, J. F.; MacMillan, D. W. C. *J. Am. Chem. Soc.* **2002**, *124*, 1172 - 1173.

[37] Brown, S. P.; Goodwin, N. C.; MacMillan, D. W. C. *J. Am. Chem. Soc.* **2003**, *125*, 1192 - 1194.

[38] Brochu, M. P.; Brown, S. P.; MacMillan, D. W. C. *J. Am. Chem. Soc.* **2004**, *126*, 4108 - 4109.

[39] Ouellet, S. G.; Tuttle, J. B.; MacMillan, D. W. C. *J. Am. Chem. Soc.* **2005**, *127*, 32 - 33.

[40] Kunz, R. K; MacMillan, D. W. C. *J. Am. Chem. Soc.* **2005**, *127*, 3240 - 3241.

[41] Beeson, T. D.; MacMillan, D. W. C. *J. Am. Chem. Soc.* **2005**, *127*, 8826 - 8828.

[42] (a) Singh, R.; Ghosh, S. K. *Tetrahedron* **2010,** *66*, 2284 - 2292. (b) Selkälä, S. A.; Koskinen, A. M. P. *Eur. J. Org. Chem.* **2005**, 1620 - 1624. (c) Kumpulainen, E. T. T.; Koskinen, A. M. P.; Rissanen, K. *Org. Lett.* **2007**, *9*, 5043 - 5045. (d) Jacobs, W. C.; Christmann, M. *Synlett.* **2008**,

247 - 251. (e) Voith, M.; Fröhlich, R.; Christmann, M. *Synlett.* 2007, 391 - 394. (f) Sun, B. -F.; Wang, C. -L.; Ding, R.; Xu, J. -Y.; Lin, G. -Q. *Tetrahedron Lett.* **2011**, *52*, 2155 - 2158**.** (g) Barykina, O. V.; Rossi, K. L.; Rybak, M. J.; Snider, B. B. *Org. Lett.* **2007**, *11*, 5334 - 5533. (h) Flores, B.; Molinski, T. F. *Org. Lett. 2011*, **13**, 3932 - 3935. (i) Fernandez, N.; Carillo, L.; Vicaio, J. L.; Badia, D.; Reyes, E. *Chem. Commun.* **2011**, 12313 - 12315.

[43] (a) Van Rhijn, W. M.; De Vos, D. E.; Sels, B. F. Bossaert,W. D.; Jacobs, P. A. *Chem. Commun*. **1998**, 317 - 318. (b) Maggi, R.; Raveendran, S. N.; Santacroce, Y.; Maestri, G.; *Beilstein J. Org. Chem.* **2016**, *12*, 2173 - 2180. (c) Sajjadifar, S.; Mansouri, G.; Miraninezhad, S. *Asian J. Nano. Sci. Mat.* **2018**, *1*, 9 - 15. (d) Du, Y.; Barber, T.; Lim, S. E.; Rzepa, H. S.; Baxendale I. R.; Whiting, A. *Chem. Commun.* **2019**, *55*, 2916 - 2919. (e) Rathod, P. B.; Kumar, K. S. A.; Athawale A. A.; Pandey, A. K.; Chattopadhyay S. *Eur. J. Org. Chem.* **2018**, 5980 - 5987. (f) Breslow, R. *Science* **1982**, *218*, 532 -537.

[44] (a) Regen, S. L. *J. Am. Chem. Soc.* **1975**, *97*, 5956 - 5057. (b) Regen, S. L. *J. Am. Chem. Soc.* **1976**, *98*, 6270 - 6274. (c) (34) Regen, S. L. *Angew. Chem., Int. Ed. Engl.* **1979**, *18*, 421 - 429.

[45] (a) Haraguchi, N.; Itsuno, S. in *Polymeric Chiral Catalyst Design and Chiral Polymer Synthesis* (Itsuno, S. Eid), Wiley, Hoboken, 2011, Chap. 2, pp. 17 - 61. (b) Kristensen, T. E. in *Comprehensive Enantioselective Organocatalysis* (Dalko, P. I. Eid.), Wiley-VCH, Weinheim, 2013, Chap. 23. (c) Altava, B.; Burguete, M. I.; Luis, S. V. in *The Power of Functional Resins in Organic Synthesis* (Puche, J. T.; Albricias, F. Eids.), Wiley-VCH, Weinheim, 2008, Chap. 10, pp. 247 - 308. (d) Kristensen, T. E.; Hansen, T. Eur. *J. Org. Chem.* **2010**, 3179 - 3204. (e) Cozzi, F. *Adv. Synth. Catal.* **2006**, *348*, 1367 - 1390.

[46] (a) Chinchila, R.; Mazón, P.; Nájera, C. *Tetrahedron: Asymmetry* **2000**, *11***,** 3277 - 3281. (b) Chinchila, R.; Mazón, P.; Nájera, C. *Adv. Synth. Catal.* **2004**, *346***,** 1186 - 1194.

[47] Denelli, T.; Annunziata, R.; Benaglia, M.; Cinquini, M.; Cozzi, F.; Tocco, G. *Tetrahedron: Asymmetry* **2003**, *14*, 46 - 467.

[48] Wang, X.; Yin, L.; Yang, T.; Wang, Y. *Org. Biomol. Chem*. **2007**, *5*, 406 - 430.

[49] Benaglia, M.; Celentano, G.; Cinquini, M.; Puglisi A.; Cozzi, F. *Adv. Synth. Catal*. **2002**, *344*, 149 - 152.

[50] S. A. Selkälä, J. Tois, P. M. Pihko, A. M. P. Koskinen, *Adv. Synth. Catal.* **2002**, *344*, 941 - 945.

[51] Zhang, Y.; Zhao, L.; Lee, S. S.; Ying, J. Y. *Adv. Synth. Catal.* **2006**, *348*, 2027 - 2032.

[52] Puglisi, A.; Benaglia, M.; Cinquini, M.; Cozzi F.; Celentano, G. Eur. *J. Org. Chem.* **2004**, 567 - 573.

[53] Kristensen, T. E.; Vestli, K.; M. Jakobsen, G.; Hansen F. K.; Hansen, T. J. *J. Org. Chem.* **2010**, *75*, 1620 - 1629.

[54] Wu, Y.; Zhang, Y.; Yu, M.; Zhao, G.; Wang, S. *Org. Lett.* **2006**, *8*, 4417 - 4420.

[55] (a) Gruttadauria, M.; Riela, S.; Aprile, C.; Lo Meo, P.; D'Anna, F.; Noto, R. *Adv. Synth. Catal.* **2006**, *348*, 82 - 92. (b) An, Z.; Zhang, W.; Shi, H.; He, J. *J. Catal*. **2006**, *241*, 319 - 327. (c) Vijaikumar, S.; Dhakshinamoorthy, A.; Pitchumani, K. *Appl. Catal., A* **2008**, *340*, 25 - 32.

[56] Mitsudome, T.; Nose, K.; Mizugaki, T.; Jitsukawa, K.; Kaneda, K. *Tetrahedron Lett. 2008 49*, 5464 - 5466.

[57] Hagiwara, H.; Kuroda, T.; Hoshi T.; Suzuki, T. Adv. *Synth. Catal.* **2010**, *352*, 909 - 916.

[58] Arakawa, Y.; Haraguchi, N.; Itsuno, S. *Angew. Chem. Int. Ed.* **2008**, *47*, 8232 - 8235.

[59] Haraguchi, N.; Takemura Y.; Itsuno, S. *Tetrahedron Lett.* **2010**, *51*, 1205 - 1208.

[60] Haraguchi, N.; Kiyono, H.; Takemura, Y.; Itsuno, S. *Chem. Commun.* **2012**, *48*, 4011 - 4013.

[61] Itsuno, S.; Oonami, T.; Takenaka, N.; Haraguchia, N. *Adv. Synth. Catal.* **2015**, *357*, 3995 - 4002.

[62] Haraguchi, N.; Nguyen, T. L.; Itsuno, S. *ChemCatChem* **2017**, *9*, 3786 - 3794.

[63] Haraguchi, N.; Takenaka, N.; Najwa, A.; Takahara, Y.; Kar Mun, M.; Itsuno. S. *Adv. Synth. Catal.* **2018**, *360*, 112 - 123.

[64] (a) Li, X.; Yang, B.; Zhang, S.; Jia, X.; Hu, Z. *Colloid. Polym. Sci.* **2017**, *295*, 573 - 582. (b) Haraguchi, N.; Nishiyama, A.; Itsuno, S. *J. Polym. Sci. Part A: Polym. Chem.* **2010**, *48*, 3340 - 3349.

[65] Li, W. H.; Stöver. H. D. H. *J. Polym. Sci. Part A: Polym. Chem.* **1998**, *36*, 1543 - 1551.

[66] Perrier-Cornet, R.; Héroguez, V.; Thienpont, A.; Babot, O.; Toupance, T. *J. Chromatogr. A* **2008**, *1179*, 2 - 8.

[67] Li, K.; Stöver, H. D. H. *J. Polym. Sci. Polym. Chem. Ed.* **1993**, *31*, 3257 - 3263.

[68] Koprinarov, I.; Hitchcock, A. P.; Li, W. H.; Heng, Y. M.; Stöver, H. D. H. *Macromolecules* **2001**, *34*, 4424 - 4429.

[69] (a) Zheng, G.; Stöver, H. D. H. *Macromolecules* **2002**, *35*, 6828 - 6834.
(b) Zheng, G.; Stöver, H. D. H. *Macromolecules* **2002**, *35*, 7612 - 7619.

[70] (a) Zheng, G.; Stöver, H. D. H. *Macromolecules* **2003**, *36*, 1808 - 1814. (b) Zheng, G.; Stöver, H. D. H. *Macromolecules* **2003**, *36*, 7439 -7445. (c) Zhang, M.; Liu, L.; Wu, C.; Fu, G.; Zhao, H.; He, B. *Polymer* **2007**, *48*, 1989 – 1997.

[71] (a) Holderle, M.; Baumert, M.; Mulhaupt, R. *Macromolecules* **1997**, *30*, 3420 - 3422. (b) Gabaston, L. I.; Jackson, R. A.; Armes, S. P. *Macromolecules* **1998**, *31*, 2883 - 2888. (c) Song, J. S.; Winnik, M. A. *Macromolecules* **2006**, *39*, 8318 - 8325. (d) Min, K.; Matyjaszewski, K. *Macromolecules* **2007**, *40*, 7217 - 7222. (e) Sugihara, S.; Sugihara, K.; Armes, S. P.; Ahmad, H.; Lewis, A. L. *Macromolecules* **2010**, *43*, 6321 - 6329. (f) Shim, S. E.; Jung, H.; Lee, H.; Biswas, J.; Choe, S. *Polymer* **2003**, *44*, 5563 - 5572. (g) Ki, B.; Yu, Y. C.; Jeon, H. J.; Yu, W.-R.; Ryu, H. W.; Youk, J. H. *Fibers Polym.* **2012**, *13*, 135 - 138. (h) Warren, N. J.; Armes, S. P. *J. Am. Chem. Soc*. **2014**, *136*, 10174 - 10185. (i) Oh, J. K.; Tang, C.; Gao, H.; Tsarevsky, N. V.;

Matyjaszewski, K. *J. Am. Chem. Soc.* **2006**, *128*, 5578–5584. (j) Zheng, G.; Pan, C. *Macromolecules* **2006**, *39*, 95 - 102. (k) Wan, W.; Pan, C. *Macromolecules* **2007**, *40*, 8897 - 8905. (l) An, Z.; Shi, Q.; Tang, W.; Tsung, C. K.; Hawker, C. J.; Stucky, G. D. *J. Am. Chem. Soc.* **2007**, *129*, 14493 - 14499. (m) Thurecht, K. J.; Gregory, A. M.; Wang, W.; Howdle, S. M. *Macromolecules* **2007**, *40*, 2965 - 2967. (n) Grignard, B.; Jérôme, C.; Calberg, C.; Jérôme, R.; Wang, W.; Howdle, S. M.; Detrembleur, C. *Macromolecules* **2008**, *41*, 8575 - 8583. (o) Min, K.; Gao, H.; Yoon, J. A.; Wu, W.; Kowalewski, T.; Matyjaszewski, K. *Macromolecules* **2009**, *42*, 1597 - 1603. (p) Shen, W.; Chang, Y.; Liu, G.; Wang, H.; Cao, A.; An, Z. *Macromolecules* **2011**, *44*, 2524 - 2530.

[72] (a) Zu, B.; Pan, G.; Guo, X., Zhang H. *J. Polym. Sci. Part A: Polym. Chem.* **2009**, *47*, 3257 - 3270. (b) Jiang, J.; Zhang, Y.; Guo, X.; Zhang, H. *Macromolecules* **2011**, *44*, 5893 - 5904. (c) Jiang, J.; Zhang, Y.; Guo X.; Zhang. H. *RSC Advances* **2012**, *2*, 5651 - 5662. (d) Fang, L.; Chen, S.; Guo, X.; Zhang, Y.; Zhang, H. *Langmuir* **2012**, *28*, 9767 - 9777.

[73] Li, J.; Zu, B.; Zhang, Y.; Guo, X.; Zhang, H. *J. Polym. Sci. Part A: Polym. Chem.* **2010**, *48*, 3217 - 3228.

[74] (a) Zhang, Y.; Zhang, H. *Chin. J. React. Polym.* **2008**, *17*, 1 - 11. (b) Pan, G.; Zu, B.; Guo, X.; Zhang, Y.; Li, C.; Zhang, H. *Polymer* **2009**, *50*, 2819 - 2825. (c) Pan, G.; Zhang, Y.; Guo, X.; Li, C.; Zhang, H. *Biosens. Bioelectron.* **2010**, *26*, 976 - 982. (d) Pan, G.; Ma, Y.; Zhang, Y.; Guo, X.; Li, C.; Zhang, H. *Soft Matter* **2011**, *7*, 8428 - 8439. (e) Pan, G.; Zhang, Y.; Ma, Y.; Li, C.; Zhang, H. *Angew. Chem. Int. Ed.* **2011**, 50, 11731 - 11734. (f) Ma, Y.; Zhang, Y.; Zhao, M.; Guo, X.; Zhang, H. *Chem. Commun*. **2012**, *48*, 6217 - 6219. (g) Ma, Y.; Zhang, Y.; Zhao, M.; Guo. X.; Zhang, H. *Mol. Imprinting* **2012**, 3 - 16.

[75] (a) Lindenblatt, G.; Schartl, W.; Pakula, T.; Schmidt, M. *Macromolecules* **2000**, *33*, 9340 - 9347. (b) Zhu, M. Q.; Wang, L. Q.; Exarhos, G. J.; Li, A. D. Q. *J. Am. Chem. Soc.* **2004**, *126*, 2656 - 2657.

[76] (a) Pyun, J.; Kowalewski, T.; Matyjaszewski, K. Macromol. *Rapid Commun.* **2003**, *24*, 1043 - 1059. (b) Mandal, T. K.; Fleming, M. S.; Walt, D. R. *Nano Lett.* **2002**, *2*, 3 - 7. (c) Sill, K.; Emrick, T. *Chem. Mater.* **2004**, *16*, 1240 - 1243. (d) Kickelbick, G.; Holzinger, D.; Brick, C.; Trimmel, G.; Moons, E. *Chem. Mater*. **2002**, *14*, 4382 - 4389. (e) Vestal, C. R.; Zhang, Z. *J. Am. Chem. Soc.* **2002**, *124*, 14312 - 14313.

[77] Henze, M.; Mädge, D.; Prucker, O.; Rühe J. *Macromolecules* **2014**, *47*, 2929 - 2937.

[78] Xu, F.; Neoh, K.; Kang, *E. Prog. Polym. Sci.* **2009**, *34*, 719 - 761.

[79] Otsu, T. *J. Polym. Sci. Part A: Polym. Chem.* **2000**, *38*, 2121 - 2136.

[80] Hawker, C. J.; Bosman, A. W.; Harth, E. *Chem. Rev*. **2001**, *101*, 3661 - 3688.

[81] (a) Matyjaszewski, K.; Xia, J. *Chem. Rev.* **2001**, *101*, 2921 - 2990. (b) Kamigaito, M.; Ando, T.; Sawamoto, M. *Chem. Rev.* **2001**, *101*, 3689 - 3745. (c) Percec, V.; Barboiu, B. *Macromolecules* **1995**, *28*, 7970 - 7972.

[82] (a) Mcleary, J. B.; Klumperman, B. *Soft Matter*. **2006**, *2*, 45 - 53. (b) Lowe, A. B.; McCormick, C. L. *Prog. Polym. Sci.* **2007**, *32*, 283 - 351. (c) Moad, G.; Rizzardo, E.; Thang, S. H. *Polymer* **2008**, *49*, 1079 - 1131.

[83] Huang, X. Y.; Wirth, M. *J. Anal. Chem.* **1997**, *69*, 4577 - 4580.

[84] Ejaz, M.; Yamamoto, S.; Ohno, K.; Tsujii, Y.; Fukuda, T. *Macromolecules* **1998**, *31*, 5934 - 5936.

[85] (a) Zou, H.; Wu, S.; Shen, J. *Chem. Rev.* **2008**, *108*, 3893 - 3957. (b) Wu, L.; Glebe, U.; Boöker, A. *Polym. Chem.* **2015**, *6*, 5143 - 5184. (c) Wu, L.; Glebe, U.; Böker, A. *Macromolecules* **2016**, *49*, 9586 - 9596. (d) Ohno, K.; Morinaga, T.; Koh, K.; Tsujii, Y.; Fukuda, T. *Macromolecules* **2005** *38*, 2137 - 2142. (e) Wu, T.; Zhang, Y.; Liu, S. *Chem. Mater.* **2008,** *20*, 101 - 109.

CHAPTER II

Synthesis of Polymer Microsphere Functionalized with Benzyl Halide Moiety by Precipitation Polymerization

2.1 Introduction

Functional polymer microspheres play an important role in a variety of industrial areas such as medicines, paints, adhesives, cosmetics, and electronics.[1–4] To develop a variety of functional polymeric particles, the surface modification and the control of morphology, as well as the size control and the narrow size distribution, are significant. These polymer particles can be directly prepared using functional monomers by heterogeneous polymerization techniques such as emulsion polymerization,[5] dispersion polymerization,[6] suspension polymerization,[7] and precipitation polymerization. They can also be obtained by another method where the surface modification of existing polymer microspheres is required. These particles may be colloidally stabilized by electrostatic, steric, and electrostatic forces. In precipitation polymerization, steric stabilization through a self-renewing surface gel layer can prevent coagulation of particles and can lead to stabilizer-free, narrow-disperse spherical functional polymer microspheres with controllable surface chemistry. They have many characteristic features, including large specific surface area, high mobility, high mechanical strength, easy recovery from the dispersion and reversible dispersibility, etc. These features can be utilized for the exhibition of the functions of polymer microspheres. Optical and optoelectrical functions of these polymer particles have also been attracted much attention.

Among the diverse heterogeneous polymerization techniques, suspension, emulsion, and dispersion polymerizations have played important roles in industrial production. The suspension polymerization involves well-dispersed liquid monomer droplets in an aqueous system with a steric stabilizer and vigorous stirring to yield the polymer particles as a dispersed solid phase. It is challenging to control the size uniformity of the polymer particles because a dynamic process control influences such an approach. Steric stabilizers like poly(*N*-vinylpyrrolidone) (PVP) must be utilized to stabilize the polymer microspheres and prevent them from coagulation. Emulsion polymerization starts in micelles, resulting in the colloidal latex particles stabilized by (micelle forming) surfactants. Later in the process, the surfactant molecules also supply electrostatic stabilization. This process usually utilizes water-soluble initiators and is most suitable for water-insoluble monomers. Dispersion polymerization begins from a homogeneous solution of all the starting materials (i.e., the monomer, initiator, and stabilizer). In contrast, the polymer microspheres precipitate out during the progress of the polymerization. Accordingly, this polymerization should be carried out in good solvents for the monomers but poor solvents for the polymer particles being formed. Also, in dispersion polymerization, steric stabilizers

like PVP or poly(vinyl alcohol) (PVA) must be utilized to stabilize the polymer microspheres and prevent them from aggregation. For all these processes, the complete removal of the surfactant or stabilizer from the resultant polymer particles is very difficult. It can lead to problems for obtaining clean and smooth surfaces, which may be difficult to apply in some fields.

Precipitation polymerization has been unique for the synthesis of monodisperse functional polymer micro-/nanospheres because of its easy experimental setup and no need for any surfactants or stabilizers.[8-33] This technique starts as a homogeneous mixture of the monomer(s), initiator, and solvents. The polymer microspheres are formed *via* polymerization of the monomers/crosslinkers and precipitate out from the homogeneous solution. During the polymerization, the growing polymer chains precipitate from the continuous medium by enthalpic precipitation or entropic precipitation, in those cases where cross-linking prevents the polymer and solvent from mixing.[26] Even though the combination of monomer and solvent is quite limited and the yield of resulting polymer particle is moderate, precipitation polymerization can afford narrowly dispersed spherical polymer microspheres. In addition, the diameter of polymer microspheres can be controlled by the monomer concentration, molar ratio of crosslinker, and the initiator concentration.

Initially, this technique did not attract much attention due to the difficulty in controlling the polymer particle uniformly[9]. Stöver and coworkers have established precipitation polymerization of divinylbenzene (DVB)[10-13]. The technique is expanded to the copolymerization of chloromethylstyrene (4-vinylbenzyl chloride),[14] maleic anhydride,[15,16], or methacrylic monomers[17] with DVB as a precise synthetic method for preparing narrowly disperse polymer microspheres[10-17]. The precipitation polymerization was carried out by using DVB or functional monomers with DVB below 5 vol% in acetonitrile, mixtures of acetonitrile and toluene, or mixtures of methyl ethyl ketone (MEK) and heptane, by free radical polymerization using AIBN as an initiator. They found that the particles increase in size by a reactive growth mechanism (also called entropic precipitation mechanism)[12,16] in which soluble oligomeric radicals are captured from solution by reaction with surface double bonds on existing particles (Scheme 2.1). The captured oligomers on the surface swell in the reaction medium and provide

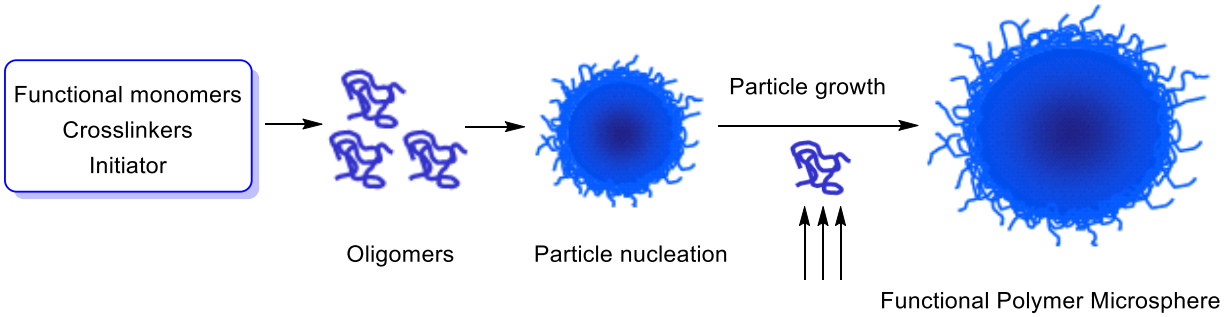

Scheme 2.1 Synthesis of functional polymer microsphere by precipitation polymerization.

steric stabilization,[17] by forming a solvated gel layer on the particle surface. Such a transient gel layer prevents inter-particle coagulation and at the same time, continues to crosslink, and desolvate until it transforms into microspheres. Nearly monodisperse, spherical particles can be routinely prepared in good yield by this method, and tuning the size and porosity of the resulting particles can be achieved via the polymerization conditions.

Stöver et al. also reported the synthesis of monodisperse crosslinked core-shell polymer microspheres by two-stage precipitation polymerization in which multifunctional groups were introduced into the shell of poly(DVB) microspheres.[27] Distillation precipitation polymerization was reported in 2004 by Yang's group to synthesize monodisperse polymer microspheres with various functional groups, core-shell polymer microspheres, inorganic/polymer core-shell composite/hybrid microspheres, and multilayer structured microspheres.[28] In the distillation precipitation polymerization, the solvent is partially distilled out during the polymerization. The main difference between the normal precipitation polymerization and distillation precipitation is the agitation of the polymerization system. Precipitation polymerization is performed by rolling the reaction system on a shaking-bed or a rotary-evaporator equipment in the lab. Distillation precipitation polymerization is carried out via distilling part of the solvent out of the polymer nano-/microspheres and bumping. Photo-initiated precipitation polymerization was subsequently developed by Irgum's group in 2007 for the synthesis of monodisperse poly(DVB) particles with AIBN as UV-initiator in acetonitrile.[29] UV initiation allowed the polymerization to proceed at or below room temperature to minimize temperature-dependent side reactions, such as chain transfer.[30] Two recent reviews cover microspheres with complex internal structures prepared by precipitation polymerization.[31,32]

Functional polymer microspheres were widely used in different fields, including separation resins, drug delivery systems, and microreactors. R. Perrier-Cornet et al. reported the synthesis of narrow dispersed crosslinked poly(4-vinylbenzyl chloride (VBC)) particles by precipitation polymerization with a porous structure that was used as a stationary phase in high-performance liquid chromatography.[33]

In this Chapter, monodisperse polymer microspheres having benzyl halide moiety were synthesized by the precipitation polymerization of various comonomers (styrene, methyl methacrylate (MMA), or 2-hydroxyethyl methacrylate (HEMA)), DVB with VBC as a dual functional monomer using AIBN as an initiator in acetonitrile or mixtures of acetonitrile and toluene. In the synthesis of these microspheres, the effect of comonomers and the molar ratio of monomers on the diameter and dispersity were investigated. These polymer microspheres can be used as macroinitiators without further modifications in surface-initiated atom transfer radical polymerization (SI-ATRP). Besides, the benzyl halide moiety in these polymer particles can also be reacted with primary, secondary, and tertiary amines, and other

nucleophiles, resulting in the synthesis of hydrophilic and biocompatible polymer particles. These polymer microspheres were characterized by FT-IR, optical microscope, and SEM.

2.2 Results and Discussion

2.2.1 Synthesis of monodisperse poly(DVB-St-VBC) microspheres with benzyl chloride moiety ***1d$_x$sC$_z$*** *by precipitation polymerization*

A series of poly(DVB-St-VBC) microspheres having benzyl chloride moiety **1d$_x$sC$_z$** was prepared by the precipitation polymerization of styrene, DVB, and VBC with AIBN in CH_3CN as illustrated in

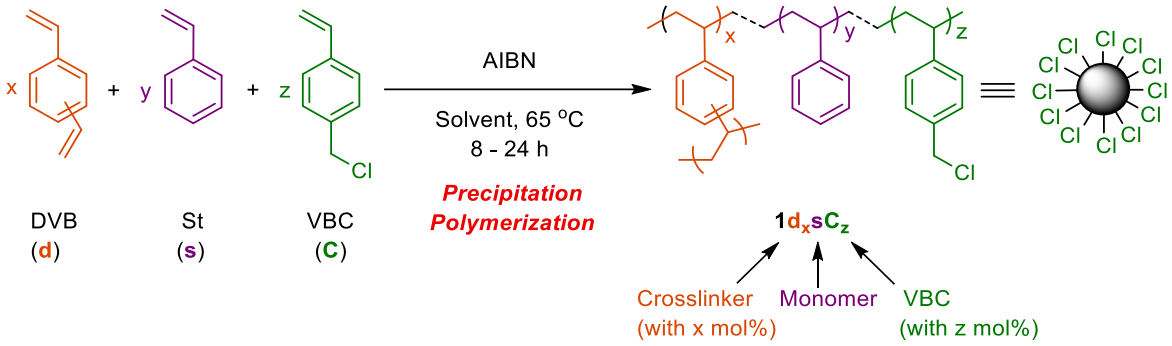

Scheme 2.2 Synthesis of polymer microsphere having benzyl chloride moiety **1d$_x$sC$_z$** by precipitation polymerization.

Table 2.1 Characterization of polymer microsphere having benzyl chloride moiety **1d$_x$sC$_z$**[a].

Entry	Polymer Microsphere	Time (h)	Yield (%)	D_n (μm)[b]	U (D_w/D_n)[b]	Cl Content (mmol g^{-1})[c]		Cl density (nm^{-3})
						Cl_{calcd}	$Cl_{measured}$	
1	**1d$_{20}$sC$_5$**	24	26	2.95	1.02	0.451	0.566	0.34
2	**1d$_{20}$sC$_{10}$**	12	14	2.94	1.00	0.880	0.910	0.55
3	**1d$_{20}$sC$_{10}$**	24	26	3.96	1.01	0.884	0.978	0.59
4	**1d$_{20}$sC$_{20}$**	8	8	2.94	1.00	1.68	1.64	0.99
5	**1d$_{20}$sC$_{20}$**	24	24	4.40	1.02	1.69	1.68	1.0
6	**1d$_{20}$sC$_{20}$**	48	37	5.86	1.00	1.68	1.69	1.0
7[d]	**1d$_{20}$sS$_{30}$**	24	-	-	-	n.d	n.d	n.d
8[d,e]	**1d$_{20}$sS$_{30}$**	24	12	5.08	1.25	1.04	0.391	n.d

[a] All the polymerizations were performed in CH_3CN at 65 °C using 4.3 wt% monomers relative to the reaction medium and 2 wt% AIBN relative to the total monomers.

[b] Measured from SEM images.

[c] Determined by titrimetric method.

[d] ATRP initiator system (BnBr/CuBr/2,2′-bipyridine) was used instead of AIBN. **S**: Phenyl *p*-styrenesulfonate.

[e] ATRPP was carried out using 8.0 wt% monomers relative to the reaction medium.

Scheme 2.2. The molar ratio of DVB was set to 20 mol%, and that of VBC was changed to 5, 10, and 20 mol%, respectively. The precipitation polymerization proceeded as expected, and micron-sized polymer particle was successfully obtained. These characterizations were summarized in Table 2.1. The isolated yield was relatively low (8%-26%) due to the minimum molar ratio of DVB to form a micro-sized particle was used.[10] When the molar ratio of DVB is increased, the yield can be increased. Monodisperse spherical polymer particles could be synthesized regardless of the VBC molar ratio by the precipitation polymerization. We found that a high VBC molar ratio resulted in the increase of particle diameter when the polymerization time was constant (entry 5). For the synthesis of the polymer microspheres with the same diameter (ca. 3.0 μm) and different benzyl halide content (**1d$_x$sC$_z$**), the polymerization time was adjusted. Unfortunately, polymer microsphere was not obtained when ATRP initiator, that is, BnBr/CuBr/bipyridine instead of AIBN was used loading 4.0 wt% of monomers relative to acetonitrile in the precipitation polymerization. Polymer microsphere was formed when atom transfer radical polymerization (ATRP) was carried out using 8.0 wt% of monomer concentration in the precipitation polymerization where particle was somewhat aggregated.

From these SEM photographs of **1d$_x$sC$_z$**, spherical and uniform microspheres were successfully obtained (Figure 2.1a, b and c). The number averaged diameters (D_n) measured from SEM images, and

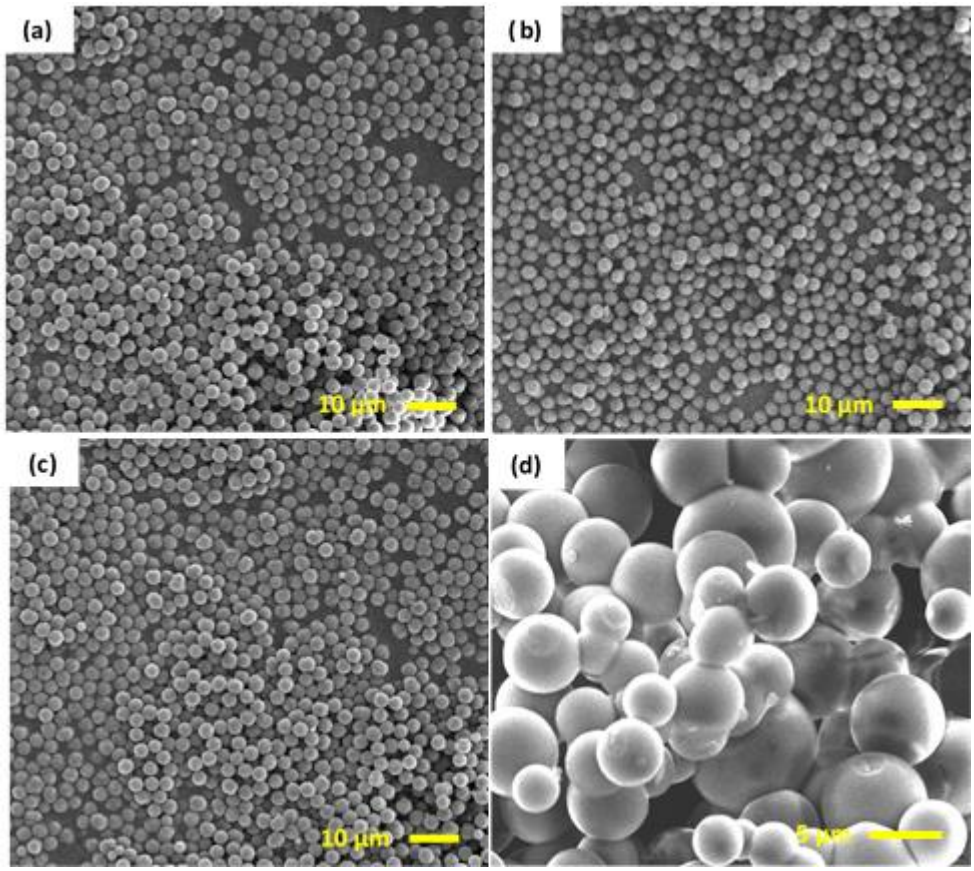

Figure 2.1 SEM images of **1d$_x$sC$_z$**: **1d$_{20}$sC$_5$** (a), **1d$_{20}$sC$_{10}$** (b), **1d$_{20}$sC$_{20}$** (c), and **1d$_{20}$sS$_{30}$** (d).

polydispersity indexes (*U*) are 2.95 μm and 1.02 for **1d$_{20}$sC$_5$**, 2.94 μm and 1.00 for **1d$_{20}$sC$_{10}$**, and 2.94 μm and 1.00 for **1d$_{20}$sC$_{20}$**, respectively. D_n of **1d$_{20}$sC$_{20}$** was increased when the polymerization time was increased (entry 6). From the FT-IR spectra of **1d$_x$sC$_z$**, the characteristic C−Cl absorption peak at 1265 cm^{-1} derived from benzyl chloride moiety was observed (Figure 2.2). The intensity of the absorption peak for the C−Cl bond increased with increasing of the VBC contents in **1d$_x$sC$_z$**. The chlorine content in **1d$_x$sC$_z$** determined by a titrimetric method was increased with the increase of VBC molar ratio. These measured chlorine contents were close to those calculated based on the molar ratio of monomers. Chlorine densities calculated from the chlorine content were in the range from 0.34 to 1.0 nm^{-3}. These results indicate that monodisperse **1d$_x$sC$_z$** with the same diameter, but with different molar ratio of benzyl chloride moiety were successfully prepared by the precipitation polymerization.

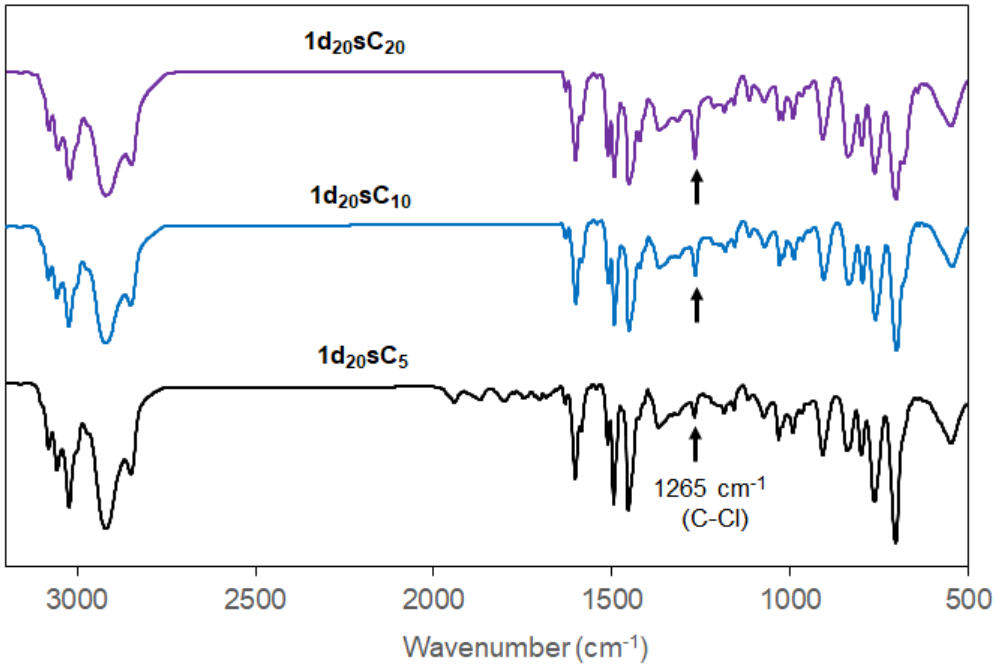

Figure 2.2 FT-IR spectra of **1d$_x$sC$_z$**.

*2.2.2 Synthesis of polymer microspheres having benzyl chloride moiety **1d$_x$yC$_z$** by precipitation polymerization of various comonomers (**y**), divinylbenzene (DVB (**d**)) and 4-vinylbenzyl chloride (VBC (**C**))*

To check the effect of comonomer, polymer microsphere having benzyl chloride moiety **1d$_x$yC$_z$** was synthesized by the precipitation polymerization of 60 mol% of comonomer (styrene, methyl methacrylate (MMA), or 2-hydroxyethyl methacrylate (HEMA)), 20 mol% of divinylbenzene (DVB) with 20 mol% of 4-vinylbenzyl chloride (VBC) as illustrated in Scheme 2.3. The molar ratio of DVB and VBC was kept fixed, and that of the comonomer was changed from St to HEMA with a constant molar ratio. The characterizations of **1d$_x$yC$_z$** were summarized in Table 2.2. For the synthesis of polymer microspheres with the same diameter (Ca. 1.0 μm), the polymerization time was adjusted. The isolated

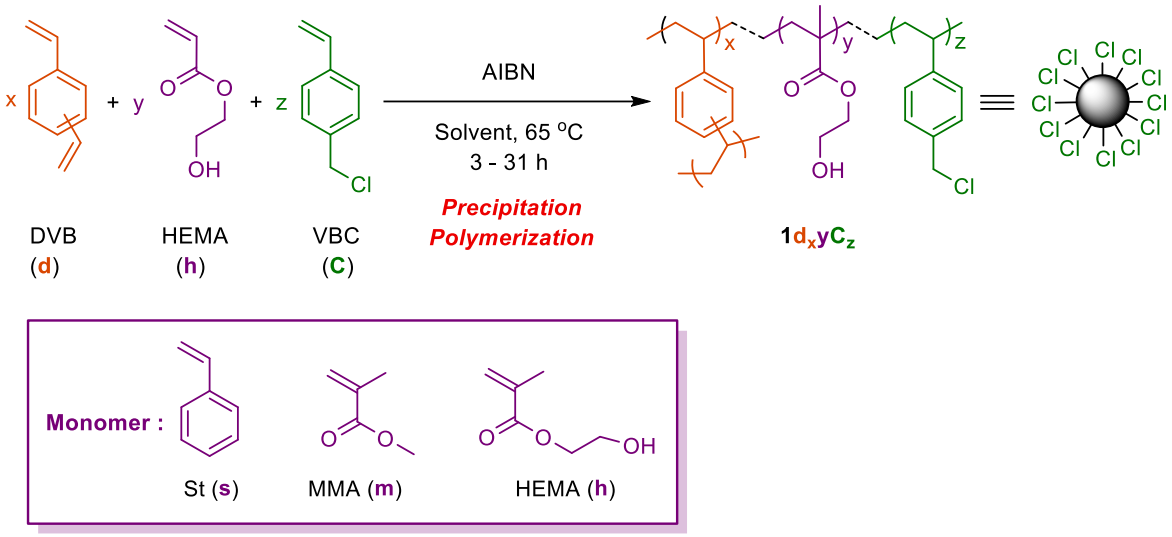

Scheme 2.3 Synthesis of polymer microsphere having benzyl chloride moiety **1d$_x$yC$_x$** by precipitation polymerization.

Table 2.2 Characterization of polymer microsphere having benzyl chloride moiety **1d$_x$yC$_z$**[a].

Entry	Polymer Microsphere	Time (h)	Yield (%)	D_n (μm)[b]	U (D_w/D_n)[b]	Cl Content (mmol g^{-1})[c]	
						Cl_{calcd}	$Cl_{measured}$
1	**1d$_{20}$sC$_{20}$**	3	3	1.14	1.00	1.68	1.67
2	**1d$_{20}$sC$_{20}$**	24	24	4.41	1.00	1.69	1.68
3	**1d$_{20}$mC$_{20}$**	2	4	1.12	1.00	1.71	1.76
4	**1d$_{20}$mC$_{20}$**	24	28	9.14	1.01	1.73	1.80
5[d]	**1d$_{20}$hC$_{20}$**	24	24	0.80	1.14	1.49	1.56

[a] All the polymerizations were performed in CH_3CN at 65 °C using 4.3 wt% monomers relative to the reaction medium and 2 wt% AIBN relative to the total monomers.

[b] Measured from SEM images.

[c] Determined by titrimetric method.

[d] CH_3CN:Toluene = 9:1 was used as a solvent.

yield was relatively low (3-24%). The number-averaged diameters (D_n) measured from SEM photographs were 1.14 μm for **1d$_{20}$sC$_{20}$**, 1.12 μm for **1d$_{20}$mC$_{20}$**, and 0.80 μm for **1d$_{20}$hC$_{20}$**, respectively (Figure 2.3a, c and e). D_n of **1d$_{20}$sC$_{20}$** and **1d$_{20}$mC$_{20}$** were increased with 4.41 μm and 9.14 μm, respectively (Figure 2.3b and d) when the polymerization time was constant. When HEMA was used as a comonomer, a smaller microsphere was obtained compared to styrene or MMA at constant polymerization time (entry 5). The distributions (D_w/D_n) were narrow being in the range of 1.00 and 1.14. Chlorine contents in **1d$_x$yC$_z$** determined by titrimetric were in good agreement with calculated ones. In the FT-IR spectra of **1d$_x$yC$_z$**, the characteristic FT-IR band was appeared at 1265 cm^{-1} due to the C–Cl bond (Figure 2.4). The strong peaks were found at 1602, 1509, 1451 cm^{-1} and 3059, 3024 cm^{-}

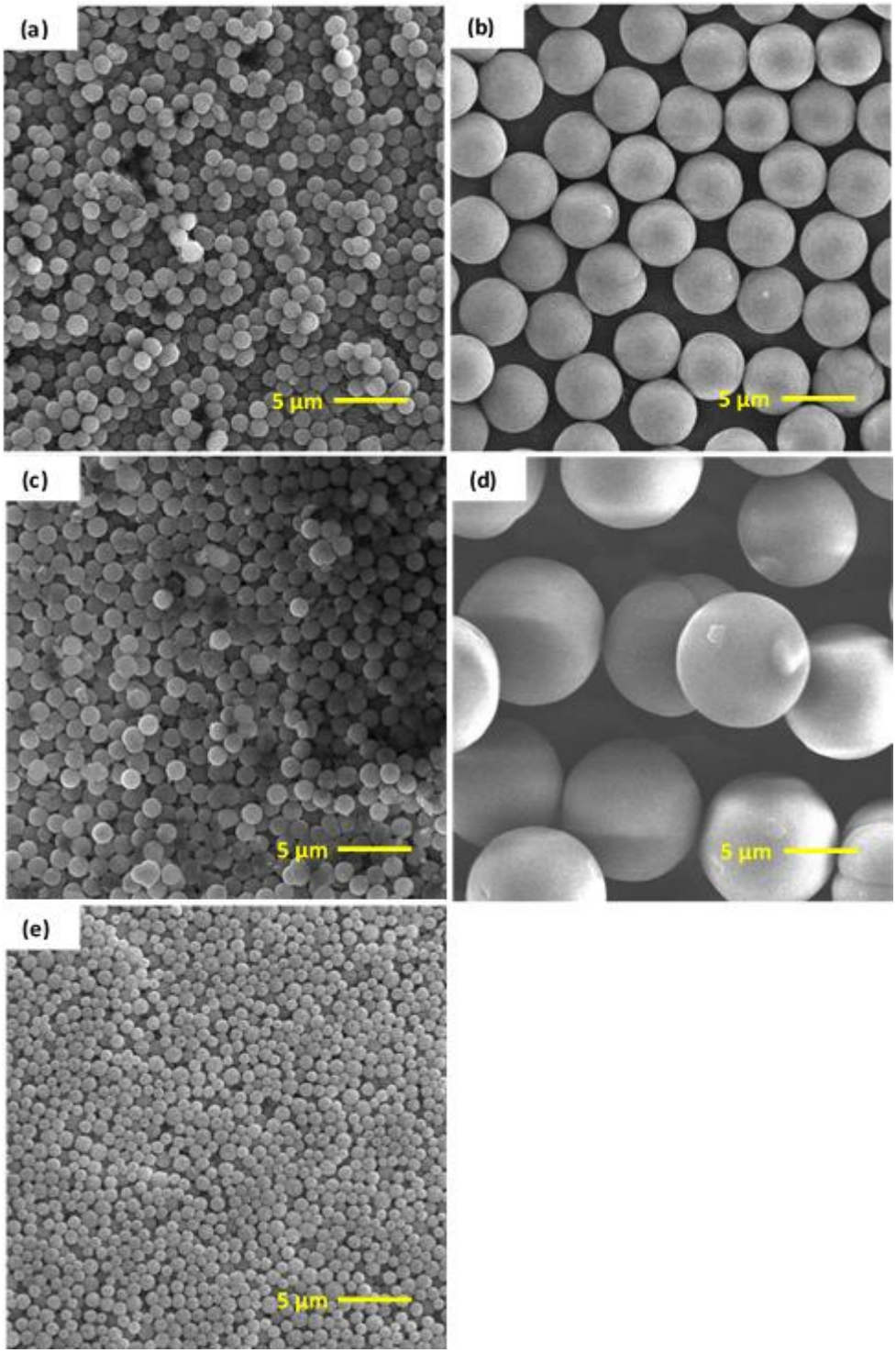

Figure 2.3 SEM images of $\mathbf{1d_xyC_z}$: $\mathbf{1d_{20}sC_{20}}$ (a), $\mathbf{1d_{20}sC_{20}}$ (b) (entry 2), $\mathbf{1d_{20}mC_{20}}$ (c), $\mathbf{1d_{20}mC_{20}}$ (d) (entry 4), and $\mathbf{1d_{20}hC_{20}}$ (e).

[1] due to C=C and C−H bonds in the aromatic ring of $\mathbf{1d_{20}sC_{20}}$, respectively. The stretching absorption frequency of the C=O bond was observed at 1728 and 1720 cm^{-1} in $\mathbf{1d_{20}mC_{20}}$ and $\mathbf{1d_{20}hC_{20}}$, respectively. A broad peak for O-H in $\mathbf{1d_{20}hC_{20}}$ was observed at 3446 cm^{-1}.

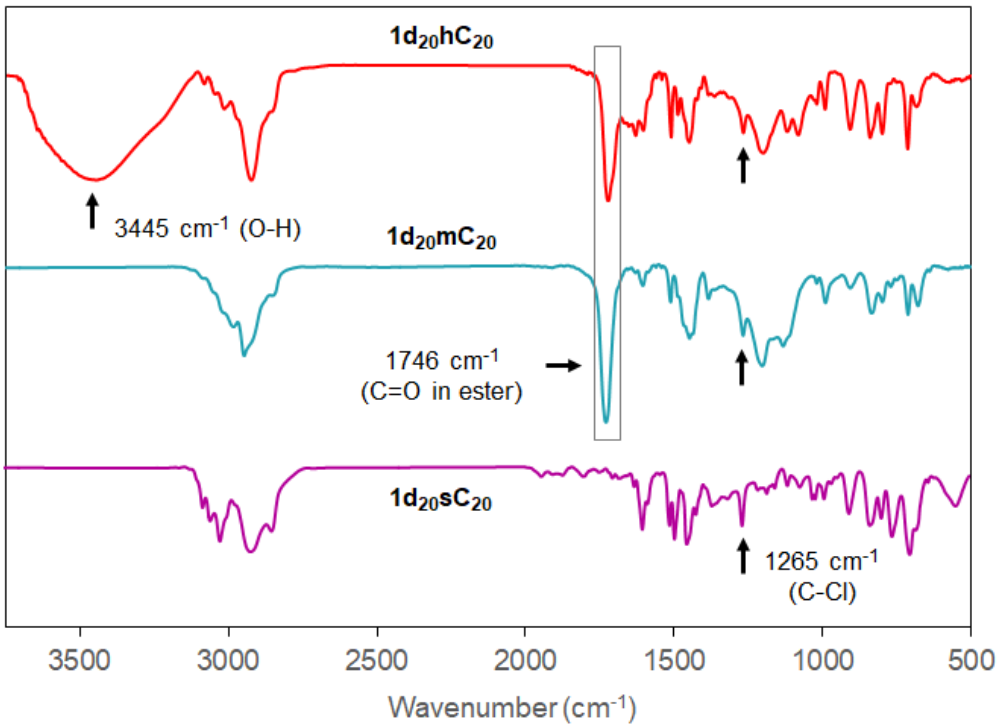

Figure 2.4 FT-IR spectra of **1d$_x$yC$_z$** (**y = s, m, h**).

Table 2.3 Characterization of polymer microsphere having benzyl chloride **1d$_x$hC$_z$**[a].

Entry	**1d$_x$hC$_z$** **x/z**	Time (h)	Yield (%)	D_n (μm)[b]	U (D_w/D_n)[b]	Cl Content (mmol g^{-1})[c]	
						Cl_{calcd}	$Cl_{measured}$
1	**20/5**	8	12	1.07	1.03	0.38	0.51
2	**20/10**	11	17	1.41	1.07	0.75	0.88
3	**20/20**	24	24	0.80	1.14	1.49	1.56
4	**20/30**	31	29	1.11	1.04	2.19	2.11
5	**30/20**	19	28	0.94	1.04	1.49	1.38
6	**40/20**	6	6	1.45	1.00	1.48	1.37
7	**50/20**	4	4	2.20	1.34	1.48	1.47
8	**20/20-BPO**[d]	24	40	2.00	1.05	1.38	1.49

[a] All the polymerizations were performed in CH_3CN:Toluene = 9:1 at 65 °C using 4.3 wt% monomers relative to the reaction medium and 2 wt% AIBN relative to the total monomers.

[b] Measured from SEM images.

[c] Determined by titrimetric method.

[d] Benzoyl peroxide (BPO) was used instead of AIBN.

A series of poly(DVB-HEMA-VBC) microspheres **1d$_x$hC$_z$** was then synthesized with different monomer ratios by precipitation polymerization (Scheme 2.4). The molar ratio of DVB was set to 20 mol%, and that of VBC was changed to 5, 10, 20, and 30 mol%, respectively (Cl series: **1d$_{20}$hC$_z$**). In

addition, the VBC ratio was constant at 20 mol%, and that of DVB was changed to 20, 30, 40, and 50 mol%, respectively (DVB series: **1d$_x$hC$_{20}$**). The characterization data were summarized in Table 2.3. In

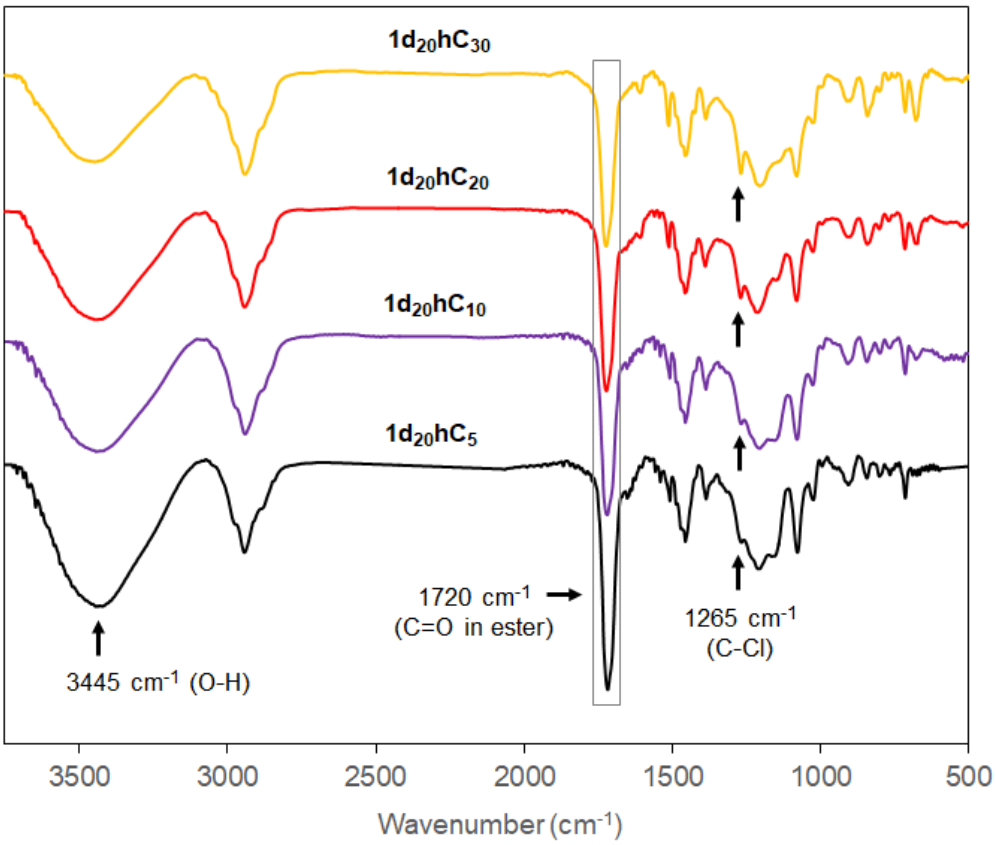

Figure 2.5 FT-IR spectra of **1d$_{20}$hC$_z$ (Cl series)**.

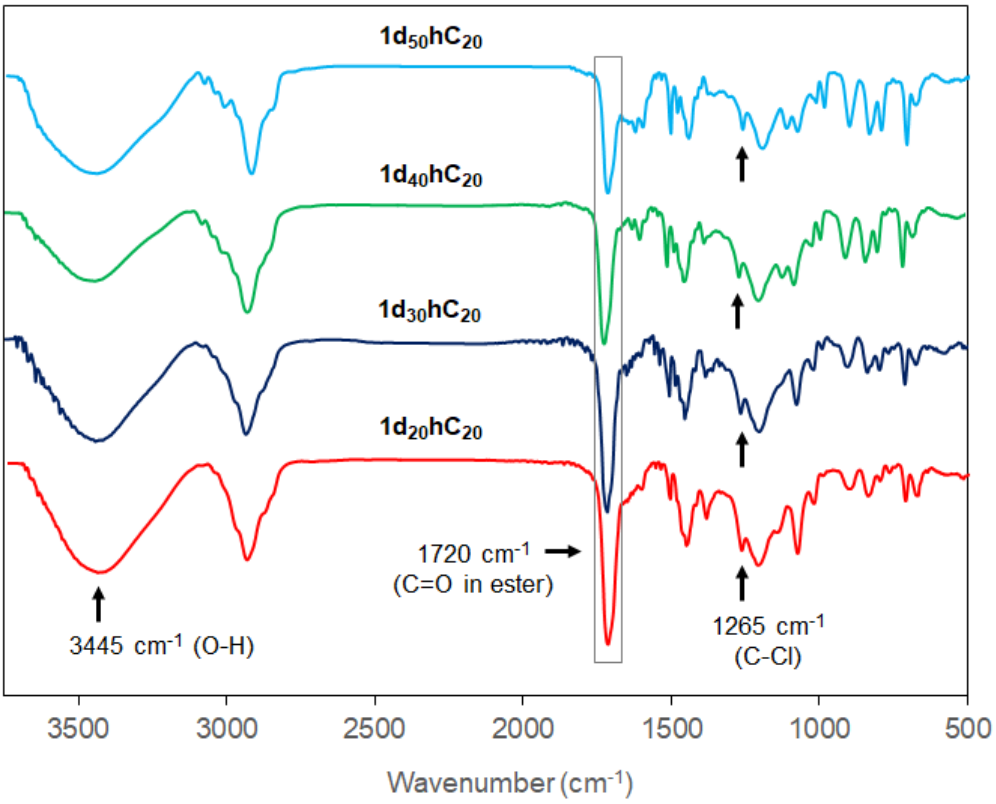

Figure 2.6 FT-IR spectra of **1d$_x$hC$_{20}$ (DVB series)**.

the Cl series, the particle growth rate was decreased with increasing Cl content at constant DVB, whereas the rate was increased with increasing DVB content at constant VBC in DVB series. D_n of **1d$_{20}$hC$_{20}$** synthesized using benzoyl peroxide (BPO) instead of AIBN as an initiator was 2.00 μm with a polydispersity index being 1.05 (entry 8). The use of BPO instead of AIBN as an initiator gave **1d$_x$hC$_z$** with larger D_n. The D_n for **1d$_x$hC$_z$** were in the range of 0.80 and 2.20 μm, and these distributions were relatively narrow. FT-IR spectra of **1d$_x$hC$_z$** exhibited that both absorption peaks assigned to stretching vibration of C−Cl and C=O bonds. In the case of **1d$_{20}$hC$_z$** (Cl series), the peak intensity of C−Cl bond is increased with increasing of z value (Cl content), and the intensity of absorption peak for C=O bond is decreased with the expense of HEMA monomer (Figure 2.5), whereas in case of **1d$_x$hC$_{20}$** (DVB series) with constant z value, that of the peak intensity for C−Cl bond was similar (Figure 2.6). Chlorine contents in **1d$_x$hC$_z$** were also in good agreement with calculated ones. These results clearly indicated that monodispersed polymer microspheres having benzyl chloride moiety **1d$_x$hC$_z$** were successfully synthesized by the precipitation polymerization.

*2.2.3 Synthesis of low cross-linked polymer microspheres having benzyl bromide moiety **1d$_x$sB$_z$** by precipitation polymerization of styrene, divinylbenzene (DVB (**d**)) and a divinyl crosslinker **M1**, followed by transformation reaction.*

The isolated yield of polymer microsphere synthesized using DVB as a crosslinker was relatively low. We have successfully synthesized polymer microsphere **1d$_x$sM1$_z$** by the precipitation polymerization of x mol% of St, y mol% of DVB, and z mol% of a divinyl crosslinker **M1** with relatively

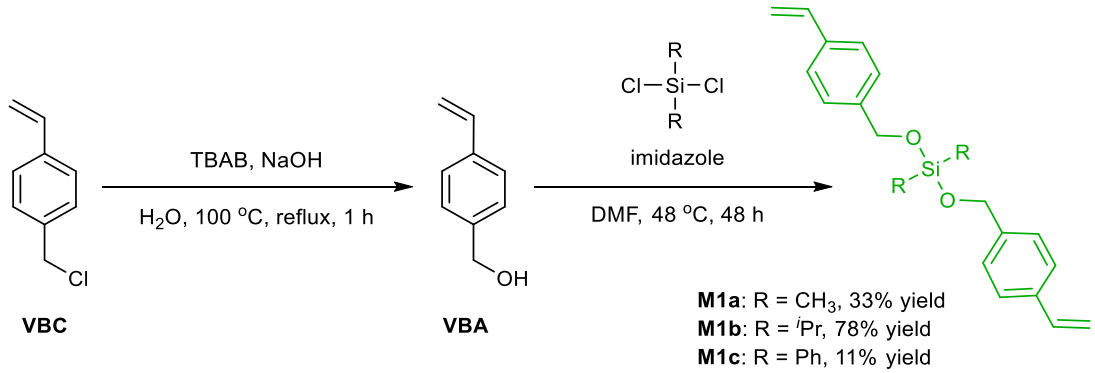

Scheme 2.4 Synthesis of **M1**

higher yield (37-40%) as illustrated in Scheme 2.5. The characterization of **1d$_x$sM1$_z$** was summarized in Table 2.4. High yield with large D_n was found when a high molar ratio of crosslinker was used (entry 1 vs 2) (Figure 2.7a and b). The nature of R in **M1** did not affect the yield of polymer microspheres. Polymer microsphere **1d$_{10}$sM1$_{10}$-1** with relatively high D_n was obtained when **M1a** was used as a divinyl crosslinker at a constant molar ratio of monomers during polymerization (entries 1, 3 and 5). Low crosslinked polymer microsphere having benzyl bromide moiety **1d$_x$sB$_{2z}$** was synthesized by alkyl

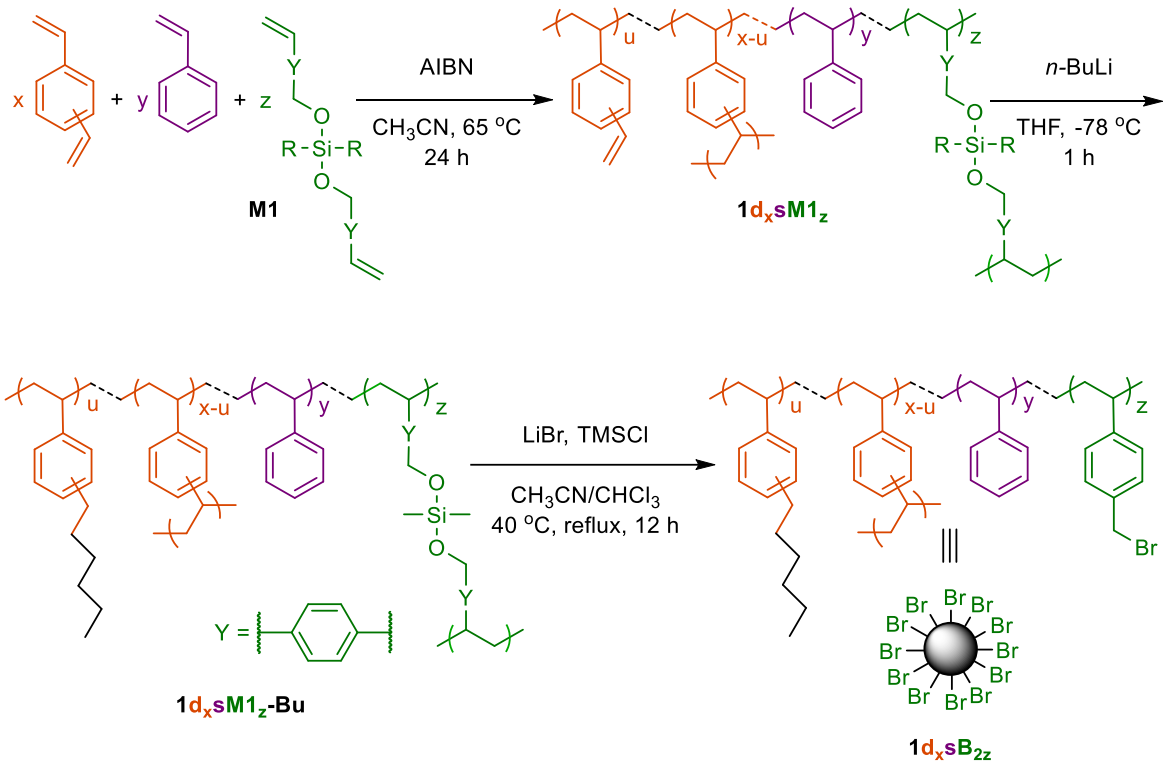

Scheme 2.5 Synthesis of low crosslinked polymer microsphere having benzyl bromide **1d$_x$sB$_{2z}$** by precipitation polymerization.

Table 2.4 Characterization of low crosslinked polymer microsphere having benzyl bromide **1d$_x$sB$_{2z}$**[a].

Entry	**1d$_x$sB$_{2z}$**	R	x/y/z	Yield (%)	D_n (μm)[b]	U (D_w/D_n)[b]	Br Content (mmol g^{-1})[c]	
							Br_{calcd}	$Br_{measured}$
1	**1d$_{10}$sB$_{20}$-1**	CH_3	10/80/10	37	2.77	1.15	1.42	1.89 1.66[d]
2	**1d$_{20}$sB$_{20}$-1**	CH_3	20/70/10	42	4.44	1.04	1.41	-
3	**1d$_{10}$sB$_{20}$-2**	^{i}Pr	10/80/10	38	2.41	1.13	1.43	-
4	**1d$_5$sB$_{10}$-2**	^{i}Pr	05/90/05	24	2.69	1.34	0.81	1.24 1.27[d]
5	**1d$_{10}$sB$_{20}$-3**	Ph	10/80/10	40	2.52	1.16	1.42	-
6	**1d$_5$sB$_{10}$-3**	Ph	05/90/05	25	2.01	1.25	083	-

[a] All the polymerizations were performed in CH_3CN at 70 °C using 4.3 wt% monomers relative to the reaction medium and 2 wt% AIBN relative to the total monomers.

[b] Measured from SEM images.

[c] Determined by titrimetric method.

[d] Determined from elemental analysis.

lithiation to minimize residual vinyl bond in crosslinker, followed by transformation reaction as illustrated in Scheme 2.5. Since the transformation reaction was not influenced on the particle diameter,

the D_n of $\mathbf{1d_xsB_{2z}}$ was unchanged. For example, the D_n of $\mathbf{1d_{10}sM1_{10}}$ and $\mathbf{1d_{10}sB_{20}}$ were 2.79 and 2.77 μm, respectively, with narrow size distributions. Polymer microsphere $\mathbf{1d_xsM1_z}$ and $\mathbf{1d_zsB_{2z}}$ were characterized by FT-IR spectra. For example, in the FT-IR spectra of $\mathbf{1d_{10}sM1_{10}}$ (Figure 2.8), the characteristic absorption peaks for Si−C, Si−O and C−O bonds appeared at 1257, 1075 and 1019 cm^{-1}, respectively, that indicating polymerization successfully occurred. After the transformation reaction of $\mathbf{1d_{10}sM1_{10}}$, these characteristic peaks were disappeared, and two stretching vibrations of C−Br bond were observed at 1227 and 608 cm^{-1}, indicating that the transformation reaction successfully occurred. Measured bromine content in $\mathbf{1d_{10}sB_{20}}$ from the titrimetric method and the elemental analysis were somewhat higher than the calculated one.

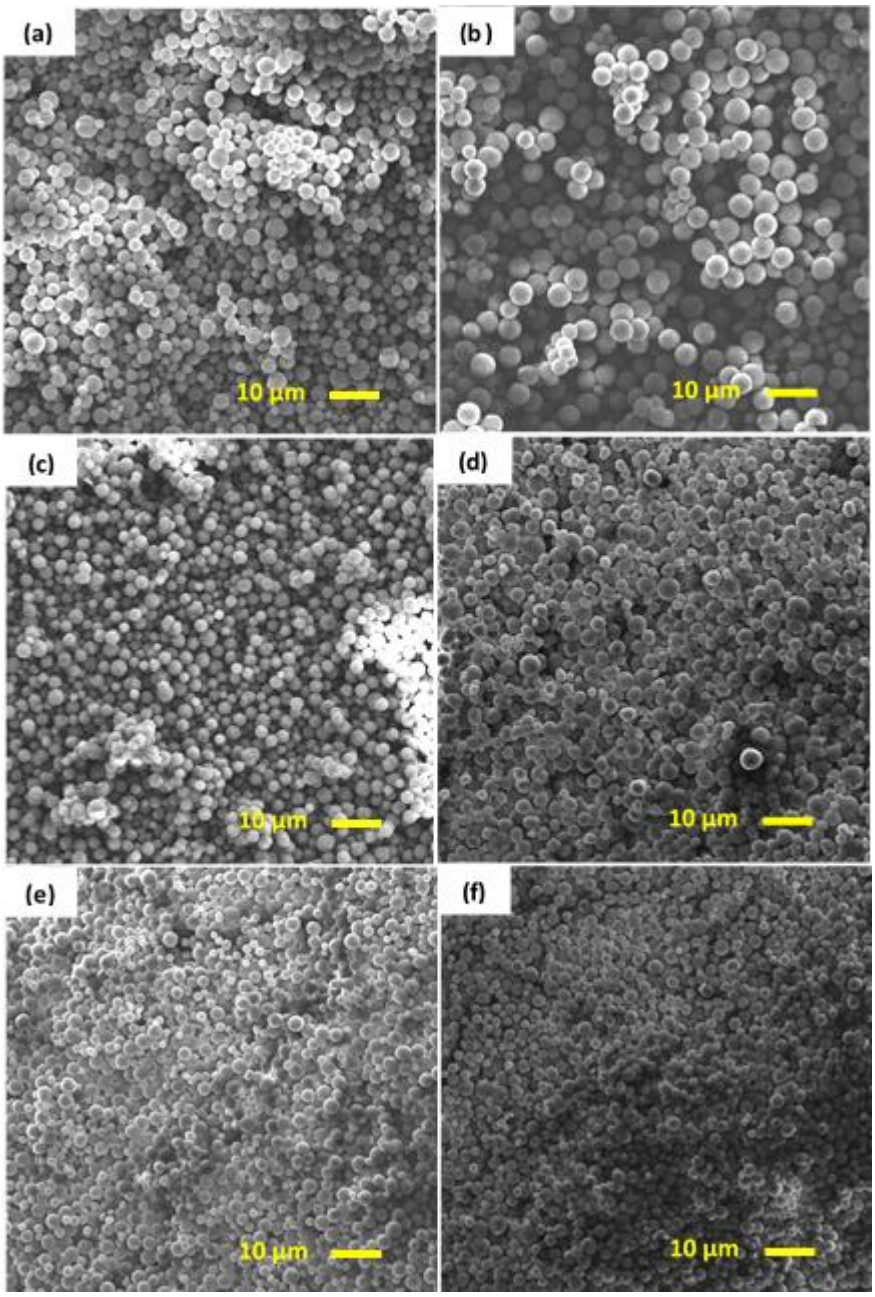

Figure 2.7 SEM images of $\mathbf{1d_xyB_{2z}}$: $\mathbf{1d_{10}B_{20}}$**-1** (a), $\mathbf{1d_{20}sB_{20}}$**-1** (b), $\mathbf{1d_{10}sB_{20}}$**-2** (c), $\mathbf{1d_5sB_{10}}$**-2** (d), $\mathbf{1d_{10}sB_{20}}$**-3** (e), and $\mathbf{1d_5sB_{10}}$**-3** (f).

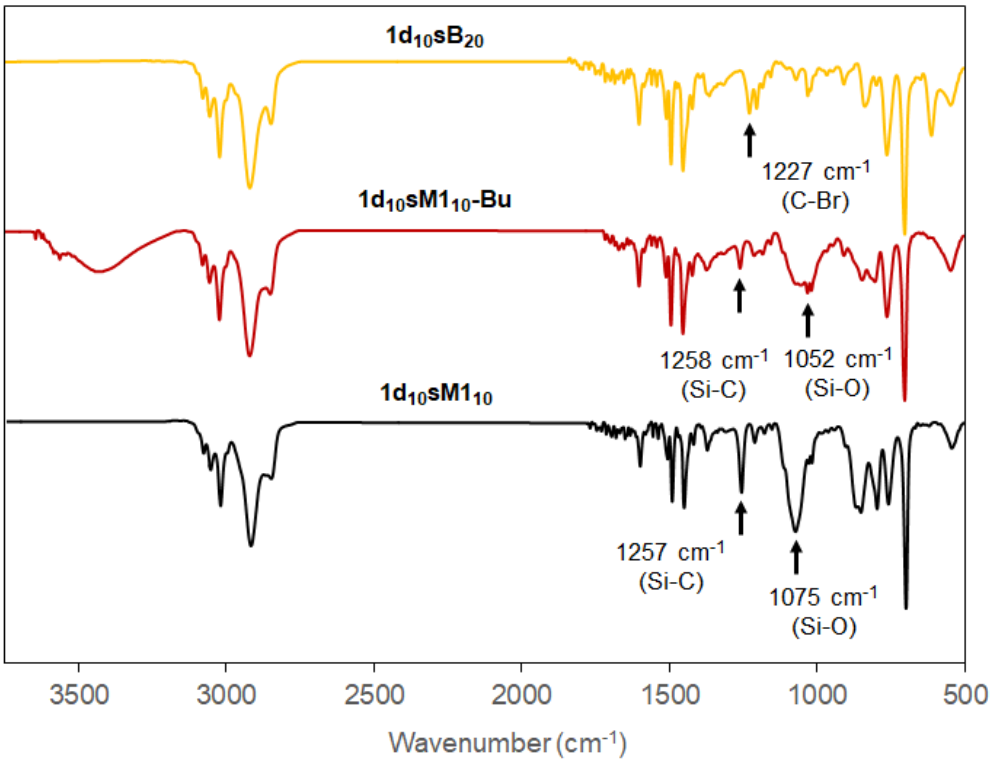

Figure 2.8 FT-IR spectra of **1d$_{10}$sM1$_{10}$** and **1d$_{10}$sB$_{20}$**.

2.3 Conclusion

Narrowly disperse functional polymer microspheres having benzyl halide moiety were successfully synthesized by precipitation polymerization of various comonomers (styrene, methyl methacrylate (MMA), or 2-hydroxyethyl methacrylate (HEMA), divinylbenzene (DVB) with 4-vinylbenzyl chloride (VBC) using AIBN as an initiator in acetonitrile or mixtures of acetonitrile and toluene. In the synthesis of polymer microspheres, the nature of comonomers and the molar ratio of monomers affected the yield and diameter of polymer microspheres. Polymer microspheres functionalized with benzyl halide moiety prepared via precipitation polymerization, which was used as macroinitiators for the synthesis of hairy or core-corona polymer microspheres by surface-initiated atom transfer radical polymerization (SI-ATRP) in Chapter **III**.

2.4 Experimental

2.4.1 Materials and measurements

Styrene (Kishida Chemical Co. Ltd., Osaka, Japan) and divinylbenzene obtained from Nippon & Sumikin Chemical Co. Ltd., Japan, were washed with aqueous 10% NaOH and water, followed by distilling with CaH_2 under reduced pressure. Methyl methacrylate (Sigma-Aldrich), 2-hydroxyethyl methacrylate and 4-vinylbenzyl chloride (Wako Pure Chemical Industries Ltd., Japan), were distilled under reduced pressure.

Chlorine contents in polymer microspheres were measured by the titrimetric method. FT-IR spectra were recorded with a JEOL JIR-7000 FT-IR spectrometer and are reported in reciprocal centimeter (cm^{-1}). SEM measurements were conducted by using JSM-IT100 at an acceleration voltage of 10.0 kV. The number-average diameter (D_n) and the dispersity index (U) were determined from the SEM image.

Number-averaged diameter (D_n), weight-averaged diameter (D_w), and polydispersity index (U) of polymer microsphere were calculated using the following equations by counting at least a hundred of individual particles from the SEM images.

$$D_n = \frac{\sum n_i d_i}{\sum n_i} \quad (1)$$

$$D_w = \frac{\sum n_i d_i^4}{\sum n_i d_i^3} \quad (2)$$

$$U = \frac{D_w}{D_n} \quad (3)$$

Where n_i is the number of particles with d_i.

2.4.2 Synthesis of poly(St-DVB-VBC) microspheres ***1d$_x$sC$_z$*** *by precipitation polymerization*

A series of monodisperse polymer microspheres having benzyl chloride with variable molar ratio was synthesized by precipitation polymerization of styrene, divinylbenzene, and 4-vinylbenzyl chloride using AIBN as an initiator in acetonitrile. In all batches, DVB content was kept constant (20 mol%), but VBC/styrene content was changed.

Representative synthesis procedure for ***1d$_{20}$sC$_5$***: A 60 mL HDPE narrow-mouth bottle was charged with DVB (0.468 g, 3.59 mmol), styrene (1.40 g, 13.4 mmol), VBC (0.138 g, 0.904 mmol), AIBN (0.040 g, 0.24 mmol, 2 wt% relative to the total monomers), and 60 mL of CH_3CN under N_2 gas. Precipitation polymerization was carried out in an incubator at a constant temperature of 65 ^oC with rolling the bottle horizontally at 9 rpm for 24 h. The reaction mixture was cooled to room temperature, and the insoluble fraction was collected by centrifugation and washed with THF, methanol, and acetone. The solid product was dried under vacuum at 40 ^oC for 24 h.

1d$_{20}$sC$_5$: 0.530 g, 26% yield. FT-IR (KBr): ν = 1266 (C−Cl), 1601, 1493, 1452 (C=C in aromatic ring), 3059, 3025 (C−H in aromatic ring), 2922, and 2851 (C−H in alkyl) cm^{-1}. Chlorine contents: 0.566 mmol g^{-1}.

1d$_{20}$sC$_{10}$: 0.282 g, 14% yield. FT-IR (KBr): ν = 1265 (C-Cl), 1602, 1493, 1452 (C=C in aromatic ring), 3059, 3025 (C−H in aromatic ring), 2922, and 2850 (C-H in alkyl) cm^{-1}. Chlorine contents: 0.910 mmol g^{-1}.

1d$_{20}$sC$_{20}$: 0.151 g, 8% yield. FT-IR (KBr): ν = 1265 (C−Cl), 1602, 1493, 1451(C=C in aromatic ring), 3059, 3025 (C−H in aromatic ring), 2922, and 2851 (C−H in alkyl) cm^{-1}. Chlorine contents: 1.64 mmol g^{-1}.

2.4.3 *Synthesis of polymer microspheres having benzyl chloride moiety* ***1d$_x$yC$_z$*** *by precipitation polymerization of various comonomers and divinylbenzene (DVB) with 4-vinylbenzyl chloride (VBC)*

Monodisperse polymer microspheres having benzyl chloride were synthesized by the precipitation polymerization of various comonomers (styrene, methyl methacrylate (MMA), or 2-hydroxyethyl methacrylate (HEMA)) and DVB with VBC using AIBN as a radical initiator in acetonitrile or acetonitrile: toluene = 9:1.

General procedure for ***1d$_{20}$yC$_{20}$ (y = s, m, or h)****:* A 30 mL HDPE narrow-mouth bottle was charged with 20 mol% of DVB (**d**), 60 mol% of commoner (**y**), 20 mol% of VBC (**C**), AIBN (2 wt% relative to the total monomers), and 30 mL of solvent under N_2 gas. In all cases, the total monomers (1.0 g) were kept constant.

Representative synthesis procedure for ***1d$_{20}$hC$_{20}$***: A 30 mL HDPE narrow-mouth bottle was charged with DVB (0.194 g, 1.49 mmol), HEMA (0.580 g, 5.57 mmol)), VBC (0.228 g, 1.49 mmol), AIBN (0.020 g, 0.12 mmol) and a mixture of solvent (27 mL of CH_3CN and 3 mL of toluene) under N_2 gas. Polymerization was carried out in an incubator at a constant temperature of 65 ^oC with rolling the bottle horizontally at 9 rpm for 24 h. The reaction mixture was cooled to room temperature, and the insoluble fraction was collected by centrifugation and washed with THF, methanol, and acetone. The solid product was dried under vacuum at 40 ^oC for 24 h.

1d$_{20}$sC$_{20}$: 0.238 g, 24% yield; FT-IR (KBr): *v* = 1265 (C−Cl), 1602, 1509, 1451 (C=C in aromatic ring), 3059, 3024 (C−H in aromatic ring), 2921, and 2849 (C−H in alkyl) cm^{-1}. Chlorine contents: 1.68 mmol g^{-1}.

1d$_{20}$mC$_{20}$: 0.286 g, 28% yield; FT-IR (KBr): *v* = 1266 (C−Cl), 1604, 1510, 1446 (C=C in aromatic ring), 1728 (C=O in ester), 2946, and 2848 (C−H in alkyl) cm^{-1}. Chlorine contents: 1.80 mmol g^{-1}.

1d$_{20}$hC$_{20}$: 0.237 g, 24% yield; FT-IR (KBr): *v* = 1267 (C−Cl), 1606, 1509, 1455 (C=C in aromatic ring), 1720 (C=O in ester), 2941 (C−H in alkyl), and 3446 (O−H) cm^{-1}. Chlorine contents: 1.56 mmol g^{-1}.

2.4.4 Synthesis of ***M1***

The compound ***M1*** *was synthesized by the following steps*:

Synthesis of VBA*:* Tetra *n*-butylammonium bromide (TBAB) (10.7 g, 33.2 mmol) and NaOH (0.462 g, 11.2 mmol) was taken in a 500 mL round-bottom flask. 4-Vinylbenzyl chloride (11.0 mL, 78.1

mmol) and 300 mL of water were then added. The reaction was heated at 100 °C for 1 h. The crude product was extracted with ethyl acetate (300 mL × 3) and dried over $MgSO_4$. After removing $MgSO_4$ by filtration, the extracted solvent (AcOEt) was removed by rotary evaporator. The crude product was purified by column chromatography on silica gel with ethyl acetate: hexane = 1:4 as eluents to afford the compound, 4-vinylbenzyl alcohol (**VBA**) as colorless liquid (R_f =0.18; 11.0 g, 92% yield). ^{1}H NMR (400 MHz, $CDCl_3$, δ = 7.26 ($CDCl_3$, TMS): δ = 4.69 (d, J = 5.80 Hz, 2H), 5.25 (d, J = 11.0 Hz, 1H), 5.75 (d, J = 17.7 Hz, 1H), 6.72 (dd, J = 10.7, 17.7 Hz, 1H), 7.33 (d, J = 8.2 Hz, 2H), 7.41 (d, J = 8.2 Hz, 2H). ^{13}C NMR (100 MHz, $CDCl_3$, δ = 77.19 ($CDCl_3$), TMS): δ = 65.05, 113.98, 126.48, 127.32, 136.58, 140.51.

Synthesis of M1a: A 100-mL round-bottomed flask with a magnetic stirring bar was charged with VBA (11.0 g, 81.7 mmol) and imidazole (6.02 g, 88.4 mmol), and pumped up to remove moisture for 10-30 min. Dry DMF (50 mL) was added at room temperature under argon gas. Dichlorodimethyl silane **a** (4.70 mL, 40.2 mmol) was added slowly into the mixture at room temperature. The reaction was continued at 40 °C for 48 h. After the reaction, saturated $NaHCO_3$ was added to make basic medium (pH 7~8). The reaction mixture was transferred into a reparatory funnel and extracted with a 1:1 ratio of H_2O-hexane (800 mL × 3). The organic phase was further extracted by water (400 mL) and dried over $MgSO_4$. After removing $MgSO_4$ by filtration, the solvent was removed by rotary evaporator and pumped up. The crude product was purified by column chromatography on silica gel with ethyl acetate: hexane = 1:20 as eluents to afford the compound **M1a** as colorless liquid (R_f = 0.31; 3.63 g, 33% yield). ^{1}H NMR (400 MHz, $CDCl_3$, δ = 7.26 ($CDCl_3$, TMS): δ = 0.19 (s, 6H), 5.21 (d, J = 10.7 Hz, 2H), 5.72 (d, J = 17.7 Hz, 2H), 6.70 (dd, J = 11.0, 17.4 Hz, 2H), 7.26 (d, J = 6.1 Hz, 4H), 7.36 (d, J = 8.2 Hz, 4H). ^{13}C NMR (100 MHz, $CDCl_3$, δ = 77.15 ($CDCl_3$), TMS): δ = -2.84, 64.39, 113.69, 126.31, 126.94, 136.70, 140.21. HRMS (ESI, *m/z*): $[M + Na]^+$ calcd. for $C_{20}H_{24}NaO_2Si$: 347.1438, found: 347.1458.

M1b: 78% yield. ^{1}H NMR (400 MHz, $CDCl_3$, δ = 7.26 ($CDCl_3$, TMS): δ = 1.09 (d, J = 4.27 Hz, 12H), 1.53-1.55 (m, 2H), 4.81(s, 4H), 5.21 (d, J = 11.0 Hz, 2H), 5.72 (d, J = 17.4 Hz, 2H), 6.70 (dd, J = 11.0, 17.7 Hz, 2H), 7.26 (d, J = 8.85 Hz, 4H), 7.36 (d, J = 8.24 Hz, 4H).. ^{13}C NMR (100 MHz, $CDCl_3$, δ = 77.13 ($CDCl_3$), TMS): δ = 12.34, 17.54, 64.51, 113.49, 126.21, 126.31, 136.45, 136.77, 140.77.

M1c: 11% yield. ^{1}H NMR (400 MHz, $CDCl_3$, δ = 7.26 ($CDCl_3$, TMS): δ = 4.81 (s, 4H), 5.22 (d, J = 11.0 Hz, 2H), 5.73 (d, J = 17.7 Hz, 2H), 6.70 (dd, J = 10.7, 17.4 Hz, 2H), 7.26 (d, J = 8.24 Hz, 4H), 7.34-7.47 (m, 10H), 7.72 (d, J = 7.63 Hz, 4H).

*2.4.5 Synthesis of low crosslinked polymer microspheres having benzyl bromide moiety **1d$_{10}$sB$_{20}$** by precipitation polymerization, followed by transformation reaction*

***1d$_{10}$sB$_{20}$** was synthesized by the following steps:*

Synthesis of 1d$_{20}$sM1a$_{10}$: A 180 mL HDPE narrow-mouth bottle was charged with 10 mol% of DVB (626 mg, 4.81 mmol), 80 mol% of styrene (3.99 g, 38.4 mmol), 10 mol% of **M1a** (1.47 g, 4.52 mmol), AIBN (120 mg, 0.72 mmol) and 184 mL of CH_3CN under N_2 gas. Polymerization was carried out in an incubator at a constant temperature of 65 °C with rolling the bottle horizontally at 9 rpm for 3 h. The reaction mixture was cooled to room temperature, and the insoluble fraction was collected by centrifugation and washed with THF, methanol, and acetone. The solid product was dried under vacuum at 40 °C for 24 h. 2.253 g, 37% yield; FT-IR (KBr): ν = 1257 (Si−C), 1075 (Si−O), 1019 (C−O), 1602, 1508, 1452 (C=C in aromatic ring), 3059, 3025 (C−H in aromatic ring), 2922, 2853 (C−H in alkyl) cm^{-1}.

Synthesis of 1d$_{20}$sM1a$_{10}$-Bu: To **1d$_{10}$sM1a$_{10}$** (1.96 g, DVB contents: 0.202 g, 1.55 mmol) in dry THF (20 mL), *n*-BuLi (5 mL) was added at -78 °C. The reaction was continued at -78 °C for 1h. After 1 h, 20 mL MeOH was added slowly into the reaction mixture at room temperature. Polymer particles were collected by centrifugation and washed several times with MeOH, a 1:1 ratio of H_2O-THF, and acetone. The solid product was dried under vacuum at 40 °C for 24 h. 1.83 g, 93% yield; FT-IR (KBr): ν = 1258 (Si−C), 1052 (Si−O), 1016 (C−O), 1602, 1509, 1452 (C=C in aromatic ring), 3059, 3025 (C−H in aromatic ring), 2922, 2852 (C−H in alkyl) cm^{-1}.

Synthesis of 1d$_{10}$sB$_{20}$: A 100-mL round-bottomed flask with a magnetic stirring bar was charged with **1**d$_{20}$sM1$_{10}$-Bu (1.79 g, 1.33 mmol of **M1a** moiety) and LiBr (6.11 g, 70.3 mmol) at room temperature. Dry $CHCl_3$ (33 mL) and CH_3CN (8 mL) were then added as soon as possible. Finally, TMSCl (8.45 mL, 66.6 mmol) was added into the mixture. The mixture was refluxed at 40 °C for 12 h under N_2 gas. Polymer particles were collected by centrifugation and washed several times using a 1:1 ratio of MeOH-THF after stirring in the same mixed solvent for 48 h. After that, the polymer particle was further stirred in a 1:1 ratio of MeOH-H_2O for 24 h and then washed. Finally, **1d$_{10}$sB$_{20}$** was washed with water and acetone. The solid product was dried under vacuum at 40 °C for 24 h. 1.840 g, 98% yield; FT-IR (KBr): ν = 1227 (C−Br), 1602, 1508, 1452 (C=C in aromatic ring), 3058, 3025 (C−H in aromatic ring), 2922, 2850 (C−H in alkyl) cm^{-1}. Bromine content measured from titrimetric method and elemental analysis were 1.89 and 1.66 mmol g^{-1}, respectively.

References

[1] Xia, Y.; Gates, B.; Yin, Y.; Lu, Y. *Adv. Mater.* **2000**, *12*, 693 - 713.

[2] Wang, J.; Cormack, P. A. G.; Sherrington, D. C.; Khoshdel, E. *Angew. Chem. Int. Ed.* **2003**, *42*, 5336 - 5338.

[3] Ye, L.; Mosbach, K. *Chem. Mater.* **2008**, *20*, 859 - 868.

[4] Barner, L. *Adv. Mater.* **2009**, *21*, 2547 - 2553.

[5] Gorsd, M. N.; Blanco, M. N.; Pizzio, L. R. *Procedia Mat. Sci.* **2012**, *1*, 432 - 438.

[6] (a) Eslami, H.; Hosseinzadeh, S.; Saadat, Y.; Afshar-Taromi, F. Rimaz, M. *Colloid Polym. Sci.* **2012**, *290*, 1463. (b) Antonietti, M.; Bremser, W.; Schmidt, M. *Macromolecules* **1990**, *23*, 3796 - 3805.

[7] Okubo, M.; Konishi, Y.; Minam, H. *Colloid Polym. Sci*. **1998**, *276*, 638 - 642.

[8] Naka, Y.; Kaetsu, I.; Yamamoto, Y.; Hayashi, K. *J. Polym. Sci., Part A: Polym. Chem.* **1991**, *29*, 1197 - 1202.

[9] (a) Romack, T. J., Maury, E. E.; DeSimone, J. M. *Macromolecules* **1995**, *28*, 912 - 915. (b) Laska, Widlarz, J.; Woźny, E. *J. Polym. Sci. Part A: Polym. Chem.* **2002**, *40*, 3562 - 3569. (c) Liu, T.; Garner, P.; DeSimone, J. M.; Roberts, G. W.; Bothun, G. D. *Macromolecules* **2006**, *39*, 6489 - 6494.

[10] Li, K.; Stöver, H. D. H. *J. Polym. Sci., Part A: Polym. Chem.* **1993**, *31*, 3257 - 3263.

[11] Li, W. H.; Stöver, H. D. H. *J. Polym. Sci., Part A: Polym. Chem.* **1998**, *36*, 1543 -1551.

[12] Downey, J.; Frank, R. S.; Li, W.; H. Stöver, H. D. H. *Macromolecules* **1999**, *32*, 2838 - 2844.

[13] Downey, J.; McIsaac, G.; Frank, R. S.; Stöver, H. D. H. *Macromolecules* **2001**, *34*, 4534 - 4541.

[14] Li, W. H., Li, K.; Stöver, H. D. H. *J. Polym. Sci. Part A: Polym. Chem.* **1999**, *37*, 2295 - 2303

[15] Frank, R. S.; Downey, J. S.; Stöver, H. D. H. *J. Polym. Sci. Part A: Polym. Chem.* **1998**, *36*, 2223 - 2227.

[16] Frank, R. S.; Downey, J.; Yu, K.; Stöver, H. D. H. *Macromolecules* **2002**, *35*, 2728 - 2735.

[17] Li, W. H.; Stöver, H. D. H. *J. Polym. Sci. Part A: Polym. Chem.* **1999**, *37*, 2899 -2907.

[18] Ye, L.; Weiss, R.; Mosbach, K. *Macromolecules* **2000**, *33*, 8239 - 8245.

[19] Bai, F.; Yang, X.; Huang, W. *Macromolecules* **2004**, *37*, 9746 - 9752.

[20] Shim, S. E.; Yang, S.; Choe, S. J. Polym. Sci., Part A: Polym. Chem. **2004**, *42*, 3967 - 3774.

[21] Jin, J. M.; Yang, S.; Shim, S. E.; Choe, S. *J. Polym. Sci., Part A: Polym. Chem.* **2005**, *43*, 5343 - 5346.

[22] Joso, R.; Pan, E. H.; Stenzel, M. H.; Davis, T. P.; Barner-Kowollik, C.; Barner, L. *J. Polym. Sci., Part A: Polym. Chem.* **2007**, *45*, 3482 - 3487.

[23] Yan, Q.; Bai, Y.; Meng, Z.; Yang, W. *J. Phys. Chem. B* **2008**, *112*, 6914 - 6922.

[24] Yan, Q.; Zhao, T.; Bai, Y.; Zhang, F.; Yang, W. *J. Phys. Chem. B* **2009**, *113*, 3008 - 3014.

[25] Medina-Castillo, A. L.; Fernandez-Sanchez, J. F.; Segura- Carretero, A.; Fernandez-Gutierrez A., *Macromolecules* **2010**, *43*, 5804 - 5813.

[26] Sosnowski, S.; Gadzinowski, M.; Slomkowski, S. *Macromolecules* **1996**, *29*, 4556 - 4564.

[27] (a) Li, W. H.; Stöver, H. D. H. *Macromolecules* **2000**, *33*, 4354 - 4360. (b) Koprinarov, I.; Hitchcock, A. P.; Li, W. H.; Heng, Y. M.; Stöver, H. D. H. *Macromolecules* **2001**, *34*, 4424 - 4429.

(c) Takekoh, R.; Li, W. H.; Burke, N. A. D.; Stöver, H. D. H. *J. Am. Chem. Soc.* **2006**, *128*, 240 - 244.

[28] (a) Bai, F.; Yang, X.; Huang, W. *Macromolecules* **2004**, *37*, 9746 - 9752. (b) Bai, F.; Yang, X.; Huang, W. *Eur. Polym. J.* **2006**. *42*, 2088 - 2097. (c) Bai, F.; Yang, X.; Li, R.; Huang, B. *Polymer* **2006**, *47*, 5775 - 5784. (d) Bai, F.; Li, R.; Yang, X.; Li, S. *Polym. Int.* **2006**, *55*, 319 - 325. (e) Bai, F.; Huang, B; Yang, X.; Huang, W. *Eur. Polym. J.* **2007**, *43*, 3923 - 3932.

[29] (a) Limé, F.; Irgum, K. *Macromolecules* **2007**, *40*, 1962 - 1968. (b) Limé, F.; Irgum, K. *Macromolecules* **2009**, *42*, 4436 - 4442.

[30] Joso, R.; Pan, E. H.; Stenzel, M. H.; Davis T. P.; Barner-Kowollik, C.; Barner, L. *J. Polym. Sci. Part A: Polym. Chem*. **2007**, *45*, 3482 - 3487.

[31] Ghosh Chaudhuri, R.; Paria, S. *Chem. Rev.* **2011**, *112*, 2373 - 2433.

[32] Li, G. L.; Möhwald, H.; Shchukin, D. G. *Chem. Soc. Rev.* **201**3, *42*, 3628 - 3646.

[33] Perrier-Cornet, R.; Héroguez, V.; Thienpont, A.; Babot, O.; Toupance, T. *J. Chromatogr. A* **2008**, *1179*, 2 - 8.

CHAPTER III

Synthesis of Well-defined Hairy Polymer Microspheres by Surface-initiated Atom Transfer Radical Polymerization

3.1 Introduction

Well-defined core-corona or hairy type polymer microspheres are one of the core-shell microspheres in which well-defined linear polymer chains are grafted onto the surface of core-corona polymer microspheres. These graft chains make the nature of polymer microsphere more flexible and reactive. The rigidity and stability of core, as well as flexibility, processability, functionality of corona, enlarge the potential applications of core-corona polymer microspheres. These polymer microspheres can be synthesized by either a "grafting onto"[1,2] or a "grafting from"[3-7] approach. In the "grafting onto" approach (Figure 3.1**A**), the linear polymer chains with active species react with reactive sites of the surface of core to afford core-corona polymer microsphere. The active species can be located either at the end or on the backbone of the polymer chain or be part of side chains. However, this approach often allows low grafting densities due to steric hindrance between the polymer chains. In the ''grafting from" approach (Figure 3.1**B**), graft polymerization of monomer is performed with plural initiators on the surface of core to afford core-corona polymer microsphere. The ''grafting from" and ''grafting to" techniques can also be implemented together.[9] For instance, Berger reported the synthesis of stimuli-responsive bicomponent core-corona Janus particles by both approaches where the first polymer could be immobilized onto one side of silica particles using the ''grafting from" approach and the second

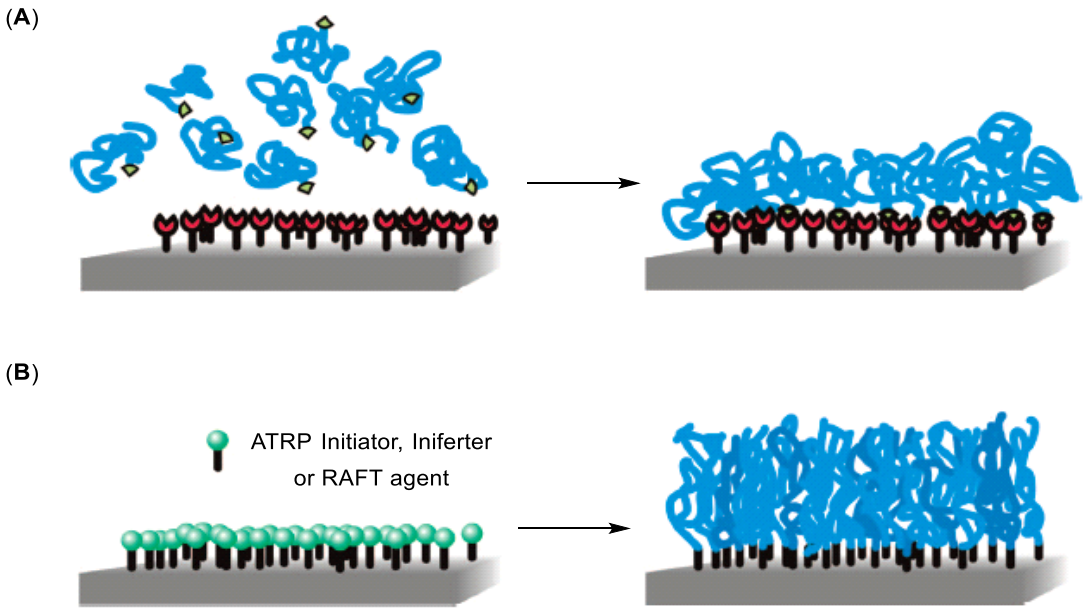

Scheme 3.1[9] Schematic illustration of different techniques of chemical grafting of linear polymer chains onto a solid surfaces: (**A**) "grafting onto" and (**B**) "grafting from".

polymer was grafted onto the other side of the particle surface via the ‘‘grafting to” approach.[8] The third one “grafting through” which is based on the use of surface-attached monomer groups, or in other word, surfaces carrying a self-assembled monolayer containing polymerizable groups.[10] The attachment of a polymer chain through such a process consists from a principle point of view of both “grafting to” and “grafting from” steps. Despite the fact that such processes are widely applied, even in industrial applications, mostly for adhesion promotion (so-called application of a “primer”), surprisingly, the “grafting through” approach is from a scientific point of view not extensively explored and the details of the mechanism are not well understood. This technique also provides limited grafting densities. The predictable number-average molecular weight (M_n) and narrow polydispersity (M_w/M_n) of grafted polymer can be obtained when living or controlled polymerization technique is used for the synthesis.

Among the above approaches, grafting from method by various surface-initiated controlled/‘‘living’’ radical polymerizations (CRPs) such as iniferter-induced living radical polymerization (ILRP),[11] nitroxide-mediated radical polymerization (NMP),[12] atom transfer radical polymerization (ATRP),[13-15] and reversible addition-fragmentation chain transfer (RAFT) polymerization,[16-18] has been widely used for the synthesis of highly grafted and well-defined core-corona polymer microspheres because of their good control over the length of polymer chains, grafting densities, broad applicability to a wide range of monomers, and mild reaction conditions. These living techniques can also be used to generate

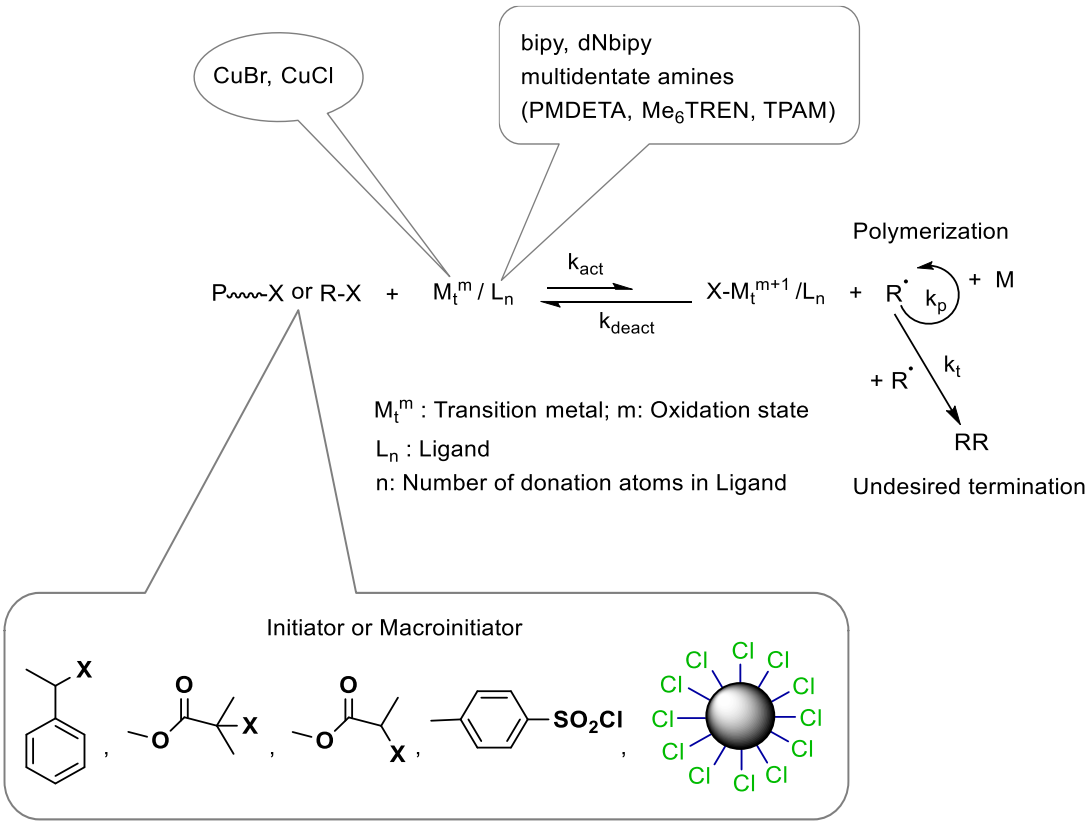

Scheme 3.2 The proposed mechanism for ATRP.

grafted homopolymers, copolymers, and block copolymers.

In comparison with other CRPs, ATRP has been particularly attractive because of its versatility and robustness, good control over narrow polydispersity and degree of chain end functionalities. ATRP was first reported in 1995 by Matyjaszewski et al.[15,19,20] ATRP relies on the reversible redox activation of a dormant alkyl halide-terminated polymer chain end by a halogen transfer to a transition metal complex (The proposed mechanism for ATRP is shown in Scheme 3.2). The formal homolytic cleavage of the carbon-halogen bond, which results from this process, generates a free and active carbon-centered radical species at the polymer chain end. This activation step is based on a single electron transfer from the transition metal complex to the halogen atom, which leads to the oxidation of the transition metal complex. Then, in a fast, reversible reaction, the oxidized form of the catalyst reconverts the propagating radical chain end to the corresponding halogen-capped dormant species.

Patten et al. first reported the surface-initiated ATRP on silica nanoparticles.[21,22] They successfully demonstrated that styrene (St) and MMA could be controllably polymerized from 75 nm silica nanoparticles. According to similar principles, a variety of other monomers such as *n*-butyl acrylate (*n*BA), *tert*-butyl acrylate (*t*BA), 2-hydroxyethyl methacrylate (HEMA), and oligo(ethylene glycol) methyl ether methacrylate (OEGMA) have been polymerized silica nanoparticles *via* surface-initiated ATRP.[23-26]

Kohji Ohno et al. synthesized high-density PMMA brushes by SI-ATRP on silica particles (SiPs) with average diameters 290 and 740 nm.[27] Lei Wu et al. reported the introduction of ATRP initiator moiety on commercially available silica particles with an average diameter 123 nm that are used for graft polymerization of *N*-isopropylacrylamide (NIPAm), and the resulting PNIPAm grafted SiPs are used as living initiators for the second graft polymerization of 4-vinylpyridine (4VP) monomer.[28] The subsequent quaternization of the outer poly(4VP) block with CH_3I led to the synthesized hybrid nanoparticles being well dispersed in aqueous solution. There have also been several reports on polymer grafted-SNPs synthesized by SI-ATRP using surface modified SNPs as core considering their potential applications in various areas such as colloid chemistry, catalysis, nanopatterning, photonics, drug delivery, and biosensing.[29-31]

Stöver's group reported the addition of hydrogen chloride to residual C−C bond on the surface of poly(DVB) particles and the subsequent surface-initiated atom transfer radical polymerization (SI-ATRP) from resulting surface-bound 1-phenylethyl chloride initiator groups.[32] The resulting grafted-poly(DVB) particles are used as a macroinitiator for graft polymerization of the second monomer. They also reported the synthesis of ATRP macroinitiator by hydroboration/oxidation reaction of residual vinyl groups on poly(DVB) microsphere. The SI-ATRP of HEMA and 2-(dimethylamino)ethyl methacrylate initiated by the macroinitiator gave hydrophilic grafted microspheres.[33]

In this Chapter, we synthesized hairy type or core-corona polymer microspheres using monodisperse polymer microspheres having benzyl halide moiety prepared from precipitation polymerization as multifunctional initiator. The SI-ATRP of St, MMA, HEMA, *n*BA, *n*BMA, *t*BMA, and NIPAm were carried out from benzyl chloride moiety of P(DVB-St-VBC) microspheres to synthesize hairy polymer microspheres having homopolymer chains in their hairs. These core-corona polymer microspheres were also synthesized from graft copolymerization of an achiral monomer (St, MMA, HEMA, or NIPAm) with phenyl *p*-styrenesulfonate using polymer microspheres having benzyl halide as a macroinitiator by SI-ATRP. In the synthesis of these polymer microsphere, the effect of the molar ratio of monomers and molar ratio of VBC in core, size and nature of core on the grafting density were investigated. These core-corona polymer microspheres were characterized by FT-IR, GPC, optical microscope, and SEM.

3.2 Results and Discussion

3.2.1 Synthesis of monodisperse poly(DVB-St-VBC) microspheres with benzyl halide moiety $\mathbf{I_z}$ *by precipitation polymerization*

A series of poly(DVB-St-VBC) polymer microspheres having benzyl chloride moiety $\mathbf{1d_xsC_z}$ (or $\mathbf{I_z}$) was prepared by the precipitation polymerization of styrene, DVB, and VBC with AIBN in CH_3CN as illustrated in Scheme 3.3. The molar ratio of DVB was set to 20 mol%, and that of VBC was changed to 5, 10, and 20 mol%, respectively. The precipitation polymerization proceeded as expected, and micron-sized polymer particle was successfully obtained. These characterizations were summarized in Table 2.1 of Chapter **II** that were discussed in details there. The isolated yield was relatively low (8%-26%) due to the minimum molar ratio of DVB to form micro-sized particle was used. To synthesize the

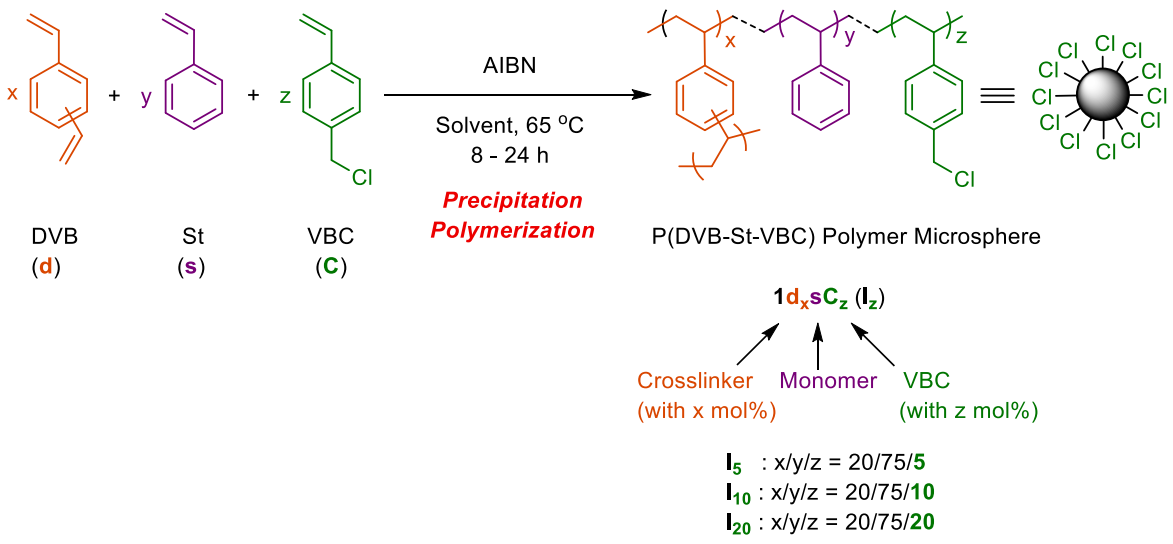

Scheme 3.3 Synthesis of polymer microsphere having benzyl chloride moiety $\mathbf{I_z}$ by precipitation polymerization.

same diameter (ca. 3.0 μm) of polymer microspheres with different benzyl halide content $\mathbf{I_z}$, the polymerization time was adjusted.

3.2.2 Synthesis of polymer microspheres having benzyl chloride moiety ***1d$_x$yC$_z$*** *by precipitation polymerization of various Comonomers (**y**), divinylbenzene (DVB (**d**)) and 4-vinylbenzyl chloride (VBC (**C**))*

To check the effect of comonomer, polymer microspheres having benzyl chloride moiety $\mathbf{1d_xyC_z}$ were synthesized by the precipitation polymerization of 60 mol% of comonomer (styrene, methyl methacrylate (MMA), or 2-hydroxyethyl methacrylate (HEMA)), 20 mol% of DVB with 20 mol% of VBC as illustrated in Scheme 3.4. The molar ratio of DVB and VBC was kept fixed, and that of comonomer was changed from St to HEMA with constant molar ratio. The characterizations of $\mathbf{1d_xyC_z}$ were summarized in Table 2.2 of Chapter **II**. To synthesize the same diameter (Ca. 1.0 μm) of polymer microspheres, the polymerization time was adjusted. The isolated yield was relatively low (3-24%). The number-averaged diameters (D_n) measured from SEM photographs were 1.14 μm for $\mathbf{1d_{20}sC_{20}}$, 1.12 μm for $\mathbf{1d_{20}mC_{20}}$, and 0.80 μm for $\mathbf{1d_{20}hC_{20}}$, respectively. D_n of $\mathbf{1d_{20}sC_{20}}$ and $\mathbf{1d_{20}mC_{20}}$ were increased that were 4.41 μm and 9.14 μm, respectively when the polymerization time was constant. When HEMA was used as comonomer, smaller microsphere was obtained compared to styrene or MMA monomer at constant polymerization time. The distributions (D_w/D_n) were narrow being in the range of 1.00 and 1.14. Chlorine contents in $\mathbf{1d_xyC_z}$ determined by titrimetric were in good agreement with calculated ones. In the FT-IR spectra of $\mathbf{1d_xyC_z}$, the characteristic FT-IR band was appeared at 1265 cm^{-1} due to C–Cl bond. The strong peaks were found at 1602, 1509, 1451 cm^{-1} and 3059, 3024 cm^{-1} due to C=C and C–H bonds in the aromatic ring of $\mathbf{1d_{20}sC_{20}}$, respectively. The stretching absorption frequency of C=O bond was

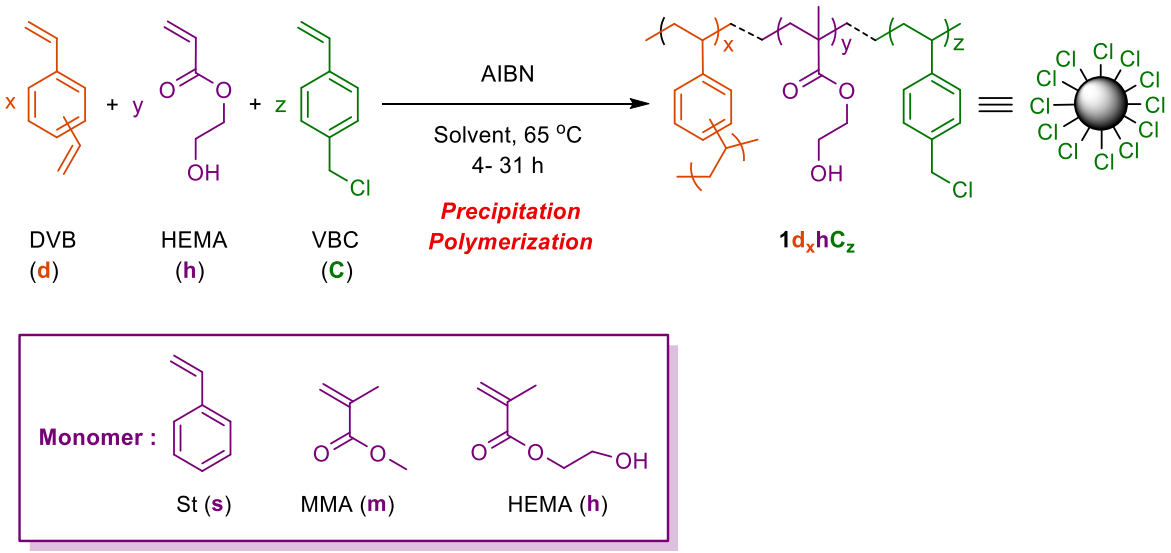

Scheme 3.4 Synthesis of polymer microsphere having benzyl chloride $\mathbf{1d_xhC_z}$ by precipitation polymerization.

observed at 1728 and 1720 cm^{-1} in **1d$_{20}$mC$_{20}$** and **1d$_{20}$hC$_{20}$**, respectively. A broad peak for O-H in **1d$_{20}$hC$_{20}$** was observed at 3446 cm^{-1}.

A series of poly(DVB-HEMA-VBC) microspheres **1d$_x$hC$_z$** was then synthesized with different monomer ratio by precipitation polymerization (Scheme 3.4). The molar ratio of DVB was set to 20 mol%, and that of VBC was changed to 5, 10, 20, and 30 mol%, respectively (Cl series: **1d$_{20}$hC$_z$**). In addition, the VBC ratio was constant at 20 mol%, and that of DVB was changed to 20, 30, 40, and 50 mol%, respectively (DVB series: **1d$_x$hC$_{20}$**). The characterization data was summarized in Table 2.3 of Chapter **II** that was briefly discussed. In Cl series, the particle growth rate was decreased with increasing Cl content at constant DVB, whereas the rate was increased with increasing DVB content at constant VBC in DVB series. D_n of **1d$_{20}$hC$_{20}$** synthesized using benzoylperoxide (BPO) instead of AIBN as an initiator was 2.00 μm with a polydispersity index being 1.05 (entry 8, Table 2.3 in Chapter **II**). The use of BPO instead of AIBN as an initiator gave **1d$_x$hC$_z$** with larger D_n. The D_n for **1d$_x$hC$_z$** were in the range of 0.80 and 2.20 μm, and these distributions were relatively narrow. FT-IR spectra of **1d$_x$hC$_z$** exhibited that both absorption peaks assigned to stretching vibration of C−Cl and C=O bonds. Chlorine contents in **1d$_x$hC$_z$** were also in good agreement with calculated ones. These results clearly indicated that monodispersed polymer microspheres having benzyl chloride moiety **1d$_x$hC$_z$** were successfully synthesized by the precipitation polymerization.

*3.2.3 Synthesis of hairy polymer microspheres **H** using **I$_z$** as multifunctional polymeric initiator by surface-initiated ATRP*

Benzyl halide moiety of **I$_z$** can be utilized as the initiator system of ATRP. Herein, surface-initiated ATRP (SI-ATRP) initiated with **I$_z$** was performed for the synthesis of hairy polymer microspheres **H** (Scheme 3.5). According to the monomer of SI-ATRP, polymerization system was changed. Basically, 2,2′-bipyridine as a ligand and diphenyl ether (DPE) as a solvent were used for the SI-ATRP of styrene,

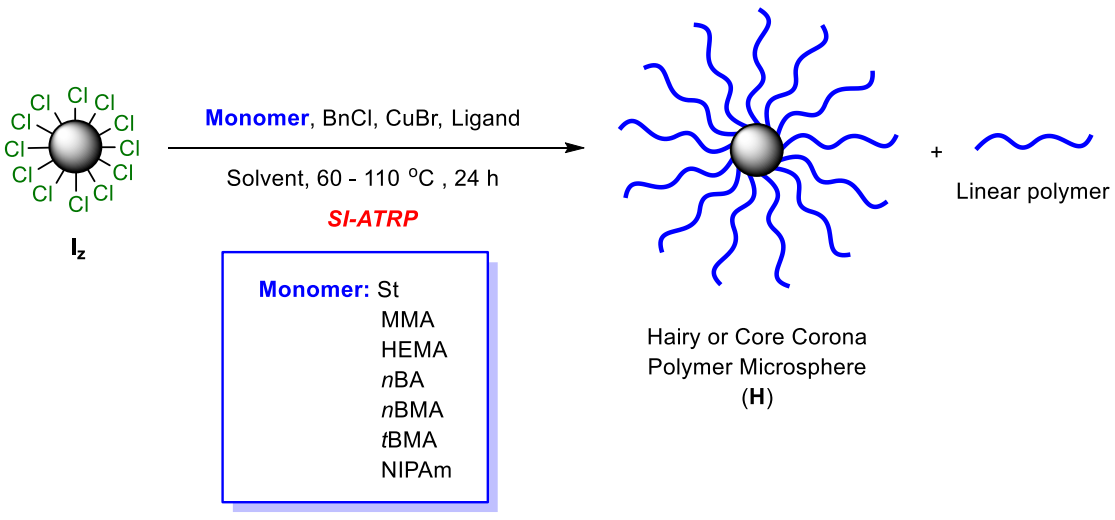

Scheme 3.5 Synthesis of hairy polymer microsphere **H** by SI-ATRP.

MMA, and HEMA. For the polymerization of *n*BA, *n*BMA, and *t*BMA, *N*,*N*,*N*′,*N*″,*N*″-PMDETA as a ligand and anisole as a solvent were employed.

NIPAm has not been controllably polymerized by ATRP when 2,2′-bipyridine was employed as the ligand. Masci et al. prepared PNIPAm with low polydispersity via ATRP in DMF/water mixed solvent using CuCl/Me_6TREN as the catalyst.[34] Stöver et al. proved that NIPAm can be controllably

Table 3.1 Synthesis of hairy polymer microsphere **H** using $\mathbf{I_z}$ by SI-ARTP[a].

Entry	**H**	$\mathbf{I_z}$	M/I	Monomer	ΔW (%)[b]	Grafted polymer		D_n(**I**) (μm)[b]	D_n(**H**) (μm)[b]	U (**H**)[b]	C.V.[d]
						$M_{n,SEC}$	M_w/M_n				
1[e]	$\mathbf{H_{5\text{-}50}}$	$\mathbf{I_5}$	50	St	35	7,240	1.20	2.95	3.75	1.00	0.72
2[e]	$\mathbf{H_{10\text{-}50}}$	$\mathbf{I_{10}}$	50	St	73	7,040	1.21	2.94	3.62	1.01	0.77
3[f]	$\mathbf{H_{10\text{-}50}}$	$\mathbf{I_{10}}$	50	St	70	8,310	1.32	2.94	3.68	1.00	1.5
4[f,g]	$\mathbf{H_{10\text{-}50}}$	$\mathbf{I_{10}}$	50	St	74	8,490	1.30	2.94	3.70	1.00	1.0
5[e]	$\mathbf{H_{20\text{-}50}}$	$\mathbf{I_{20}}$	50	St	130	5,640	1.14	2.94	3.11	1.01	0.68
6[e]	$\mathbf{H_{20\text{-}150}}$	$\mathbf{I_{20}}$	150	St	189	11,900	1.30	2.94	3.85	1.01	0.72
7[e]	$\mathbf{H_{20\text{-}300}}$	$\mathbf{I_{20}}$	300	St	552	32,000	1.64	2.94	6.99	1.17	3.0
8[e]	$\mathbf{H_{20\text{-}500}}$	$\mathbf{I_{20}}$	500	St	957	51,600	1.65	2.94	8.10	1.03	2.0
9[e,h]	$\mathbf{H_{(MMA)}}$	$\mathbf{I_{20}}$	50	MMA	75	32,300	1.44	2.94	3.14	1.02	1.8
10[e,i]	$\mathbf{H_{(HEMA)}}$	$\mathbf{I_{20}}$	50	HEMA	130	6,800	1.16	2.94	7.98	1.02	0.93
11[f,j]	$\mathbf{H_{(}$*n*$\mathbf{BA)}}$	$\mathbf{I_{20}}$	50	*n*BA	10	10,700	1.45	2.94	3.31	1.01	1.4
12[f,j]	$\mathbf{H_{(}$*n*$\mathbf{BMA)}}$	$\mathbf{I_{20}}$	50	*n*BMA	77	11,100	1.50	2.94	3.03	1.00	1.5
13[f,j]	$\mathbf{H_{(}$*t*$\mathbf{BMA)}}$	$\mathbf{I_{20}}$	50	*t*BMA	15	11,100	1.50	2.94	3.38	1.01	1.6
14[k,l]	$\mathbf{H_{(NIPAm)}}$	$\mathbf{I_{20}}$	50	NIPAm	19	12,600	1.32	2.94	3.42	1.01	1.2

$[Monomer]_o$ = 6.0 M, $[Cl]_o$ = $[CuBr]_o$ = 0.12 M, and $[ligand]_o$ = 0.36 M.

[a] The polymerizations were performed at 110 °C for 24 h with $[Monomer]_o/[Cl]_o/[CuBr]_o/[ligand]_o$ = 100/2/2/6.

[b] $$\text{Weight increase } (\Delta W\%) = \frac{\text{Weight of hairy polymer microspheres } (Wt_{HP}) - \text{Weight of polymer microspheres } (Wt_{PM})}{\text{Weight of polymer microspheres } (Wt_{PM})} \times 100$$

[c] Measured from SEM images.

[d] Determined by particle size distribution analyzer.

[e] 2,2′-bipyridine (ligand) and DPE (solvent) were used.

[f] PMDETA (ligand) was used.

[g] Toluene (solvent) was used.

[h] Polymerization was performed at 90 °C.

[i] Polymerization was performed at 80 °C.

[j] Anisole (solvent) was used.

[k] Me_6TREN (ligand) and MeOH (solvent) were used.

[l] Polymerizations were performed at 60 °C.

polymerized in various alcohols at ambient temperature by ATRP under similar conditions.[35] We used CuBr/Me_6TREN catalyst system in MeOH for the polymerization of NIPAm. The characterization data were summarized in Table 3.1. For example, $\mathbf{H_{5\text{-}50}}$ represents the hairy microsphere synthesized by $\mathbf{I_5}$ as a macroinitiator with molar ratio of styrene to initiators (M/I) = 50.

In all cases, the weight increase of $\mathbf{I_z}$ was observed after the polymerization, which suggested that the SI-ATRP of monomer proceeded from benzyl chloride moiety of $\mathbf{I_z}$. The increase of ΔW% is proportional to that of $[Cl]_o$ in $\mathbf{I_z}$ (entries 1-5). The polymerization was carried out with the addition of a predetermined amount of benzyl chloride (BnCl) as a sacrificial initiator. The free polymer generated in the polymerization was then isolated from the solution and characterized by ^{1}H NMR and SEC. In

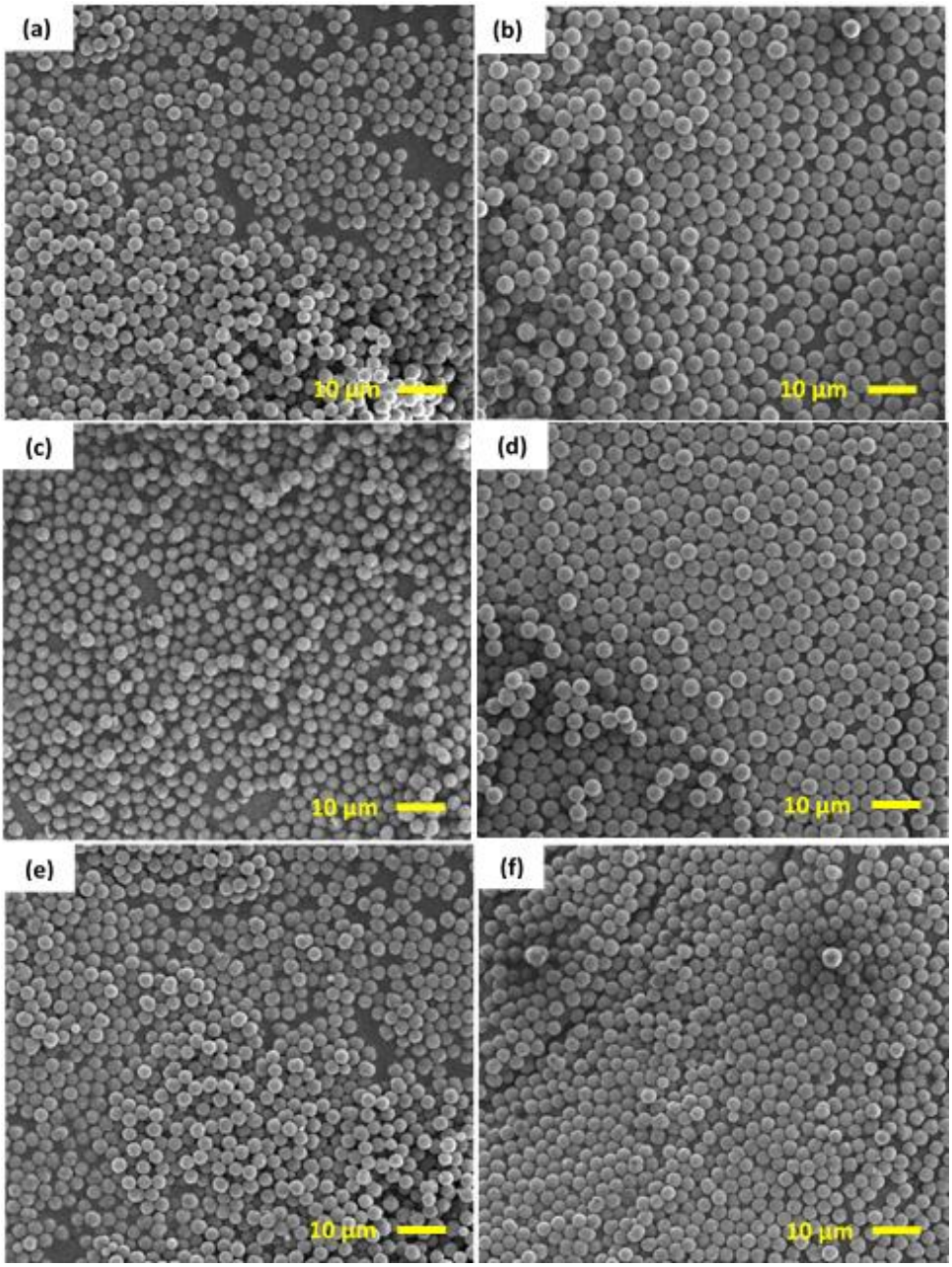

Figure 3.1 SEM images of polymer microsphere $\mathbf{I_z}$ and hairy polymer microsphere $\mathbf{H_{z\text{-}50}}$: $\mathbf{I_5}$ (a), $\mathbf{H_{5\text{-}50}}$ (b), $\mathbf{I_{10}}$ (c), $\mathbf{H_{10\text{-}50}}$ (d), $\mathbf{I_{20}}$ (e), and $\mathbf{H_{20\text{-}50}}$ (f).

SI-ATRP, the initiation efficiency of macroinitiator can be regarded as similar to that of benzyl chloride.[47,48] The number-averaged molecular weight (M_n) and polydispersity (M_w/M_n) of the grafted polymers were measured by those of free polymer. SEC curve of the free polystyrene was almost monomodal with small tailing and the top was shifted to earlier retention time with maintaining the shape of trace. M_n of grafted polymer were somewhat higher than those calculated (ca. 5,000 g mol^{-1}) likely due to the bimolecular termination at the early stage of the polymerization (entries 1 and 2). The use of PMDETA instead of 2,2′-bipyridine as a ligand or toluene instead of DPE as a solvent did not suppress the side reaction (entries 3 and 4). From these SEM photographs of **H**, spherical and uniform microspheres as well as $\mathbf{I_z}$ were successfully obtained (Figure 3.1b, d and f). In addition, D_n of hairy polymer microspheres (D_n(**H**)) were increased to some extent (Table 2, entries 1, 2, 5). The polydispersity indexes (U) were quite narrow and the coefficient of variations (C.V.) was less than 1.0

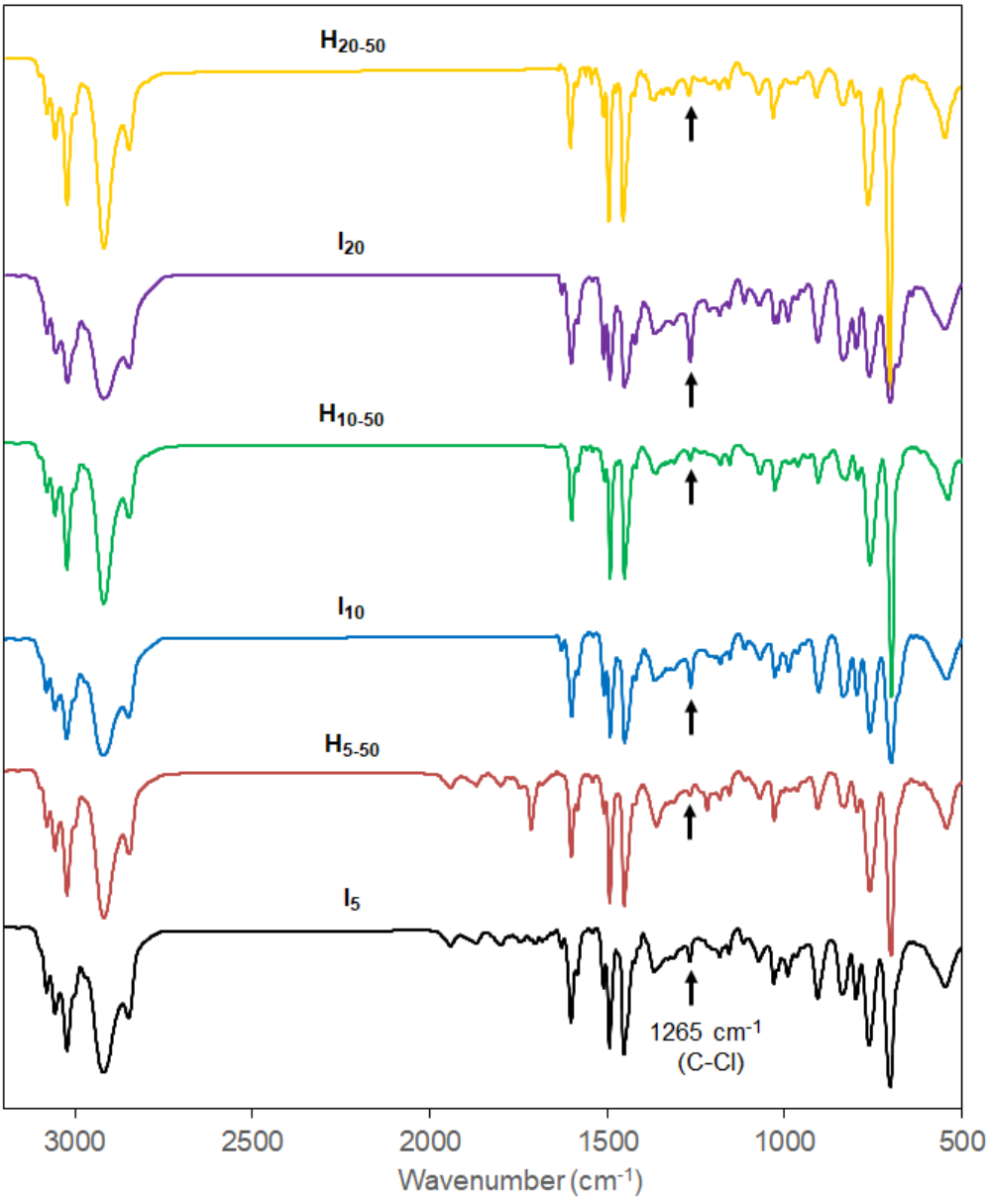

Figure 3.2 FT-IR spectra of $\mathbf{I_z}$ and the corresponding grafted polymer microsphere $\mathbf{H_{z\text{-}50}}$.

in all cases. In the FT-IR spectra of **H**, the characteristic C−Cl absorption peak at 1265 cm^{-1} derived from the macroinitiator moiety was observed (Figure 3.2). As expected, the peak intensity was smaller than that of the corresponding $\mathbf{I_z}$ due to the relative reduction of the peak intensity after the SI-ATRP. The Cl content in **H** determined by the titrimetric method were in the range from 0.346 to 1.07 mmol g^{-1}, smaller than those in $\mathbf{I_z}$, however, in good agreement with the corresponding calculated values.

*Effect of ratio of styrene to initiators (M/I) on the synthesis of **H***

Next, the effect of ratio of styrene to initiators (M/I) on the synthesis of **H** was investigated. $\mathbf{I_{20}}$ was used as a macroinitiator and M/I was set to 50, 150, 300, and 500, respectively. These results were also summarized in entries 5-8 in Table 2. The ΔW% was increased with the increase of M/I. M_n of the grafted polymer was in good agreement with those calculated (ca. 5,000, 15,000, 30,000, and 50,000 g mol^{-1}, respectively). Figure 3.3 exhibits the dependence of M_n and M_w/M_n on M/I. The M_n was increased linearly with the increase of M/I. This result indicated that the SI-ATRP was proceeded in a controlled manner. With the increase of M/I, M_w/M_n exhibited somewhat higher value. Interestingly, the D_n(**H**) was dramatically increased in the case of $\mathbf{H_{20\text{-}300}}$ and $\mathbf{H_{20\text{-}500}}$ (entries 7 and 8) (Figure 3.4). The range of diameter increase when the SI-ATRP proceeded from the surface can be estimated between 20 and 100

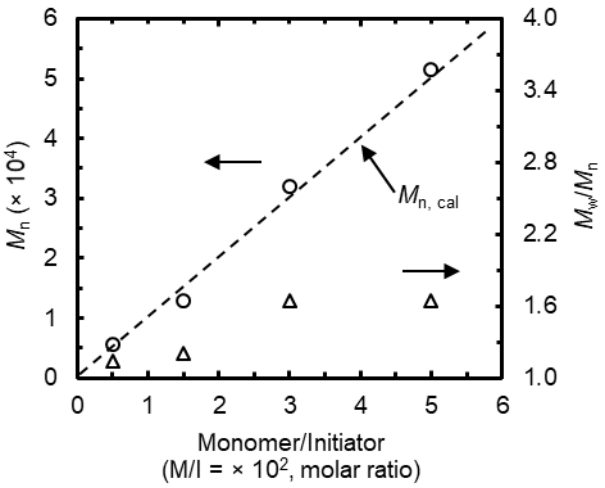

Figure 3.3 Relationship between M_n (o) or M_w/M_n (Δ) and M/I.

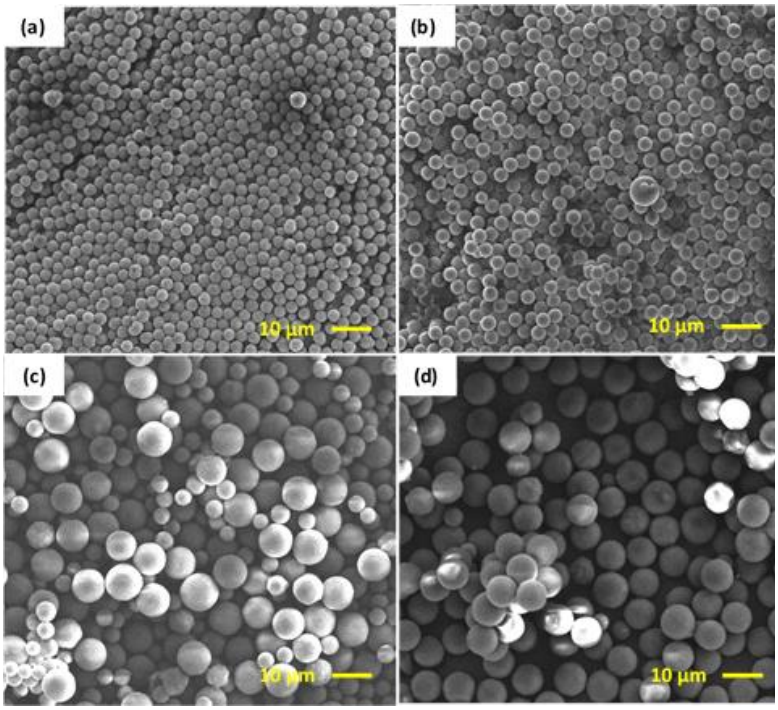

Figure 3.4 SEM images of hairy polymer microspheres $\mathbf{H_{20\text{-}M/I}}$: $\mathbf{H_{20\text{-}50}}$ (a), $\mathbf{H_{20\text{-}150}}$ (b), $\mathbf{H_{20\text{-}300}}$ (c), and $\mathbf{H_{20\text{-}500}}$ (d).

nm. The drastic increase of D_n cannot be explained by only the polymerization of styrene from the surface of core. The reason is not clear, but we anticipated that polystyrene longer chain propagated not only from the surface of core but from the inside immobilized the core structure, which was swollen in diphenyl ether with higher concentration of monomer at high temperature as illustrated in Scheme 3.6. Actually, **I$_{20}$** was well swollen under these conditions. The swelling nature of **I$_{20}$** was further investigated in Table 3.2. Under these conditions, polydispersity index (M_w/M_n) of grafted polymer was influenced on the C.V. of corresponding hairy microsphere. In addition, due to the swelling nature of **I$_{20}$**, the grafting density was overestimated and the quantification was difficult. We have also studied kinetics with monomer conversions for confirming whether the polymerization proceeds either in controlled manner or not. The plot of time versus ln[M]$_o$/[M] in the surface-initiated ATRP of styrene using **I$_{20}$** as multifunctional initiator is shown in Figure 3.5, which shows linear first-order kinetic. This result indicated that the graft polymerization of styrene proceeds in a controlled fashion. These results clearly indicate that the SI-

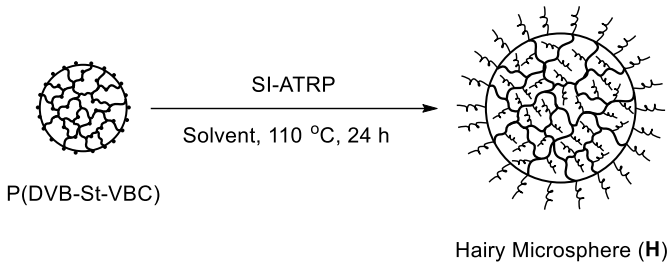

Scheme 3.6 Internal structure of hairy polymer microsphere **H**.

Table 3.2 Swelling property of **I$_{20}$**.

Polymer Microsphere	D_n (μm)[a]	Solvent	Monomer	Temp. (°C)	Time (h)	D_n (μm)[a]	D_n (μm) in solid state[a]
I$_{20}$	3.14	DPE	-	rt.	1.30	3.16	-
					24	3.23	3.13
				110	24	3.69	3.16
		-	St	rt.	1.30	3.18	-
					24	3.61	3.13

[a] Measured from optical microscope images.

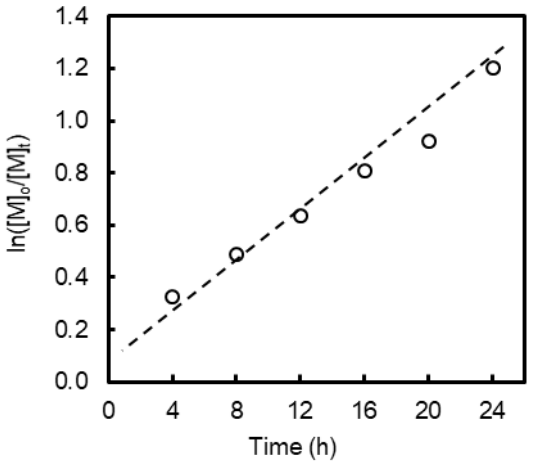

Figure 3.5 Plot of ln[M]$_o$/[M] versus reaction time for the graft polymerization of styrene (St) in DPE at 110 °C with **I$_{20}$** used as multifunctional initiator: [St]$_o$/[(**I**]$_o$/[Cu(I)Br]$_o$ /[2,2′-bipyridine]$_o$ = 100/2/2/6

ATRP of styrene (M/I ≤ 150) using **I_{20}** as a macroinitiator proceeded smoothly in a controlled grafting from polymerization manner to afford well-defined hairy polymer microspheres.

*Effect of monomer on the synthesis of **H***

Next, we synthesized different types of hairy polymer microspheres using **I_{20}** as multifunctional initiator from graft polymerization of MMA, HEMA, *n*BA, *n*BMA, *t*BMA, and NIPAm, as illustrated in Scheme 3.5. The characterization data were summarized in entries 9-14 in Table 3.1 In all cases, the increase of ΔW% was observed after the polymerization. The M_n of hair in **$H_{(MMA)}$** and **$H_{(NIPAm)}$** was higher than the M_n calculated (ca. 5,000 and 5,600, g mol^{-1}, respectively) likely due to the chain termination at the end of polymerization (entries 9 and 14). In **$H_{(nBA)}$**, **$H_{(nBMA)}$**, and **$H_{(tBMA)}$**, the M_n was close to, but somewhat higher than the M_n calculated (ca. 7,000, g mol^{-1}) due to the bimolecular

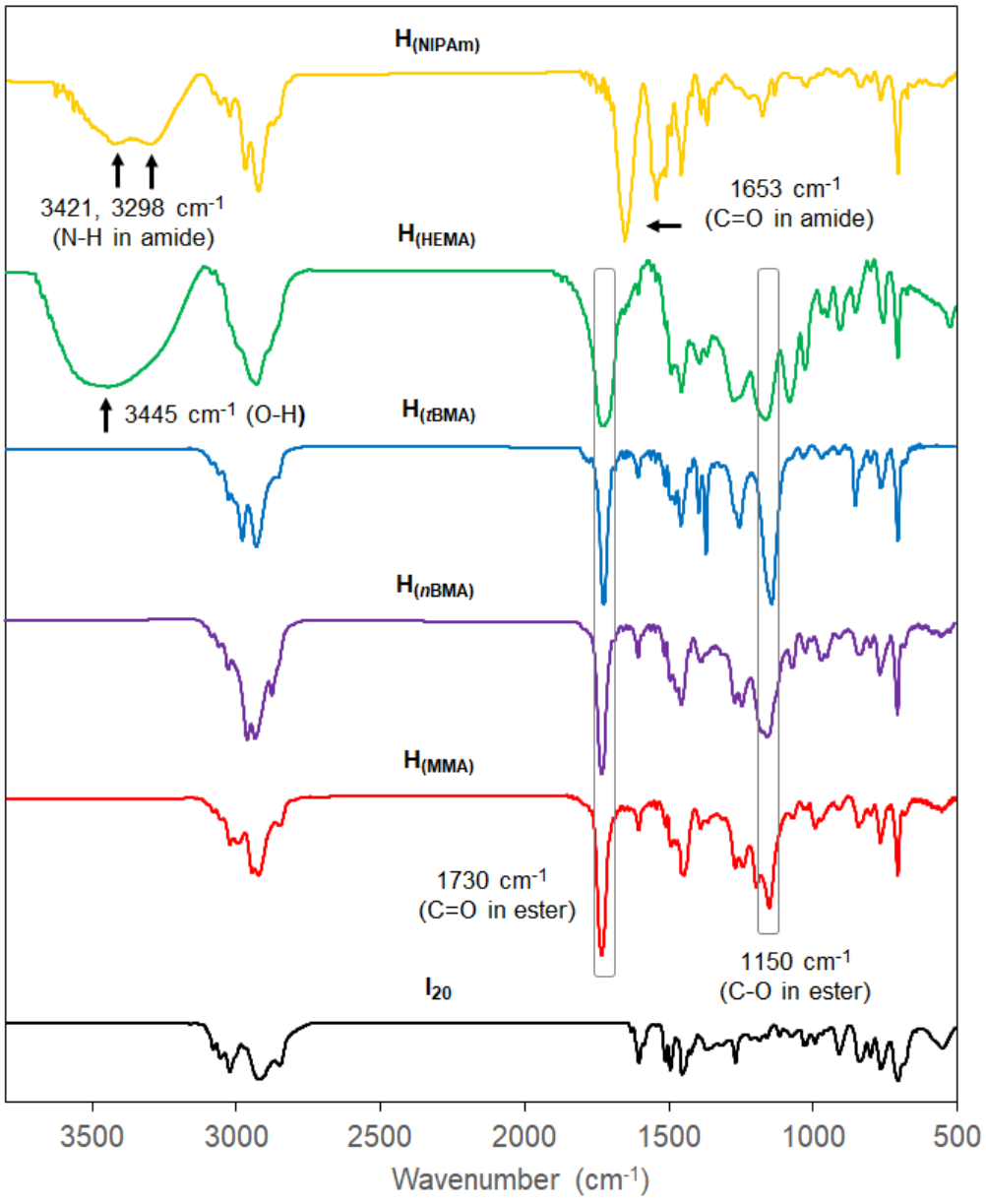

Figure 3.6 FT-IR spectra of **I_{20}** and the corresponding grafted polymer microsphere **H**.

termination at the early stage of the polymerization (entries 11-13). These M_w/M_n values are relatively high. By contrast, the M_n of hair in **H$_{(HEMA)}$** was in good agreement with the M_n calculated (ca. 6,500 g mol^{-1}). In addition, the polydispersity was enough narrow (M_w/M_n = 1.16) and C.V. was less than 1.0. These results indicate that SI-ATRP of HEMA using **I$_{20}$** proceeded in a controlled manner. Unfortunately, the control of SI-ATRP of MMA and NIPAm was difficult.

The D_n of **H** was increased from 2.94 μm of **I$_{20}$** to 3.14-3.42 μm (entries 9, 12-14), indicating the successful grafting of PMMA, P*n*BA, P*n*BMA, P*t*BMA, and PNIPAm chains onto the surface of **I$_{20}$**. In the case of **H$_{(HEMA)}$**, the D_n became approximately 8 μm. The phenomenon can be considered as same as that observed in the case of SI-ATRP of polystyrene (M/I ≥ 300). In all cases, the C.V. was less than 2.0.

Figure 3.6 shows the FT-IR spectra of hairy polymer microsphere **H**. The characteristic absorption peak found at 1653 cm^{-1} due to C−O in amide and the two absorption bands are appeared at 3421 and 3298 cm^{-1} due to N− H in amide were observed in **H$_{(NIPAm)}$**. In anothers, the characteristic strong absorption peak at 1730 cm^{-1} due to C−O in ester was apparently observed. A broad peak for O-H in grafted PHEMA chains is observed at 3445 cm^{-1} in **H$_{(HEMA)}$**. These characteristic FT-IR signals indicate that ester and amide type polymer chains were grafted onto the surface of **I$_{20}$**.

The Cl contents in **H** determined by titrimetric method were in the range of 0.792 and 1.25 mmol g^{-1}, smaller than that in **I$_{20}$** (1.64 mmol g^{-1}), which also supported the grafting PMMA, PHEMA, P*n*BA, P*n*BMA, P*t*BMA, and PNIPAm chains onto the polymer microsphere. As a result, hairy polymer microspheres having P*n*BA, P*n*BMA, or P*t*BMA chains on the surface were successfully synthesized by SI-ATRP using a monodisperse microsphere having benzyl chloride moiety.

*3.2.4 Synthesis of sulfonate core-corona polymer microsphere **2** from graft copolymerization of an achiral vinyl monomer and phenyl p-styrene sulfonate using **1** as a macroinitiator by SI-ATRP*

Polymer microsphere **1** can be used as a macroinitiator of ATRP since **1** posesses pural benzyl chloride moiety. Core-corona polymer microsphere **2** has been synthesized by SI-ATRP of styrene and phenyl *p*-styrenesulfonate using **1** as a macroinitiator, as illustrated in Scheme 3.7.

The weight increase of core-corona polymer microsphere and grafting density of corona are calculated by the following equations:

$$\text{Weight increase } (\Delta W\%) = \frac{\text{Weight of } \mathbf{2}\ (Wt_{\mathbf{2}}) - \text{Weight of } \mathbf{1}\ (Wt_{\mathbf{1}})}{\text{Weight of } \mathbf{1}\ (Wt_{\mathbf{1}})} \times 100 \quad (1)$$

$$\text{Grafting density (G.D) (chains/nm}^2) = \frac{\Delta W\% \times N_A \times V \times \rho}{S \times M_{\text{Grafted polymer}}} \quad (2)$$

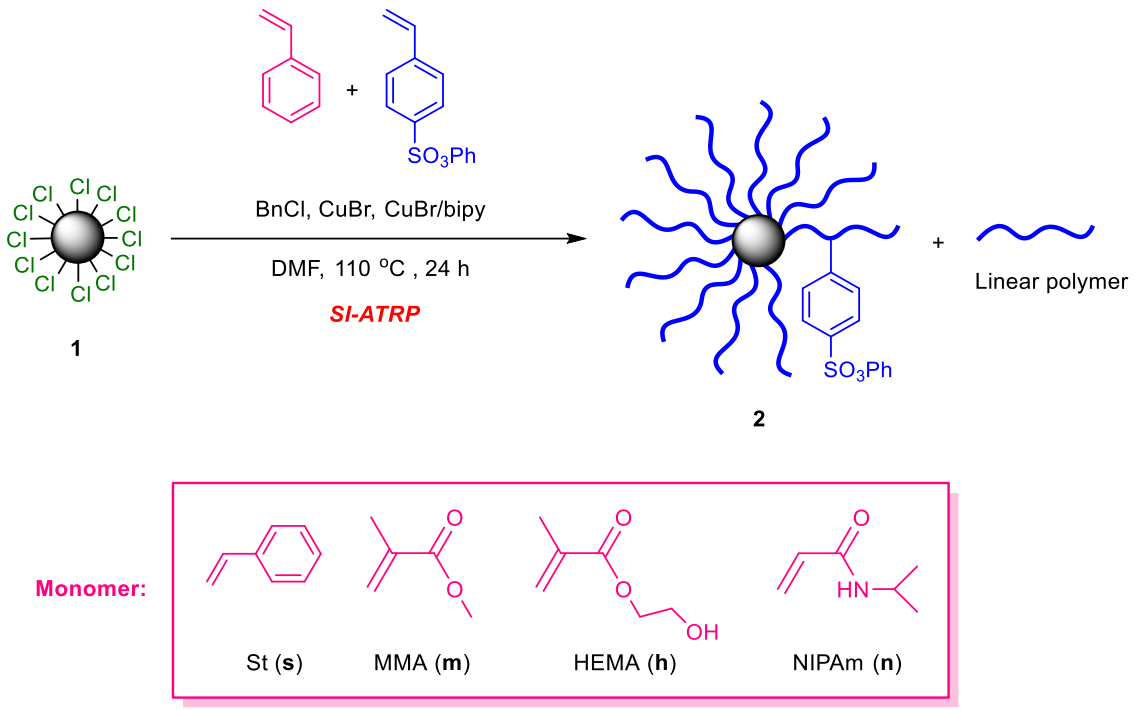

Scheme 3.7 Synthesis of sulfonate core-corona polymer microsphere **2** by SI-ATRP.

$M_{\text{Grafted polymer}}$ is M_n of grafted polymer, $V = (\frac{4}{3}) \times \pi \times (\frac{D_n}{2})^3$, $S = 4\pi \times (\frac{D_n}{2})^2$,

N_A is the Avogadro constant, ρ presents an average density 1g cm^{-3} for the core microsphere.

To measure the number-averaged molecular weight (M_n) and polydispersity (M_w/M_n) of the grafted polymers onto the surface of the polymer microspheres **1**, all the polymerization reactions were performed with the addition of a predetermined amount of the sacrificial initiator, benzyl chloride (BnCl). The free polymer formed in the polymerization reaction was then isolated for SEC analysis. The characterization of **2** was summarized in Table 3.3.

In FT-IR spectra of core-corona polymer microsphere **2,** two absorption peaks are appeared at 1375 cm^{-1} (strong) and 1175 cm^{-1} (weak) for stretching vibration of S=O bond. The peak intensity of S=O bond is increased with increasing Cl content in **1** (Figure 3.7). The signal intensity for the aromatic region is also slightly stronger than that of the corresponding **1**. The weight increase (ΔW) calculated by equation 1 was generally less than 25% when styrene and phenyl *p*-styrenesulfonate were polymerized with use of $\mathbf{1d_xhC_z}$. With the increase of z value (content of benzyl chloride moiety), ΔW was increased which was also confirmed by the intensity of absorption peaks for S=O bond in the FT-IR spectra (entries 1-4; Figure 3.7). On the other hand, ΔW was constant when the x value (content of DVB) was increased (entries 3, 5-7). Core-corona microspheres with different kind of monomer in the corona were synthesized using MMA (m), HEMA (h), and NIPAm (n) as comonomer with phenyl *p*-styrenesulfonate,

Table 3.3 Characterization of core-corona polymer microsphere **2**[a].

Entry	$\mathbf{2d_xhC_z}$	ΔW (%)[b]	Graft polymer		D_n(**1**) (μm)[b]	D_n(**2**) (μm)[b]	G.D. (chains/nm^2)[e]
	x/z		M_n[c, SEC]	M_w/M_n[c]			
1	**20/5**	3	8,300	1.29	1.07	1.12	0.40
2	**20/10**	4	6,800	1.21	1.41	1.43	0.80
3	**20/20**	16	11,200	1.40	0.80	1.02	1.0
4	**20/30**	20	8,600	1.12	1.11	1.15	2.6
5	**30/20**	21	11,900	1.41	0.94	1.07	1.7
6	**40/20**	25	9,200	1.14	1.45	1.66	4.0
7	**50/20**	20	9,700	1.22	2.20	2.25	4.6
8[f]	**20/20-A**	14	6,900	1.17	2.00	2.22	4.1
9[g,h]	**20/20-200**	33	26,400	1.54	1.12	1.32	1.4
10[g,i]	**20/20-300**	38	45,300	1.65	1.12	1.52	1.0
11[g,j]	**20/20-m**	153	14,800	1.23	1.12	1.58	1.1
12[g,k]	**20/20-h**	145	19,900	1.79	1.12	1.65	8.2
13[g,l]	**20/20-n**	31	13,200	1.80	1.12	1.40	2.6
14[m]	$\mathbf{2d_{20}sC_{20}}$	72	7,630	1.18	1.14	1.34	n.d.
15[m,n]	$\mathbf{2d_{20}sC_{20}}$	78	10,800	1.25	4.41	5.33	n.d.
16[m]	$\mathbf{2d_{20}mC_{20}}$	89	7,950	1.19	1.12	1.30	n.d.
17[m,o]	$\mathbf{2d_{20}mC_{20}}$	91	9,000	1.22	9.14	9.25	n.d.

[a] SI-ATRPs of styrene (70 mol%) and *p*-phenyl styrenesulfonate (30 mol%) were performed in the precence of $\mathbf{1d_{20}hC_{20}}$ (D_n : 0.80 μm) in DMF at 110 °C for 24 h. M/I =50.

[b] Calculated by equation 1.

[c] Determined by SEC using DMF as an eluent at a flow rate of 1.0 mL min^{-1} at 40 °C (polystyrene standards).

[d] Measured from SEM images.

[e] Calculated by equation 2.

[f] $\mathbf{1d_{20}hC_{20}}$**-BPO** was used as macroinitiator.

[g] 1.12 μm of $\mathbf{1d_{20}hC_{20}}$ was used as macroinitiator.

[h] M/I =200.

[i] M/I =300.

[j] MMA was used instead of styrene.

[k] HEMA was used instead of styrene.

[l] NIPAm was used instead of styrene.

[m] Diphenyl ether (DPE) was used as solvent.

[n] 4.41 μm of $\mathbf{1d_{20}sC_{20}}$ was used as macroinitiator.

[o] 9.14 μm of $\mathbf{1d_{20}mC_{20}}$ was used as macroinitiator.

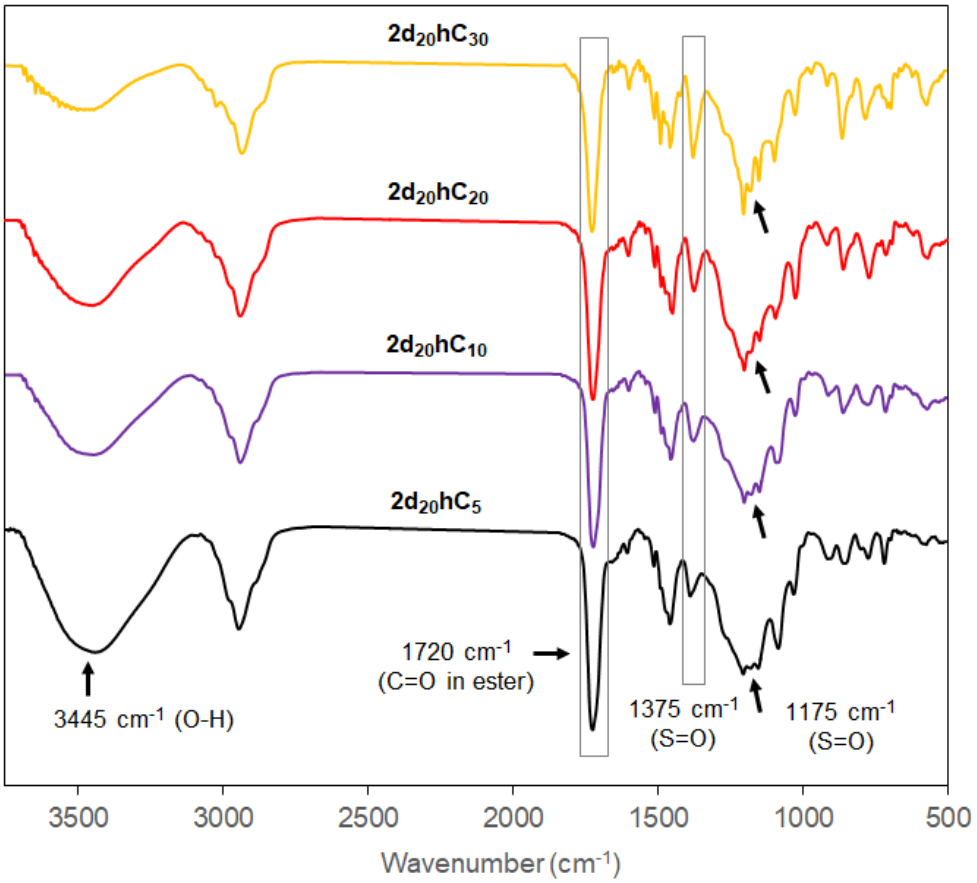

Figure 3.7 FT-IR spectra of **$2d_{20}hC_z$** (**z = 5, 10, 20, 30**).

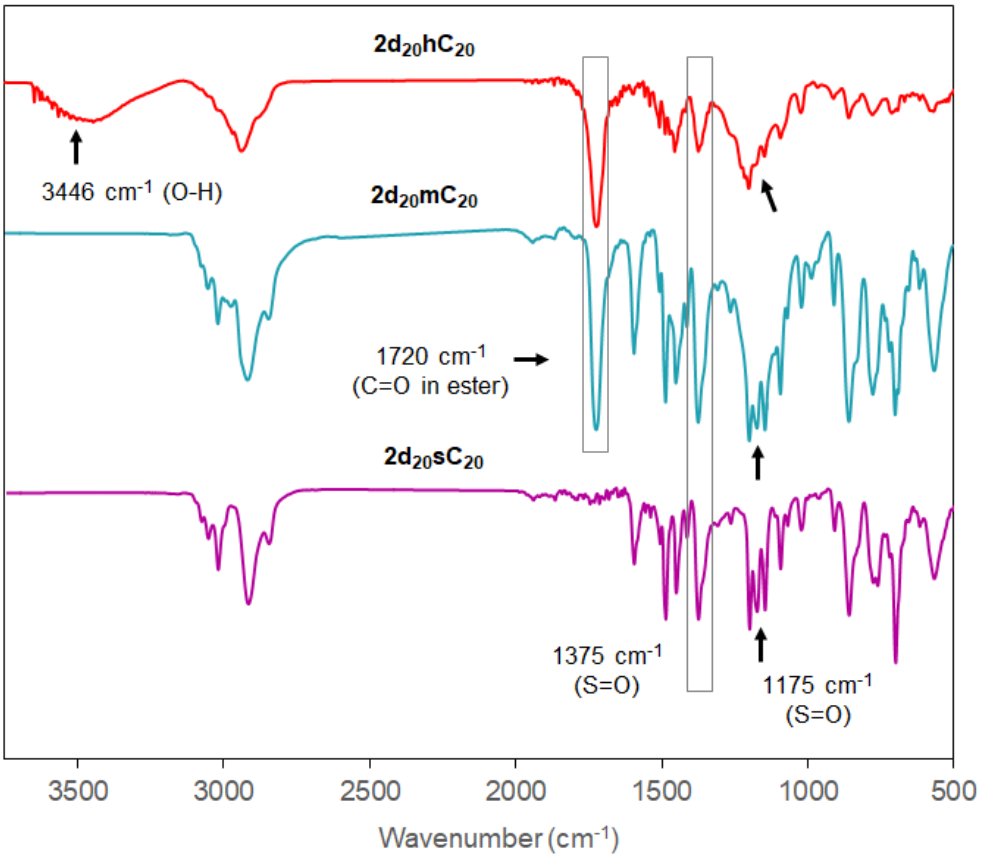

Figure 3.8 FT-IR spectra of **$2d_{20}yC_{20}$** (**y = s, m, h**).

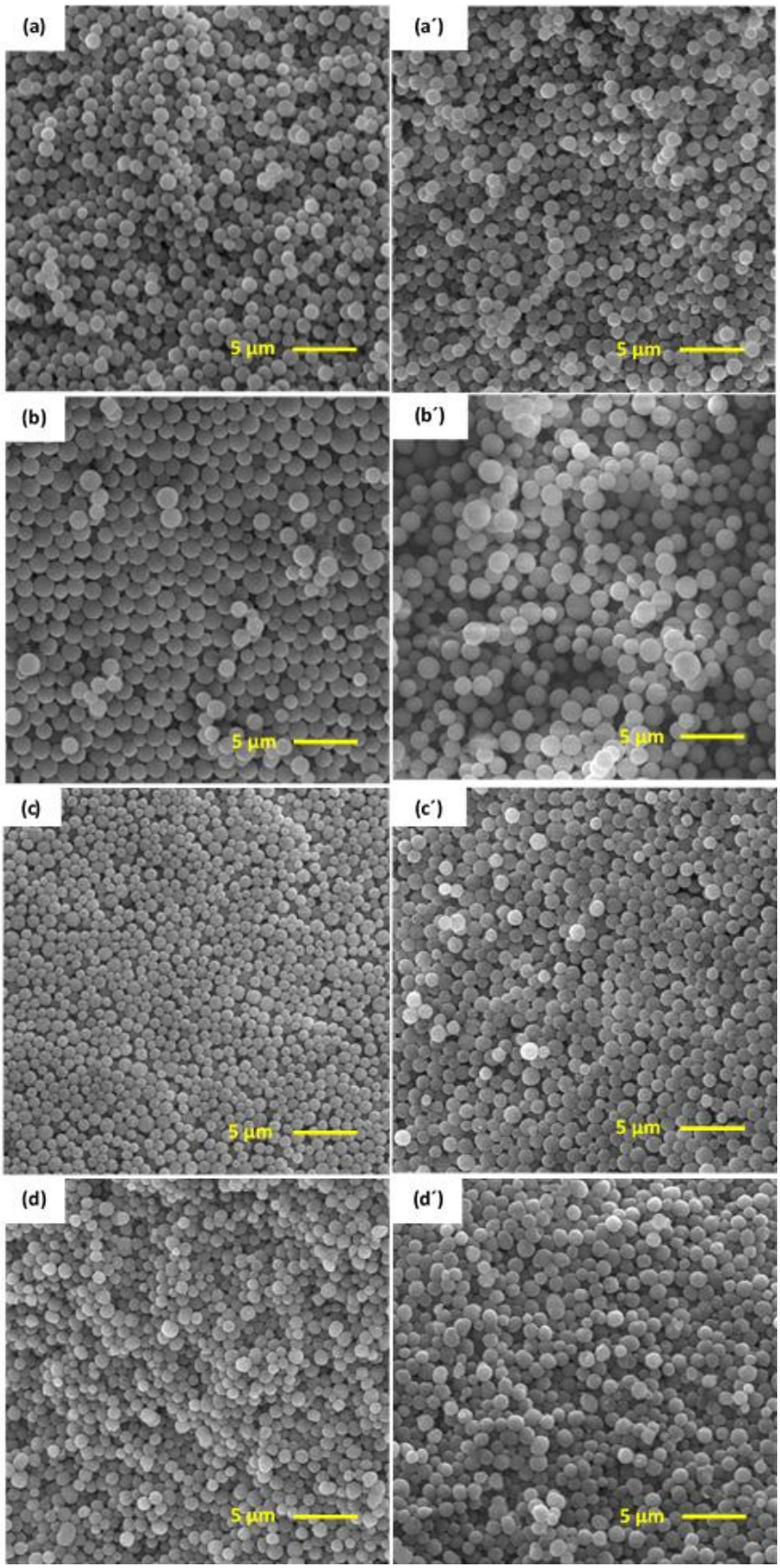

Figure 3.9 SEM images of polymer microsphere **1** and the corresponding core-corona polymer microsphere **2**: **1d$_{20}$hC$_5$** (a), **2d$_{20}$hC$_5$** (a′), **1d$_{20}$hC$_{10}$** (b), **2d$_{20}$hC$_{10}$** (b′), **1d$_{20}$hC$_{20}$** (c), **2d$_{20}$hC$_{20}$** (c′), **1d$_{20}$hC$_{30}$** (d), and **2d$_{20}$hC$_{30}$** (d′).

respectively. High ΔW was obtained when a comonomer such as MMA and HEMA was used, probably due to the high M_n of graft polymer (entries 11 and 12). ΔW was increased when **1d$_{20}$sC$_{20}$** or **1d$_{20}$mC$_{20}$** was used in the polymerization (entries 14-17) which was confirmed by FT-IR spectra of the corresponding core-corona polymer microspheres (Figure 3.8). Because in these cases, the intensity of the characteristics absorption peaks for S=O bond were increased compared to that of **2d$_{20}$hC$_{20}$** synthesized using **1d$_{20}$hC$_{20}$**. The M_n of corona estimated from the characterization of free polymer are in good agreement with the calculated value (Ca. 8,000 g mol^{-1}) and the M_w/M_n values are low (1.12-1.41) (entries 1-8). The M_n of corona in **2d$_{20}$hC$_{20}$-200** and **2d$_{20}$hC$_{20}$-300** are also in good agreement with those calculated (Ca. 32,000 and 48,000 g mol^{-1}) (entries 9 and 10). In **2d$_{20}$hC$_{20}$-m** and **2d$_{20}$hC$_{20}$-n**, the M_n of the corona (14,800 and 13,200 g mol^{-1}) were somewhat higher than those calculated, due to the bimolecular termination at the early stage of the polymerization as well as the M_w/M_n values are moderate (1.23 and 1.80, respectively) (entries 11 and 13). In **2d$_{20}$hC$_{20}$-h**, the M_n of the corona was higher than those calculated due to the chain termination at the end of polymerization as well as the M_w/M_n value is also moderate (entry 12). From these results, we found that the graft copolymerization of styrene and phenyl *p*-styrenesulfonate proceeds in a controlled manner, affording well-defined core-corona polymer microsphere **2**. Compared with the D_n of **1**, that of **2** is increased by the corona. SI-ATRP by only the surface initiator would lead to small size increase. Actually, the diameters increased in the range between 20 and 220 nm (entries 1-8, Figure 3.9 for entries 1-4). With the increase of M/I in the polymerization, **2** with high D_n was obtained (entries 3, 9 and 10). When MMA and HEMA were used instead of styrene as a comonomer, relatively larger polymer microspheres were obtained (entries 11 and 12). In the case of **2d$_{20}$sC$_{20}$**, apparently large microsphere with 5.33 μm of D_n from 4.41 μm of **1** was obtained (entry 15). The large increase of D_n may occur because the poly(styrene-*co*-phenyl *p*-styrenesulfonate) chain grows not only from the surface of **1** but also from the interior of **1**. The phenomenon only occurs when the polymer microsphere is being well swellen in the polymerization [82]. The grafting density (G.D.) was eligible, approximately 1.0 chain/nm^2. Both the z (Cl content) and x values (DVB molar ratio) affected on the G.D. (entries 1-7). As expected, higher G.D. was obtained when the larger size of core particle was used (entry 3 vs 8). G.D. was almost independent of M/I (entries 3, 9, and 10).

These results indicated that well-defined sulfonated core-corona polymer microspheres **2** were successfully synthesized by the SI-ATRP with phenyl *p*-styrenesulfonate using polymer microspheres having benzyl chloride prepared via precipitation polymerization as macroinitiators.

3.3 Conclusion

We have successfully synthesized well-defined hairy polymer microspheres **H** by the surface-initiated atom transfer radical polymerization (SI-ATRP) of styrene by using narrowly dispersed polymer microsphere having benzyl chloride moiety $\mathbf{I_z}$ prepared from precipitation polymerization. The M_n of grafted polymer can be controlled up to 15,000 g mol^{-1} by changing the M/I, and the M_w/M_n was lower than 1.30 when M/I $\leq$ 150. In addition, hairy polymer microspheres having poly(*n*BA), poly(*n*BMA), or poly(*t*BMA) chains on the surface were successfully synthesized by SI-ATRP. The living nature of the ATRP in the present PS grafted polymer microspheres and the property of swollen hairy microspheres are now for further investigation.

Monodispersed sulfonated core-corona polymer microsphere **2** was successfully synthesized by the SI-ATRP of monomer such as styrene, MMA, HEMA, and NIPAm and phenyl *p*-styrenesulfonate with monodispersed polymer microsphere having benzyl chloride moiety **1** prepared *via* precipitation polymerization as a macroinitiator. We found that the graft copolymerization of styrene and phenyl *p*-styrenesulfonate proceeded in a controlled manner, affording well-defined core-corona polymer microsphere **2** when poly(DVB-HEMA-VBC) microsphere $\mathbf{1d_xhC_z}$ having ATRP initiator moiety was used as a macroinitiator. In Chapter **IV** and **V**, these core-corona polymer microspheres functionalized with sulfonate were used as polymeric supports for the ionic immobilization of chiral cinchonidinium salt and MacMillan catalyst precursor, respectively.

3.4 Experimental

3.4.1 Materials and measurements

Styrene (Kishida Chemical Co. Ltd., Osaka, Japan) and divinylbenzene obtained from Nippon & Sumikin Chemical Co. Ltd., Japan, were washed with aqueous 10% NaOH and water, followed by distilling with CaH_2 under reduced pressure. *n*-Butyl acrylate, *n*-butyl methacrylate, and *tert*-butyl methacrylate (Kishida Chemical Co. Ltd.), 2-hydroxyethyl methacrylate (Wako Pure Chemical Industries Ltd., Japan), methyl methacrylate (Sigma-Aldrich) and 4-vinylbenzyl chloride were distilled under reduced pressure. *N*-Isopropylacrylamide (TCI, Japan) was recrystallized from a mixture of hexane and acetone (90/10, *v*/*v*) and dried at a low temperature under vacuum. Copper (I) bromide was stirred with glacial acetic acid overnight and filtered, followed by washing three times with methanol and diethyl ether and then dried under vacuum. 2,2′-Bipyridine (Nacalai Tesque, Japan), *N,N,N′,N″,N″*-pentamethyldiethylenetriamine (Sigma-Aldrich), and tris [2-(dimethylamino)ethyl]amine (Wako Pure Chemical Industries Ltd., Japan) were used as received without further purification. Diphenyl ether (Wako Pure Chemical Industries Ltd., Japan) and anisole (Kishida Chemical Co. Ltd., Japan) were

purified through passing alumina column. Methanol (Wako Pure Chemical Industries Ltd., Japan) was distilled.

Chlorine contents in hairy polymer microspheres were measured by the titrimetric method. FT-IR spectra were recorded with a JEOL JIR-7000 FT-IR spectrometer and are reported in reciprocal centimeter (cm^{-1}). SEM measurements were conducted by using JSM-IT100 at an acceleration voltage of 10.0 kV. The number-average diameter (D_n) and the dispersity index (U) were determined from the SEM image.

Number-averaged diameter (D_n), weight-averaged diameter (D_w), and polydispersity index (U) of polymer microsphere were calculated using the following equations by counting at least a hundred of individual particles from the SEM images.

$$D_n = \frac{\sum n_i d_i}{\sum n_i} \quad (3)$$

$$D_w = \frac{\sum n_i d_i^4}{\sum n_i d_i^3} \quad (4)$$

$$U = \frac{D_w}{D_n} \quad (5)$$

Where n_i is the number of particles with d_i.

The coefficient of variation (C.V.) of hairy polymer microsphere was measured by a particle size distribution analyzer (SALD-2300, Shimadzu) in THF.

3.4.2 Synthesis of hairy polymer microspheres using $\mathbf{I_z}$ *as multifunctional initiator by surface-initiated ATRP*

Representative Synthesis Procedure for $\mathbf{H_{5\text{-}50}}$: To a 6 mL vial with magnetic stir bar, CuBr (0.017 g, 0.12 mmol), $\mathbf{I_5}$ (0.176 g, 0.100 mmol of benzyl chloride moiety), and 1 mL of diphenyl ether were added. The reaction mixture was purged with Ar gas for 5 min and 2, 2′-bipyridine (56 mg, 0.36 mmol) was added. After additional 5 min of Ar gas bubbling, styrene (0.625 g, 6.00 mmol), and sacrificial initiator (benzyl chloride, 0.0025 g, 0.020 mmol) were added in the mixture. $[St]_o/[Cl]_o$ (in $\mathbf{I_5}$ and BnCl)/ $[CuBr]_o/[bipy]_o$ (molar ratio) is set to 100/2/2/6. The polymerization was carried out in oil bath at 110 ^oC for 24 h with stirring at 400 rpm. The resulting blue-green polymer particles were isolated by centrifugation and washed with THF three times, and washed with methanol and glacial acetic acid (95/5, *v/v*) several times until resulting solids became almost white. Finally, these solids were washed with diethyl ether twice. These hairy polymer particles were dried at 40 ^oC under vacuum oven.

The free polymers were collected from the supernatant by precipitation into MeOH that were further purified. The resulting linear polymers were dried at 40 ^oC under vacuum oven to afford white powders.

$H_{5\text{-}50}$: FT-IR (KBr): *v* = 1267 (C−Cl), 1601, 1493, 1452 (C=C in aromatic ring), 3059, 3025 (C−H in aromatic ring), 2921, and 2849 (C−H in alkyl) cm^{-1}. Chlorine content: 0.346 mmol g^{-1}.

$H_{10\text{-}50}$: FT-IR (KBr): *v* = 1266 (C−Cl), 1601, 1493, 1452 (C=C in aromatic ring), 3059, 3025 (C−H in aromatic ring), 2921, and 2849 (C−H in alkyl) cm^{-1}. Chlorine content: 0.805 mmol g^{-1}.

$H_{20\text{-}50}$: FT-IR (KBr): *v* = 1266 (C−Cl), 1601, 1493, 1452 (C=C in aromatic ring), 3059, 3025 (C−H in aromatic ring), 2921, and 2849 (C−H in alkyl) cm^{-1}. Chlorine content: 1.07 mmol g^{-1}.

$H_{20\text{-}150}$: FT-IR (KBr): *v* = 1266 (C−Cl), 1602, 1493, 1452 (C=C in aromatic ring), 3059, 3025 (C−H in aromatic ring), 2919, and 2848 (C−H in alkyl) cm^{-1}. Chlorine content: 1.06 mmol g^{-1}.

$H_{20\text{-}300}$: FT-IR (KBr): *v* = 1266 (C−Cl), 1601, 1493, 1452 (C=C in aromatic ring), 3059, 3025 (C−H in aromatic ring), 2921, and 2849 (C−H in alkyl) cm^{-1}. Chlorine content: 0.720 mmol g^{-1}.

$H_{20\text{-}500}$: FT-IR (KBr): *v* = 1601, 1493, 1451 (C=C in aromatic ring), 3059, 3024 (C−H in aromatic ring), 2920, and 2847 (C−H in alkyl) cm^{-1}. Chlorine content: 0.165 mmol g^{-1}.

$H_{(MMA)}$: FT-IR (KBr): *v* = 1731 (C=O in ester), 1193, and 1148 (C−O) cm^{-1}. Chlorine content: 1.07 mmol g^{-1}.

$H_{(HEMA)}$: FT-IR (KBr): *v* = 1726 (C=O in ester), 1270, 1159 (C−O), and 3446 (O−H) cm^{-1}. Chlorine content: 0.792 mmol g^{-1}.

$H_{(nBA)}$: FT-IR (KBr): *v* = 1733 (C=O in ester), 1168, and 1077 (C−O) cm^{-1}. Chlorine content: 1.25 mmol g^{-1}.

$H_{(nBMA)}$: FT-IR (KBr): *v* = 1727 (C=O in ester), 1236, 1161 (C−O) cm^{-1}. Chlorine content: 0.990 mmol g^{-1}.

$H_{(tBMA)}$: FT-IR (KBr): *v* = 1718 (C=O in ester), 1250, 1141 (C−O) cm^{-1}. Chlorine content: 1.21 mmol g^{-1}.

$H_{(NIPAm)}$: FT-IR (KBr): *v* = 1653 (C=O in amide), 1236, 1161 (C−O), 3421, 3308 (N−H), 1456 (C−N) cm^{-1}. Chlorine content: 0.978 mmol g^{-1}.

*3.4.3 Synthesis of p-phenyl styrenesulfonate (**S**)*

3.4.3.1 Synthesis of p-styrenesulfonyl chloride

A 100-mL round-bottomed flask with a magnetic stirring bar was slowly charged with thionyl chloride (12.4 mL, 171 mmol) under N_2 gas at room temperature and then *p*-styrenesulfonic acid sodium salt (5.01 g, 24.3 mmol) was added to the solution. Immediately, the flask was transferred in an ice bath and 7.5 mL of dry DMF was added via a syringe in very slowly at 0 °C. The ice bath was removed after adding DMF. The flask was covered by aluminium foil, and the reaction was continued for 12 h at room

temperature under N_2 gas. The crude product was extracted with Et_2O (50 mL × 3). Et_2O was removed by rotary evaporator and pumped up for 10 min. The purified compound, *p*-styrenesulfonyl chloride is light yellow liquid. 4.77 g, 95% Yield. ^{1}H NMR (400 MHz, $CDCl_3$, δ = 7.26 ($CDCl_3$, TMS): δ = 5.55 (d, $^3J_{cis}$ (H,H) = 11.0 Hz, 1H; =CH), 5.98 (d, $^3J_{trans}$ (H,H) = 17.7 Hz, 1H; =CH), 6.79 (dd, $^3J_{cis}$ (H,H) = 11.0 and $^3J_{trans}$ (H,H) = 17.7 Hz, 1H; =$CH_{cis}H_{trans}$), 7.62 (d, ^3J (H,H) = 8.5 Hz, 2H; Ar), 8.00 (d, ^3J (H,H) = 8.5 Hz, 2H; Ar).

*3.4.3.2 Synthesis of p-phenyl styrenesulfonate (**S**)*

To a 100-mL round bottomed flask with a magnetic stirr bar, phenol (2.18 g, 23.2 mmol) and pyridine (9.95 mL, 124 mmol) was added at room temperature. The mixure was then cooled to 0 °C and *p*-styrenesulfonyl chloride (4.77 g, 23.6 mmol) was added at 0 °C. The flask was covered by aluminium foil, and the mixture was kept at room temperature for 24 h. After the reaction, 1 M HCl (60 mL) was added, and the crude product was extracted with $CHCl_3$ (30 mL×3). The organic layer was washed with 1M HCl (60 mL) and 5% K_2CO_3 (50 mL × 2), respectively. The solvent ($CHCl_3$) was removed by rotary evaporator. The crude product was purified by column chromatography on silica gel with 3:2 hexane/CH_2Cl_2 as eluents to afford phenyl *p*-styrenesulfonate as yellowish liquid. 2.61 g, 55% Yield, R_f = 0.51. ^{1}H NMR (400 MHz, $CDCl_3$, δ = 7.26 ($CDCl_3$), TMS): δ = 5.48 (d, $^3J_{cis}$ (H,H) = 10.7 Hz, 1H; =CH), 5.92 (d, $^3J_{trans}$ (H,H) = 17.7 Hz, 1H; =CH), 6.75 (dd, $^3J_{cis}$ (H,H) = 11.0 and $^3J_{trans}$ (H,H) = 17.7 Hz, 1H; =$CH_{cis}H_{trans}$), 6.99 (d, ^3J (H,H) = 7.9 Hz, 2H; Ar), 7.24-7.31 (m, 3H; Ar), 7.51 (d, ^3J (H,H) = 8.5 Hz, 2H; Ar). ^{13}C NMR (100 MHz, $CDCl_3$, δ = 77.1 ($CDCl_3$)): δ = 118.4, 122.4, 126.7, 127.2, 128.8, 129.7, 129.9, 134.0, 135.1, 143.3, 149.6.

*3.4.4 Synthesis of core-corona polymer microspheres **2** from graft copolymerization of monomer (styrene, MMA, HEMA, and NIPAm) and phenyl p-styrenesulfonate (**S**) using **1** as multifunctional Initiator by SI-ATRP*

*Representative synthesis procedure for **2d$_{20}$hC$_{20}$***: To a 6 mL vial with magnetic stir bar, CuBr (0.035 g, 0.24 mmol), **1d$_{20}$hC$_{20}$** (0.128 g, 0.200 mmol), and dry DMF (2 mL) were added. The reaction mixture was purged with Ar gas for 5 min and 2, 2′-bipyridine (0.114 g, 0.730 mmol) was added. After additional 5 min of Ar bubbling, 70 mol% of styrene (0.879 g, 8.44 mmol), 30 mol% of *p*-phenyl styrenesulfonate (0.939 g, 3.61 mmol) and a sacrificial initiator (benzyl chloride, 0.0050 g, 0.039 mmol) were added in the mixture. $[St+S]_o/[Cl]_o$ (in **1d$_{20}$hC$_{20}$** and BnCl)/ $[CuBr]_o/[bipy]_o$ (molar ratio) was set to 100/2/2/6. The polymerization was carried out at 110 °C for 24 h. The resulting blue-green polymer particles were isolated by centrifugation, and washed with THF three times, and washed with methanol and glacial acetic acid (95/5, *v/v*)) several times until resulting solids became almost white. Finally, these solids

were washed with Et_2O twice. These core-corona polymer microspheres were dried at 40 °C under vacuum oven.

The free polymer was collected from the supernatant by the precipitation into MeOH (125 mL). The crude polymer was then dissolved in THF and passed over alumina column to remove metals. Finally, the resulting polymer was collected by dropwise adding in MeOH, followed by filtration and then dried at 40 °C under vacuum oven to provide a white powder.

$2d_{20}hC_{20}$ ($2d_{20}hC_{20}$-s): FT-IR (KBr): ν = 1374, 1176 (S=O), 1597, 1488, 1453 (C=C in aromatic ring), 1726 (C=O in ester), 2939 (C−H in alkyl), and 3447 (O−H) cm^{-1}.

$2d_{20}hC_{20}$-m: FT-IR (KBr): ν = 1376, 1147 (S=O), 1597, 1488, 1455 (C=C in aromatic ring), 1725 (C=O in ester), 2948 (C−H in alkyl), and 3489 (O−H) cm^{-1}.

$2d_{20}hC_{20}$-h: FT-IR (KBr): ν = 1373, 1175 (S=O), 1597, 1488, 1456 (C=C in aromatic ring), 1724 (C=O in ester), 3058 (C−H in aromatic ring), 2945 (C−H in alkyl), and 3446 (O−H) cm^{-1}.

$2d_{20}hC_{20}$-n: FT-IR (KBr): ν = 1374, 1176 (S=O), 1597, 1488, 1455 (C=C in aromatic ring), 1725 (C=O in ester), 1660 (C=O in amide), 2937 (C−H in alkyl), and 3422 (O−H) cm^{-1}.

$2d_{20}mC_{20}$: FT-IR (KBr): ν = 1376, 1174 (S=O), 1601, 1487, 1448 (C=C in aromatic ring), 3058, 3023, (C−H in aromatic ring), 1726 (C=O in ester), and 2921, 2850 (C−H in alkyl) cm^{-1}.

$2d_{20}sC_{20}$: FT-IR (KBr): ν = 1377, 1177 (S=O), 1597, 1489, 1453 (C=C in aromatic ring), 3058, 3024, (C−H in aromatic ring), and 2921, 2850 (C−H in alkyl) cm^{-1}.

References

[1] Lindenblatt, G.; Schartl, W.; Pakula, T.; Schmidt, M. *Macromolecules* **2000**, *33*, 9340 - 9347.

[2] Zhu, M. Q.; Wang, L. Q.; Exarhos, G. J.; Li, A. D. Q. *J. Am. Chem. Soc.* **2004**, *126*, 2656 - 2657.

[3] Pyun, J.; Kowalewski, T.; Matyjaszewski, K. Macromol. *Rapid Commun.* **2003**, *24*, 1043 - 1059.

[4] Mandal, T. K.; Fleming, M. S.; Walt, D. R. *Nano Lett.* **2002**, *2*, 3 - 7.

[5] Sill, K.; Emrick, T. *Chem. Mater.* **2004**, *16*, 1240 - 1243.

[6] Kickelbick, G.; Holzinger, D.; Brick, C.; Trimmel, G.; Moons, E. *Chem. Mater.* **2002**, *14*, 4382 - 4389.

[7] Vestal, C. R.; Zhang, Z. *J. Am. Chem. Soc.* **2002**, *124*, 14312 - 14313.

[8] Xu, F.; Neoh, K.; Kang, *E. Prog. Polym. Sci.* **2009**, *34*, 719 - 761.

[9] Berger, S.; Synytska, A.; Ionov, L.; Eichhorn, K.; Stamm, M. *Macromolecules* **2008**, *41*, 9669 - 9676.

[10] Henze, M.; Mädge, D.; Prucker, O.; Rühe J. *Macromolecules* **2014**, *47*, 2929 - 2937.

[11] Otsu, T. *J. Polym. Sci. Part A: Polym. Chem.* **2000**, *38*, 2121 - 2136.

[12] Hawker, C. J.; Bosman, A. W.; Harth, E. *Chem. Rev.* **2001**, *101*, 3661 - 3688.

[13] Matyjaszewski, K.; Xia, J. *Chem. Rev.* **2001**, *101*, 2921 - 2990.

[14] Kamigaito, M.; Ando, T.; Sawamoto, M. *Chem. Rev.* **2001**, *101*, 3689 - 3745.

[15] Percec, V.; Barboiu, B. *Macromolecules* **1995**, *28*, 7970 - 7972.

[16] Mcleary, J. B.; Klumperman, B. *Soft Matter.* **2006**, *2*, 45 - 53.

[17] Lowe, A. B.; McCormick, C. L. *Prog. Polym. Sci.* **2007**, *32*, 283 - 351.

[18] Moad, G.; Rizzardo, E.; Thang, S. H. *Polymer* **2008**, *49*, 1079 - 1131.

[19] Wang, J.-S.; Matyjaszewski, K. *J. Am. Chem. Soc.* **1995**, *117*, 5614 - 5615.

[20] Kato, M.; Kamigaito, M.; Sawamoto, M.; Higashimura, T. *Macromolecules* **1995**, *28*, 1721 - 1723.

[21] von Werne, T.; Patten, T. E. *J. Am. Chem. Soc.* **1999**, *121*, 7409 - 7410.

[22] von Werne, T.; Patten, T. E. *J. Am. Chem. Soc.* **2001**, *123*, 7497 -7505.

[23] Carrot, G.; Diamanti, S.; Manuszak, M.; Charleux, B.; Vairon, I. P. *J. Polym. Sci., Part A: Polym. Chem.* **2001**, *39*, 4294 - 4301.

[24] Pyun, J.; Matyjaszewski, K.; Kowalewski, T.; Savin, D.; Patterson, G. D.; Kickelbick, G.; Huesing, N. *J. Am. Chem. Soc.* **2001**, *123*, 9445 - 9446.

[25] Pyun, J.; Jia, S. J.; Kowalewski, T.; Patterson, G. D.; Matyjaszewski, K. *Macromolecules* **2003**, *36*, 5094 - 5104.

[26] Carrot, G.; El Harrak, A.; Oberdisse, J.; Jestin, J.; Boue, F. *Soft Matter* **2006**, *2*, 1043 - 1047.

[27] Ohno, K.; Morinaga, T.; Koh, K.; Tsujii, Y.; Fukuda, T. *Macromolecules* **2005** *38*, 2137 - 2142.

[28] Wu, L.; Glebe, U.; Böker, A. *Macromolecules* **2016**, *49*, 9586 - 9596.

[29] Zou, H.; Wu, S.; Shen, J. *Chem. Rev.* **2008**, *108*, 3893 - 3957.

[30] Wu, L.; Glebe, U.; Boöker, A. *Polym. Chem.* **2015**, *6*, 5143 - 5184.

[31] Wu, T.; Zhang, Y.; Liu, S. *Chem. Mater.* **2008,** *20*, 101 - 109.

[32] Zheng, G.; Stöver, H. D. H. *Macromolecules* **2002**, *35*, 6828 - 6834.

[33] Zheng, G.; Stöver, H. D. H. *Macromolecules* **2003**, *36*, 1808 - 1814.

[34] Masci, G.; Giacomelli, L.; Crescenzi, V. *Macromol. Rapid Commun.* **2004**, *25*, 559 - 564.

[35] Xia, Y.; Yin, X. C.; Burke, N. A. D.; Stöver, H. D. H. *Macromolecules* **2005**, *38*, 5937 - 5943.

CHAPTER IV

Synthesis of Core-corona Polymer Microsphere-supported Cinchonidinium Salt and Its Application to Asymmetric Synthesis

4.1 Introduction

Asymmetric synthesis using a chiral quaternary ammonium salt as organocatalyst has been extensively studied in past decades. Since the pioneering work by a research group at Merck in 1984, chiral quaternary ammonium salts derived from cinchona alkaloid have been widely used as chiral organocatalyst in various asymmetric reactions.[1-10] Employing a chiral organocatalyst under a homogeneous condition, a tedious work-up procedure is often required to isolate and purify the product form a reaction mixture. Regarding the production of fine chemicals without contamination of catalysts, recovery of chiral organocatalysts is very essential considering the principles of sustainable development. Immobilization of chiral quaternary ammonium salt onto solid support has been an attractive approach for catalytic asymmetric reactions because of the enhancement of sustainability. Although there have been numerous reports on covalently bonded polymer-immobilized chiral quaternary ammonium salts for asymmetric alkylation reaction,[11-25] these heterogeneous catalysts sometimes offer inherent disadvantages, such as low selectivity and low catalytic activity. Itsuno et al. have developed two methods for the ionically immobilization of chiral quaternary ammonium salts.[26] The first method involves the polymerization of a chiral quaternary ammonium sulfonate monomer, and the second one is the immobilization of a chiral quaternary ammonium salt onto a sulfonated polymer through an ion exchange reaction. The latter is a facile and general technique for the immobilization of ammonium onto sulfonated polymers regardless of kinds of ammonium and sulfonated polymer. These polymeric chiral quaternary ammonium salts were successfully used as polymeric organocatalysts in the asymmetric alkylation of a glycine derivative. They have also developed the ammonium sulfonate formation for the synthesis of main-chain ionic polymers and successfully applied for asymmetric reactions.[27,28] The catalytic ability of these main-chain chiral ionic polymers were also tested in the benzylation of *N*-diphenylmethylene gylcine *tert*-butyl ester, showing increased enantioselectivity but loss of activity.

As well as linear or crosslinked polymer, polymer microsphere can be used as support polymer for catalyst. Some polymer microspheres functionalized with catalyst have been applied to organic reactions. For example, poly(DVB-*co*-methacrylic acid) microsphere-stabilized gold metallic colloids were used in the reduction of nitrophenol with $NaBH_4$ in water.[29] Chitosan microsphere-supported palladium complexes were applied in Mizoroki-Heck reaction of aryl halides with phenylboronic acid.[30] Core-shell poly(styrene-methyl methacrylate) microspheres with palladium-iminodiacetic acid were used as

a catalyst in Suzuki and Heck reactions in aqueous media.[31] Our research group was developed uniform-, core-shell-, and core-corona-type polymer microsphere-supported chiral ligands in an asymmetric transfer hydrogenation.[32] The introduction site of the chiral catalyst and the hydrophobicity of the microspheres, as well as the degree of crosslinking, were significantly affected on this reaction. Recently, micron-/nano-sized hairy microsphere-supported MacMillan catalyst was used in the Diels–Alder reaction in water.[33]

Nevertheless of the efficiency of polymer microsphere as polymer support, there is no report on the immobilization of chiral cinchonidinium salt onto polymer microspheres. Monodisperse sulfonated uniform microspheres or sulfonated core-corona polymer microspheres seem to be suitable solid-supports for the ionic immobilization of chiral cinchonidinium salt because of their high surface area, facile dispersibility, and mechanical strength. In addition, an advantage of polymer microspheres is the ability to control their hydrophilic-hydrophobic balance, which offers suitable microenvironments for catalytic asymmetric reactions. In our recent work, we have successfully synthesized hairy polymer microspheres by surface-initiated atom transfer radical polymerization (SI-ATRP) using monodisperse polymer microspheres having benzyl chloride moiety synthesized via precipitation polymerization as a macroinitiator.[34]

In this Chapter, core-corona microsphere-supported chiral cinchonidinium salts were synthesized by the ion exchange reaction of sulfonated core-corona microspheres with chiral cinchonidinium salt. These core-corona microsphere-supported chiral cinchonidinium salts were applied as heterogeneous organocatalysts in the asymmetric alkylation reaction of glycine Schiff base. The effect of nature of core and corona (kinds of monomer, composition, diameter, and length of corona) on the catalytic activity was investigated in detail.

4.2 Results and Discussion

*4.2.1 Synthesis of sulfonate core-corona polymer microsphere **2** from the graft copolymerization of an of achiral vinyl monomer and phenyl p-styrene sulfonate using **1** as a macroinitiator by SI-ATRP*

Core-corona polymer microsphere **2** was synthesized by surface-initiated atom transfer radical polymerization (SI-ATRP) of an achiral monomer (styrene, MMA, HEMA, or NIPAm) and phenyl *p*-styrenesulfonate (**S**) using **1** prepared vai precipitation polymerization as a macroinitiator, as illustrated in Scheme 4.1. The characterization of **2** was summarized in Table 3.2 of Chapter **III**. We found that the graft copolymerization of styrene and phenyl *p*-styrenesulfonate proceeded in a controlled manner when poly(DVB-HEMA-VBC) microsphere $\mathbf{1d_xhC_z}$ was used as a macroinitiator, affording well-defined core-corona polymer microsphere **2**. Compared with the D_n of **1**, that of **2** was increased by the

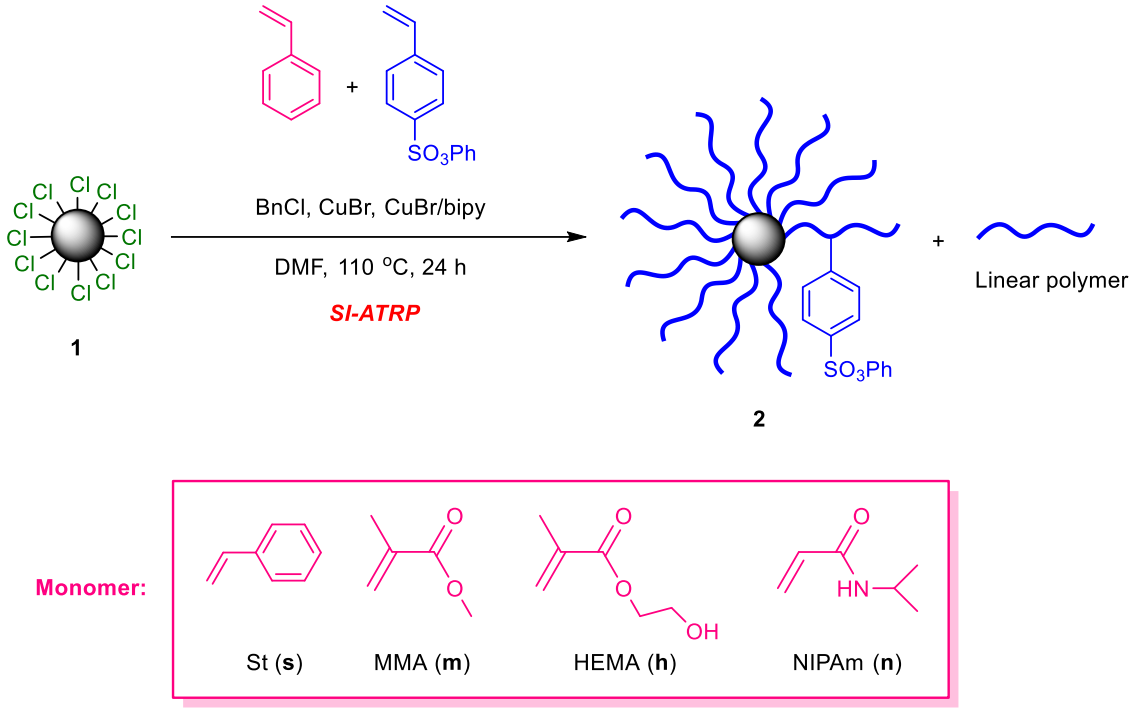

Scheme 4.1 Synthesis of sulfonate core-corona polymer microsphere **2** by SI-ATRP.

corona. SI-ATRP by only the surface initiator would lead to small size increase. Actually, the diameters increased in the range between 20 and 220 nm.

*4.2.2 Synthesis of core-corona polymer microsphere-supported chiral cinchonidinium salt **5** by ion exchange reaction*

Core-corona polymer microsphere-supported chiral cinchonidinium salt **5** was prepared by the ion exchange reaction[26] between core-corona polymer microsphere having sodium sulfonate moiety **3** and chiral cinchonidinium salt **4**, as illustrated in Scheme 4.2. **3** was synthesized by adding three equivalents

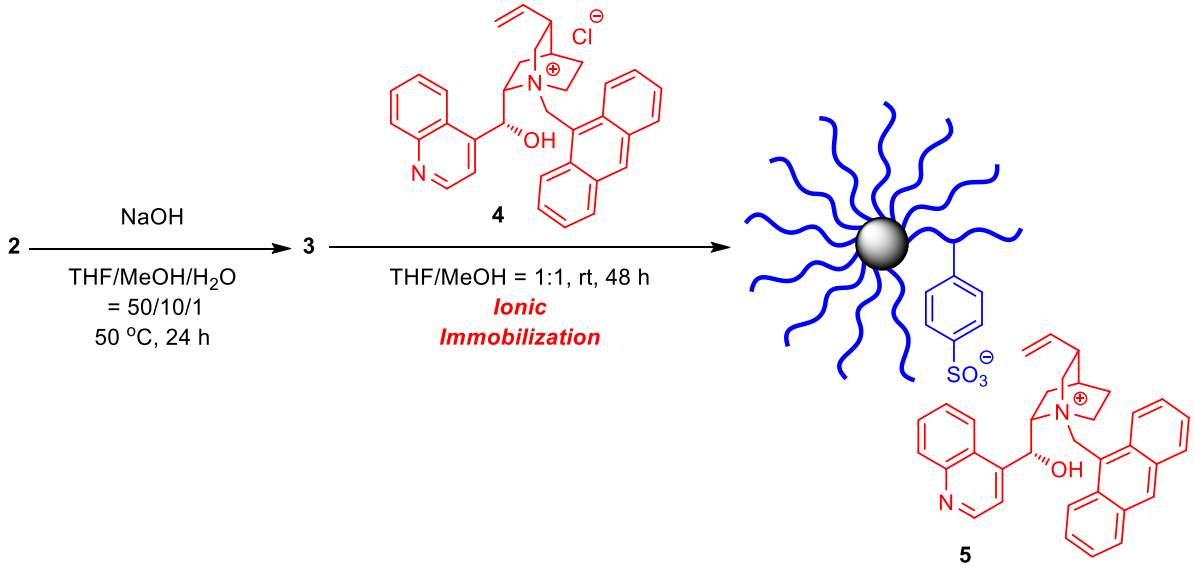

Scheme 4.2 Synthesis of core-corona polymer microsphere-supported chiral cinchonidinium catalyst **5**.

Table 4.1 Characterization of sodium sulfonate core-corona polymer microsphere **3** and core-corona polymer microsphere-supported chiral cinchonidinium catalyst **5**.

Entry	**3d$_x$hC$_z$** **x/z**	Yield (%)[b]	Sodium Sulfonate Content (mmol g^{-1})	**5d$_x$hC$_z$** **x/z**	Degree of Immobilization (%)	Catalyst Content (mmol g^{-1})[a]
1	**3d$_{20}$sC$_{20}$**	94	0.921	**5d$_{20}$sC$_{20}$**	41	0.326
2	**3d$_{20}$mC$_{20}$**	90	1.01	**5d$_{20}$mC$_{20}$**	43	0.365
3	**20/5**	94	0.0495	**20/5**	73	0.0354
4	**20/10**	95	0.0874	**20/10**	76	0.0644
5	**20/20**	93	0.273	**20/20**	100	0.377
6	**20/30**	83	0.447	**20/30**	50	0.355
7	**30/20**	89	0.841	**30/20**	65	0.468
8	**40/20**	100	0.925	**40/20**	70	0.484
9	**50/20**	97	0.931	**50/20**	86	0.200
10	**20/20-A**	92	0.250	**20/20-A**	58	0.342
11	**20/20-200**	85	0.718	**20/20-200**	59	0.278
12	**20/20-300**	76	0.553	**20/20-300**	88	0.756
13	**20/20-m**	88	1.32	**20/20-m**	68	0.558
14	**20/20-h**	91	1.11	**20/20-h**	100	0.377
15	**20/20-n**	81	0.459	**20/20-n**	100	0.377

[a] Determined based on recovered catalyst.

of NaOH to phenylsulfonate moiety of **2** in 50:10:1 THF:MeOH:H_2O mixed solvent at 50 ^oC for 24 h. The yield and sodium sulfonate content were summarized in Table 4.1. The ion exchange reaction was conducted by adding CH_3OH solution of **4** (2 equiv.) to THF solution of **3** at room temperature. The resulting light yellow polymer particles were obtained after centrifugation, washed with solvents, and dryness. The yield, degree of immobilization of **4**, and catalyst content were also summarized in Table 4.1.

The degree of immobilization in **5** were moderate to quantitative, which was depend on the property of **2**. The degree of immobilization was decreased when hydrophobic crosslinked polymer microspheres were used as core. The catalyst content in **5** determined based on the recovered catalyst was in the range of 0.0356 and 0.756 mmol g^{-1}. Unfortunately, from FT-IR spectra of **5**, the characteristic absorptions peaks for C=C and O−H bonds in cinchonidinium moiety were not observed due to the overlap with the C=C and broad O−H peaks by the core. The D_n of **3d$_{20}$hC$_{20}$** and **5d$_{20}$hC$_{20}$** were 1.02

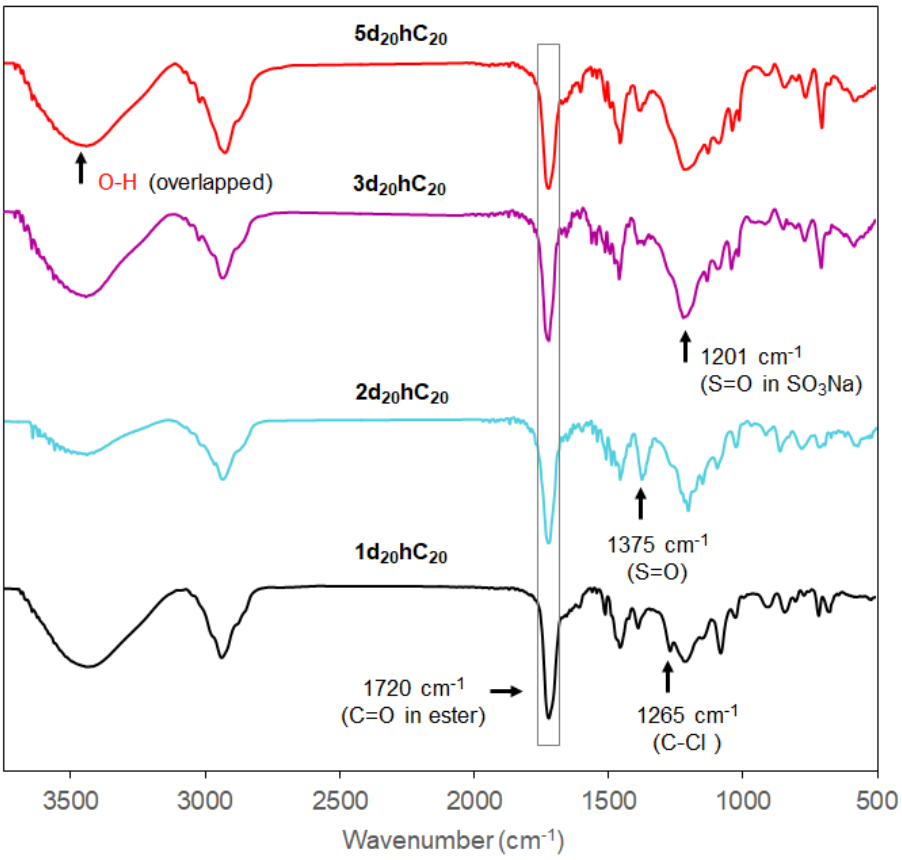

Figure 4.1 FT-IR spectra of **1d$_{20}$hC$_{20}$**, **2d$_{20}$hC$_{20}$**, **3d$_{20}$hC$_{20}$**, and **5d$_{20}$hC$_{20}$**.

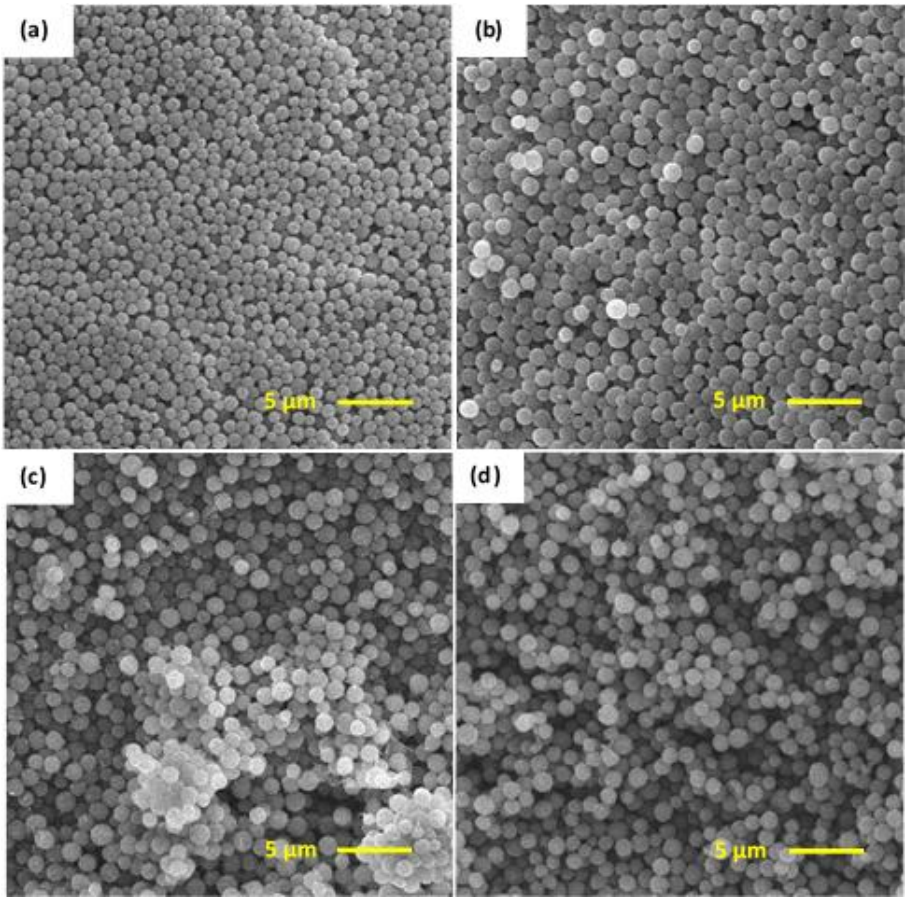

Figure 4.2 SEM images of **1d$_{20}$hC$_{20}$** (a), **2d$_{20}$hC$_{20}$** (b), **3d$_{20}$hC$_{20}$** (c), and **5d$_{20}$hC$_{20}$** (d).

and 1.04 μm, respectively (Figure 4.2c and d). Since both the deprotection of phenyl sulfonate and ionic immobilization were not influenced on the particle diameter, the D_n of **5** was as same as that of **2**. From the elemental analysis, measured nitrogen content in **5d$_{20}$hC$_{20}$** was good agreement with calculated one. These results indicated that chiral cinchonidinium salt **4** was successfully immobilized onto the side chain of corona of **3** to afford core-corona polymer microsphere-supported chiral cinchonidinium catalyst **5**.

*4.2.3 Asymmetric benzylation reaction using core-corona polymer microsphere-supported chiral cinchonidinium catalyst **5***

In order to evaluate the catalytic performance of core-corona polymer microsphere-supported chiral cinchonidinium catalysts **5**, the asymmetric alkylation of *N*-diphenylmethylene glycine *tert*-butyl ester **6** with benzyl bromide **7** was investigated. The reaction was carried out with 10 mol% of catalyst in a toluene: $CHCl_3$ (7/3, *v/v*) mixed solvent at 0 °C. These results were summarized in Table 4.3. The 9-anthracenemethyl derivative of the cinchonidine based quaternary ammonium salt **4** was originally developed by Lygo and co-workers as a powerful catalyst for the asymmetric alkylation of **6**.[35-37] By using **4** in the reaction, phenylalanine derivative **8** was obtained with 95% ee (entry 1). Firstly, we examined the effect of comonomer (styrene, MMA, and HEMA) on the catalytic reactivity and enantioselectivity. These catalysts showed higher reactivity and somewhat high enantioselectivity than gel type polymer-supported catalysts[26] (entries 2-4). Among them, **5d$_{20}$hC$_{20}$** gave the best yield (99%) with excellent enantioselectivity (97% ee) probably due to its hydrophilic nature. Using the catalyst **5d$_x$hC$_z$**, the effect of grafting density (G.D.) and DVB content were checked on the catalytic activity and enantioselectivity. The G.D. of **5** can be considered as same as that of **2** (Table 3.2 in Chapter III). We expected that lowering the G.D. enhanced catalytic activity. Interestingly, both the reactivity and enantioselectivity of **5d$_x$hC$_z$** was increased with increasing the grafting density (entries 4-6). The reason is not clear, but the high ratio of total volume occupied by core-corona microsphere-supported catalyst **5** against the solvent may restrict the mobility of catalytic site. By contrast, the catalytic reactivity of **5d$_{20}$hC$_{30}$** is decreased with increasing G.D. (entry 4 vs 7). The DVB contents in these cores were slightly affected on the reactivity of the catalyst **5d$_x$hC$_z$** however, the DVB contents had no effect on the ee values (entries 4 and 8-10).

Next, the effect of core size on the catalytic reactivity was examined. The catalytic activity is decreased with increasing size of the core (entry 4 vs 11). Both catalytic reactivity and enantioselectivity were decreased due to probably steric hindrance of the longer chain on corona (entries 12 and 13). We found that core-corona catalyst having hydrophobic corona exhibited high catalytic activity (entries 4, 14 and 16). By contrast, the catalyst containing hydrophilic corona **5d$_{20}$hC$_{20}$-h** showed relatively poor reactivity and enantioselectivity (entry 15).

Table 4.2 Asymmetric alkylation reaction using core-corona polymer microsphere-supported chiral cinchonidinium catalyst **5**[a].

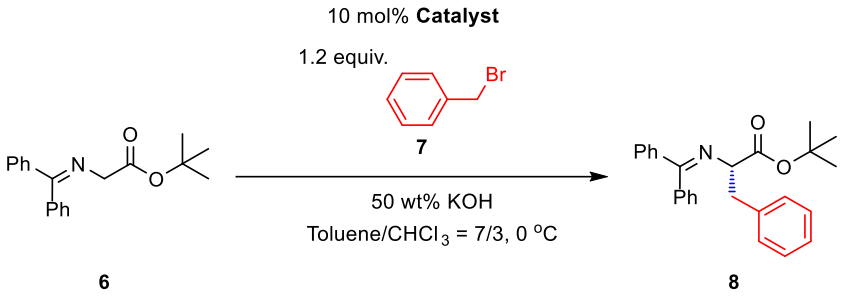

Entry	**$5_d hC_z$** **x/z**	Time (h)	Yield (%)[b]	ee (%)[c]
1	**4**	12	87	95
2	**$5d_{20}sC_{20}$**	20	99	95
3	**$5d_{20}mC_{20}$**	18	98	95
4	**20/20 ($5d_{20}hC_{20}$)**	11	99	97
5	**20/5**	30	20	22
6	**20/10**	24	91	78
7	**20/30**	14	96	95
8	**30/20**	16	93	96
9	**40/20**	14	97	95
10	**50/20**	22	95	96
11	**20/20-A**	15	92	96
12	**20/20-200**	24	97	92
13	**20/20-300**	29	95	91
14	**20/20-m**	19	97	96
15	**20/20-h**	64	71	86
16	**20/20-n**	11	90	96
17	**$9d_{20}hS_{30}$**	24	33	95
18	**$10sS_{30}$**	10	98	96
19	**$10S_{100}$**	49	93	95
20 [23][d]	**11**	15	84	81
21 [18][d,e,f]	**11**	17	90	90
22 [26][d]	**12**	24	73	95
23 [27]	**13**	48	83	87

[a] Reactions were conducted with benzyl bromide (1.2 equiv.), 50 wt% aqueous KOH, and **catalyst** (10 mol%) in toluene/$CHCl_3$ (7/3, *v/v*) at 0 °C.

[b] Determined by ^{1}H NMR.

[c] Determined by HPLC (Chiralcel OD-H).

[d] Toluene was used as a catalyst.

[e] *N*-diphenylmethylene glycine isopropyl ester was used as a substrate.

[f] 25% aq. NaOH was used as a base.

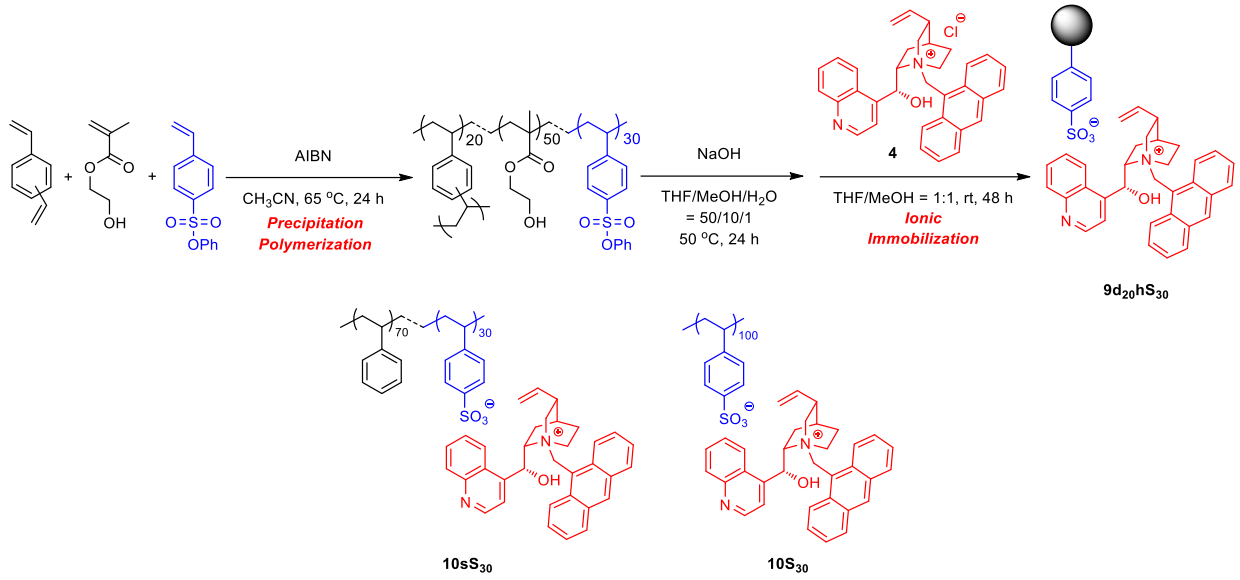

Figure 4.3 Model polymeric catalyst, **9d$_{20}$hS$_{30}$**, **10sS$_{30}$,** and **10S$_{100}$**.

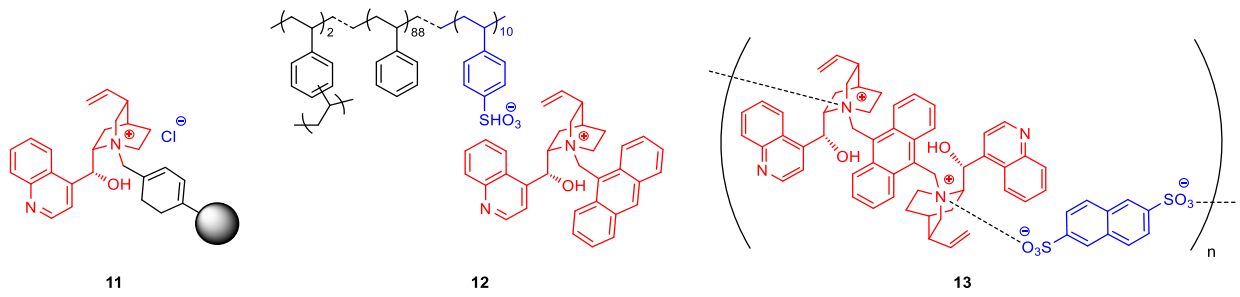

Figure 4.4 Polymeric cinchonidinium catalyst, **11**, **12**, and **13**.

To evaluate the efficiency of **5d$_{20}$hC$_{20}$** in the reaction, some polymeric catalysts, **9d$_{20}$hS$_{30}$**, **10sS$_{30}$**, and **10S$_{100}$** were tested (Figure 4.3). When we used uniform-type microsphere-supported catalyst **9d$_{20}$hS$_{30}$**, in which catalyst was directly immobilized onto microsphere, the yield was found to be poor due to the less flexible polymeric chain (entry 4 vs 17). The almost similar yield and enantioselectivity were found using both **5d$_{20}$hC$_{20}$** and linear polymer-supported catalyst **10sS$_{30}$** (entry 4 vs 18) whereas linear polymer-supported catalyst **10S$_{100}$** showed moderate reactivity as well as slightly low enantioselectivity due to the steric hindrance of cinchonidinium moiety (entry 19). In addition, the catalytic activity of **5d$_{20}$hC$_{20}$** was compared with that of polymeric cinchonidinium previously reported (Figure 4.4) (entries 20-23). Considering the reactivity and enantioselectivity, **5d$_{20}$hC$_{20}$** is proved to be one of the most efficient heterogeneous catalysts in our investigation.

*4.2.4 Optimization of reaction conditions in the asymmetric benzylation reaction using **5d$_{20}$hC$_{20}$***

In order to establish the optimal reaction conditions for the asymmetric benzylation reaction, the solvent and temperature effects were briefly examined. The results have been summarized in Table 4.3. There has a significant solvent effect on the catalytic activity.[38] The catalyst **5d$_{20}$hC$_{20}$** showed excellent affinity to a mixed solvent (Toluene:$CHCl_3$ = 7/3 or 3/7) at 0 °C while it gave low yield and enantioselectivity when toluene or $CHCl_3$ used as a solvent (entries 1-4). For achieving better enantioselectivity, the reaction temperature was lowered to -20 °C. Fortunately, **8** was successfully obtained with 98% ee, however, the reactivity was slightly decreased (entry 5). When the reaction temperature was lowered to -40 °C, the ee value was not improved (entry 6). When the reaction temperature was increased to room temperature, the catalytic activity was increased, but enantioselectivity decreased to 87% ee (entry 8). From these results, the optimized conditions for the asymmetric alkylation of **6** with **7** were determined a follows; toluene/$CHCl_3$ = 7/3 (*v/v*), and 50% aqueous KOH at 0 °C.

Table 4.3 Asymmetric benzylation reaction using **5d$_{20}$hC$_{20}$**[a].

Entry	Solvent (Toluene/$CHCl_3$)	Temp. (°C)	Time ([h)	Yield (%)[b]	ee (%)[c]
1	$CHCl_3$	0	20	86	95
2	3/7	0	11	91	96
3	7/3	0	11	99	97
4	Toluene	0	51	81	92
5	7/3	-20	46	97	98
6	7/3	-40	72	47	98
7	7/3	rt	8	87	87

[a] Reactions were conducted with benzyl bromide (1.2 equiv.), 50 wt% aqueous KOH, and **5d$_{20}$hC$_{20}$** (10 mol%).
[b] Determined by ^{1}H NMR.
[c] Determined by HPLC (Chiralcel OD-H).

4.2.5 Substrate generality in the asymmetric alkylation reaction using 5d$_{20}$hC$_{20}$

With the optimal reaction conditions in hand, the scope of the substrate was studied. A variety of monosubstituted and one disubstituted benzyl bromides, and saturated alkyl bromides **7a-g** were tested for the alkylation reaction of **6**, and the results are shown in Table 4.4. A variety of substituents such as halogen (Br and I), electronwithdrawing (trifluoromethyl group) and electron-donating (methyl group) were well tolerated under the alkylation conditions, affording the desired products **8a-g**. When benzyl bromides containing strong electron-withdrawing groups were used, the corresponding α-phenylalanine derivatives were prepared in excellent yields with high enantioselectivity. The allyl and propargyl bromides exhibited 98% and <99% ee, respectively. The reaction mechanism using ionically polymer-

supported chinconidinium salt is not the conventional phase transfer catalysis, but a mechanism involving the transition state in which ion pairs formed by polymeric sulfonate, cinchonidinium cation, enolate of substrate, and alkylating reagent.[26]

Table 4.4 Asymmetric alkylation of **6** with **7a-g** catalyzed by **5d$_{20}$hC$_{20}$**[a].

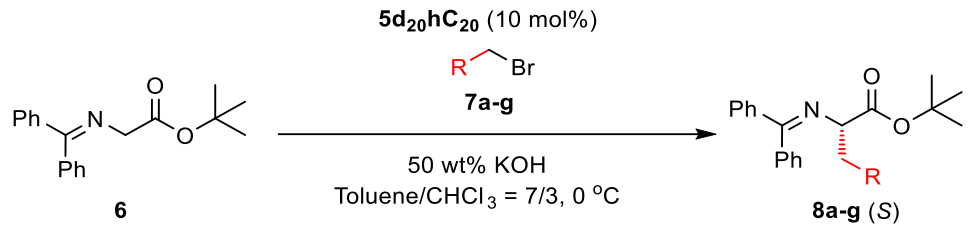

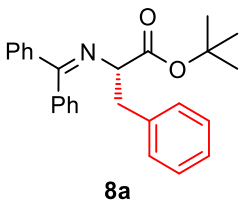

11 h, 99% yield
92% isolated yield
97% ee

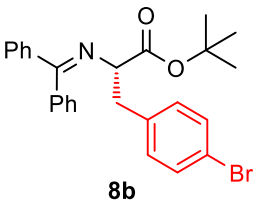

15 h, 97% yield
96% ee

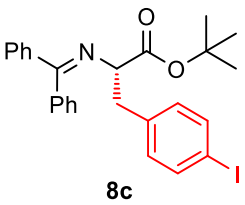

22 h, 98% yield
96% ee

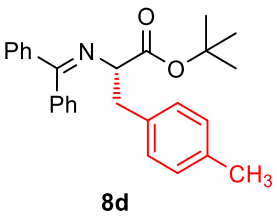

27 h, 91% yield
96% ee

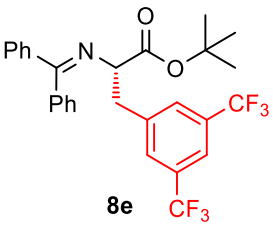

13 h, 80% yield
97% ee

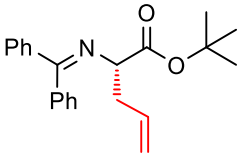

20 h, 99% yield
98% ee

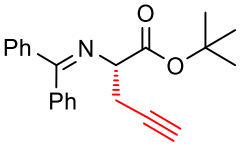

36 h, 93% yield
> 99% ee

[a] Reactions were conducted with benzyl bromide (1.2 equiv.), 50 wt% aqueous KOH, and **5d$_{20}$hC$_{20}$** (10 mol%) in toluene/$CHCl_3$ (7/3, *v/v*) at 0 °C. The yield was determined by ^{1}H NMR. The ee was determined by HPLC (Chiralcel OD-H).

4.2.6 Reusability

To confirm the reusability of the catalyst, **5d$_{20}$hC$_{20}$** was used as a catalyst in the asymmetric benzylation of **6**. Micron-sized polymer microsphere can be easily and quantitatively separated from reaction mixture by centrifugation. After completion of the reaction in each cycle, the catalyst was separated by centrifugation, followed by washing with solvents, and reused in the next cycle. The results of the catalytic reactivity and enantioselectivity were shown in Figure 4.5. The catalytic reactivity was slightly decreased with the repeated reaction. By contrast, the enantioselectivity was not changed at all in the reuse. Even though the ionic bonding between sulfonate and ammonium is not as stable as the

covalent bonding, leaching of cinchonidinium salt was not observed at all after the reaction. The structure of flesh catalyst and 5th reused catalyst was compared by FT-IR and SEM. No difference can be detected by the FT-IR spectra or SEM images of **5d$_{20}$hC$_{20}$** before and after the reuse.

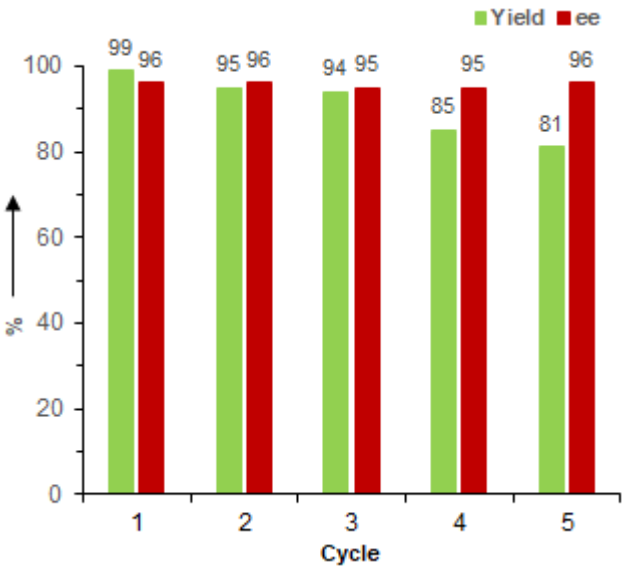

Figure 4.5 Reusability of **5d$_{20}$hC$_{20}$** in the asymmetric benzylation of **6**.

4.2.7 Proposed mechanism of the alkylation reaction catalyzed by 5

The proposed mechanism was illustrated in Scheme 4.3 as the following:

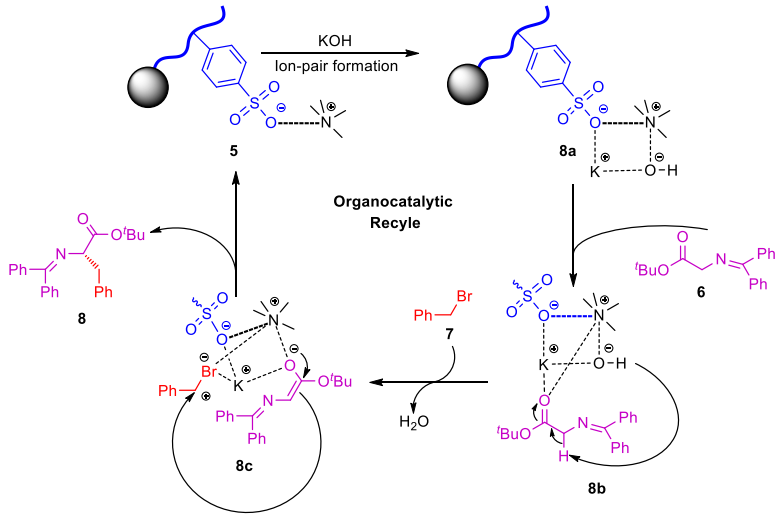

Scheme 4.3 Proposed mechanism of the alkylation reaction catalyzed by **5**.

Step 1 (Ion-pair formation): In this step, core-corona microsphere-supported quaternary ammonium sulfonate ion-pairs **5a** was formed.

Step 2 (Enolate formation): Compound **5a** was transformed into its potassium enolate. In this step, core-corona microsphere-supported quaternary ammonium sulfonate is not always necessary to form the enolate.

Step 3: The enolate of compound **5a** and bromide were incorporated into polymeric quaternary ammonium sulfonate to form mixed ionic complex. The hydrophobic-hydrophilic balance in the core and hydrophobic corona might assist to attract the substrate organic molecules.

Step 4: Alkylation of enolate to form the chiral product, which has no longer interaction with ionic

species on the catalyst. Concurrent KBr precipitation was occurred in 50% KOH aqueous solution. As a result, the original core-corona microsphere-supported quaternary ammonium sulfonate **5** was released and entered the next catalytic cycle.

4.3 Conclusion

Monodispersed, sulfonated core-corona polymer microsphere **3** was successfully synthesized by the surface-initiated ATRP (SI-ATRP) of monomer such as styrene, MMA, HEMA, and NIPAm and phenyl *p*-styrenesulfonate with monodispersed polymer microsphere having benzyl chloride moiety **1** prepared via precipitation polymerization as a macroinitiator, followed by the treatment of NaOH. The size of core, kind of monomer, chain length of corona can be changed as expected. Core-corona polymer microsphere-supported chiral cinchonidinium salt **5** was prepared by the ion exchange reaction of sodium sulfonate moiety at the side chain of corona in **3** with chiral cinchonidinium salt **4**. These polymer microspheres were used as heterogeneous chiral organocatalysts in the asymmetric alkylation reaction. The catalyst $\mathbf{5d_{20}hC_{20}}$ containing hydrophilic core $\mathbf{1d_{20}hC_{20}}$ gave best yield and high ee value in the asymmetric benzylation reaction. We found that the degree of cross-linking in the core and the core size affected the catalytic activity in the reaction. The catalytic activity was decreased with longer corona probably due to the steric hindrance of cinchonidinium moiety. The best catalyst $\mathbf{5d_{20}hC_{20}}$ showed high reactivity and excellent enantioselectivity, comparable to those corresponding low molecular weight catalyst, gel type polymer-supported catalyst, $\mathbf{9d_{20}hS_{30}}$ as well as $\mathbf{10S_{100}}$. We explored the scope of the substrate containing substituents, such as halo, electron-withdrawing and electron-donating groups. When the benzyl bromide containing strong electron-withdrawing group was used, the corresponding phenylalanine derivative was obtained in excellent yield with high enantioselectivity (up to 97%). The propargyl bromide showed excellent enantioselectivity (up to <99%). The catalyst could be reused several times without loss of the enantioselectivity.

4.4 Experimental

4.4.1 Materials and measurements

Styrene (Kishida Chemical Co. Ltd., Osaka, Japan) and divinylbenzene obtained from Nippon & Sumikin Chemical Co. Ltd., Japan, were washed with aqueous 10% NaOH and water, followed by distilling with CaH_2 under reduced pressure. 2-Hydroxyethyl methacrylate (Wako Pure Chemical Industries Ltd., Japan), methyl methacrylate (Sigma-Aldrich) and 4-vinylbenzyl chloride were distilled under reduced pressure. *N*-Isopropylacrylamide (TCI, Japan) was recrystallized from a mixture of hexane and acetone (90/10, *v/v*) and dried at a low temperature under vacuum. Copper (I) bromide was stirred with glacial acetic acid overnight and filtered, followed by washing three times with methanol

and diethyl ether and then dried under vacuum. 2,2′-Bipyridine (Nacalai Tesque, Japan) was used as received without further purification. Diphenyl ether (Wako Pure Chemical Industries Ltd., Japan) and anisole (Kishida Chemical Co. Ltd., Japan) was purified through passing alumina column.

Chlorine contents in polymer microspheres were measured by the titrimetric method. FT-IR spectra were recorded with a JEOL JIR-7000 FT-IR spectrometer and are reported in reciprocal centimeter (cm−1). SEM measurements were conducted by using JSM-IT100 at an acceleration voltage of 10.0 kV. The number-average diameter (D_n) and the dispersity index (U) were determined from the SEM image.

Number-averaged diameter (D_n), weight-averaged diameter (D_w), and polydispersity index (U) of polymer microsphere were calculated using the following equations by counting at least a hundred of individual particles from the SEM images.

$$D_n = \frac{\sum n_i d_i}{\sum n_i} \quad (1)$$

$$D_w = \frac{\sum n_i d_i^4}{\sum n_i d_i^3} \quad (2)$$

$$U = \frac{D_w}{D_n} \quad (3)$$

Where n_i is the number of particles with d_i.

*4.4.2 Synthesis of core-corona polymer microsphere-supported sodium sulfoante **3***

Representative synthesis procedure for ***3d$_{20}$hC$_{20}$***: **2d$_{20}$hC$_{20}$** (0.143 g, 0.0385 mmol of phenylsulfonate moiety) and NaOH (0.0050 g, 0.12 mmol) were taken in a flask with magnetic stir bar and the mixture of solvents (THF/MeOH/H_2O=0.65/0.13/0.013 (mL)) was added. The reaction was carried out in an oil bath at 50 °C for 24 h. The reaction mixture was cooled to room temperature, and the particles was collected by centrifugation and washed with methanol, water, and acetone several times. The solid product was dried at 40 °C under vacuum for 12 h. 0.131 g, 93% yield; sodium sulfonate content: 0.273 mmol g^{-1}. FT-IR (KBr): ν = 1216 (S=O stretching in SO_3Na), 1558, 1490, 1455 (C=C in aromatic ring), 1718 (C=O in ester), 3023 (C−H in aromatic ring), 2936 (C−H in alkyl), and 3466 (O−H) cm^{-1}.

*4.4.3 Synthesis of cinchonidinium salt **4***

To a 50-mL round-bottomed flask with a magnetic stirrer bar, cinchonidine (0.295 g, 1.00 mmol), 9-chloromethylanthracene (0.227 g, 1.00 mmol) and 6.0 mL of toluene were added. The mixture was heated to reflux at 130 °C for 3 h. Within 30 min all of the materials were dissolved and then the products began to crystallize. After 3 h, the mixture was cooled to room temperature and 6.0 mL of Et_2O was added over 1 min. The slurry was stirred for 20 min and then filtered through a sintered glass, washed

with hot toluene, followed by diethyl ether and dried at 40 °C under vacuum overnight to afford *N*-(9-anthracenemethyl) cinchonidinium chloride **4** as a light yellow crystalline solid. 0.415 g, 80% yield. ^{1}H NMR (400 MHz, $CDCl_3$, δ = 7.26 ($CDCl_3$), TMS): δ = 1.00 (m, 1 H), 1.11 (m, 1 H), 1.69 (bs, 1 H), 1.79 (m, 2 H), 2.12 (bs, 1 H), 2.42 (app, t, *J* = 11.0 Hz, 1 H), 2.58 (dd, *J* = 11.0 and 12.5 Hz, 1 H), 4.06 (bd, *J* = 13.1 Hz, 1 H), 4.72 (m, 2 H), 4.90 (dd, *J* = 0.92 and 11.3 Hz, 1 H), 5.25 (dd, *J* = 0.92 and 17.4 Hz, 1H), 5.42 (m, 1 H), 6.69 (d, *J* =13.7 Hz, 1 H), 6.84 (d, *J* =13.7 Hz, 1 H), 7.07 (m, 2 H; Ar), 7.21 (m, 4 H; Ar), 7.38 (m, 1 H; Ar), 7.58 (d, *J* = 8.2 Hz, 1 H; Ar), 7.62 (m, 1 H; Ar), 7.67 (d, *J* = 7.9 Hz, 1 H; Ar), 7.98 (s, 1 H), 8.03 (d, *J* = 4.6 Hz, 1 H; Ar), 8.21 (d, *J* = 5.2 Hz, 1 H; Ar), 8.74 (d, *J* = 9.2 Hz, 1 H; Ar), 8.85 (m, 2 H; Ar), 9.06 (d, *J* = 8.2 Hz, 1 H; Ar). ^{13}C NMR (100 MHz, $CDCl_3$, δ = 77.1 ($CDCl_3$)): δ = 15.34, 23.51, 25.73, 25.90, 38.50, 50.35, 54.69, 61.32, 65.91, 66.76, 67.42, 117.74, 118.20, 120.10, 124.23, 124.70, 124.85, 125.56, 126.44, 126.85, 127.38, 127.59, 128.24, 128.46, 128.65, 129.12, 131.07, 136.45, 145.80, 147.04, 149.36.

*4.4.4 Immobilization of N-(9-anthracenemethyl)cinchonidinium chloride **4** onto the side chain of the corona of **3***

Representative synthesis procedure for ***5d$_{20}$hC$_{20}$***: **3d$_{20}$hC$_{20}$** (0.120 g, 0.0778 mmol of sodium sulfonate moiety) was taken in a Schlenk tube with a magnetic stir bar and **4** (0.082 g, 0.16 mmol) was dissolved 0.80 mL of MeOH. The MeOH solution of **4** was added into the tube and then THF (0.80 mL) was added. The mixture was stirred at room temperature for 48 h. The resulting light yellow polymer particle was isolated by centrifugation and redispersed in MeOH, two times in water and acetone. The core-corona polymeric catalyst was dried at 40 °C under vacuum. The unreacted catalyst was recovered from the collected supernatant by removing solvent mixtures through vacuum evaporator, followed by dissolving in CH_2Cl_2, filtration and then dried at 40 °C under vacuum oven. The degree of immobilization and catalyst content was 67% and 0.361 mmol g^{-1}, respectively. Elemental analysis calcd. for $C_{25.6}H_{27.4}N_{0.6}O_{3.0}S_{0.3}Cl_{0.2}$: C 75.32%, H 6.77%, N 2.06%: found: C 68.94%, H 6.77%, N 1.60%. . FT-IR (KBr): ν = 1214 (S=O), 1601, 1490, 1454 (C=C in aromatic ring), 1722 (C=O in ester), 3023 (C−H in aromatic ring), 2928 (C−H in alkyl), and 3466 (O−H) cm^{-1}.

*4.4.5 Synthesis of **9d$_{20}$sS$_{30}$***

9d$_{20}$sS$_{30}$ was synthesized by the following steps:

Synthesis of ***M-d$_{20}$sS$_{30}$****, or simply,* ***M-S***: A 30 mL HDPE narrow-mouth bottle was charged with DVB (0.154 g, 1.18 mmol) HEMA (0.389 g, 2.99 mmol), **S** (0.468 g, 180 mmol), AIBN (0.020 g), and 30 mL of acetonitrile under N_2 gas. Polymerization was carried out in an incubator at a constant temperature of 65 ^{o}C with rolling the bottle horizontally at 9 rpm. The reaction mixture was cooled to room temperature, and the insoluble fraction was collected by centrifugation and washed with THF,

methanol, and acetone. The solid product was dried under vacuum at 40 °C for 24 h. 0.409 g, 40% yield; sulfonate content: 1.78 mmol g^{-1}. FT-IR (KBr): ν = 1373, 1176 (S=O), 1596, 1488, 1455 (C=C in aromatic ring), 1722 (C=O in ester), 3062 (C−H in aromatic ring), 2936 (C−H in alkyl), and 3447 (O−H) cm^{-1}. The number-average diameter (D_n) and polydispersity index (D_w/D_n) measured from SEM image was found 1.79 μm and 1.74, respectively.

*Synthesis of **M-SNa***: **M-S** (225 mg, 0.400 mmol of sulfonate moiety) and NaOH (0.049 g, 1.2 mmol) were taken in a flask with a magnetic stir bar inside and a mixture of solvent (THF/MeOH/H_2O (50/10/1) = 6.72/1.34/0.134) was added. The reaction was carried out in an oil bath at 50 °C for 24 h. The reaction mixture was cooled to room temperature, and the particles were collected by centrifugation and washed with methanol, water and acetone. The solid product was dried at 40 °C under vacuum for 24 h. 0.213 g, >99% yield; sodium sulfonate content: 1.97 mmol g^{-1}; FT-IR (KBr): ν = 1189 (S=O stretching in SO_3Na), 1601, 1555, 1453 (C=C in aromatic ring), 1715 (C=O in ester), 2932 (C−H in alkyl), and 3448 (O−H) cm^{-1}.

*Synthesis of **$9d_{20}hS_{30}$***: **M-SNa** (0.045 g, 0.089 mmol of sodium sulfonate moiety) was taken in a flask with a magnetic stir bar inside and **4** (0.091 g, 0.17 mmol) was dissolved in 0.85 mL of MeOH. The solution of **4** was added into the test tube and then 0.85 mL of THF was added. The reaction was continued at room temperature for 48 h. The resulting light yellow polymer particles were isolated by centrifugation and redispersed in MeOH, two times in water and acetone. The catalyst immobilized onto the surface of polymer particles were dried at 40 °C under vacuum. The unreacted catalysts were recovered from the collected supernatant by removing solvent mixtures through vacuum evaporator, followed by dissolving in dichloromethane, filtration and then dried at 40 °C under vacuum oven. The degree of immobilization and catalyst content was 61% and 0.771 mmol g^{-1}, respectively. D_n of **$9d_{20}hS_{30}$** was as same as that of **M-S**.

*4.4.6 Synthesis of **$10sS_{30}$***

$10sS_{30}$ was synthesized by the following steps:

*Synthesis of **$P\text{-}s_{70}S_{30}$**, or simply, **sS_{30}***: CuBr (0.014 g, 0.098 mmol), St (0.365 g, 3.50 mmol), **S** (0.392 g, 1.51 mmol), and diphenyl ether (1.25 mL) were added to 6 mL vial successively. The reaction mixture was purged with argon for 5 min and then PMDETA (0.052 g, 0.30 mmol) was added. After another 5 min of argon bubbling, initiator, 1-phenyl ethyl bromide (1-PEBr) (0.020 g, 0.11 mmol) was added into the system. The reaction was carried out for 24 h at a stirring rate of 400 rpm in an oil bath at 110 °C temperature. The resulting polymers were collected by drop wise adding in MeOH (100 ~ 125 mL). The polymers were collected by filtration which then dried at 40 °C temperature to provide a white powder. 0.347 g, 45% yield. $M_{n,\,NMR}$ = 9,200 g mol^{-1}; $M_{n,\,SEC}$ = 19,000; M_n/M_w = 1.53. FT-IR

(KBr): ν = 1376, 1175 (S=O stretching), 1597, 1489, 1453 (C=C in aromatic ring), 3060, 3025 (C−H in aromatic ring), and 2924, 2850 (C−H in alkyl) cm^{-1}.

Synthesis of ***sSNa$_{30}$***: **sSNa$_{30}$** was synthesized using the similar reaction conditions of **M-SNa**. The resulting polymers were collected by drop wise adding in ether. The insoluble fraction was collected by centrifugation and washed with small amount of methanol, and acetone. The solid product was dried under vacuum at 40 ^{o}C for 24 h. 89% yield; sodium sulfonate content: 2.17 mmol g^{-1}; FT-IR (KBr): ν = 1190 (S=O stretching in SO_3Na), 1601, 1493, and 1452 (C=C in aromatic ring), 3060, 3025 (C−H in aromatic ring), 2924, 2848 (C−H in alkyl), and 3447(O-H) cm^{-1}.

Synthesis of ***10sS$_{30}$***: The synthesis procedure was similar to that of **10S$_{100}$.** The resulting light yellow polymers were isolated by centrifugation and washed with MeOH, water, and acetone. The catalyst immobilized onto the polymers were dried at 40 ^{o}C under vacuum. The unreacted catalysts were recovered from the collected supernatant by removing solvent mixtures through vacuum evaporator, followed by dissolving in dichloromethane, filtration and then dried at 40 ^{o}C under vacuum oven. The degree of immobilization and catalyst content was 86% and 1.00 mmol g^{-1}, respectively.

4.4.7 Synthesis of ***10S$_{30}$***

10S$_{100}$ was synthesized by the following steps:

Synthesis of ***P-s$_0$S$_{100}$****, or simply,* ***S$_{100}$***: The synthesis procedure was as same as that of **sS$_{30}$**. 0.845 g, 64% yield. $M_{n,\,NMR}$ = 8,800 g mol^{-1}; $M_{n,\,SEC}$ = 14,000; M_n/M_w = 1.31. FTIR (KBr): ν = 1374, 1181 (S=O stretching), 1596, 1488, 1456 (C=C in aromatic ring), 3065 (C−H in aromatic ring), and 2928 (C-H in alkyl) cm^{-1}.

Synthesis of ***SNa$_{100}$***: The reaction conditions were similar to that of **sSNa$_{30}$**. The reaction mixture was cooled to room temperature, and the insoluble fraction was collected by centrifugation and washed with THF, methanol, and acetone. The solid product was dried under vacuum at 40 ^{o}C for 24 h. 86% yield; sodium sulfonate content: 4.76 mmol g^{-1}. FT-IR (KBr): ν = 1190 (S=O stretching in SO_3Na), 1645, 1602, and 1449 (C=C in aromatic ring), 3063 (C−H in aromatic ring), 2925, 2850 (C-H in alkyl), and 3464 (O-H) cm^{-1}.

Synthesis of ***10S$_{100}$***: **10S$_{100}$** was synthesized using the same procedure for **10sS$_{30}$**. The degree of immobilization and catalyst content was 29% and 0.846 mmol g^{-1}, respectively.

4.4.8 Representative asymmetric benzylation of N-diphenylmethylene glycine tert-butyl ester ***6*** *using* ***5d$_{20}$hC$_{20}$***

A mixture of *N*-diphenylmethylene glycine *tert*-butyl ester **6** (59 mg, 0.20 mmol), **5d$_{20}$hC$_{20}$** (0.055 g, 0.020 mmol), 50 wt% aqueous KOH solution (0.25 mL), and toluene/CHCl3 (7/3, *v*/*v*, 0.80 mL) was

cooled to 0 °C. After stirring for 5 min, a mixture of benzyl bromide **7** (0.028 mL, 0.24 mmol) and toluene/$CHCl_3$ (0.20 mL) was added slowly. The reaction mixture was then stirred vigorously for 11 h. The polymeric catalyst was isolated by centrifugation, followed by washing using the reaction solvent twice. Saturated NaCl aqueous solution (5.0 mL) and ethyl acetate (5.0 mL) was then added in the supernatant collected from the reaction mixture by centrifugation. The organic layer by the extraction was separated and concentrated in vacuo, followed by pumped up to give the crude product (colorless liquid). ^{1}H NMR (400 MHz, $CDCl_3$, δ = 0 ($(CH_3)_4Si$): δ = 1.44 (s, 9H), 3.13-3.25 (m, 2H, CH), 4.10 (dd, *J* = 9.16, 4.27 Hz, 1H, CH_2), 6.60 (br, d, *J* = 5.80 Hz, 2H, Ar), 7.04-7.06 (m, 2H, Ar), 7.15-7.21 (m, 3H, Ar), 7.28-7.38 (m, 6H, Ar), 7.56-7.58 (m, 2H, Ar). ^{13}C NMR (100 MHz, $CDCl_3$, δ = 77.1 ($CDCl_3$): δ = 28.1, 39.6, 68.0, 81.1, 126.2, 127.7, 127.9, 128.0, 128.1, 128.2, 128.7, 129.9, 130.1, 136.4, 138.4, 139.6, 170.3, 170.9. The yield was determined by ^{1}H NMR spectroscopy (99%). The enantioselectivity (97% ee) was determined by HPLC on a chiral stationary phase using a Chiralcel OD-H column; eluent: 2-propanol/n-hexane=1:100; flow rate: 0.3 mL min^{-1}, λ = 254 nm, 25 °C; retention time: *R* enantiomer = 25.1 min, *S* enantiomer = 41.4 min.

References

[1] Dolling, U. -H.; Davis, P. Grabowski, E. J. J. *J. Am. Chem. Soc.* **1984**, *106*, 446 - 447.

[2] Hughes, D. L.; Dolling, U. -H.; Ryan, K. M.; Schenewaldt, E. F.; Grabowski, E. J. J. *J. Org. Chem.* **1987**, *52*, 4745 - 4752.

[3] O' onnel, M. J. *Acc. Chem. Res.* **2004**, *7*, 506 - 517.

[4] Tian, S. K.; Chen, Y.; Hang, J.; Tang, L.; McDaid, P.; Deng, L. *Acc. Chem. Res*. **2004**, *37*, 621-631.

[5] Ooi, T.; Maruoka, K. *Acc. Chem. Res*. **2004**, *37*, 526 - 533.

[6] Lygo, B.; Andrews, B. *Acc. Chem. Res.* **2004**, *37*, 518 - 525.

[7] Ooi, T.; Maruoka, K. *Angew. Chem.* **2007**, *119*, 4300 - 4345.

[8] Ooi, T.; Maruoka, K. *Angew. Chem. Int. Ed.* **2007**, *46*, 4222 - 4266.

[9] Maruoka, K.; Ooi, T.; Kano, T. *Chem. Commun.* **2007**, *0*, 1487 - 1495.

[10] Jin, L.; Zhao, S.; Chen, X. *Molecules* **2018**, *23*, 1421.

[11] Benaglia, M.; Puglisi, A.; Cozzi, F. *Chem. Rev.* **2003**, *103*, 3401 - 3429.

[12] Cozzi, F. *Adv. Synth. Catal.* **2006**, *348*, 1367 - 1390.

[13] De Vos, D. E.; Vankelecom, I. F. J.; Jacobs P. A. (Eds.), Chiral Catalyst Immobilization and Recycling, Wiley-VCH, Weinheim, 2000.

[14] Chiellini, E.; Solaro, R. *J. Chem. Soc. Chem. Commun.* **1977**, 231 - 232.

[15] Colonna, S.; Fornasier, R.; Pfeiffer, U. *J. Chem. Soc. Perkin Trans*. **1978**, *1*, 8 - 11.

[16] Kobayashi, N.; Iwai, K. *Makromol. Chem. Rapid Commun*. **1981**, *2*, 105 - 108.

[17] Hodge, P.; Khoshdel, E.; Waterhouse, J. *J. Chem. Soc. Perkin Trans*. **1983**, *1*, 2205 - 2209.

[18] Chinchilla, R.; Mazón, P.; Nájera, C. *Tetrahedron: Asymmetry* **2000**, *11*, 3277 - 3281.

[19] Chinchilla, R.; Mazón, P.; Nájera, C. *Adv. Synth. Catal.* **2004**, *346*, 1186 - 1194.

[20] Thierry, B.; Plaquevent, J. -C.; Cahard, D. *Tetrahedron: Asymmetry* **2001**, *12*, 983 - 986.

[21] Thierry, B.; Perrard, T.; Audouard, C.; Plaquevent, J. C.; Cahard, D. *Synthesis* **2001**, 1742 - 1746.

[22] Shi, Q.; Lee, Y. J.; Song, H.; Cheng, M.; Jew, S. S.; Park, H. G.; Jeong, B. S. *Chem. Lett.* **2008**, *37*, 436 - 437.

[23] Thierry, B.; Plaquevent, J. -C.; Cahard, D. *Tetrahedron: Asymmetry* **2003**, *14*, 1671 - 1677.

[24] Danelli, T.; Annunziata, R.; Benaglia, M;. Cinquini, M.; Cozzi, F.; Tocco, G. *Tetrahedron: Asymmetry* **2003**, *14*, 461 - 467.

[25] Wang, X.; Yin, L.; Yang, T.; Wang, Y. *Tetrahedron: Asymmetry* **2007**, *18*, 108 - 114.

[26] Arakawa, Y.; Haraguchi, N.; Itsuno, S. *Angew. Chem. Int. Ed*. **2008**, *47*, 8232 - 8235.

[27] Parvez, M. M.; Haraguchi, N.; Itsuno, S. *Macromolecules* **2014**, *47*, 922 - 1928.

[28] Islam, M. R.; Ahamed, P.; Haraguchi, N.; Itsuno, S. *Tetrahedron: Asymmetry* **2014**, *25*, 1309 - 1915.

[29] Liu, W.; Yang, X.; Hung, W. J. *Colloid. Interface Sci.* **2006**, *340*, 160 - 165.

[30] Zhang, H. F.; Zhang, L.; Cui, Y. C. *React. Funct. Polym.* **2007**, *67*, 322 - 328.

[31] Zhang, J.; Zhang, W.; Wang, Y.; Zhang, M. *Adv. Synth. Catal.* **2008**, *50*, 2065 - 2076.

[32] Haraguchi, N.; Nishiyama, A.; Itsuno, S. *J. Polym. Sci. Part A: Polym. Chem*. **2010**, *48*, 3340 - 3349.

[33] Li, X.; Yang, B.; Zhang, S.; Jia, X.; Hu, Z. *Colloid. Polym. Sci.* **2017**, *295*, 573 - 582.

[34] Ullah, M. W.; Haraguchi, N. *J. Polym. Sci. Part A: Polym. Chem.* **2019**, *57*, 1296 - 1304

[35] Lygo, B.; Wainwright, P. G. *Tetrahedron Lett.* **1997**, *38*, 8595 - 8598.

[36] Lygo, B.; Crosby, J.; Lowdon, T. R.; Wainwright, P. G. *Tetrahedron* **2001**, *57*, 2391 - 2402.

[37] Lygo, B.; Crosby, J.; Lowdon, T. R.; Peterson, J. A.; Wainwright, P. G. *Tetrahedron* **2001**, *57*, 2403 - 2409.

[38] Lee, J. -H.; Yoo, M. -S.; Jung, J. -H.; Jew, S.; Park, H. *Tetrahedron* **2007**, *63*, 7906 -7915.

CHAPTER V

Synthesis of Core-Corona Polymer Microsphere-supported MacMillan Catalyst and Its Application to Asymmetric Diels-Alder Reaction

5.1 Introduction

Chiral organocatalysts have received considerable attention for their use in the synthesis of optically active compounds.[1] Unlike the conventional metal catalysts, they have several advantages in catalytic asymmetric reaction especially in the synthesis of medicines, agrichemicals, and pharmaceuticals because of metal-free catalyst which can avoid metal contamination of the product. Among a variety of organocatalysts, one of the efficient organocatalysts, originally developed by D. W. C and coworkers, which are designed at present is the chiral imidazolidin-4-one derivative (Imidazolidinium salt) **5**.[2] The imminium salt can be applied to a variety of catalytic asymmetric reactions, including the Diels–Alder reaction,[3] 1,3-dipolar cycloaddition,[4] Friedel-Crafts alkylation,[5] indole alkylation,[6] α-chlorination of aldehydes,[7] α-fluorination of aldehydes,[8] direct aldol reaction,[9] intramolecular Michael

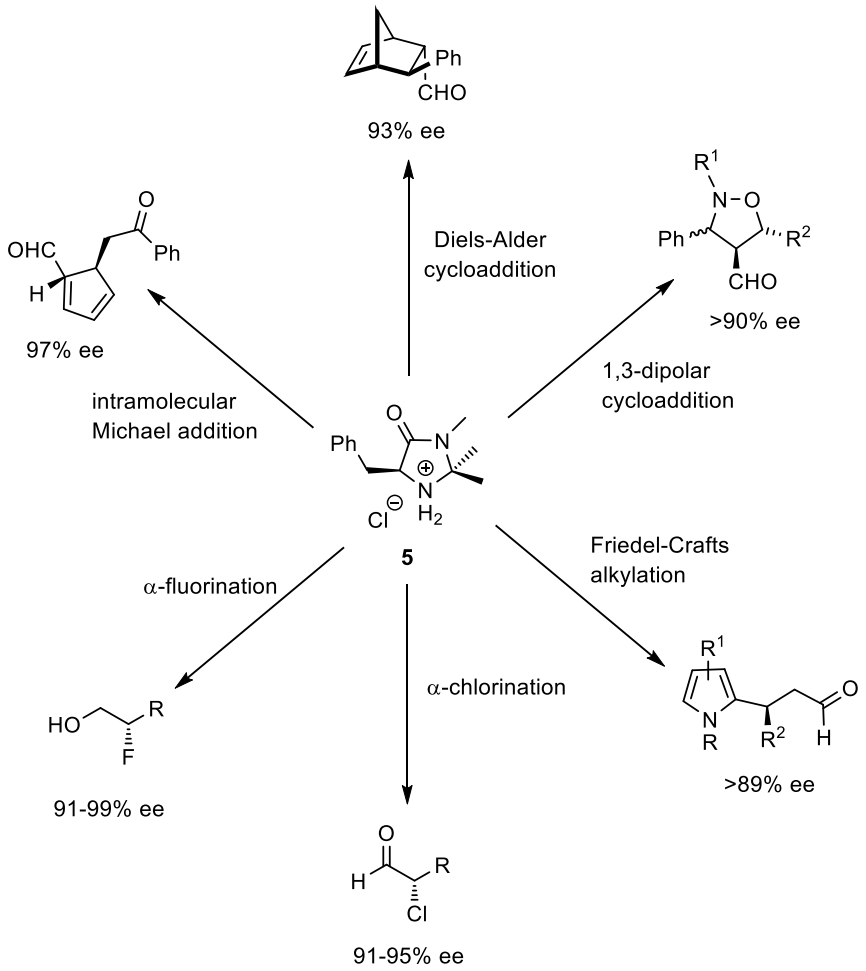

Scheme 5.1 Examples of asymmetric reactions catalyzed by MacMillan catalyst **5**.

reaction,[10] epoxidation,[11] α-allylation of aldehydes,[12] α-allylation of ketones,[13] α-alkylation of aldehydes,[14] hydride addition,[15] and cyclopropanation.[16]

With the development of new organocatalysts and organocatalytic reactions, high enantioselectivities have been obtained in various asymmetric reactions through the use of these chiral imidazolidinone organocatalysts. Unfortunately, a relatively high catalyst loading (over 10 mol% in most cases) is required to facilitate reactions at a reasonable rate. Furthermore, somewhat burdensome purification, such as silica gel column chromatography, is necessary to separate the catalyst from the product. In addition, it is typically difficult to recover and reuse the catalyst.

To facilitate the separation, recovery, and reuse of the catalyst, chiral imidazolidinones have been immobilized on polymeric or inorganic supports.[17-34] The first example was reported by Benagila and Cozzi in 2002. They prepared poly(ethylene glycol)-supported chiral imidazolidin-4-one and the salt was used for asymmetric Diels–Alder cycloaddition[18] and 1,3-dipolar cycloaddition.[20] Pihko et al. used JandaJel for the polymer-support and **5** was immobilized from *N*-position of amide moiety.[19] Ying and coworkers immobilized **5** onto siliceous and polymer-coated mesocellular forms and the resulting polymer-supported organocatalyst was used for asymmetric Friedel-Crafts alkylation and Diels–Alder reaction.[21] In all these polymeric catalysts, the MacMillan catalyst was covalently bonded to the polymer support. However, the covalently bonded polymer-supported organocatalysts have some disadvantages, including multi-step preparations and deactivation of the inherent catalysis due to the modifications necessity to anchor the organocatalysts to supports. It can be interpreted in terms of direct covalent-bonding of organocatalysts to the support material, decreasing the intrinsic properties of steric sensitivity of organocatalyst on asymmetric synthesis.

To solve the above problem, an alternative strategy involving the immobilization of organocatalysts on support materials using an ion-exchange reaction has been reported.[35] This method can be expected to allow for simple and facile preparation, easily separation from the reaction mixture, reusability of the immobilized catalyst, and higher enantioselectivity due to increased steric steering by the support material. Recently, some examples of ionically immobilized MacMillan catalysts have been reported.[36-38] Montmorillonite clay was found to readily entrap MacMillan catalysts, and the resulting heterogeneous chiral organocatalyst was utilized in Diels–Alder reactions.[36] In another case, silica gel soaked in an ionic liquid such as a medium containing 1-butyl-3-methylimidazolium salt was used for the immobilization of MacMillan catalysts.[37] In 2008, Itsuno et al. have first reported an efficient method for the ionic immobilization of chiral quaternary ammonium salts onto support polymer.[38] This method is a facile and general technique for the immobilization of ammonium onto sulfonated polymers regardless of kinds of ammonium and sulfonated polymer, which can be employed in mild conditions. Interestingly, the catalytic activity is comparable to the model molecular catalyst. In addition, the

polymeric catalyst was reused without loss of its catalytic activity. Haraguchi et al. applied this strategy for the ionic immobilization of a MacMillan catalyst on a gel type polymer.[39] The gel type polymer-immobilized MacMillan catalyst was easily obtained by polymerization of the MacMillan monomer or by ion exchange reaction between MacMillan chloride and the sulfonated polymer that was used as a heterogeneous catalyst in the Diels-Alder reaction. They have also developed several main-chain chiral polymers containing imidazolidinone repeating units by ionic bond formation between imidazolidinones and sulfonates.[40-44] These main-chain chiral ionic polyesters and polyethers containing imidazolidinone units were synthesized by ion-exchange polymerization and used as heterogeneous catalysts in the asymmetric Diels-Alder reactions. These main-chain type immobilized catalysts gave the Diels-Alder adducts with quantitative yield and excellent enantioselectivity of up to 98% ee for the *endo* isomer that were higher than that of the corresponding monomeric chiral imidazolidinone salts.

One of the interesting applications of functionalized polymer microspheres is as heterogeneous polymeric supports. Some polymer microspheres functionalized with catalyst have been applied to organic reactions.[33,45-47] We have developed uniform-type, core-shell-type and core-corona-type polymer microsphere-supported chiral ligand in the asymmetric transfer hydrogenation.[46] The introduction position of the chiral catalyst onto the polymer microsphere and the degree of crosslinkage as well as the structure and hydrophobicity of polymer microsphere greatly influenced the catalytic performance.

To date, there have been little reports about polymer microsphere-supported chiral organocatalyst which was used in asymmetric synthesis.[33] Recently, X. Li et al. have been reported covalently bonded micron-/nano-sized hairy microsphere-supported MacMillan catalyst in the asymmetric Diels–Alder reaction in water.[33] The results in their investigations showed that the chiral polymer grafted on the nanoparticles had better dispersion in the reaction media than those grafted on the microspheres and exhibited better catalytic activity and selectivity in the asymmetric Diels–Alder reaction between *trans*-cinnamaldehyde and 1,3-cyclopentadiene.

Core-corona polymer microspheres are a kind of core shell particles whose shell is composed of linear polymer chains. These polymer microspheres are more flexible and high dispersible which can provide less steric hindrance for catalytic site. In addition, they are more efficient to offer microenvironments for catalytic asymmetric reactions because of their abilities to control hydrophobic-hydrophilic balance. The nano-sized core also provides a more efficient catalytic microenvironment.[48,49]

In our previous work, we have successfully synthesized core-corona microsphere-supported cinchonidinium salt which was used as a heterogeneous catalyst in the asymmetric alkylation reaction.[50] Cinchonidinium salt was successfully immobilized onto sulfonated core-corona polymer

microsphere via ionic bond. The core size, the grafting density of corona, the chain length of corona, and the polymer structure that affected on the catalytic performance were investigated. As a result, the core-corona polymer microsphere-supported having hydrophilic core and hydrophobic corona with short corona exhibited high catalytic activity. The catalytic activity was decreased with increasing size of the core. The catalytic activity was also decreased with longer corona probably due to the steric hindrance of cinchonidinium moiety. The catalyst showed high reactivity and excellent enantioselectivity, comparable to those corresponding low molecular weight catalyst, gel type polymer-supported, uniform type polymer microsphere-supported, as well as linear homopolymer-supported catalyst.

From these findings, sulfonated core-corona polymer microsphere will be a suitable solid support for the ionically immobilization of chiral imidazolidinone salt. In this Chapter, we reported the synthesis of core-corona polymer microspheres-supported MacMillan catalysts by the neutralization reaction of core-corona polymer microsphere having sulfonic acid moiety with the precursor of MacMillan catalyst. These catalysts were used as heterogeneous catalysts in a representative asymmetric Diels–Alder reaction of *trans*-cinnamaldehyde and 1,3-cyclopentadiene in MeOH/H_2O (95/5, *v/v*). The effect of core and corona (kinds of monomer, diameter, and length of corona) on the catalytic activity was investigated in detail.

5.2 Results and Discussion

*5.2.1 Synthesis of polymer microspheres having benzyl chloride moiety **1** by precipitation polymerization*

Monodisperse polymer microspheres having benzyl chloride moiety **1** were synthesized by precipitation polymerization of 60 mol% of comonomer (St, MMA, or HEMA), 20 mol% of divinylbenzene (DVB) with 20 mol% of 4-vinylbenzyl chloride (VBC). The molar ratio of DVB and VBC was kept fixed, and that of comonomer was changed from St to HEMA. These characterizations were summarized in Table 5.1.

In the FT-IR spectra of **1**, the characteristic FT-IR band was appeared at 1265 cm^{-1} due to C−Cl bond. The strong peaks were found at 1602, 1509, 1451 cm^{-1} and 3059, 3024 cm^{-1} due to C=C and C−H in the aromatic ring, respectively in **1d$_{20}$sC$_{20}$**. The stretching absorption frequency of C=O bond was observed at 1728 and 1720 cm^{-1} in **1d$_{20}$mC$_{20}$** and **1d$_{20}$hC$_{20}$**, respectively. A broad peak for O−H in **1d$_{20}$hC$_{20}$** was observed at 3446 cm^{-1}.

Table 5.1 Characterization of polymer microsphere **1**[a].

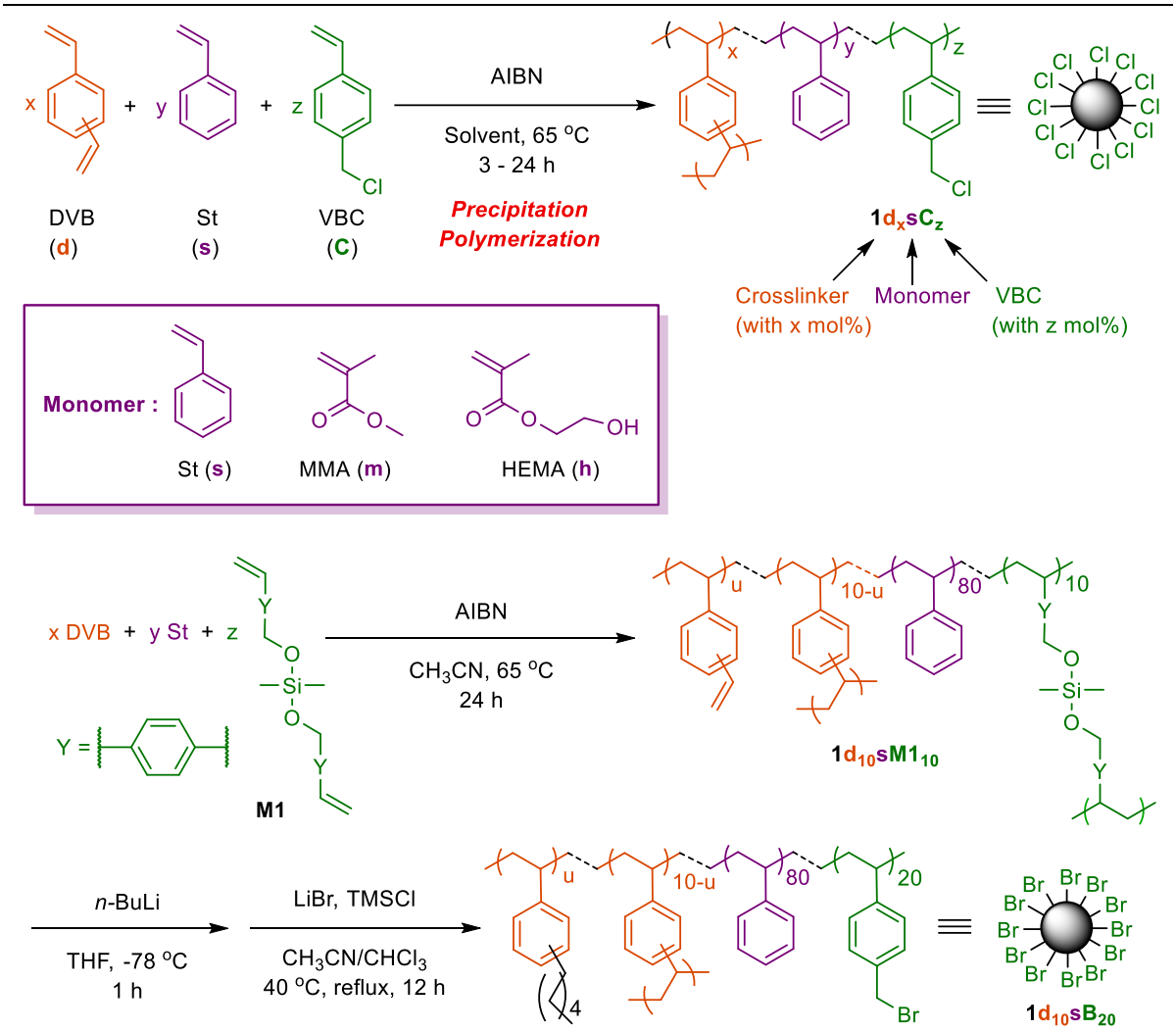

Entry	Polymer Microsphere	Time (h)	Yield (%)	D_n (μm)[c]	U[b]	Cl Content (mmol g^{-1})	
						Cl_{calcd}	$Cl_{measured}$
1	**1d$_{20}$sC$_{20}$**	3	3	1.14	1.00	1.68	1.67
2	**1d$_{20}$mC$_{20}$**	2	4	1.12	1.00	1.71	1.76
3[c]	**1d$_{20}$hC$_{20}$**	24	24	0.80	1.13	1.50	1.54
4[d]	**1d$_{20}$sC$_{20}$-2**	7	8	2.22	1.00	1.67	1.67
5[d]	**1d$_{20}$sC$_{20}$-4**	24	26	4.09	1.00	1.69	1.67
6[d]	**1d$_{20}$sC$_{20}$-6**	48	37	5.86	1.00	1.68	1.69
7	**1d$_{10}$sB$_{20}$**	24	32	1.08	1.13	1.42[e]	1.89[e] 1.66[f]

[a] All the polymerizations were performed in CH_3CN at 65 °C using 4.3 wt% monomers relative to the reaction medium and 2 wt% AIBN relative to the total monomers.

[b] Measured from SEM images.

[c] 9:1 CH_3CN:Toluene mixed solvent was used.

[d] The size of corresponding polymer microspheres were denoted by **2**, **4**, and **6**.

[e] Bromine content.

[f] Bromine content determined by elemental analysis.

The number-averaged diameter (D_n) of polymer microsphere can be controlled by adjusting the polymerization time. Polymer microspheres with similar D_n (Ca. 1.0 μm) were synthesized with relatively low yield (3-24%) due to the minimum molar ratio of DVB to form micron-sized particle was used in the polymerization (entries 1-3). The polymer microspheres **1d$_{20}$sC$_{20}$-2**, **1d$_{20}$sC$_{20}$-4**, and **1d$_{20}$sC$_{20}$-6** with high D_n (2.0, 4.0, and 6.0 μm) were also prepared by extending the polymerization time (entries 4-6). These polydispersities (U) were well controlled in most cases.

In addition to the monodispersed benzyl chloride-functionalized polymer microsphere with 20 mol% crosslinker, monodispersed low crosslinked benzyl bromide-functionalized polymer microsphere moiety **1d$_{10}$sB$_{20}$** was successfully synthesized with relatively higher yield (37%) *via* precipitation polymerization of styrene, DVB, and a divinyl crosslinker **M1**, followed by the transformation reaction (entry 7).[51] **1d$_{10}$sM1$_{10}$** and **1d$_{10}$sB$_{20}$** were characterized by FT-IR spectra. The characteristic absorption peaks for Si−C, Si−O and C−O bonds in **1d$_{10}$sM1$_{10}$** were appeared at 1257, 1075 and 1019 cm^{-1}, respectively (Figure 5.1). After transformation reaction of **1d$_{10}$sM1$_{10}$**, these characteristic peaks were disappeared and a new stretching vibration of C−Br bond was observed at 1227 cm^{-1} that indicating the both polymerization and transformation reaction successfully occurred.

The number-average diameters (D_n) measured from SEM photographs were 1.14 μm for **1d$_{20}$sC$_{20}$**, 1.12 μm for **1d$_{20}$mC$_{20}$** and 0.80 μm for **1d$_{20}$hC$_{20}$**, respectively and the size distributions were quite narrow with the polydispersity index (D_w/D_n) being in the range of 1.00 and 1.13. The D_n of **1d$_{20}$sC$_{20}$-2**, **1d$_{20}$sC$_{20}$-4**, and **1d$_{20}$sC$_{20}$-6** were also 2.22 μm, 4.09 μm, and 5.86 μm, respectively. Chlorine contents in **1** determined by titrimetric method were in good agreement with those calculated. The D_n of **1d$_{10}$sB$_{20}$** was 1.08 μm with narrow size distributions. Measured bromine content in **1d$_{10}$sB$_{20}$** from the titrimetric method and the elemental analysis were somewhat higher than the calculated one. These results clearly indicated that monodispersed polymer microspheres having benzyl halide moiety **1** were successfully synthesized by the precipitation polymerization.

*5.2.2 Synthesis of core-corona polymer microsphere **2** by SI-ATRP of an achiral vinyl monomer and phenyl p-styrene sulfonate (**S**)*

Core-corona polymer microsphere **2** was synthesized by SI-ATRP of an achiral monomer and phenyl *p*-styrene sulfonate (**S**) using **1** as a macroinitiator.

The weight increase of core-corona polymer microsphere is calculated by the following equation:

$$\text{Weight increase } (\Delta W\%) = \frac{\text{Weight of } \mathbf{2}\ (Wt_{\mathbf{2}}) - \text{Weight of } \mathbf{1}\ (Wt_{\mathbf{1}})}{\text{Weight of } \mathbf{1}\ (Wt_{\mathbf{1}})} \times 100 \qquad (1)$$

To measure the number-averaged molecular weight (M_n) and polydispersity (M_w/M_n) of the grafted

Table 5.2 Characterization of core-corona polymer microsphere **2** synthesized by SI-ATRP using **1**[a].

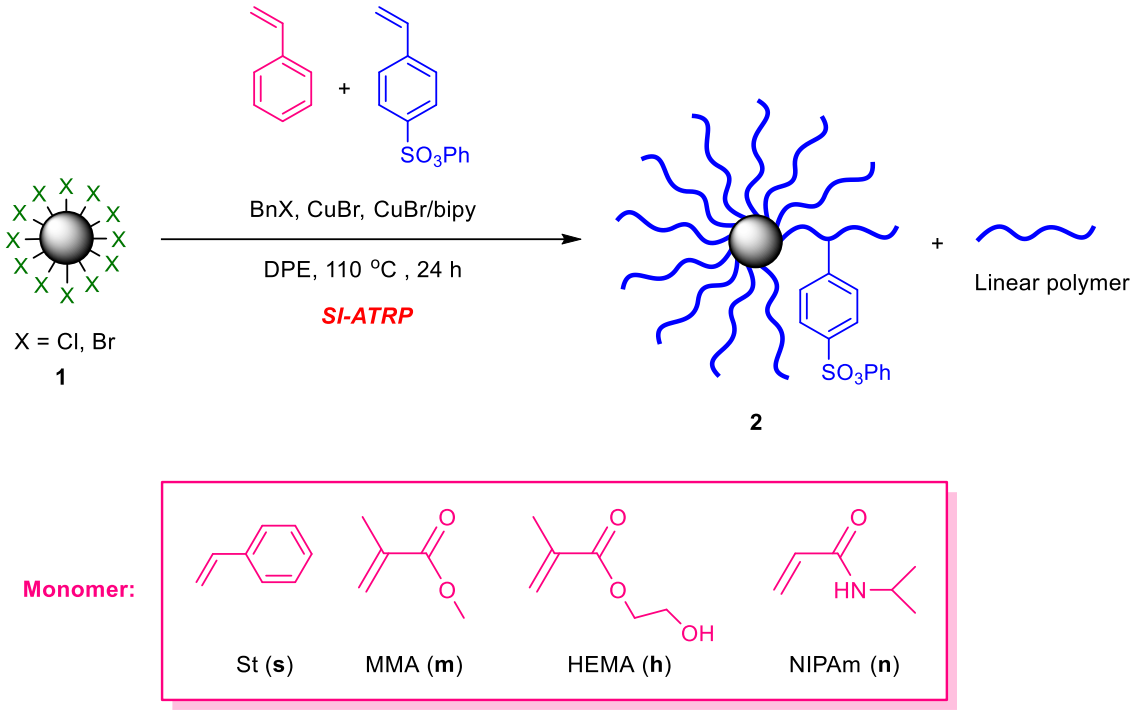

Entry	2	M/I	Comonomer	ΔW%[b]	Grafted Polymer		D_n(2) (μm)[d]	U(2)[d]
					M_n[c]	M_w/M_n[c]		
1	**2d$_{20}$sC$_{20}$**	50	St	72	7,630	1.18	1.34	1.00
2	**2d$_{20}$mC$_{20}$**	50	St	89	7,950	1.19	1.30	1.00
3[e]	**2d$_{20}$hC$_{20}$**	50	St	31	7,220	1.16	1.05	1.06
4	**2d$_{20}$sC$_{20}$-2**	50	St	68	8,090	1.20	2.79	1.01
5	**2d$_{20}$sC$_{20}$-4**	50	St	118	8,790	1.23	4.74	1.01
6	**2d$_{20}$sC$_{20}$-6**	50	St	118	7,910	1.19	6.92	1.01
7	**2d$_{10}$sB$_{20}$**	50	St	157	11,000	1.32	1.90	1.23
8	**2d$_{10}$sB$_{20}$-200**	200	St	207	30,400	1.57	1.95	1.20
9	**2d$_{10}$sB$_{20}$-300**	300	St	263	39,700	1.69	2.00	2.30
10[f]	**2d$_{10}$sB$_{20}$-m**	50	MMA	202	18,300	1.41	1.44	1.24
11	**2d$_{10}$sB$_{20}$-h**	50	HEMA	147	18,200	1.88	1.67	1.24
12	**2d$_{10}$sB$_{20}$-n**	50	NIPAm	96	6,690	1.10	1.56	1.18

[a] SI-ATRPs of **M** (70 mol%) and phenyl *p*-styrenesulfonate (30 mol%) were performed in the presence of **1** in DPE at 110 °C for 24 h. $[Monomer]_o/[X]_o$ (in **1** and BnX)/$[CuBr]_o/[bipy]_o$ (molar ratio) = 100/2/2/6 $[Monomer]_o$ = 6 M, $[X]_o = [CuBr]_o$ = 0.12 M and $[bipy]_o$ = 0.36 M.

[b] Determined by equation 1.

[c] Determined by SEC using DMF as an eluent at a flow rate of 1.0 mL min^{-1} at 40 °C (polystyrene standards).

[d] Measured from SEM images.

[e] DMF was used as solvent.

[f] Polymerization was carried out at 90 °C.

polymers onto the surface of the polymer microspheres **1**, all the polymerization reactions were carried out with the addition of a predetermined amount of the sacrificial initiator, benzyl halide (BnX). The free polymer formed in the course of the polymerization reaction was then isolated for SEC analysis. The characterization of **2** was summarized in Table 5.2.

In FT-IR spectra of core-corona polymer microsphere **2**, two absorption peaks are appeared at 1375 cm^{-1} (strong) and 1175 cm^{-1} (weak) for stretching vibration of S=O bond. The signal intensity for the aromatic region is also slightly stronger than that of the corresponding **1**.

High ΔW was obtained when hydrophobic $\mathbf{1d_{20}sC_{20}}$ or $\mathbf{1d_{20}mC_{20}}$ used as a core in the polymerization compared with $\mathbf{1d_{20}hC_{20}}$ (entries 1 and 2). The ΔW value was increased when $\mathbf{1d_{10}sB_{20}}$ used as a macroinitiator, probably due to low crosslinkage in the core (entry 1 vs 7). The ΔW value was also increased with increasing M_n of the grafted polymer chains (entries 8 and 9). Core-corona microspheres with different kind of monomer in the corona were synthesized using MMA (m), HEMA (h), or NIPAm (n) as comonomer with phenyl *p*-styrenesulfonate (**S**).

The M_n of corona estimated from the characterization of free polymer was in good agreement with the calculated value (Ca. 8,000 g mol^{-1}) and the M_w/M_n values were low (1.00-1.23) (entries 1-7 and 12). The M_n of corona in $\mathbf{2d_{10}sB_{20}}$**-200** and $\mathbf{2d_{10}sB_{20}}$**-300** were also in good agreement with those calculated (Ca. 32,000 and 48,000 g mol^{-1}) (entries 8 and 9). In $\mathbf{2d_{10}sB_{20}}$**-m** and $\mathbf{2d_{10}sB_{20}}$**-h**, the M_n of the corona (18,300 and 18,200 g mol^{-1}) were higher than those calculated, due to the chain termination at the end of polymerization as well as the M_w/M_n values were moderate (1.41 and 1.88, respectively) (entries 10 and 11). From these results, we found that the graft copolymerization of styrene or NIPAm and phenyl *p*-styrenesulfonate proceeded in a controlled manner, affording well-defined core-corona polymer microsphere **2**.

Compared with the D_n(**1**), D_n(**2**) was increased by the corona. SI-ATRP initiated by the surface initiator moiety would lead to small increase of D_n(**2**) value. Actually, the ΔD_n ($\Delta D_n = D_n(\mathbf{2}) - D_n(\mathbf{1})$) were in the range between 180 and 250 nm (entries 1-3). D_n(**2**) was increased with increasing size of core (entries 4-6). With the increase of M/I in the polymerization, higher D_n(**2**) was obtained (entries 7-9). When MMA, HEMA and NIPAm were used instead of styrene as a comonomer, relatively smaller polymer microspheres were obtained (entries 10-12). The large increase of D_n may occur because the poly(styrene-*co*-phenyl *p*-styrenesulfonate) chain grows not only from the surface of **1** but also from the interior of **1**. The phenomenon is observed when the polymer microsphere was well swollen in the polymerization mixture.[52] In most cases, the polydispersity (U) was enough low. As a result, well-defined core-corona polymer microspheres were successfully synthesized by the precipitation polymerization and SI-ATRP.

*5.2.3 Immobilization of MacMillan catalyst precursor **5** onto the side chain of corona of **4***

Core-corona polymer microsphere-supported chiral MacMillan catalyst **6** was prepared by the neutralization reaction between core-corona polymer microsphere having sulfonic acid moiety **4** and MacMillan catalyst precursor **5**. **3** was synthesized by adding three equivalents of NaOH to phenylsulfonate moiety of **2** in THF:MeOH:H_2O (50:10:1) mixed solvent at 50 ^oC for 24 h. The yield and sodium sulfonate content in **3** were summarized in Table 5.3. The acidification reaction was performed by adding twenty equivalents of H_2SO_4 to THF solution of **3** at room temperature, affording **4**. The yield and sulfonic acid content in **4** were also summarized in Table 5.3. The neutralization reaction was conducted by adding CH_3OH solution of **5** (2 equiv.) to THF solution of **4** at room temperature. The resulting polymer particles were obtained after centrifugation, washed with solvents, and dryness. The degree of immobilization and catalyst content were summarized in Table 5.4.

The degree of immobilization of **5** onto **6** was moderate to quantitative, which depend on the property of core-corona polymer microsphere **2**. The degree of immobilization was increased when hydrophilic cross-linked polymer microsphere **1d$_{20}$hC$_{20}$** were used as core (entry 3). The degree of immobilization was also increased when low cross-linked polymer microsphere **1d$_{10}$sB$_{20}$** was used as core (entry 1 vs 7). The degree of immobilization was increased when CH_2Cl_2/MeOH was used instead of THF/MeOH (entry 7 vs 8). The catalyst content in **6** determined based on recovered catalyst were in

Table 5.3 Characterization of core-corona polymer microsphere-supported sodium sulfonate **3** and core-corona polymer microsphere-supported sulfonic acid **4**.

Entry	**3**	Yield (%)	Sodium Sulfonate Content (mmol g^{-1})	**4**	Yield (%)	Sulfonic Acid Content (mmol g^{-1})
1	**3d$_{20}$sC$_{20}$**	94	0.985	**4d$_{20}$sC$_{20}$**	93	1.00
2	**3d$_{20}$mC$_{20}$**	86	0.986	**4d$_{20}$mC$_{20}$**	>99	1.00
3	**3d$_{20}$hC$_{20}$**	85	0.571	**4d$_{20}$hC$_{20}$**	92	0.792
4	**3d$_{20}$sC$_{20}$-2**	92	0.817	**4d$_{20}$sC$_{20}$-2**	93	0.825
5	**3d$_{20}$sC$_{20}$-4**	93	1.14	**4d$_{20}$sC$_{20}$-4**	94	1.18
6	**3d$_{20}$sC$_{20}$-6**	92	1.09	**4d$_{20}$sC$_{20}$-6**	94	1.12
7	**3d$_{10}$sB$_{20}$**	97	1.55	**4d$_{10}$sB$_{20}$**	97	1.61
8	**3d$_{10}$sB$_{20}$-200**	88	1.43	**3d$_{10}$sB$_{20}$-200**	97	1.48
9	**3d$_{10}$sB$_{20}$-300**	86	1.39	**4d$_{10}$sB$_{20}$-300**	98	1.44
10	**3d$_{10}$sB$_{20}$-m**	95	1.47	**4d$_{10}$sB$_{20}$-m**	96	1.52
11	**3d$_{10}$sB$_{20}$-h**	93	1.13	**4d$_{10}$sB$_{20}$-h**	98	1.15
12	**3d$_{10}$sB$_{20}$-n**	92	0.989	**4d$_{10}$sB$_{20}$-n**	99	1.01

Table 5.4 Immobilization of MacMillan catalyst precursor **5** onto the side chain of corona of **4**.

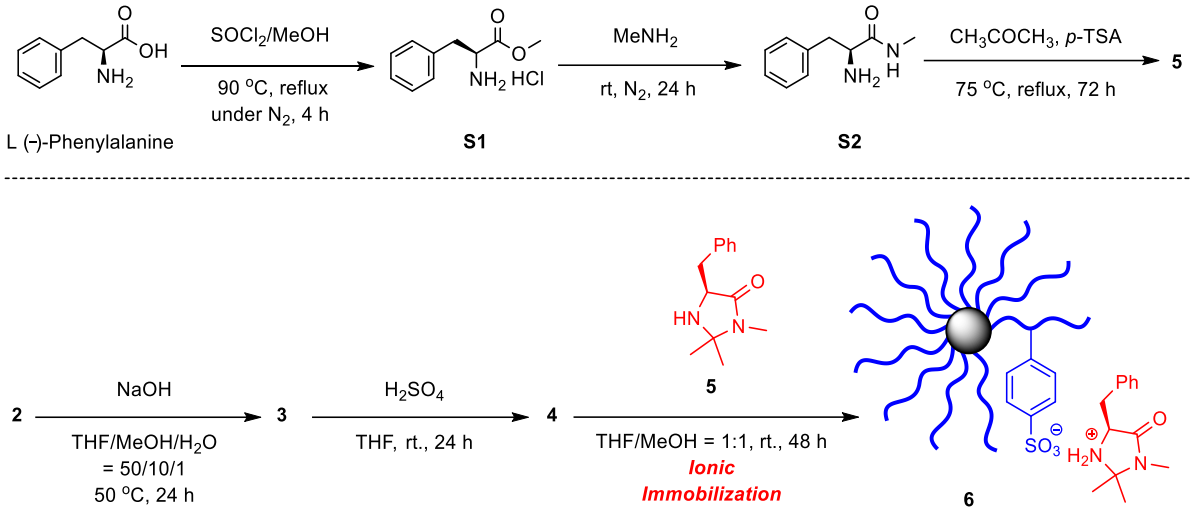

Entry	**6**	**4**	Degree of Immobilization (%)	Catalyst Content (mmol g^{-1})[a]
1	**$6d_{20}sC_{20}$**	**$4d_{20}sC_{20}$**	61	0.533
2	**$6d_{20}mC_{20}$**	**$4d_{20}mC_{20}$**	64	0.569
3	**$6d_{20}hC_{20}$**	**$4d_{20}hC_{20}$**	81	0.583
4	**$6d_{20}sC_{20}$-2**	**$4d_{20}sC_{20}$-2**	62	0.462
5	**$6d_{20}sC_{20}$-4**	**$4d_{20}sC_{20}$-4**	69	0.938
6	**$6d_{20}sC_{20}$-6**	**$4d_{20}sC_{20}$-6**	78	0.736
7	**$6d_{10}sB_{20}$**	**$4d_{10}sB_{20}$**	67	0.851
8[b]	**$6d_{10}sB_{20}$**	**$4d_{10}sB_{20}$**	86	1.06
9[b]	**$6d_{10}sB_{20}$-200**	**$3d_{10}sB_{20}$-200**	98	1.10
10[b]	**$6d_{10}sB_{20}$-300**	**$4d_{10}sB_{20}$-300**	90	1.01
11[b]	**$6d_{10}sB_{20}$-m**	**$4d_{10}sB_{20}$-m**	99	1.14
12[b]	**$6d_{10}sB_{20}$-h**	**$4d_{10}sB_{20}$-h**	87	0.842
13[b]	**$6d_{10}sB_{20}$-n**	**$4d_{10}sB_{20}$-n**	97	0.811

[a] Determined based on recovered catalyst.

[b] CH_2Cl_2/MeOH was used instead of THF/MeOH.

the range of 0.462 and 1.14 mmol g^{-1}. From FT-IR spectra of **6**, the characteristic absorption peak for C=O in imidazolidinone moiety was observed at 1721 cm^{-1} when styrene was used as comonomer in the corona. The corresponding peak was overlapped with the C=O in **$1d_{20}mC_{20}$** or **$1d_{20}hC_{20}$** which was used as the core particle. The scanning electron microsphere (SEM) images of these polymer microspheres were shown in Figure 5.2. Since the deprotection of phenyl sulfonate, the acidification of sodium sulfonate (−SO_3Na), and the ionic immobilization were not influenced on the particle diameter, the D_n(**6**) was unchanged. For example, the D_n of **$3d_{10}sB_{20}$**, **$4d_{10}sB_{20}$** and **$6d_{10}sB_{20}$** were 1.90, 1.92 and 1.91 μm, respectively (Figure 5.2c, d and e). From the elemental analysis, measured nitrogen content in **$6d_{10}sB_{20}$**

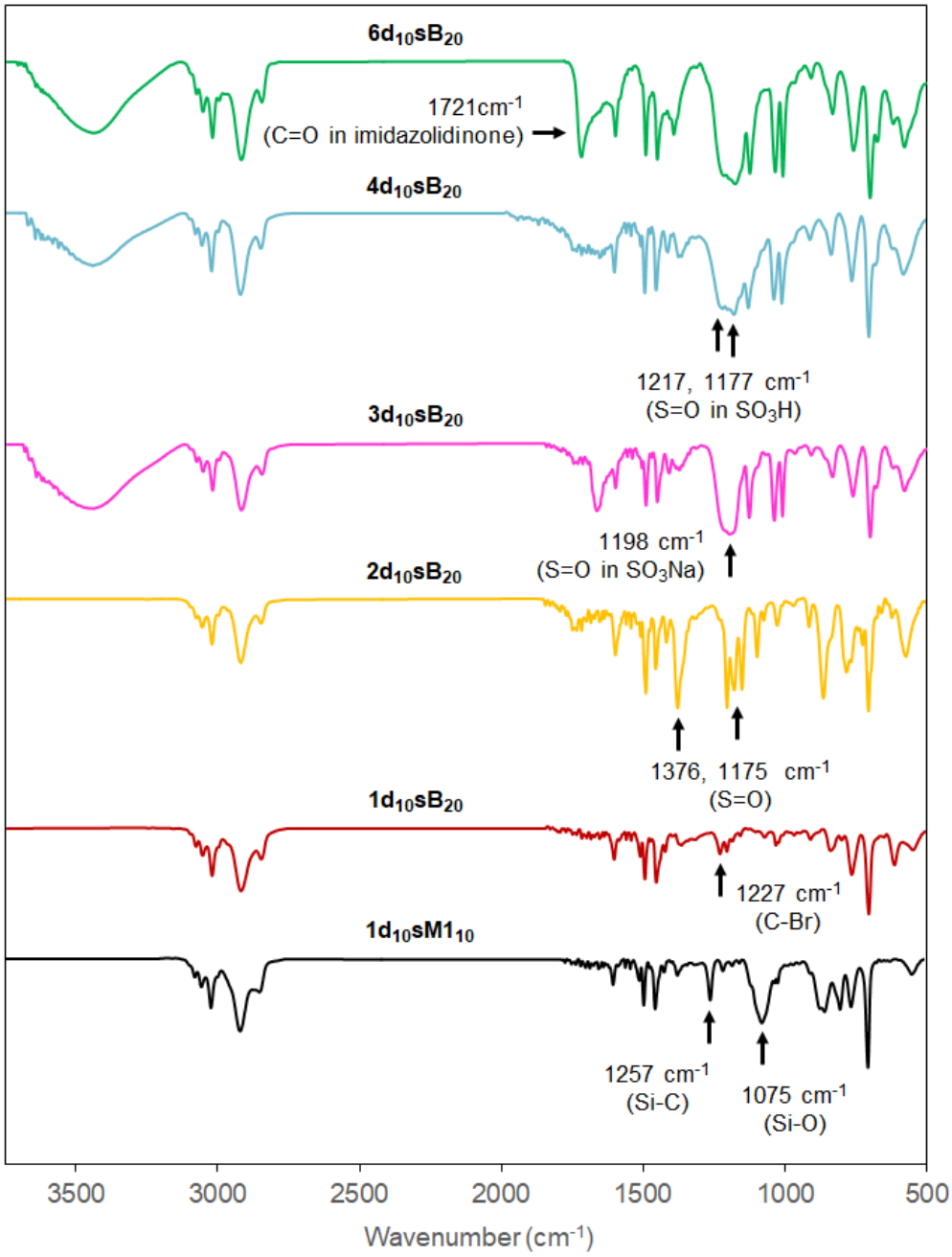

Figure 5.1 FT-IR spectra of **1d$_{10}$sM1$_{10}$**, **1d$_{10}$sB$_{20}$**, **2d$_{10}$sB$_{20}$**, **3d$_{10}$sB$_{20}$**, **4d$_{10}$sB$_{20}$**, and **6d$_{10}$sB$_{20}$**.

was good agreement with calculated one. These results indicated that MacMillan catalyst precursor **5** was successfully immobilized onto the side chain of corona of **4** with ionic bond by the neutralization reaction to afford core-corona polymer microsphere-supported MacMillan catalyst **6**.

*5.2.4 Asymmetric Diels–Alder reaction of trans-cinnamaldehyde **7** and 1,3-cyclopentadiene **8** catalyzed by **6***

In order to examine the catalytic performance of core-corona polymer microsphere-supported MacMillan catalysts **6**, the asymmetric Diels-Alder reaction of *trans*-cinnamaldehyde **7** and 1,3-cyclopentadiene **8** was performed. The reaction was carried out with 10 mol% of catalyst **6** in a

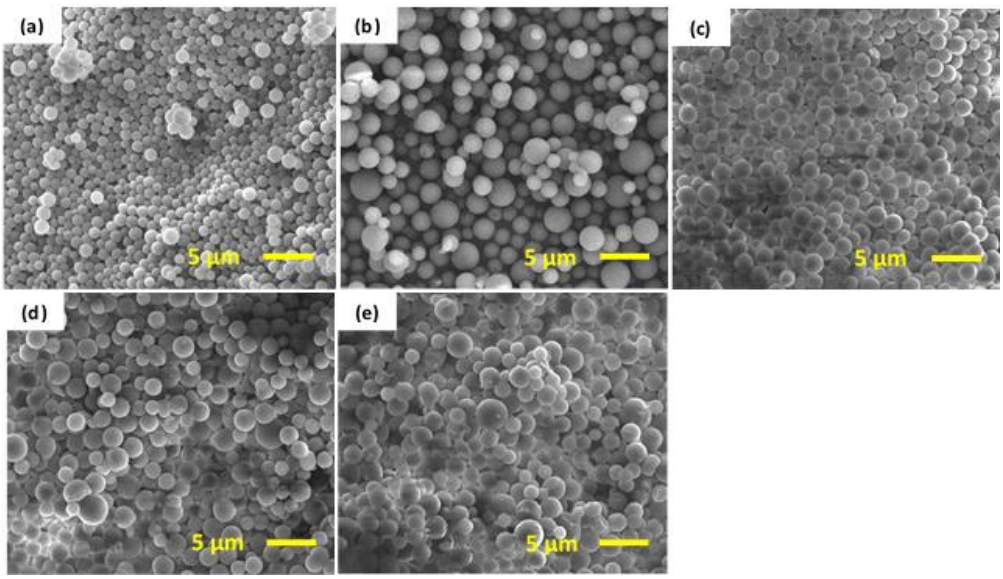

Figure 5.2 SEM images of **1d$_{10}$sB$_{20}$** (a), **2d$_{10}$sB$_{20}$** (b) **3d$_{10}$sB$_{20}$** (c), **4d$_{10}$sB$_{20}$** (d), and **6d$_{10}$sB$_{20}$** (e).

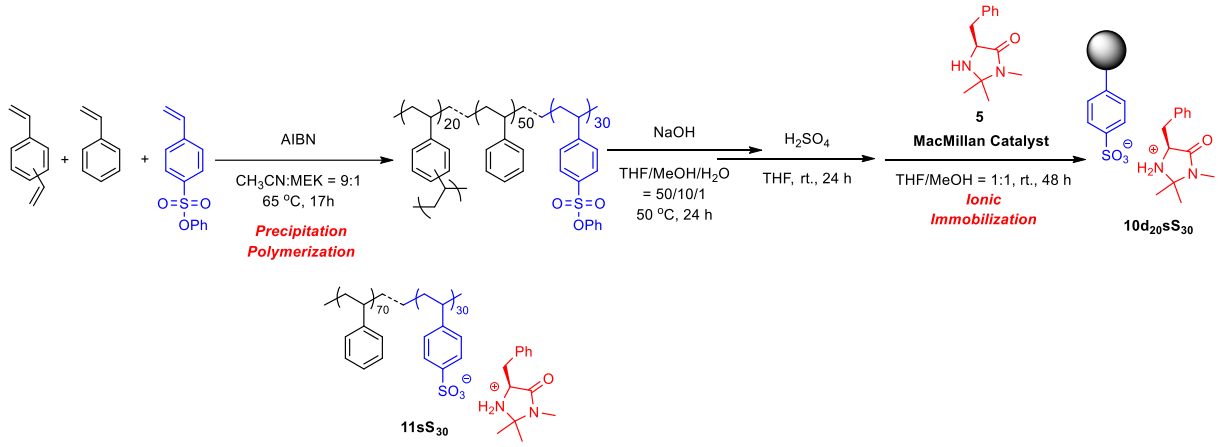

Figure 5.3 Model polymeric catalyst, **10d$_{20}$sS$_{30}$** and **11sS$_{30}$**.

MeOH:H_2O (95:5, *v/v*) mixed solvent at 25 °C, and the results were summarized in Table 5.5. Firstly, we investigated the effect of three types of comonomer (styrene, MMA, or HEMA) in the core of polymer microsphere on the catalytic performance. The catalyst with styrene comonomer **6d$_{20}$sC$_{20}$** exhibited high yield (94%) and excellent enantioselectivity (92% ee for the *exo* isomer and >99% ee for the *endo* isomer) (entry 1). When MMA or HEMA was used as a comonomer in core, the catalytic activity was decreased (entries 2 and 3). Next, the effect of core size on the catalytic performance was looked over by using the same catalyst **6d$_{20}$sC$_{20}$**. The yield of **9** was dropped when the D_n of **6d$_{20}$sC$_{20}$** was increased because the active surface area was decreased (entries 4-6). The catalyst **6d$_{10}$sB$_{20}$** containing low crosslinked core **1d$_{10}$sB$_{20}$** showed high reactivity and enantioselectivity comparable to **6d$_{20}$sC$_{20}$** (entry 1 vs 7). The ee value for *exo* isomer was increased when **6d$_{10}$sB$_{20}$** with high degree of immobilization was used (entry 7 vs 8).

Table 5.5 Catalysts screening in the asymmetric Diels–Alder reaction of *trans*-cinnamaldehyde **7** and 1,3-cyclopentadiene **8** catalyzed by **6**[a].

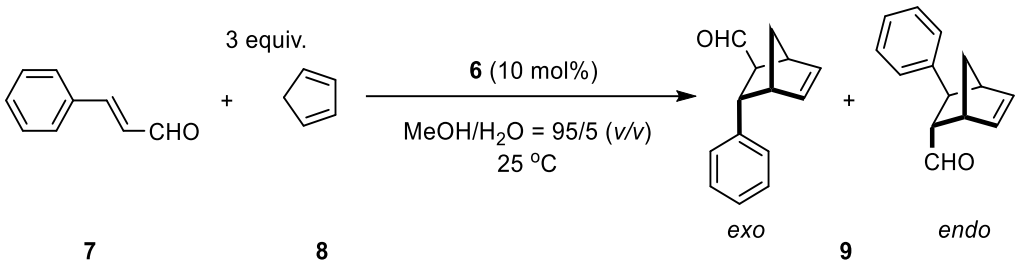

7 **8** **9**

Entry	**6**	Time (h)	**9**			
			Yield (%)[b]	*exo*/*endo*[b]	*ee* (*exo*) (%)[c]	*ee* (*endo*) (%)[c]
1	**6d$_{20}$sC$_{20}$**	36	94	54/46	92	>99
2	**6d$_{20}$mC$_{20}$**	24	50	52/48	87	>99
3	**6d$_{20}$hC$_{20}$**	50	97	53/47	90	>99
4	**6d$_{20}$sC$_{20}$-2**	60	86	54/46	83	93
5	**6d$_{20}$sC$_{20}$-4**	72	81	55/45	82	92
6	**6d$_{20}$sC$_{20}$-6**	72	68	52/48	83	93
7[d]	**6d$_{10}$sB$_{20}$**	36	99	57/43	92	>99
8	**6d$_{10}$sB$_{20}$**	38	99	52/48	99	>99
9	**6d$_{10}$sB$_{20}$-200**	60	64	51/49	91	95
10	**6d$_{10}$sB$_{20}$-300**	60	56	56/44	93	97
11	**6d$_{10}$sB$_{20}$-m**	72	72	58/42	84	>99
12	**6d$_{10}$sB$_{20}$-h**	60	71	53/47	95	97
13	**4d$_{10}$sB$_{20}$-n**	60	80	53/47	92	97
14	**10d$_{20}$sS$_{30}$**	44	97	55/45	95	>99
15	**11sS$_{30}$**	36	89	60/40	94	96

[a] Reactions were conducted with **8** (3 equiv.) in MeOH/H_2O (95/5, *v*/*v*) at 25 °C using **6** (10 mol%).

[b] Determined by ^{1}H NMR spectroscopy.

[c] Determined by GC (CHIRALDEX β-PH).

[d] Degree of immobilization was 67%.

The effect of corona length on the catalytic performance of **6d$_{10}$sB$_{20}$** was also examined. Both the yield and enantiomeric excess were decreased when **6d$_{10}$sB$_{20}$-200** or **6d$_{10}$sB$_{20}$-300** was used (entries 9 and 10). This result indicated that the increase of steric hindrance near the catalytic site significantly affected the catalytic performance. From these results, we found that **6d$_{10}$sB$_{20}$** having hydrophobic corona exhibited high catalytic activity (99% yield) with excellent enantioselectivity (99% ee (*exo*), >99% ee (*endo*)) (entry 8). By contrast, **6d$_{10}$sB$_{20}$-h** and **6d$_{10}$sB$_{20}$-n** containing hydrophilic corona showed relatively poor reactivity and enantioselectivity (entries 12 and 13).

To evaluate the efficiency of **6d$_{10}$sB$_{20}$** in the reaction, some polymeric catalysts, **10d$_{20}$sS$_{30}$** and **11sS$_{30}$** were tested in the same reaction. When uniform-type polymer microsphere-supported catalyst **10d$_{20}$sS$_{30}$**, in which MacMillan catalyst precursor **5** was directly immobilized onto the surface of polymer microsphere was used, the reactivity was found to be slightly lower, probably due to the less flexibility of polymer chain or catalytic site (entry 8 vs 14). Interestingly, the enantioselectivity by **6d$_{10}$sB$_{20}$** was somewhat higher than that obtained by the corresponding linear type polymer-supported catalyst **11sS$_{30}$** (entry 8 vs 15). Considering the reactivity and enantioselectivity, **6d$_{10}$sB$_{20}$** was one of the most efficient heterogeneous catalyst in the investigation.

*5.2.5 Optimization of reaction conditions in the asymmetric Diels–Alder reaction of **7** and **8** catalyzed by **6d$_{10}$sB$_{20}$***

In order to establish the optimal reaction conditions for the asymmetric Diels-Alder reaction of **7** and **8**, we screened the reaction solvent. The reaction solvent in the asymmetric reaction using MacMillan catalyst significantly affected the catalytic reactivity, and did when using a heterogeneous catalyst as well.[39,52] These results were summarized in Table 5.5 Both catalytic reactivity and enantioselectivity were increased with increasing polarity of the solvent used in the reaction (entries 1-

Table 5.6 Optimization of reaction conditions in the asymmetric Diels–Alder reaction of **7** and **8** catalyzed by **6d$_{10}$sB$_{20}$**[a].

Entry	Solvent	Time (h)	**9**			
			Yield (%)[b]	*exo*/*endo*[b]	ee (*exo*) (%)[c]	ee (*endo*) (%)[c]
1	THF	60	18	51/49	57	67
2	CH_2Cl_2	60	25	50/50	61	68
3	CH_3CN	60	29	52/48	66	74
4	MeOH	38	91	56/44	88	>99
5	H_2O	60	97	52/48	82	>99
6	Dry MeOH	38	92	44/56	85	94
7	THF:H_2O = 95:5	60	87	52/48	85	97
8	CHCN:H_2O = 95:5	60	96	53/47	81	92
9	MeOH:H_2O = 95:5	38	99	52/48	99	>99
10	MeOH:H_2O = 85:15	50	99	56/44	91	99
11	MeOH:H_2O = 75:25	62	99	50/50	89	98

[a] Reactions were conducted with **8** (3 equiv.) at 25 °C using **6d$_{10}$sB$_{20}$** (10 mol%) (Entry 8, Table 5.4)

[b] Determined by ^{1}H NMR spectroscopy.

[c] Determined by GC (CHIRALDEX β-PH).

4). The catalyst **6d$_{10}$sB$_{20}$** showed low reactivity with slightly low enantioselectivity (82% ee (*exo*)) when a highly polar solvent, such as H_2O, was used as the solvent, which was probably due to poor dispersity of the polymer microsphere and the hydrophobic polymer chains (entry 4 vs 5). When dry MeOH was used, enantioselectivity was decreased (entry 4 vs 6), which indicated that a trace of H_2O in the solvent assisted with increasing the ee value. There has been a report that the presence of H_2O in the Diels-Alder reaction catalyzed by the chiral imidazolidinium salt enhanced the reactivity.[53] With a 95:5 ratio

Table 5.7 Substrate generality in the asymmetric Diels-Alder reaction catalyzed by **6d$_{10}$sB$_{20}$**[a].

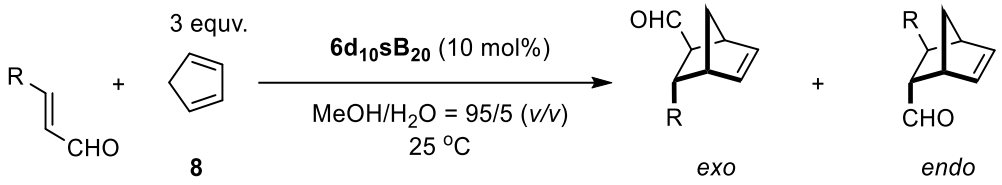

Entry	Aldehyde (R =)	Time (h)	Product	Yield (%)[b]	*exo*/*endo*[c]	ee (*exo*) (%)[d]	ee (*endo*) (%)[d]
1	4-F-Ph **12**	25	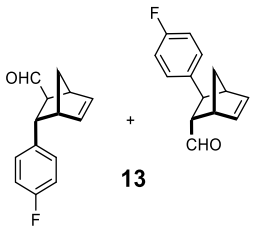 **13**	94	51/49	82	82
2	4-MeOPh **14**	32	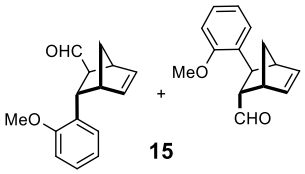 **15**	98	49/51	92	93
3	H **16**	40	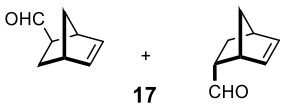 **17**	95[c]	13/87	71	n.d[e]
4[f]	H **16**	48	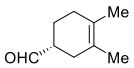 **19**	98[c]	-	95[g]	-

[a] Reaction conducted with 10 mol% of catalyst **6d$_{10}$sB$_{20}$** (Entry 8, Table 5.4).

[b] Isolated yield.

[c] Determined by ^{1}H NMR spectroscopy.

[d] Determined by HPLC after reduction of aldehydes (CHIRALCEL OJ-H).

[e] The ee (*endo*) was not determined due to peak separation problem.

[f] 2,3-dimethylbutadiene **18** was used as substrate instead of **8**.

[g] Determined by GC (CHIRALDEX β-PH).

of THF-H_2O or CH_3CN-H_2O, both reactivity and enantioselectivity were improved, compared with when only THF or CH_3CN was used as a solvent (entry 1 vs 7; entry 3 vs 8). When a 95/5 MeOH/H_2O mixed solvent was used, the catalyst **6d$_{10}$sB$_{20}$** showed excellent reactivity and enantioselectivity (99% ee (*exo*), >99% ee (*endo*)). When the amount of H_2O in the mixed solvent was increased to 25 vol%, the yield and ee were decreased due to the decrease of dispersity of the catalyst. From these results, a 95:5 ratio of MeOH-H_2O at 25 °C was accepted as the optimized conditions for the asymmetric Diels-Alder reaction.

*5.2.6 Substrate generality in the Diels-Alder reaction by **6d$_{10}$sB$_{20}$***

The substrate generality of the reaction was surveyed by the most efficient catalyst **6d$_{10}$sB$_{20}$** in 95:5 ratio of MeOH-H_2O. The reaction between 4-fluorocinnamaldehyde **12** and **8** produced **13** in quantitative yield with high ee (entry 1). The reaction between 2-methoxy cinnamaldehyde **14** and **8** afforded these adducts **15** in 98% yield and with 92% ee (*exo*) and 93% ee (*endo*) (entry 2). The reaction of acrolein **16** and **8** proceeded with moderate enantioselectivity (entry 3). The **6d$_{10}$sB$_{20}$** exhibited high enantioselectivity in the asymmetric Diels–Alder reaction of **16** and 2,3-dimethylbutadiene **18** (entry 4).

5.2.7 Reusability

One of the merits of polymeric catalyst is its facile separation and reuse. Even though linear or gel-type polymeric catalyst can be recovered by decantation or filtration, quantitative recovery of the catalyst is not always easy. By contrast, the polymer microsphere with more than 1 μm diameter can be

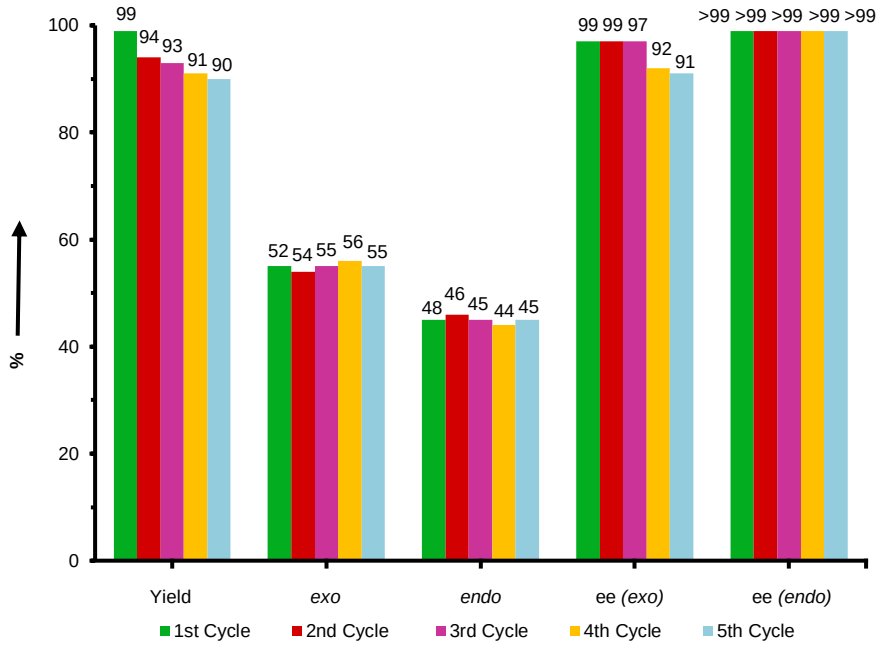

Figure 5.4 Reusability of **6d$_{10}$sB$_{20}$** in the asymmetric Diels-Alder reaction of **7** and **8**.

recovered by centrifugation quantitatively. **6d$_{10}$sB$_{20}$** was recovered with >99% yield. By using the recovered **6d$_{10}$sB$_{20}$**, the reusability was tested in the Diels-Alder reaction of **7** and **8** (Figure 5.4). With the increase of cycle, a slight decrease in the yield was observed. Interestingly, the ionic bonding between sulfonate and the imidazolidinium was found to be enough stable and no leaching of the catalyst was observed at all after the reaction. Besides, the enantioselectivity for the *endo* isomer was unchanged at all in the reuse.

*5.2.8 Reaction mechanism of Diels-Alder reaction catalyzed by **6***

Plausible reaction mechanism was illustrated in Scheme 5.2. The reaction mechanism was essentially similar to that of the original MacMillan's catalyst. Upon condensation of core-corona polymer microsphere-supported MacMillan catalyst **6** and *trans*-cinnamaldehyde **7**, an activated iminium species **9a** was formed, which reacted with 1, 3-cyclopentadiene **8** to form the transition state **9b**. Upon hydrolysis, the transient iminium species **9b** was converted to product **9** (*exo* or *endo*) and the

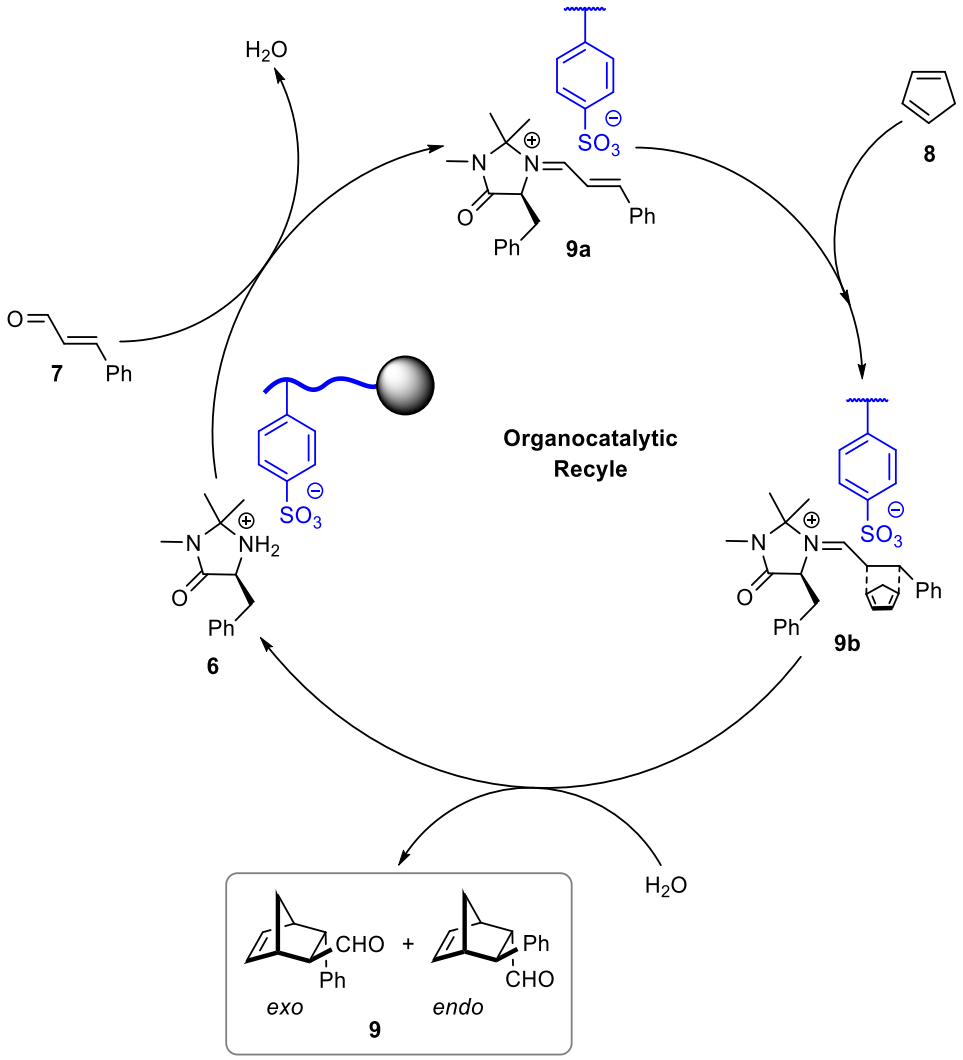

Scheme 5.2 Reaction mechanism of Diels-Alder reaction catalyzed by **6**.

immobilized catalyst **6** was released and entered the new cycle. In the course of the reaction cycle, polymeric sulfonate must be closely located by the iminium or ammonium cation owing to the strong affinity.

5.3 Conclusion

Core-corona polymer microsphere having sulfonic acid **4** was successfully synthesized by the surface-initiated ATRP (SI-ATRP) of monomer such as styrene, MMA, HEMA, and NIPAm and phenyl *p*-styrenesulfonate with monodispersed polymer microsphere having benzyl halide moiety **1** prepared *via* precipitation polymerization as a macroinitiator, followed by the treatment of NaOH and acidification by H_2SO_4. The size of core, kind of monomer, chain length of the corona can be changed as expected. Ionically core-corona polymer microsphere-supported chiral MacMillan catalyst **6** was prepared by the neutralization reaction between the sulfonic acid moiety at the side chain of corona in **4** with MacMillan catalyst precursor **5**. These polymer microsphere-supported catalysts were used as heterogeneous chiral organocatalysts in the asymmetric Diels-Alder reaction of *trans*-cinnamaldehyde **7** and 1,3-cyclopentadiene **8**. We found that the core size affected the catalytic activity in the reaction. The catalytic activity was decreased with longer corona probably due to the steric hindrance of imidazolidinium moiety. The catalyst $\mathbf{6d_{10}sB_{20}}$ containing hydrophobic core and corona gave the Diels-Alder adduct **9** in 99% yield with excellent ee values (99% ee for the *exo* isomer and >99% ee for the *endo* isomer). The best catalyst $\mathbf{6d_{10}sB_{20}}$ showed higher enantioselectivity than that of the corresponding uniform type polymer microsphere-supported catalyst $\mathbf{10d_{20}sS_{30}}$. The catalyst could be reused several times without loss of the enantioselectivity.

5.4 Experimental

5.4.1 Materials and Measurements

Styrene (Kishida Chemical Co. Ltd., Osaka, Japan) and divinylbenzene obtained from Nippon & Sumikin Chemical Co. Ltd., Japan, were washed with aqueous 10% NaOH and water, followed by distilling with CaH_2 under reduced pressure. 2-Hydroxyethyl methacrylate (Wako Pure Chemical Industries Ltd., Japan), methyl methacrylate (Sigma-Aldrich) and 4-vinaylbenzyl chloride were distilled under reduced pressure. *N*-Isopropylacrylamide (TCI, Japan) was recrystallized from a mixture of hexane and acetone (90/10, *v/v*) and dried at a low temperature under vacuum. Copper (I) bromide was stirred with glacial acetic acid overnight and filtered, followed by washing three times with methanol and diethyl ether and then dried under vacuum. 2,2′-Bipyridine (Nacalai Tesque, Japan) was used as received without further purification. Diphenyl ether (Wako Pure Chemical Industries Ltd., Japan) and anisole (Kishida Chemical Co. Ltd., Japan) was purified through passing alumina column.

Chlorine contents in polymer microspheres were measured by titrimetric method. FT-IR spectra were recorded with a JEOL JIR-7000 FT-IR spectrometer and are reported in reciprocal centimeter (cm^{-1}). SEM measurements were conducted by using JSM-IT100 at an acceleration voltage of 10.0 kV. The number-average diameter (D_n) and the dispersity index (U) were determined from the SEM image.

Number-averaged diameter (D_n), weight-averaged diameter (D_w), and polydispersity index (U) of polymer microsphere were calculated using the following equations by counting at least a hundred of individual particles from the SEM images.

$$D_n = \frac{\sum n_i d_i}{\sum n_i} \quad (2)$$

$$D_w = \frac{\sum n_i d_i^4}{\sum n_i d_i^3} \quad (3)$$

$$U = \frac{D_w}{D_n} \quad (4)$$

Where n_i is the number of particles with d_i.

*5.4.2 General procedure for the synthesis of polymer microspheres having benzyl chloride moiety **1** by precipitation polymerization*

Monodisperse polymer microspheres having benzyl chloride **1** were synthesized by precipitation polymerization of various comonomers (St, MMA, and HEMA) and divinylbenzene (DVB) with 4-vinylbenzyl chloride (VBC) using AIBN as initiator in acetonitrile or acetonitrile: toluene = 9:1.

*Representative synthesis procedure for **1d$_{20}$sC$_{20}$***: A 180 mL HDPE narrow-mouth bottle was charged with 20 mol% of DVB (1.32 g, 10.1 mmol), 60 mol% of St (3.15 g, 30.2 mmol), 20 mol% VBC (1.54 g, 10.1 mmol), AIBN (0.120 g, 0.720 mmol) and 183 mL of CH_3CN under N_2 gas. Polymerization was carried out in an incubator at a constant temperature of 65 °C with rolling the bottle horizontally at 9 rpm for 3 h. The reaction mixture was cooled to room temperature, and the insoluble fraction was collected by centrifugation and washed with THF, methanol, and acetone. The solid product was dried under vacuum at 40 °C for 24 h. 0.182 g, 3% yield; FT-IR (KBr): ν = 1265 (C−Cl), 1602, 1509, 1451 (C=C in aromatic ring), 3059, 3024 (C−H in aromatic ring), and 2921, 2849 (C−H in alkyl) cm^{-1}. Chlorine contents: 1.67 mmol g^{-1}.

1d$_{10}$sB$_{20}$: The synthesis procedure of **1d$_{10}$sB$_{20}$** was discussed in **section 2.4.5** of Chapter **II**. FT-IR (KBr): ν = 1227, 608 (C−Br), 1602, 1508, 1452 (C=C in aromatic ring), 3058, 3025 (C−H in aromatic ring), 2922, 2850 (C−H in alkyl) cm^{-1}. Elemental analysis calcd. for **1d$_{10}$sB$_{20}$** ($C_{9.2}H_{9.2}Br_{0.2}$): C 81.39%, H 6.84%, Br 11.77%; found: C 78.65%, H 6.64%, Br 13.29%. Bromine content measured from the titrimetric method and the elemental analysis were 1.89 and 1.66 mmol g^{-1}, respectively.

*5.4.3 Synthesis of core-corona polymer microspheres **2** from graft copolymerization of an achiral monomer with p-phenyl styrenesulfonate (**S**) using **1** as multifunctional Initiator by surface-initiated ATRP*

*Representative synthesis procedure for **2d$_{10}$sB$_{20}$***: To a 6 mL vial with magnetic stir bar, CuBr (0.34 g, 0.24 mmol), **1d$_{10}$sB$_{20}$** (0.106 g, 0.200 mmol) and 2 mL of diphenyl ether were added. The reaction mixture was purged with argon for 5 min and 2, 2′-bipyridine (0.112 g, 0.720 mmol) was added. After additional 5 min of argon bubbling, 70 mol% of styrene (0.875 g, 8.40 mmol), 30 mol% of *p*-phenyl styrenesulfonate (0.937 g, 3.60 mmol) and a sacrificial initiator (benzyl chloride (BnCl), 0.056 g, 0.044 mmol) were added in the mixture. $[St+S]_o/[Cl]_o$ (in **1d$_{10}$sB$_{20}$** and BnCl)/$[CuBr]_o/[bipy]_o$ (molar ratio) was set to 100/2/2/6. The polymerization was carried out in oil bath at 110 ^oC for 24 h with stirring at 400 rpm. The resulting blue-green polymer particles were isolated by centrifugation and washed with THF three times, and washed with methanol and glacial acetic acid (95/5, *v/v*)) several times until resulting solids became almost white. Finally, these solids were washed with diethyl ether twice. These core-corona polymer microspheres were dried at 40 ^oC under vacuum oven.

The free polymers were collected from the supernatant by precipitation into MeOH (100~125 mL). The polymers then were dissolved in THF and passed over alumina column for removing metal. Finally, the resulting polymers were collected by dropwise adding in MeOH, followed by filtration and then dried at 40 ^oC under vacuum oven to provide a white powder.

2d$_{10}$sB$_{20}$: FT-IR (KBr): ν = 1376, 1176 (S=O), 1600, 1489, 1454 (C=C in aromatic ring), 3060, 3025 (C−H in aromatic ring), and 2924, 2851 (C−H in alkyl) cm^{-1}.

*5.4.4 Synthesis of core-corona polymer microsphere-supported sodium sulfoante **3***

*Representative synthesis procedure for **3d$_{10}$sB$_{20}$***: **2d$_{10}$sB$_{20}$** (0.667 g, 0.954 mmol of phenylsulfonate moiety) and NaOH (0.118 g, 2.86 mmol) were taken in a flask with magnetic stir bar and the mixture of solvent (THF/MeOH/H_2O = 16.03/3.21/0.32 (mL) was added. The reaction was carried out in an oil bath at 50 °C for 24 h. The reaction mixture was cooled to room temperature, and the particles was collected by centrifugation and washed with methanol, water, and acetone several times. The solid product was dried at 40 °C under vacuum for 12 h. 0.598 g, 97% yield; sodium sulfonate content: 1.55 mmol g^{-1}. FT-IR (KBr): ν = 1198 (S=O stretching in SO_3Na), 1601, 1493, 1453 (C=C in aromatic ring), 3059, 3025 (C−H in aromatic ring), and 2923, 2850 (C−H in alkyl) cm^{-1}.

*5.4.5 Synthesis of core-corona polymer microsphere-supported sulfonic acid **4***

*Representative synthesis procedure for **4d$_{10}$sB$_{20}$***: **3d$_{10}$sB$_{20}$** (0.573 g, 0.880 mmol of sodium sulfonate moiety) was taken in a flask with a magnetic stir bar inside and then THF (47 mL) added. The diluted solution of H_2SO_4 (0.98 mL) was added slowly into the mixture. The reaction was carried out at room

temperature for 24 h. The reaction mixture was cooled to room temperature, and the particles were collected by centrifugation and washed with water, methanol and acetone. The solid product was dried at 40 °C under vacuum for 12 h. 0.539 g, 97% yield; sulfonic acid content: 1.61 mmol g^{-1}. FT-IR (KBr): ν = 1217, 1175 (S=O stretching in SO_3H), 1601, 1558, 1453 (C=C in aromatic ring), 3059, 3025 (C−H in aromatic ring), and 2923, 2850 (C−H in alkyl) cm^{-1}.

*5.5.6 Synthesis of MacMillan catalyst precursor **5***

MacMillan catalyst **5** was synthesized by the following steps:

*Synthesis of **S1***: A 100-mL round-bottomed flask with a magnetic stirring bar was charged with MeOH (40.0 mL, 90.0 mmol) and $SOCl_2$ (6.40 mL, 88.0 mmol) was added slowly under N_2 gas at 0 °C. The ice bath was removed after adding $SOCl_2$ and then L (–) - phenylalanine (3.03 g, 18.3 mmol) was added. The reaction was continued for 4 h at 90 °C under N_2 gas. The solvent used was evaporated and pumped up. The obtained crude product **S1** is a white solid (3.93 g, 99% yield). ^{1}H NMR (400 MHz, δ = 4.66 (D_2O): δ = 3.09 - 3.14 (m, 1H), 3.21 - 3.26 (m, 1H), 3.71 (s, 3H), 4.32 (dd, J = 1.8, 5.8 Hz, 1H), 7.16 - 7.32 (m, 5H).

*Synthesis of **S2***: A 100-mL round-bottomed flask with a magnetic stirring bar was charged with **S1** (3.43 g, 15.9 mmol) and $MeNH_2$ (17.0 mL, 204 mmol). The reaction was carried out for 24 h at room temperature under N_2 gas. The reaction mixture was pumped up and extracted with Et_2O (40 mL × 2). The bottom phase was evaporated by rotary evaporator and then added saturated $NaHCO_3$ to make basic medium (pH >7). The solution was transferred into separatory funnel and extracted with $CHCl_3$ (40 mL × 3). The organic phase was dried over $MgSO_4$. After removing $MgSO_4$ by filtration, the solvent ($CHCl_3$) was removed by rotary evaporator and pumped up. The obtained product **S2** is a white solid (1.74 g, 9.76 mmol, 51% yield). ^{1}H NMR (400 MHz, δ = 4.66 (D_2O): δ = 2.59 (m, 3H), 2.87 (d, J = 7.0 Hz, 2H), 3.55 (t, J = 6.7 Hz, 1H), 7.18 - 7.34 (m, 5H).

*Synthesis of MacMillan Catalyst precursor **5**:* A 100-mL round-bottomed flask with a magnetic stirring bar was charged with **S2** (1.74 g, 9.76 mmol), *p*-TSA (0.070 g, 0.037 mmol) and acetone (26.7 mL). The reaction was continued for 72 h at 75 °C. The reaction mixture was evaporated by rotary evaporator and pumped up. The crude product was purified by column chromatography on silica gel with EtOAc/Hexane = 4:1 as eluents to afford the compound, **5** as a reddish liquid (1.36 g, 78% yield; R_f = 0.14). ^{1}H NMR (400 MHz, δ = 4.66 (D_2O): δ = 1.14 (s, 3H), 1.24 (s, 3H), 2.73 (s, 3H), 2.97 - 3.01 (m, 1H), 3.11 - 3.14 (m, 1H), 3.77 (dd, J = 1.9, 4.6 Hz, 1H), 7.20 - 7.29 (m, 5H). ^{13}C NMR (100 MHz, $CDCl_3$, δ = 77.17 ($CDCl_3$), TMS): δ = 25.32, 25.39, 27.30, 37.32, 59.36, 75.65, 126.88, 128.68, 129.60, 137.24, 173.49. HRMS (ESI, *m/z*): $[M + Na]^+$ calcd. for $C_{13}H_{18}N_2NaO$: 241.1311, found: 283.0422.

*5.4.7 Immobilization of MacMillan catalyst precursor **5** onto the side chain of corona of **4***

*Representative synthesis procedure for **6d$_{10}$sB$_{20}$:*** **4d$_{10}$sB$_{20}$** (0.477 g, 0.768 mmol of sulfonic acid moiety) was taken in a Schlenk tube with a magnetic stir bar and **5** (0.335 g, 1.54 mmol) was dissolved in 6.98 mL of MeOH. The solution of **5** was added into the tube and then an equal amount of CH_2Cl_2 was added. The reaction was continued at room temperature for 48 h. The resulting polymer particles were isolated by centrifugation and redispersed in MeOH, and acetone. The catalyst immobilized core-corona polymer particles were dried at 40 °C under vacuum. The unreacted catalysts were recovered from the collected supernatant by removing solvent mixtures through vacuum evaporator, followed by pumped up. The degree of immobilization and catalyst content was 86% and 1.06 mmol g^{-1}, respectively. Elemental analysis calcd. for **6d$_{10}$sB$_{20}$** ($C_{21.2}H_{22.6}N_{0.6}O_{1.2}S_{0.3}Br_{0.2}$): C 77.01%, H 6.90%, N 2.54%; found: C 73.28%, H 6.64%, N 2.40%. Nitrogen content measured from based on the immobilized catalyst and the elemental analysis were 2.12 and 1.73 mmol g^{-1}, respectively.

5.4.8 Synthesis of 10d$_{20}$sS$_{30}$

10d$_{20}$sS$_{30}$ was synthesized by the following steps:

*Synthesis of **M-d$_{20}$sS$_{30}$** or **simply, M-S**:* A 30 mL HDPE narrow-mouth bottle was charged with DVB (0.169 g, 1.30 mmol) St (0.334 g, 3.21 mmol), S (0.507 g, 1.95 mmol), AIBN (0.020 g), and 27 mL of acetonitrile and 3 mL of MEK under N_2 gas. Polymerization was carried out in an incubator at a constant temperature of 65 °C for 17 h with rolling the bottle horizontally at 9 rpm. The reaction mixture was cooled to room temperature, and the insoluble fraction was collected by centrifugation and washed with THF, methanol, and acetone. The solid product was dried under vacuum at 40 °C for 24 h. 0.378 g, 37% yield; sulfonate monomer content: 1.90 mmol g^{-1}. FT-IR (KBr): ν = 1376, 1176 (S=O), 1596, 1488, 1454 (C=C in aromatic ring), 3060, 3025 (C−H in aromatic ring), and 2924, 2853 (C−H in alkyl) cm^{-1}. The number-average diameter (D_n) and polydispersity index (D_w/D_n) measured from SEM image was found 1.26 μm and 1.01, respectively.

*Synthesis of **M-SNa**:* **M-S** (0.299 g, 0.568 mmol of phenylsulfonate moiety) and NaOH (0.070 g, 1.6 mmol) were taken in a flask with a magnetic stir bar inside and a mixed solvent 50:10:1 THF:MeOH:H_2O (= 9.54/1.91/0.19 (mL)) was added. The reaction was carried out in an oil bath at 50 °C for 24 h. The reaction mixture was cooled to room temperature, and the particles were collected by centrifugation and washed with methanol, water and acetone. The solid product was dried at 40 °C under vacuum for 24 h. 0.282 g, >99% yield; sodium sulfonate content: 2.12 mmol g^{-1}. FT-IR (KBr): ν = 1190 (S=O stretching in SO_3Na), 1601, 1507, 1452 (C=C in aromatic ring), 3024 (C−H in aromatic ring), and 2924, 2854 (C−H in alkyl) cm^{-1}.

*Synthesis of **M-SH**:* **M-SNa** (0.165 g, 0.350 mmol of sodium sulfonate moiety) was taken in a flask

with a magnetic stir bar inside and then THF (18 mL) added. The diluted solution of H_2SO4 (0.37 mL) was added slowly into the mixture. The reaction was carried out at room temperature for 24 h. The reaction mixture was cooled to room temperature, and the particles were collected by centrifugation and washed with water, methanol and acetone. The solid product was dried at 40 ^oC under vacuum for 12 h. 0.150 g, 96% yield; sulfonic acid content: 2.23 mmol g^{-1}. FT-IR (KBr): ν = 1217, 1175 (S=O stretching in SO_3H), 1601, 1558, 1456 (C=C in aromatic ring), 3025 (C−H in aromatic ring), and 2924, 2854 (C−H in alkyl) cm^{-1}.

Synthesis of ***10d$_{20}$sS$_{30}$***: **M-SH** (0.142 g, 0.317 mmol of sulfonic acid moiety) was taken in a Schlenk tube with a magnetic stir bar inside and 5 (0.141 g, 0.646 mmol) was dissolved in 1.0 mL of MeOH. The solution of **5** was added into the tube and then 1.0 mL of CH_2Cl_2 was added. The reaction was continued at room temperature for 48 h. The resulting polymer particles were isolated by centrifugation and redispersed in MeOH, and acetone. The catalyst immobilized core-corona polymer particles were dried at 40 ^oC under vacuum. The unreacted catalysts were recovered from the collected supernatant by removing solvent mixtures through vacuum evaporator, followed by pumped up. The degree of immobilization and catalyst content was 66% and 1.12 mmol g^{-1}, respectively

5.4.9 Synthesis of ***11sS$_{30}$***

11sS$_{30}$ was synthesized by the following four steps: (i) Synthesis of **sS$_{30}$**; (ii) Synthesis of **sSNa$_{30}$**; (iii) Synthesis of **sSH$_{30}$**, and (iv) Synthesis of **11sS$_{30}$**. The synthesis procedures for **sS$_{30}$** and **sSNa$_{30}$** were discussed in **section 4.4.6** of Chapter **IV**.

Synthesis of ***sSH$_{30}$:*** The reaction conditions were similar to that of **M-SH**. The resulting polymers were collected by drop wise adding in ether. The insoluble fraction was collected by centrifugation and washed with small amount of methanol, and acetone. The solid product was dried under vacuum at 40 ^oC for 24 h. 95% yield; sulfonic acid content: 2.35 mmol g^{-1}. FT-IR (KBr): ν = 1217 (S=O stretching in SO_3H), 1601, 1494, 1454 (C=C in aromatic ring), 3059, 3025 (C−H in aromatic ring), and 2923, 2850 (C−H in alkyl) cm^{-1}.

Synthesis of ***11sS$_{30}$***: The synthesis procedure was as same as that of **10d$_{20}$sS$_{30}$**. The resulting polymers were extracted with CH_2Cl_2 (twice). The extracted solvent was evaporated and pumped up. Finally, the polymers were washed with hexane. The solid product was pumped up and dried under vacuum at 40 ^oC for 24 h. The degree of immobilization and catalyst content was 100% and 1.61 mmol g^{-1}, respectively.

5.4.10 A representative asymmetric Diels–Alder reaction of ***7*** *and* ***8*** *catalyzed by* ***6d$_{10}$sB$_{20}$***

A Schlenk tube equipped with a magnetic stirring bar was charged with **6d$_{10}$sB$_{20}$** (0.050 mmol of

catalyst), and 0.25 mL of CH_3OH/H_2O(95/5, *v*/*v*) mixed solvent. Then, **7** (0.066 g, 0.50 mmol) and **8** (0.099 g, 1.5 mmol) was added to the mixture, which was stirred at 25 °C for 36 h. The reaction mixture was transferred into a centrifuge tube and the mixture was isolated by centrifugation and washed with ether two or three times. The solvents were removed by rotary evaporator until remaining 1 mL solvents. Then CH_2Cl_2:H_2O:trifluoroacetic acid (2:2:1) was added into the flask. After stirring for 2 h, the mixture was neutralized by saturated $NaHCO_3$ aqueous solution. The mixture was extracted with 5 mL of. The organic layer was further extracted by adding 8 mL of H_2O and 5 mL of Et_2O, followed by extracting using 8 mL saturated NaCl, and the organic layer was dried with anhydrous $MgSO_4$. After removing $MgSO_4$ by filtration, the solvent of the filtrate was removed using a vacuum pump. The crude Diels-Alder adducts were obtained as liquids which were purified using silica gel column chromatography (with 1:19 ethyl acetate/hexane as an eluent). The Diels-Alder adducts 9 were obtained as colorless liquids. The yield and *exo*/*endo* ratio were determined using ^{1}H NMR through comparison of the proton signals of the aldehyde. The enantiomeric excess of *exo* and *endo* isomers was determined using GC through comparison of the peak area ratio (Astec CHIRALDEX β-PH; injection temperature of 180 °C, detection temperature of 180 °C, the column temperature was increased from 150 °C to 180 °C with 1 °C/min; retention time: 35.0 min (*exo*(*2R*)), 35.6 min (*exo*(*2S*)), 36.3 min (*endo*(*2R*)), and 37.0 min (*endo*(*2S*)).

References

[1] (a) Dalko, P. I. Ed., *Enantioselective Organocatalysis*, Wiley-VCH, Weinheim, Germany, 2007. (b) Berkessel, A.; Grçger, H. in *Asymmetric Organocatalysis: From Biomimetic Concepts to Applications in Asymmetric Synthesis*, Wiley-VCH, Weinheim, 2005. (c) Benaglia, M.; Puglisi, A.; Cozzi, F. *Chem. Rev.* **2003**, *103*, 3401 - 3429.

[2] (a) Dalko, P. I. Ed. In *Comprehensive Enantioselective Organocatalysis*, Wiley-VCH, Weinheim, 2013, Chap. 4. (b) MacMillan, D. W. C. *Nature* **2008**, *455*, 304 -308. (c) Lelais, G.; MacMillan, D. W. C. *in New Frontiers in Asymmetric Catalysis*, (Mikami, K.; Lautens M. Eds.), John Wiley & Sons, 2007, pp 319 - 331; (d) Mukherjee, S.; Yang, J. W.; Hoffmann, S.; List, B. *Chem. Rev.* **2007**, 1*07*, 5471 - 5569 (e) Erkkila, A.; Majander, I.; Pihko, P. M. *Chem. Rev.* **2007**, *107*, 5416 - 5470 (f) Lelais, G.; MacMillan, D. W. C. *Aldrichimica Acta* **2006**, *39*, 79 - 87.

[3] Ahrendt, K. A.; Borths, C. J.; MacMillan, D. W. C. *J. Am. Chem. Soc.* **2000**, *122*, 4243 - 4244.

[4] Jen, W. S.; Wiener, J. J. M.; MacMillan, D. W. C. *J. Am. Chem. Soc.* **2000**, *122*, 9874 - 9875.

[5] Paras, N. A.; MacMillan, D. W. C. *J. Am. Chem. Soc.* **2001**, *123*, 4370 - 4371.

[6] Austin, J. F.; MacMillan, D. W. C. *J. Am. Chem. Soc.* **2002**, *124*, 1172 - 1173.

[7] Brochu, M. P.; Brown, S. P.; MacMillan, D. W. C. *J. Am. Chem. Soc.* **2004**, *126*, 4108 - 4109.

[8] Beeson, T. D.; MacMillan, D. W. C. *J. Am. Chem. Soc.* **2005**, *127*, 8826 - 8828.

[9] Northrup, A. B.; MacMillan, D. W. C. *J. Am. Chem. Soc*. **2002**, *124*, 6798 - 6799.

[10] Fonseca, M. T. H.; List, B. *Angew. Chem. Int. Ed.* **2004**, *43*, 3958 - 3960.

[11] Lee, S.; MacMillan, D. W. C. *Tetrahedron* **2006**, *62*, 11413 - 11424.

[12] Pham, P. V.; Ashton, K.; MacMillan, D. W. C. *Chem. Sci*. **2011**, *2*, 1470 - 1473.

[13] Mastracchio, A.; Warkentin, A. A.; A. Walji, M.; MacMillan, D. W. C. *Proc. Natl. Acd. Sci*. USA, **2010**, *107*, 20648 - 20651.

[14] Mangion, I. K.; Northrup, A. B.; MacMillan, D. W. C. *Angew. Chem.* **2004**, *116*, 6890 - 6892; *Angew. Chem. Int. Ed.* **2004**, *43*, 6722 - 6724.

[15] Ouellet, S. G.; Tuttle, J. B.; MacMillan, D. W. C. *J. Am. Chem. Soc.* **2005**, *127*, 32 - 33.

[16] Kunz, R. K; MacMillan, D. W. C. *J. Am. Chem. Soc.* **2005**, *127*, 3240 - 3241.

[17] Haraguchi, N.; Itsuno, S. Ed. *In Polymeric Chiral Catalyst Design and Chiral Polymer Synthesis*, Wiley, Hoboken, 2011, Chap. 2, pp 17- 61.

[18] Benaglia, M.; Celentano, G.; Cinquini, M.; Puglisi, A.; Cozzi, F. *Adv. Synth. Catal.* **2002**, *344*, 149 - 152.

[19] Selkälä, S. A.; Tois, J.; Pihko, P. M.; Koskinen, A. M. P. *Adv. Synth. Catal.* **2002**, *344*, 941- 945.

[20] Puglisi, A.; Benaglia, M.; Cinquini, M.; Cozzi F.; Celentano, G. Eur. *J. Org. Chem.* **2004**, 567 - 573.

[21] Zhang, Y.; Zhao, L.; Lee, S. S.; Ying, J. Y. *Adv. Synth. Catal.* **2006**, *348*, 2027 - 2032.

[22] Mason, B. P.; Bogdan, A. R.; Goswami, A.; McQuade, D. T. *Org. Lett.* **2007**, *9*, 3449 - 3451.

[23] Kristensen, T. E.; Vestli, K.; M. Jakobsen, G.; Hansen F. K.; Hansen, T. J. *J. Org. Chem.* **2010**, *75*, 1620 - 1629.

[24] Guizetti, S.; Benaglia, M.; Siegel, J. S. *Chem. Commun.* **2012**, *48*, 3188 - 3190.

[25] Riente, P.; Yadav, J.; Pericás, M. A. *Org. Lett.* **2012**, *14*, 3668 - 3671.

[26] Moore, B. L.; Lu, A.; Longbottom, D. A.; O'Reilly, R. K. *Polym. Chem.* **2013**, *4*, 2304 - 2312.

[27] Chiroli, V.; Benaglia, M.; Cozzi, F.; Puglisi, A.; Annunziata, R.; Celentano, G. *Org. Lett.* **2013**, *15*, 3590 - 3593.

[28] Wang, C. A.; Zhang, Y.; Shi, J. Y.; Wang, W. *Chem. Asian J.* **2013**, *8*, 1110 -1114.

[29] Chiroli, V.; Benaglia, M.; Puglisi, A.; Porta, R.; Jumde, R. P.; Mandoli, A. *Green Chem.* **2014**, *16*, 2798 - 2806.

[30] Salvo, A. M. P.; Giacalone, F.; Nato, R.; Gruttadauria, M.; *ChemPlusChem* **2014**, *79*, 857 - 862.

[31] Takata, L. M. S.; Iida, H.; Shimomura, K.; Hayashi, K.; Santos, A. A. D.; Yashima, E. *Macromol. Rapid. Commun.* **2015**, *36*, 2047 - 2054.

[32] Ranjber, S.; Riente, P.; Rodriguez-Escrich, C.; Yadav, J.; Ramineni, K.; Pericás, M. A. *Org. Lett.* **2016**, *18*, 1602 - 1605.

[33] Li, X.; Yang, B.; Zhang, S.; Jia, X.; Hu, Z. *Colloid Polym. Sci*. **2017**, *295*, 573 - 582.

[34] Wang, C. A.; Li, Y. W.; Han, Y. F.; Zhang, J. P.; Wu, R. T.; He, G. F. *Polym. Chem.* **2017**, *8*, 5561 - 5569.

[35] (a) Gruttadauria, M.; Riela, S.; Aprile, C.; Lo Meo, P.; D'Anna, F.; Noto, R. *Adv. Synth. Catal.* **2006**, *348*, 82 - 92. (b) An, Z.; Zhang, W.; Shi, H.; He, J. *J. Catal.* **2006**, *241*, 319 - 327. (c) Vijaikumar, S.; Dhakshinamoorthy, A.; Pitchumani, K. *Appl. Catal. A* **2008**, *340*, 25 - 32.

[36] Mitsudome, T.; Nose, K.; Mizugaki, T.; Jitsukawa, K.; Kaneda, K. *Tetrahedron Lett.* **2008**, *49*, 5464 - 5466.

[37] Hagiwara, H.; Kuroda, T.; Hoshi T.; Suzuki, T. Adv. *Synth. Catal.* **2010**, *352*, 909 - 916.

[38] Arakawa, Y.; Haraguchi, N.; Itsuno, S. *Angew. Chem. Int. Ed.* **2008**, *47*, 8232 - 8235.

[39] Haraguchi, N.; Takemura Y.; Itsuno, S. *Tetrahedron Lett.* **2010**, *51*, 1205 - 1208.

[40] Haraguchi, N.; Kiyono, H.; Takemura, Y.; Itsuno, S. *Chem. Commun.* **2012**, *48*, 4011 - 4013.

[41] Itsuno, S.; Oonami, T.; Takenaka, N.; Haraguchia, N. *Adv. Synth. Catal.* **2015**, *357*, 3995 - 4002.

[42] Haraguchi, N.; Nguyen, T. L.; Itsuno, S. *ChemCatChem* **2017**, *9*, 3786 - 3794.

[43] Haraguchi, N.; Takenaka, N.; Najwa, A.; Takahara, Y.; Kar Mun, M.; Itsuno. S. *Adv. Synth. Catal.* **2018**, *360*, 112 - 123

[44] Itsuno, S.; Parvez, M. M.; Haraguchi, N. *Polym. Chem.* **2011**, *2*, 1942 - 1949.

[45] Zhang, J.;Zhang, W.; Wang, Y.; Zhang, M. *Adv. Synth. Catal.* **2008**, *350*, 2065 - 2076.

[46] Haraguchi, N.; Nishiyama, A.; Itsuno, S. *J. Polym. Sci. Part A: Polym. Chem.* **2010**, *48*, 3340 - 3349.

[47] Shi, J. Y.; Wang, C. A.; Li, Z. J.; Wang, Q.; Zhang, Y.; Wang, W. *Chem.: Eur. J.* **2011**, 17, 6206 - 6213.

[48] Hasan, O.E.; Niyazi, B. *React. Funct. Polym.* **2017,** *99*, 88 - 94.

[49] Carrot, G.; Rutot-Houzé, D.; Pottier, A.; Degée, P.; Hilborn, J.; Dubois, P. *Macromolecules* **2002**, *35*, 8400 - 8404.

[50] Ullah, M. W.; Thao, N. T. P.; Sugimoto, T.; Haraguchi, N. *Mol. Catal.* **2019**, *473*.

[51] Manuscript under preparation.

[52] Ullah, Haraguchi, N. *J. Polym. Sci. Part A: Poly. Chem.* **2019**, 57, 1296 - 1304.

[53] (a) Haraguchi, N.; Takemura, Y.; Itsuno, S. *Tetrahedron Lett. 2010*, 51, 1205 - 1208. (b) Sugie, H.; Hashimoto, Y., Haraguchi, N.; Itsuno, S. *J. Organomet. Chem.* **2014**, *751*, 711 - 716. (c) Brazier, J. B.; Jones, K. M.; Platts, J. A.; Tomkinson, N. C. O. *Angew. Chem. Int. Ed.* **2011**, *50*, 1613 -1616.

CHAPTER VI

Summary

In my PhD work, I have synthesized narrowly disperse functional polymer microspheres having benzyl halide moiety by precipitation polymerization which were used as macroinitiator to synthesize well-defined hairy or core-corona polymer microspheres by surface-initiated atom transfer radical polymerization. Core-corona polymer microspheres were used as solid supports for the ionically immobilization of chiral organocatalysts. These ionically core-corona microsphere-immobilized chiral organocatalysts were applied in asymmetric organocatalysis.

6.1 Synthesis of Polymer Microsphere Functionalized with Benzyl Halide Moiety by Precipitation Polymerization

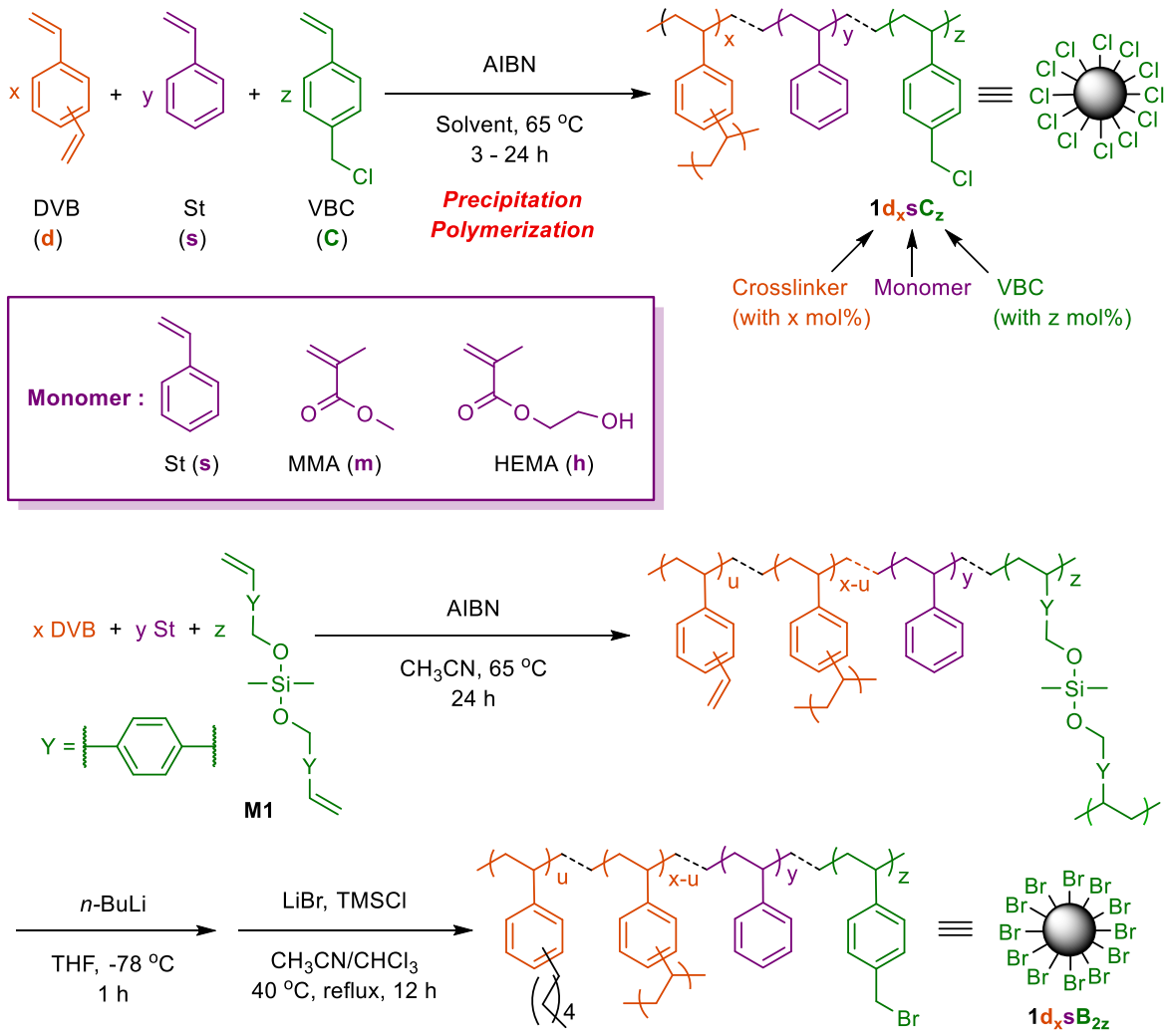

Scheme 6.1 Synthesis of polymer microsphere having benzyl chloride moiety **1** by precipitation polymerization.

Chapter **II** describes the synthesis of narrowly dispersed functional polymer microspheres having benzyl halide moiety by the precipitation polymerization of various comonomers (styrene, methyl methacrylate (MMA), or 2-hydroxyethyl methacrylate (HEMA)), divinylbenzene (DVB) with 4-vinylbenzyl chloride (VBC) using AIBN as an initiator in acetonitrile, or mixtures of acetonitrile and toluene. In precipitation polymerization, polymer particles was not obtained when DVB (<20 mol%) was used as a crosslinker. In this research, we have also successfully synthesized functional polymer microspheres using 10 mol% of crosslinker (DVB and a divinyl crosslinker) by precipitation polymerization and transformation reaction. The nature of comonomer and the molar ratio of monomers affected the yield and diameter of polymer microspheres.

6.2 Synthesis of Well-defined Hairy Polymer Microspheres by Surface-initiated Atom Transfer Radical Polymerization

In Chapter **III**, we have successfully synthesized well-defined hairy polymer microspheres **H** by the surface-initiated atom transfer radical polymerization (SI-ATRP) of styrene by using narrowly dispersed polymer microsphere having benzyl chloride moiety $\mathbf{I_z}$ prepared from precipitation polymerization. The M_n of grafted polymer can be controlled up to 15,000 g mol^{-1} by changing the M/I, and the M_w/M_n was lower than 1.30 when M/I $\leq$ 150. In addition, hairy polymer microspheres having poly(*n*BA), poly(*n*BMA), or poly(*t*BMA) chains on the surface were successfully synthesized by SI-ATRP.

In this Chapter, monodisperse sulfonate core-corona polymer microsphere **2** was successfully synthesized by the SI-ATRP of monomer such as styrene, MMA, HEMA, and NIPAm and phenyl *p*-styrenesulfonate with monodispersed polymer microsphere having benzyl chloride moiety **1** prepared *via* precipitation polymerization as a macroinitiator. We found that the graft copolymerization of styrene and phenyl *p*-styrenesulfonate proceeded in a controlled manner, affording well-defined core-corona

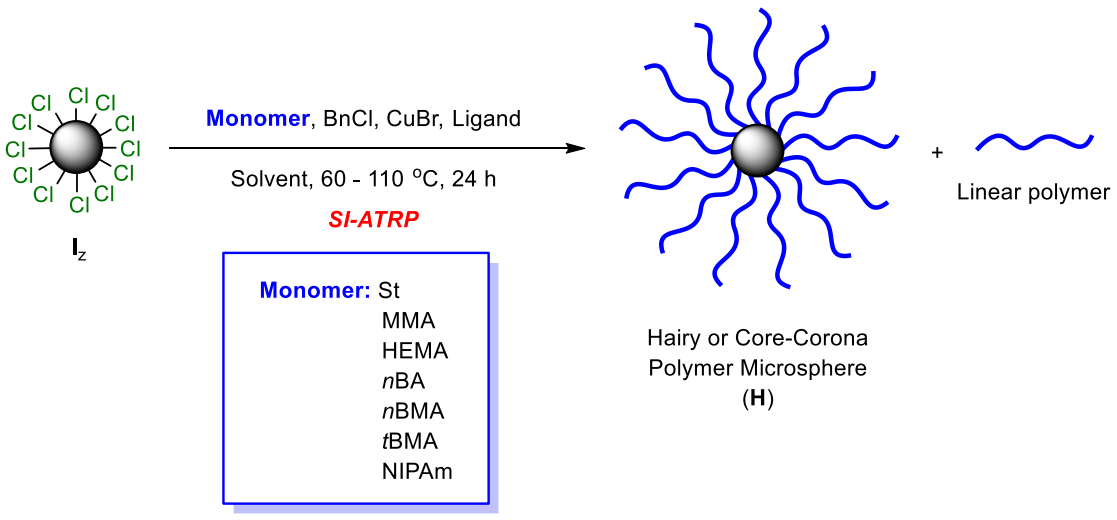

Scheme 6.2 Synthesis of hairy polymer microsphere **H** by SI-ATRP.

polymer microsphere **2** when poly(DVB-HEMA-VBC) microsphere **1d$_x$hC$_z$** having ATRP initiator moiety was used as a macroinitiator.

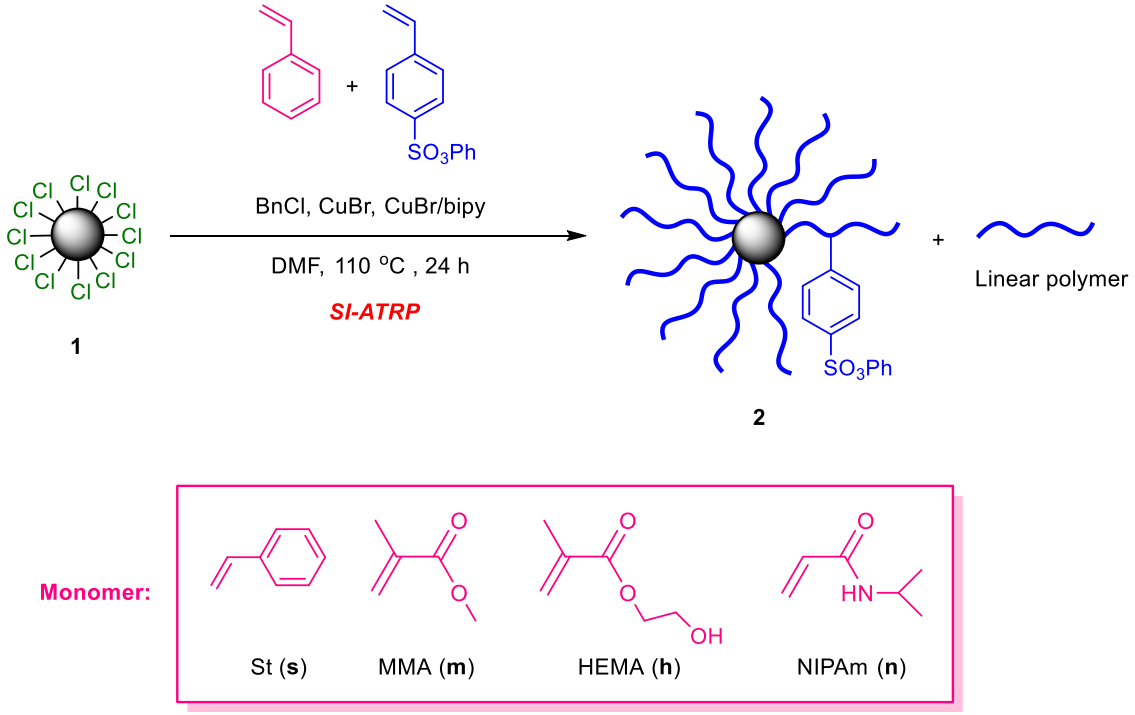

Scheme 6.3 Synthesis of sulfonate core-corona polymer microsphere **2** by SI-ATRP.

6.3 Synthesis of Core-corona Polymer Microsphere-supported Cinchonidinium Salt and Its Application to Asymmetric Synthesis

Monodispersed sulfonate core-corona polymer microsphere **3** was successfully synthesized by the surface-initiated ATRP (SI-ATRP) of monomer such as styrene, MMA, HEMA, and NIPAm and phenyl

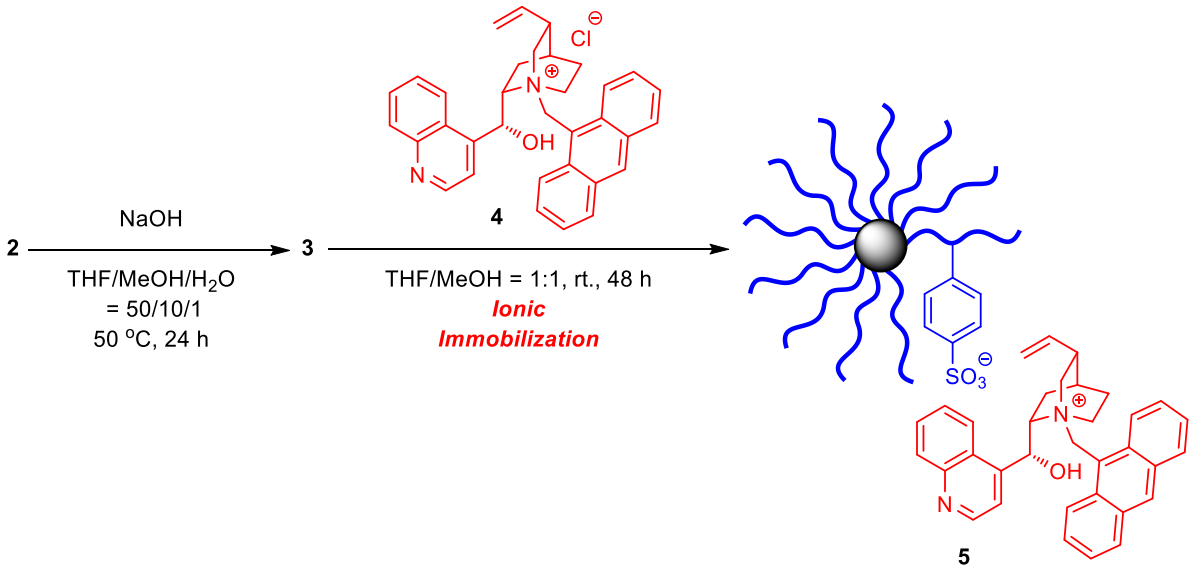

Scheme 6.4 Synthesis of core-corona polymer microsphere-supported chiral cinchonidinium catalyst **5**.

pstyrenesulfonate with monodispersed polymer microsphere having benzyl chloride moiety **1** prepared *via* precipitation polymerization as a macroinitiator, followed by the treatment of NaOH. Core-corona polymer microsphere-supported chiral cinchonidinium salt **5** was prepared by the ion exchange reaction of sodium sulfonate moiety at the side chain of corona in **3** with chiral cinchonidinium salt **4**. These polymer microspheres were used as heterogeneous chiral organocatalysts in the asymmetric alkylation

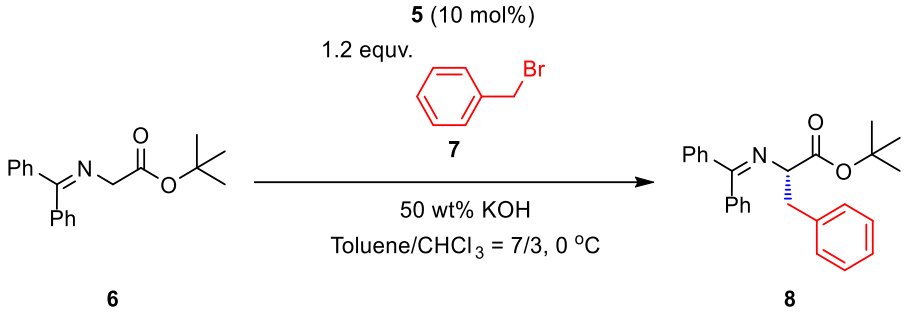

Scheme 6.5 Asymmetric benzylation reaction of **6** catalyzed by **5**.

reaction. The catalyst **5d$_{20}$hC$_{20}$** containing hydrophilic core **1d$_{20}$hC$_{20}$** gave best yield and high ee value in the asymmetric benzylation reaction. We found that the degree of cross-linking in the core and the core size affected the catalytic activity in the reaction. The catalytic activity was decreased with longer corona probably due to the steric hindrance of cinchonidinium moiety. The best catalyst **5d$_{20}$hC$_{20}$** showed high reactivity and excellent enantioselectivity, comparable to those corresponding low molecular weight catalyst, gel type polymer-supported catalyst, **9d$_{20}$hS$_{30}$** as well as **10S$_{100}$**. We explored the scope of the substrate containing substituents, such as halo, electron-withdrawing and electron-donating groups. When the benzyl bromide containing strong electron-withdrawing group was used, the corresponding phenylalanine derivative was obtained in excellent yield with high enantioselectivity (up to 97%). The propargyl bromide showed excellent enantioselectivity (up to <99%). The catalyst could be reused several times without loss of the enantioselectivity.

6.4 Synthesis of Core-Corona Polymer Microsphere-supported MacMillan Catalyst and Its Application to Asymmetric Diels-Alder Reaction

Core-corona polymer microsphere having sulfonic acid moiety **4** was successfully synthesized by the surface-initiated ATRP of monomer such as styrene, MMA, HEMA, and NIPAm and phenyl *p*-styrenesulfonate with monodispersed low-crosslinked polymer microsphere having benzyl halide moiety **1** prepared *via* precipitation polymerization as a macroinitiator, followed by the treatment of NaOH and acidification by H_2SO_4. Core-corona polymer microsphere-supported chiral MacMillan catalyst **6** was prepared by the neutralization reaction between the sulfonic acid moiety at the side chain of corona in **4** with MacMillan catalyst precursor **5**. These core-corona polymer microsphere-supported

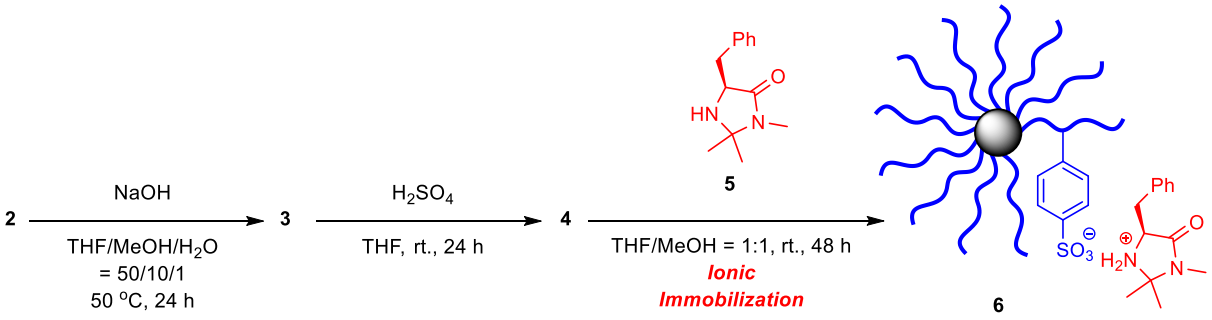

Scheme 6.6 Synthesis of core-corona polymer microsphere-supported MacMillan catalyst **6**.

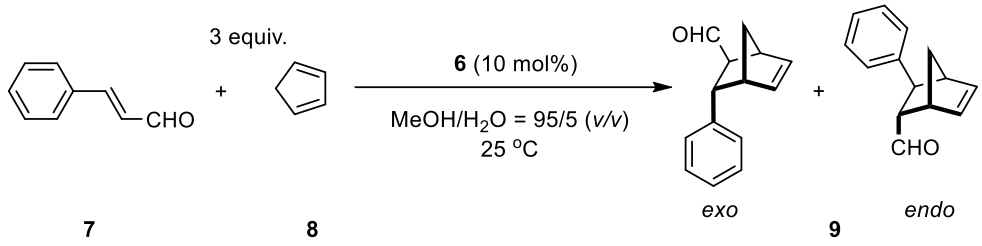

Scheme 6.7 Asymmetric Diels-Alder reaction of **7** and **8** catalyzed by **6**.

catalysts were used as heterogeneous chiral organocatalysts in the asymmetric Diels-Alder reaction. The catalyst **6d$_{10}$sB$_{20}$** containing hydrophobic core and corona gave the desired adduct in 99% yield with excellent ee value (99% ee (*exo*) and >99% ee (*endo*) in the asymmetric Diels–Alder reaction of *trans*-cinnamaldehyde **7** and 1,3-cyclopentadiene **8**. We found that the core size affected the catalytic activity in the reaction. The catalytic activity was decreased with longer corona probably due to the steric hindrance of imidazolidinium moiety. The best catalyst **6d$_{10}$sB$_{20}$** showed higher enantioselectivity than that of the corresponding uniform type polymer microsphere-supported MacMillan catalyst **10d$_{20}$sS$_{30}$**. The catalyst could be reused several times without loss of the enantioselectivity.

Achievements

A.1 List of Papers

1. **Md. Wali Ullah** and Naoki Haraguchi, "Synthesis of well-defined hairy polymer microspheres by precipitation polymerization and surface-initiated atom transfer radical polymerization," *J. Polym. Sci., Part A: Polym. Chem.* **2019**, *57*, 1296 - 1304.
2. **Md. Wali Ullah**, Nguyen Thi Phuong Thao, Takuya Sugimoto and Naoki Haraguchi, "Synthesis of core-corona polymer microsphere-supported cinchonidinium salt and its application to asymmetric synthesis," *Molecular Catalysis* **2019**, *473*. https://doi.org/10.1016/j.mcat.2019.110392.
3. **Md. Wali Ullah** and Naoki Haraguchi, "Ionic, core-corona polymer microsphere-immobilized MacMillan catalyst for asymmetric Diels-Alder reaction," *Catalysts* **2019**, *9*, 960. https://doi.org/10.3390/catal9110960.

A.2 List of Presentations at International Conferences

1. Naoki Haraguchi, **Md. Wali Ullah**, Nguyen Thi Phuong Thao, Kaito Aburaya, and Takuya Sugimoto, "Synthesis of monodisperse functional polymer microspheres by precipitation polymerization," *The 19th Malaysia International Chemistry Congress (19MICC) and International Congress on Pure & Applied Chemistry Langkawi (ICPAC Langkawi)*, **October 30 - November 02, 2018**, Langkawi, Malaysia.
2. **Md. Wali Ullah**, Takuya Sugimoto, Naoki Haraguchi and Shinichi Itsuno, "Synthesis of core-corona polymer microsphere-supported cinchonidinium salt and its application to asymmetric organocatalysis," *The 12th SPSJ International Polymer Conference (IPC 2018)*, **December 4 - 7, 2018**, Hiroshima, Japan.
3. **Md. Wali Ullah**, Nguyen Thi Phuong Thao, Takuya Sugimoto, Naoki Haraguchi and Shinichi Itsuno, "Asymmetric alkylation reaction of glycine derivatives catalyzed by core-corona polymer microsphere-supported cinchonidinium salt," *The 257th Spring 2019 ACS National Meeting and Exposition*, M**arch 31 - April 4, 2019**, Orlando, Florida, USA.

A.3 List of Presentations at Domestic Conferences

1. **Md. Wali Ullah**, Naoki Haraguchi and Shinichi Itsuno, "Synthesis of well-defined hairy polymer microspheres by precipitation polymerization and surface-initiated atom transfer radical polymerization," *The 47th Annual Meeting of Union of Chemistry-Related Societies (UCRS) in Chubu Area*, **November 11 - 12, 2017**, Gifu University, Japan.
2. **Md. Wali Ullah**, Naoki Haraguchi and Shinichi Itsuno, "Synthesis of hairy polymer microsphere-supported chiral cinchonidinium catalyst and its application to asymmetric reaction," *The 67th SPSJ Annual Meeting*, **May 23 - 25, 2018**, Nagoya Congress Center, Japan.
3. Naoki Haraguchi, **Md. Wali Ullah**, Yuya Ono and Shinichi Itsuno, "Synthesis of polymer microsphere-immobilized chiral pyrrolidine catalyst and its application to asymmetric organocatalysis," *The 67th Symposium on Macromolecules*, **September 12 - 14, 2018**, Sapporo Campus, Hokkaido University, Japan
4. **Md. Wali Ullah**, Naoki Haraguchi and Shinichi Itsuno, 'Synthesis of core-corona polymer microsphere-supported MacMillan catalyst and its application to asymmetric Diels-Alder reaction," *The 68th Symposium on Macromolecules*, **September 25 - 27, 2019**, Fukui University, Japan.
5. Takuya Sugimoto, **Md. Wali Ullah**, and Naoki Haraguchi, "Synthesis of low crosslinked monodisperse polymer microsphere by cleavage reaction," *The 68th Symposium on Macromolecules*, **September 25 - 27, 2019**, Fukui University, Japan.
6. Mithun Kumar Debnath, **Md. Wali Ullah** and Naoki Haraguchi, "Development of one-pot asymmetric Michael addition reaction catalyzed by polymer microsphere-supported chiral pyrrolidine catalyst," *The 50th Annual Meeting of Union of Chemistry-Related Societies (UCRS) in Chubu Area*, **November 9 - 10, 2019**, Shinsyu University, Japan.

Appendix A

Supporting documents for CHAPTER II

A.1 ^{1}H and ^{13}C NMR spectra

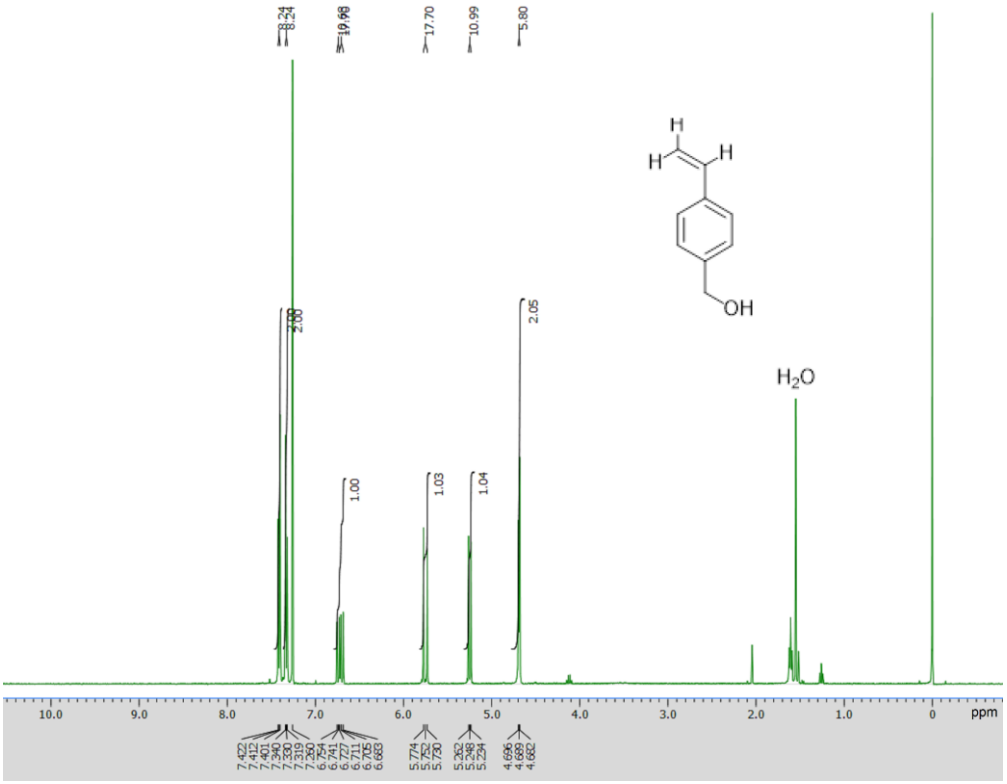

^{1}H NMR of **VBA** in $CDCl_3$

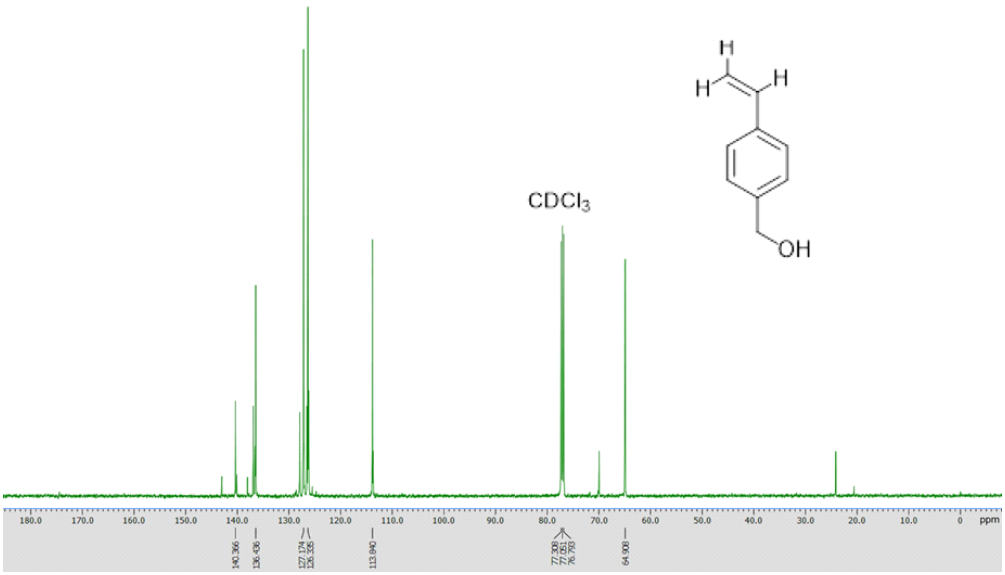

^{13}C NMR of **VBA** in $CDCl_3$

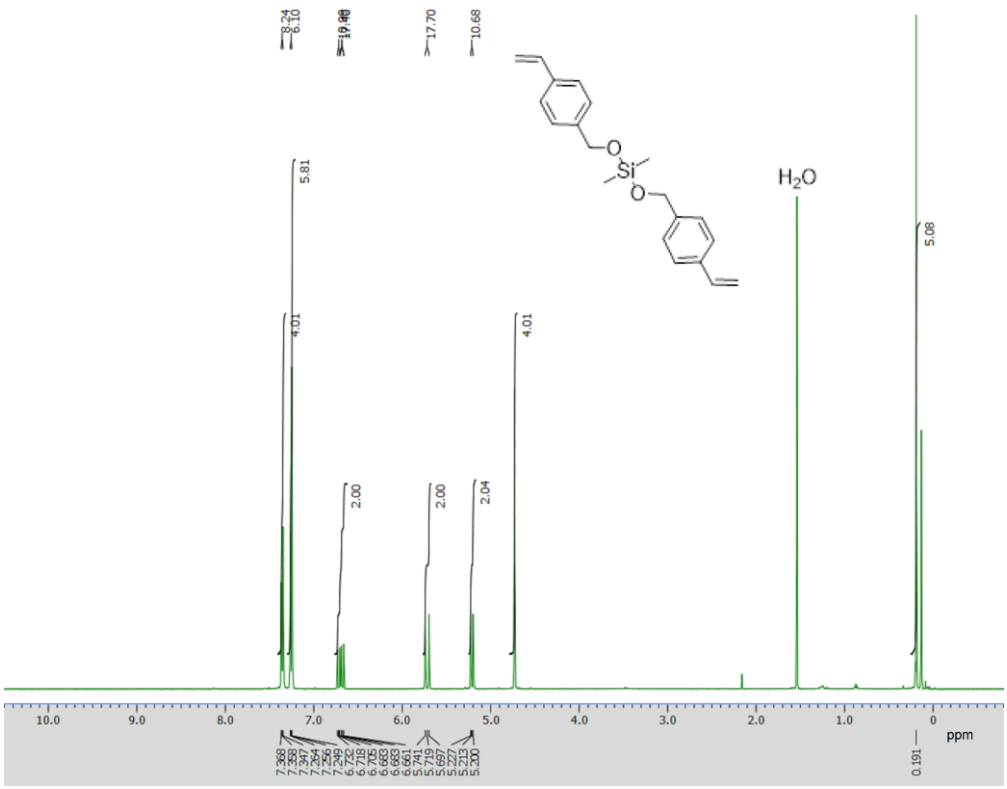

^{1}H NMR of **M1a** in $CDCl_3$

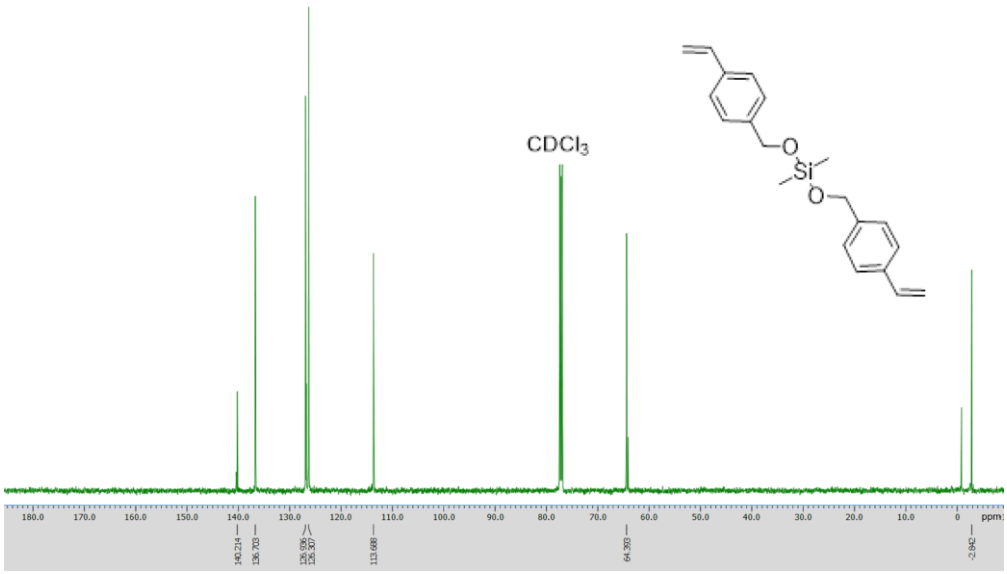

^{13}C NMR of **M1a** in $CDCl_3$

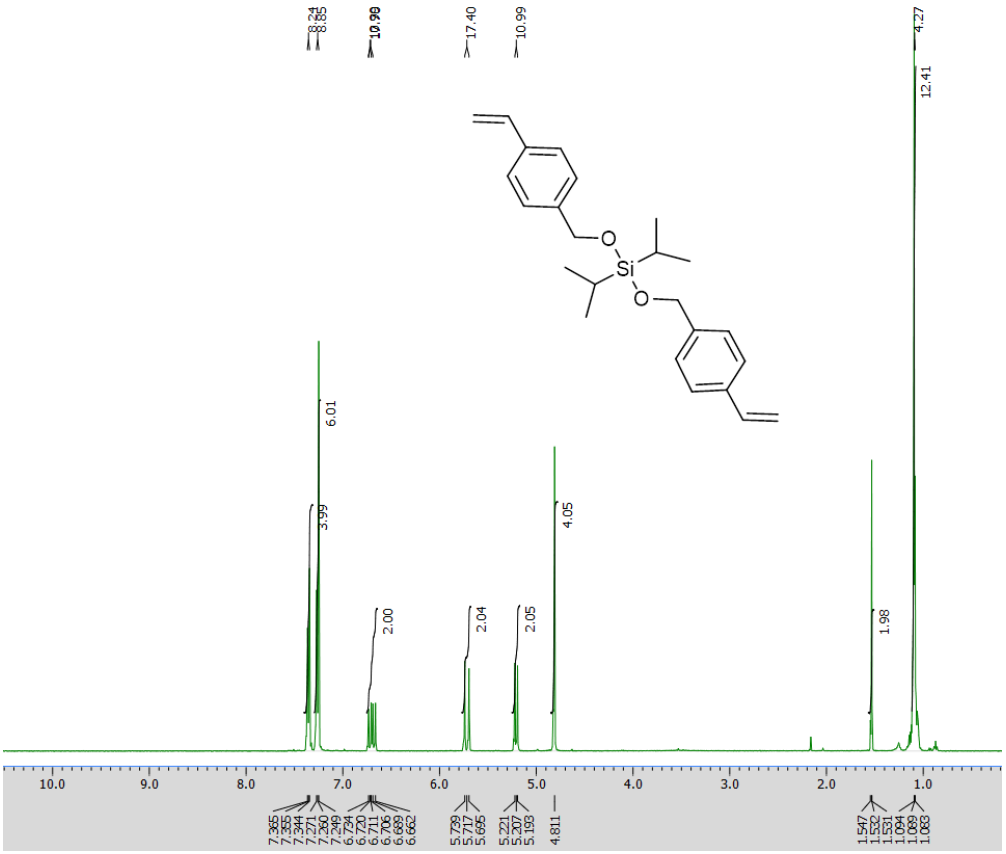

^{1}H NMR of **M1b** in $CDCl_3$

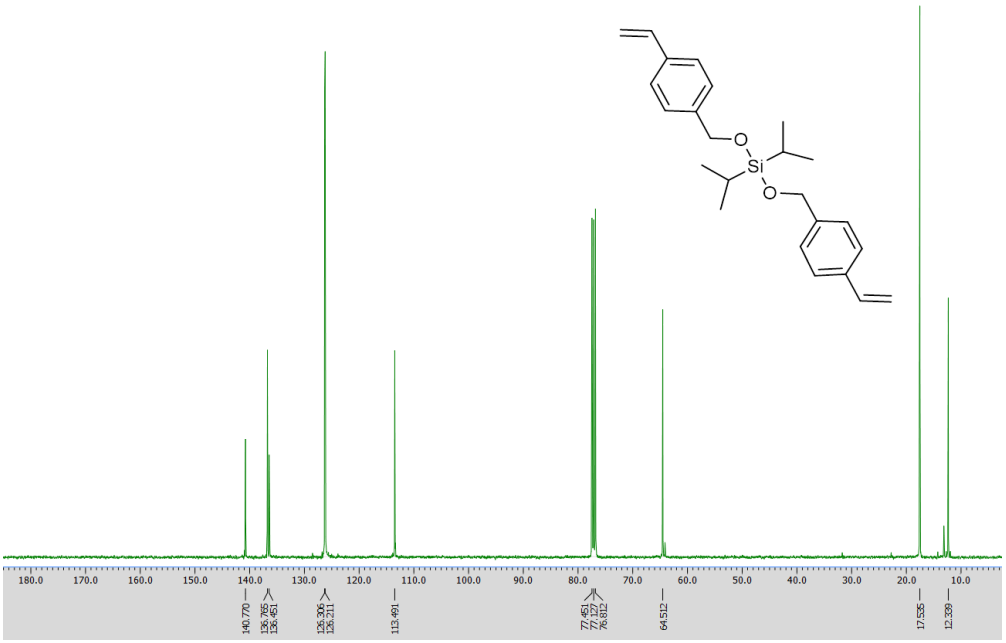

^{13}C NMR of **M1b** in $CDCl_3$

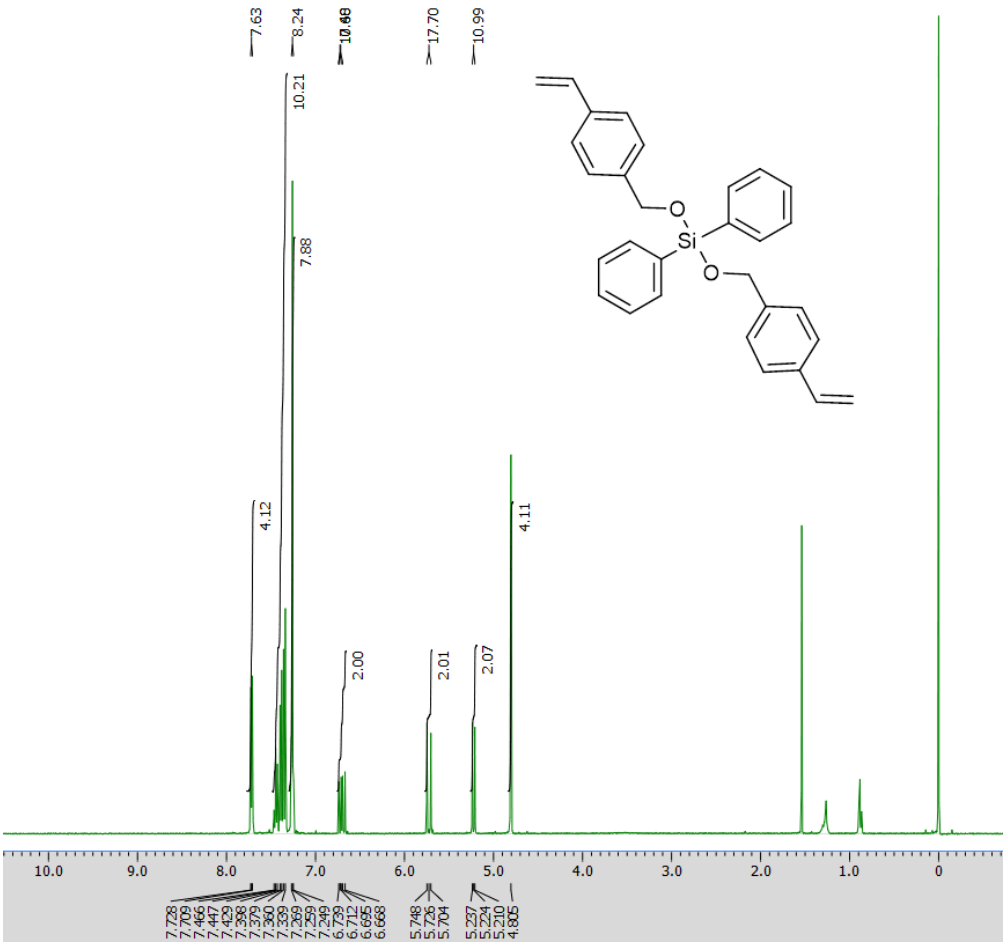

^{1}H NMR of **M1c** in $CDCl_3$

Appendix B

Supporting documents for CHAPTER III

B.1 ^{1}H NMR of linear polystyrene in $CDCl_3$ (Table 3.1)

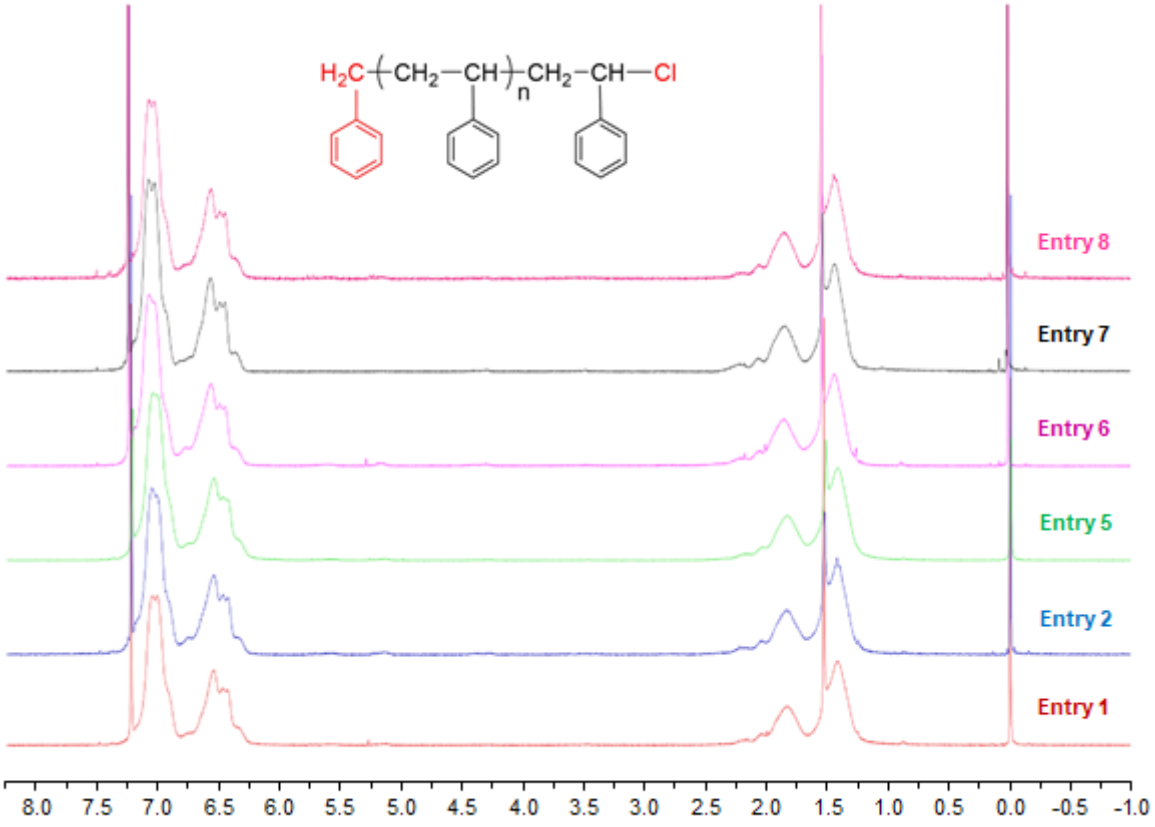

B.2 SEC traces of linear polystyrene

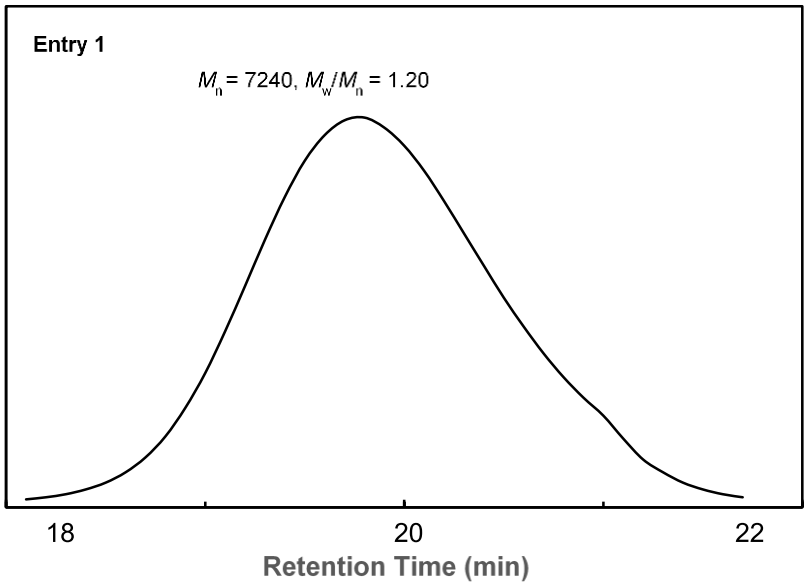

SEC curve of linear polystyrene (entry 1 in **Table 3.1**)

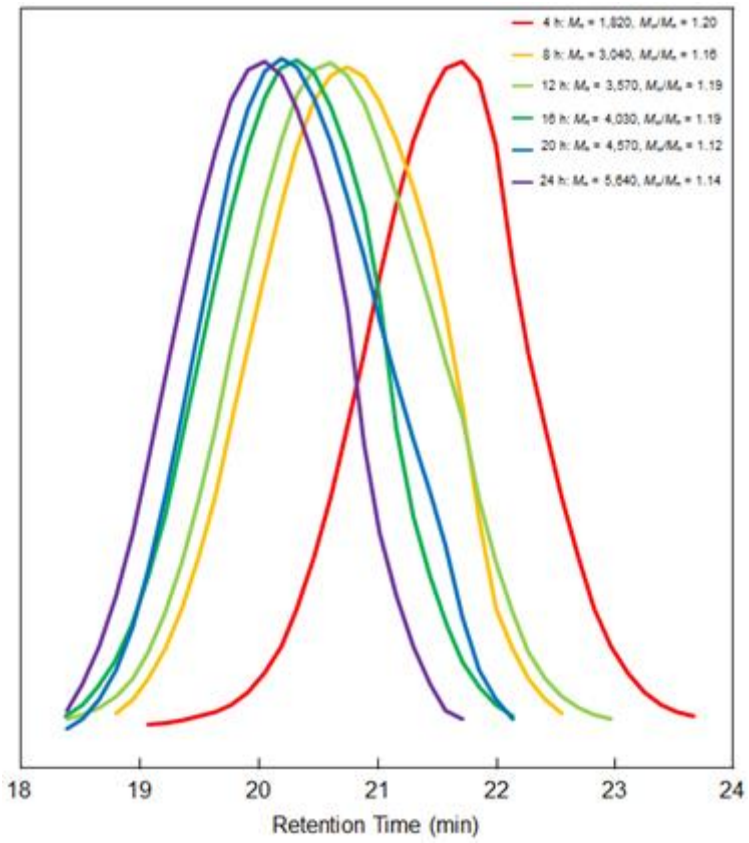

SEC curve of linear polystyrene (entry 5 in **Table 3.1**)

B.3 SEM images of hairy polymer microsphere (entries 9-14 in Table 3.1)

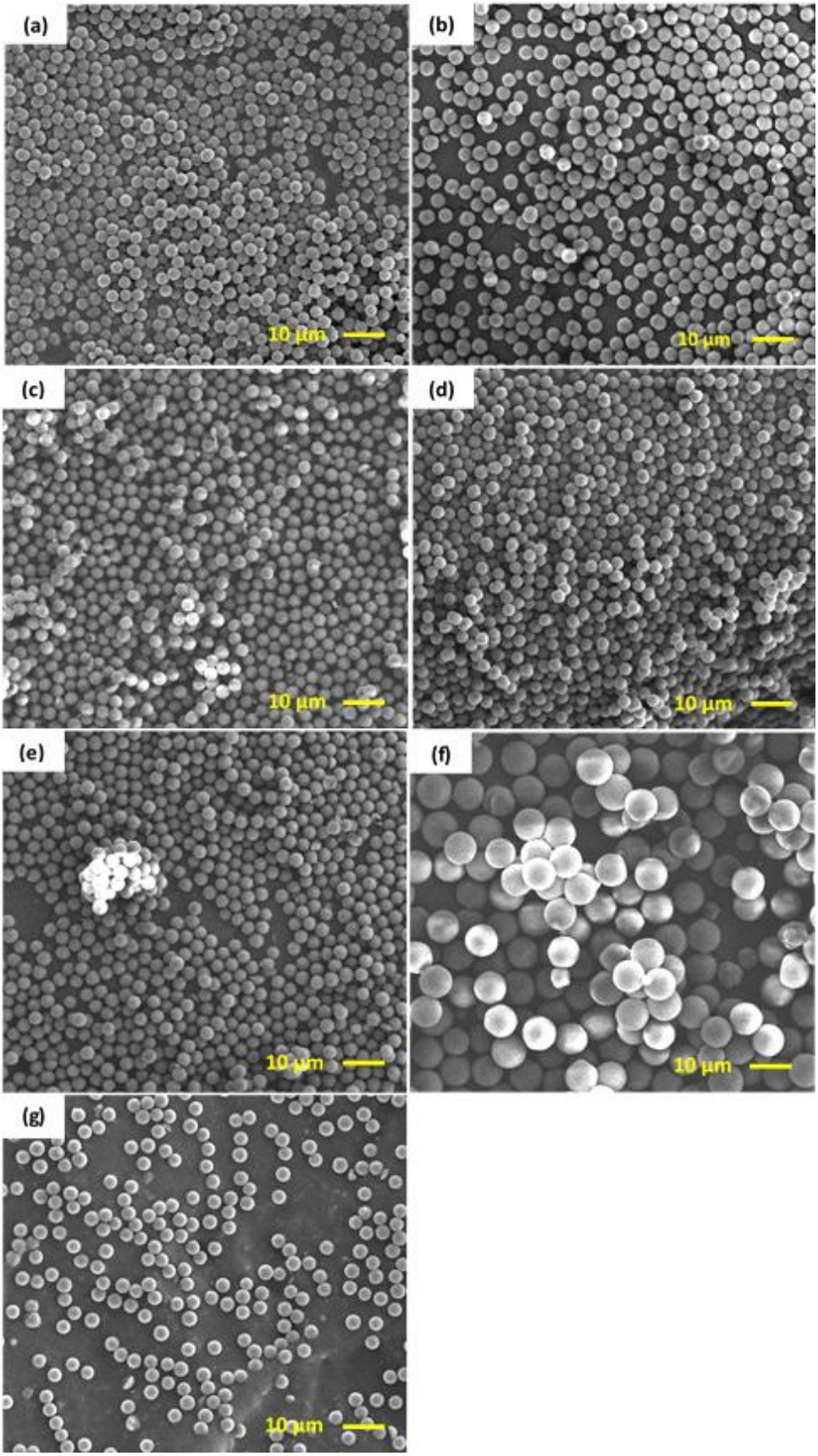

I_{20} (a), **$H_{(MMA)}$** (b), **$H_{(nBA)}$** (c), **$H_{(nBMA)}$** (d), **$H_{(tBMA)}$** (e), **$H_{(HEMA)}$** (f), and **$H_{(NIPAm)}$** (g).

B.4 FTIR of hairy polymer microsphere (entries 3, 5-7, 11-13 in Table 3.3)

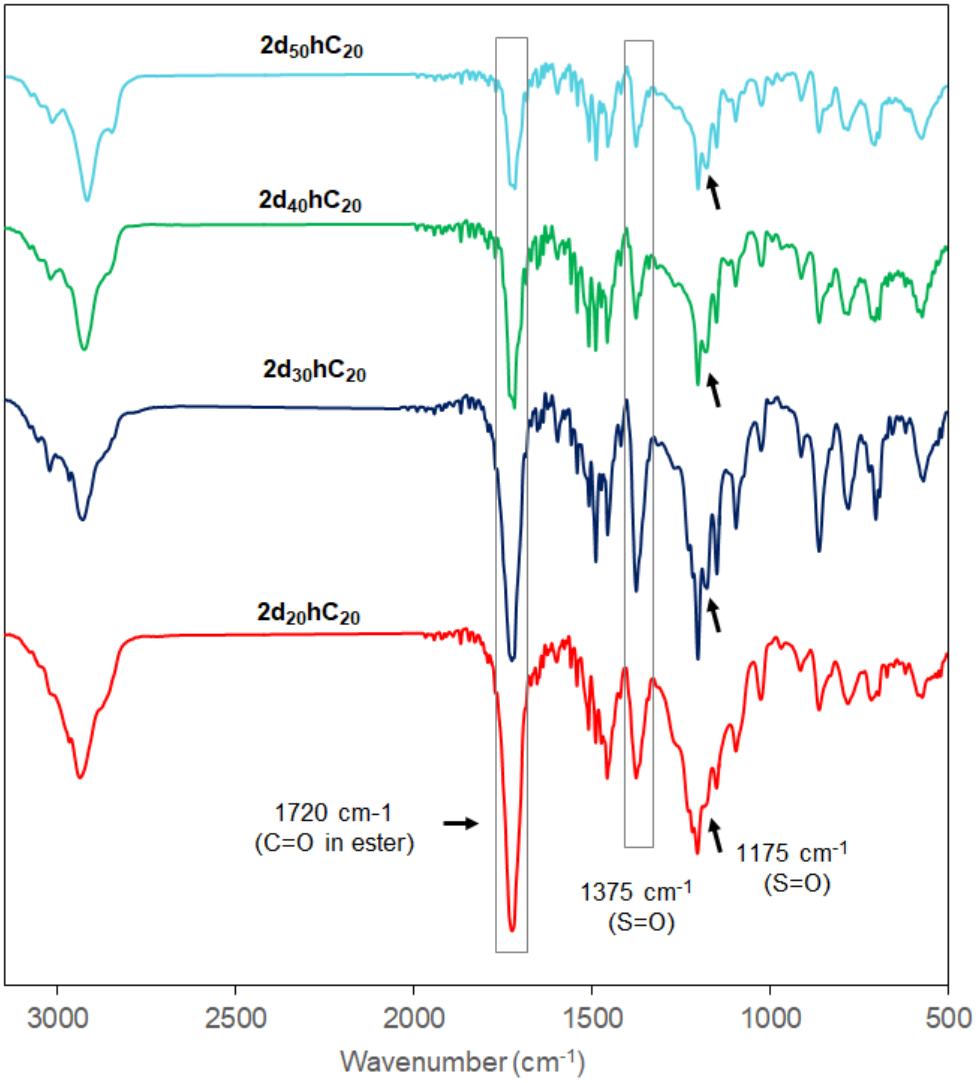

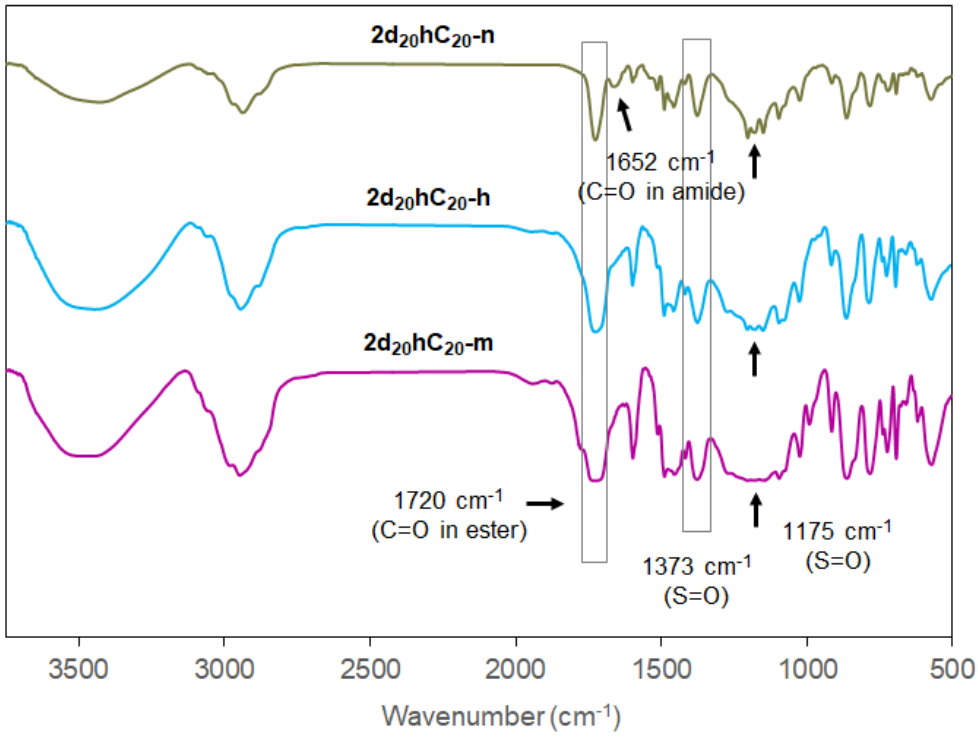

B.5 SEM images of polymer microsphere 1 and the corresponding hairy polymer microsphere 2

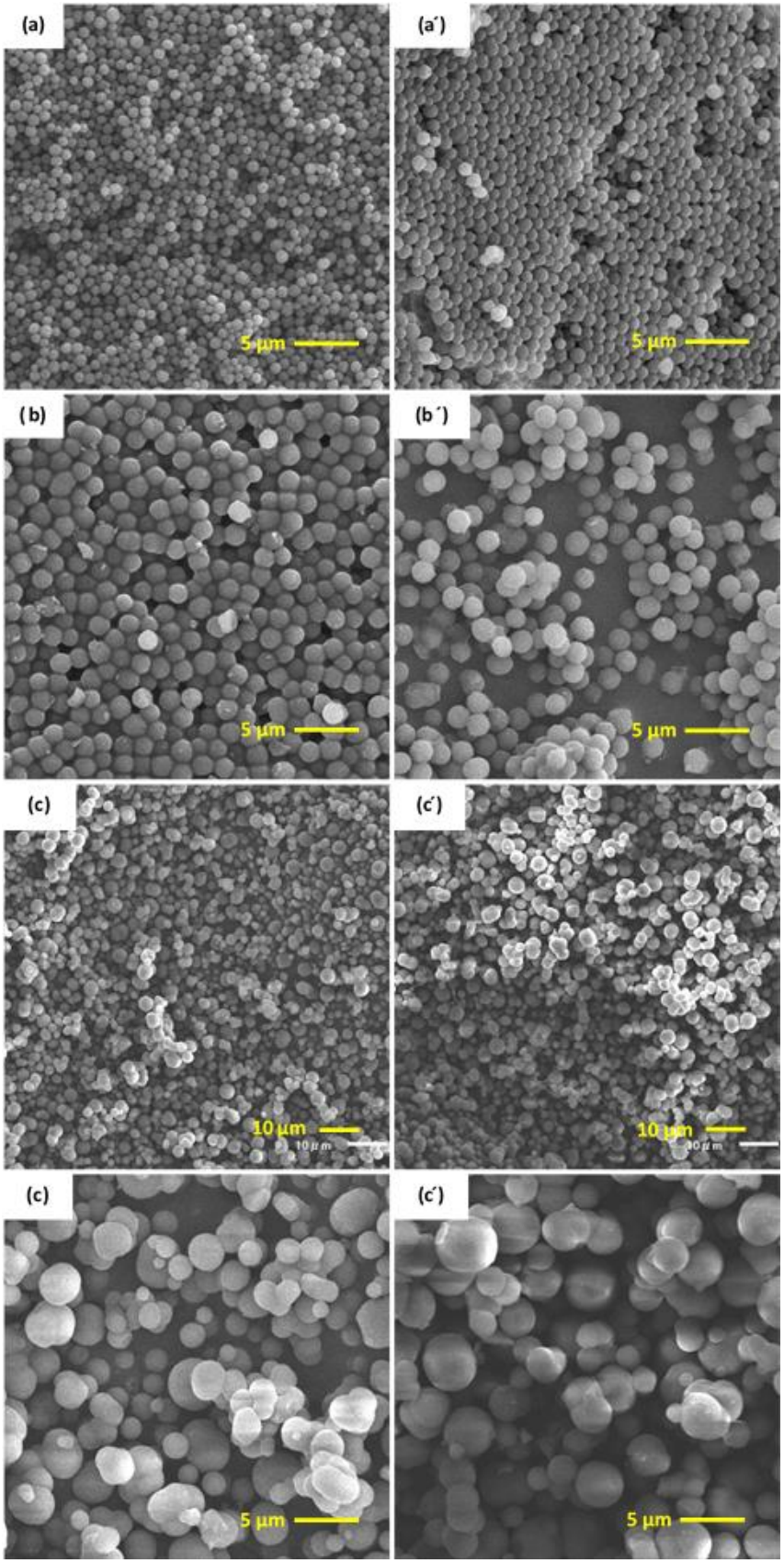

1d$_{30}$hC$_{20}$ (a), **2d$_{30}$hC$_{20}$** (a′), **1d$_{40}$hC$_{20}$** (b), **2d$_{40}$hC$_{20}$** (b′), **1d$_{50}$hC$_{20}$** (c), and **2d$_{50}$hC$_{20}$** (c′).

(**DVB series**: entries 5-7 in **Table 3.3**)

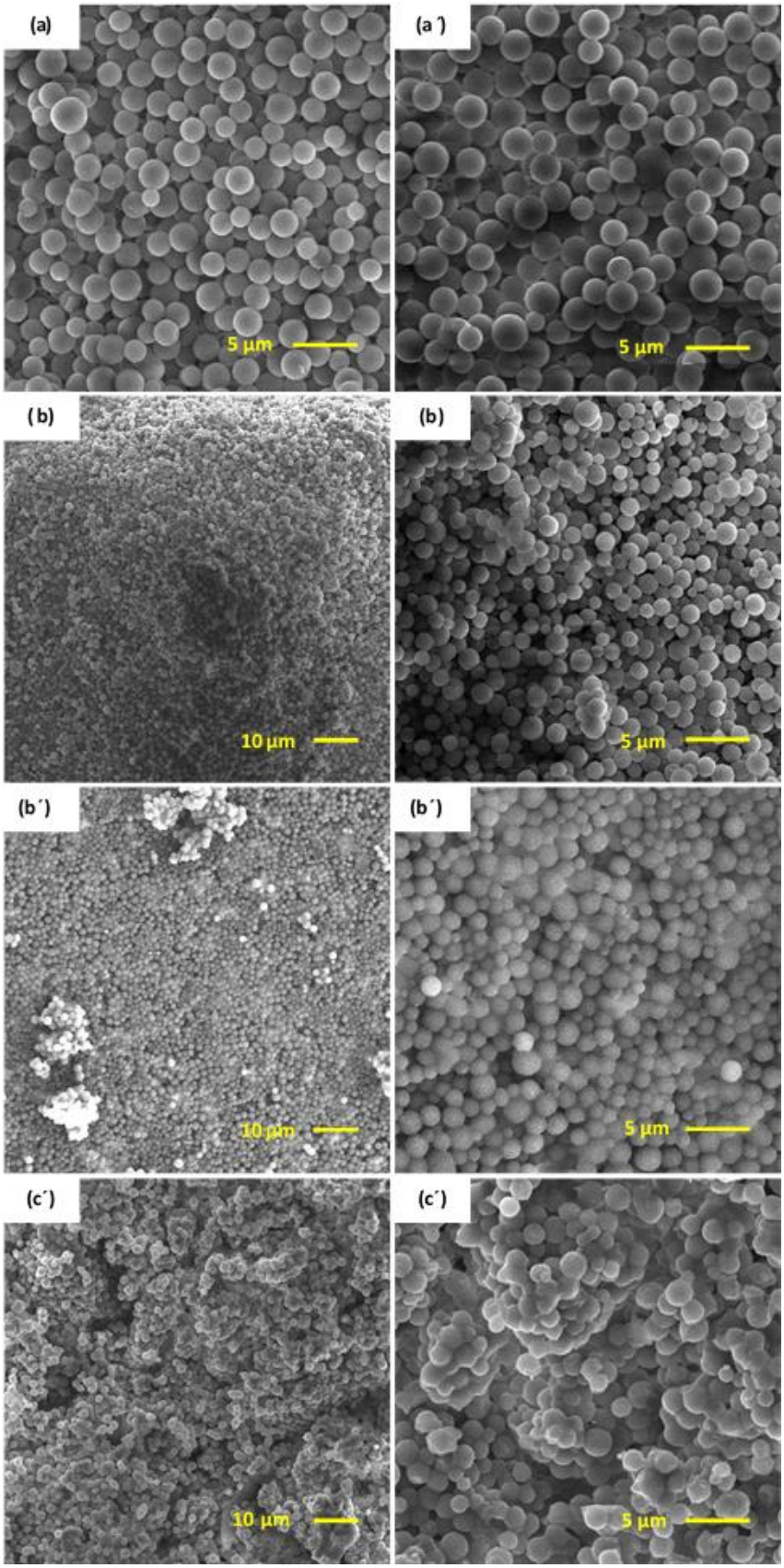

1d$_{20}$hC$_{20}$A (a), **2d$_{20}$hC$_{20}$A** (a′), **1d$_{20}$hC$_{20}$** (D_n = 1.2 µm) (b), **2d$_{20}$hC$_{20}$-200** (b′), and **2d$_{20}$hC$_{20}$-300** (c′).

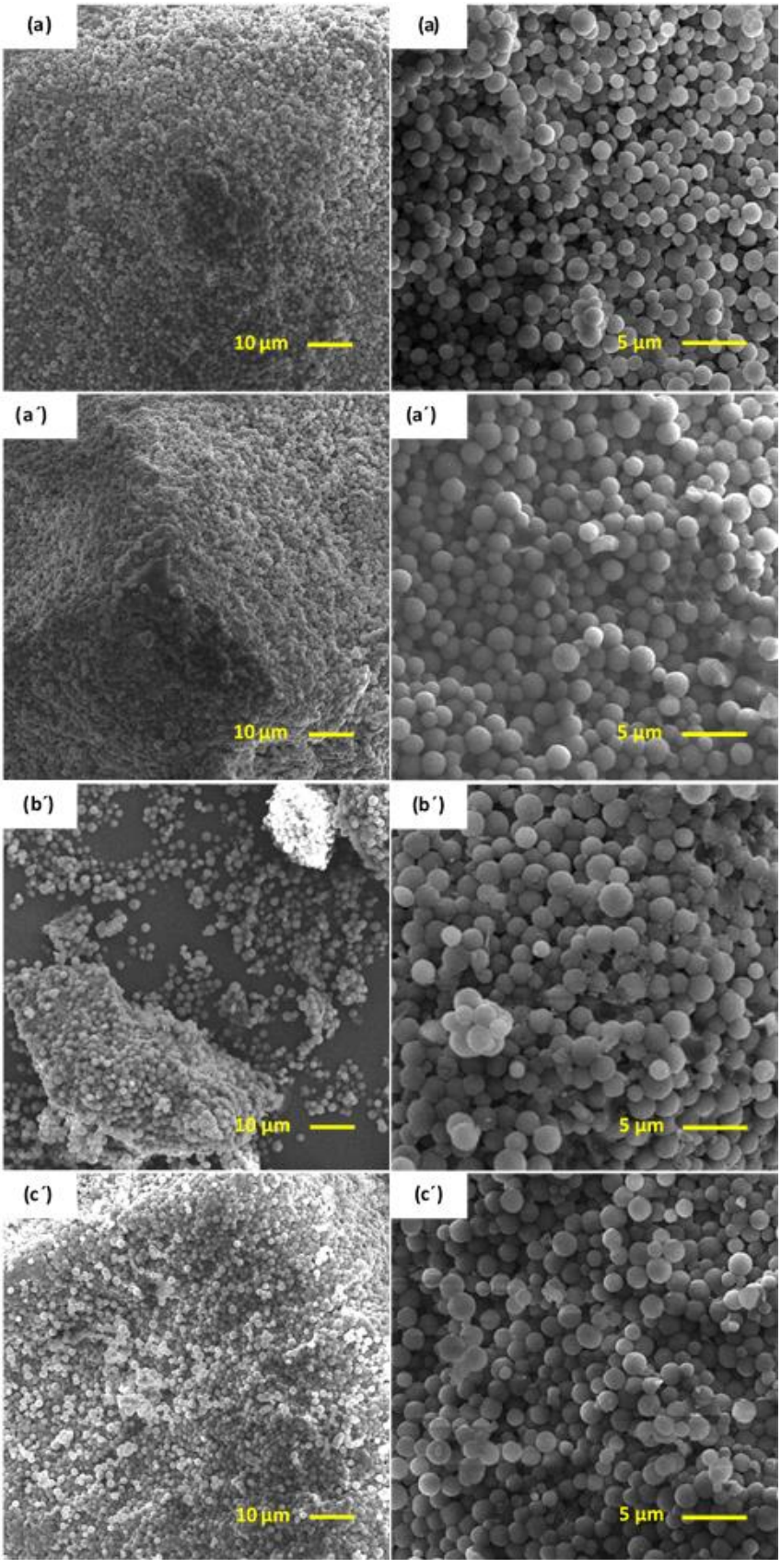

1d$_{20}$hC$_{20}$ (D_n = 12 µm) (a), **2d$_{20}$hC$_{20}$-m** (a′), **2d$_{20}$hC$_{20}$-h** (b′), and **2d$_{20}$hC$_{20}$-n** (c′).

(entries 11-13 in **Table 3.2**)

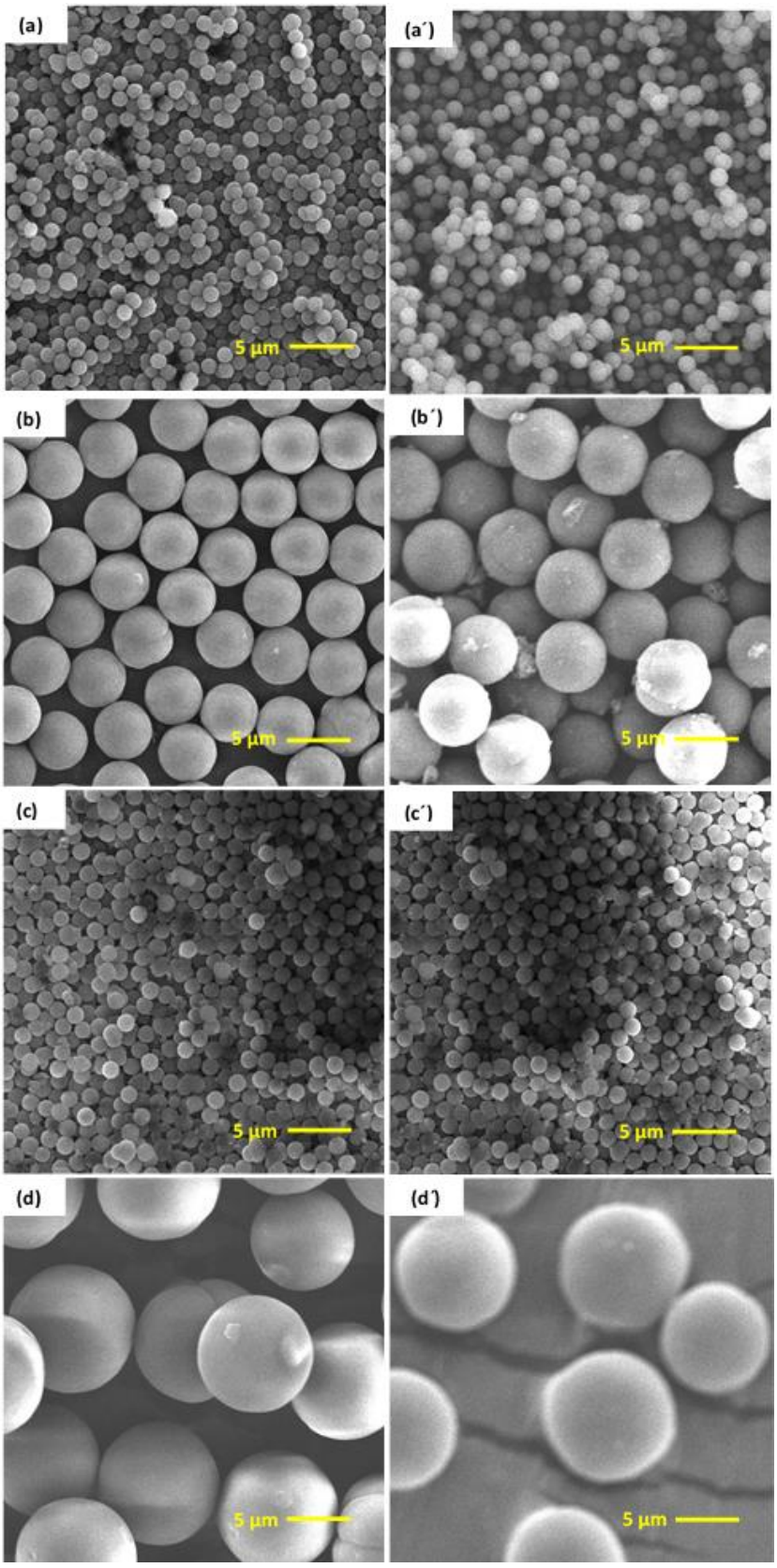

1d$_{20}$sC$_{20}$ (D_n = 1.14 µm) (a), **2d$_{20}$sC$_{20}$** (a´), **1d$_{20}$sC$_{20}$** (D_n = 4.41 µm) (b), **2d$_{20}$sC$_{20}$** (b´), **1d$_{20}$mC$_{20}$** (D_n = 1.12 µm) (c), **2d$_{20}$mC$_{20}$** (c´), **1d$_{20}$mC$_{20}$** (D_n = 9.14 µm) (d), and **2d$_{20}$mC$_{20}$** (d´). (entries 14-17 in **Table 3.2**)

B.6 ^{1}H NMR spectra

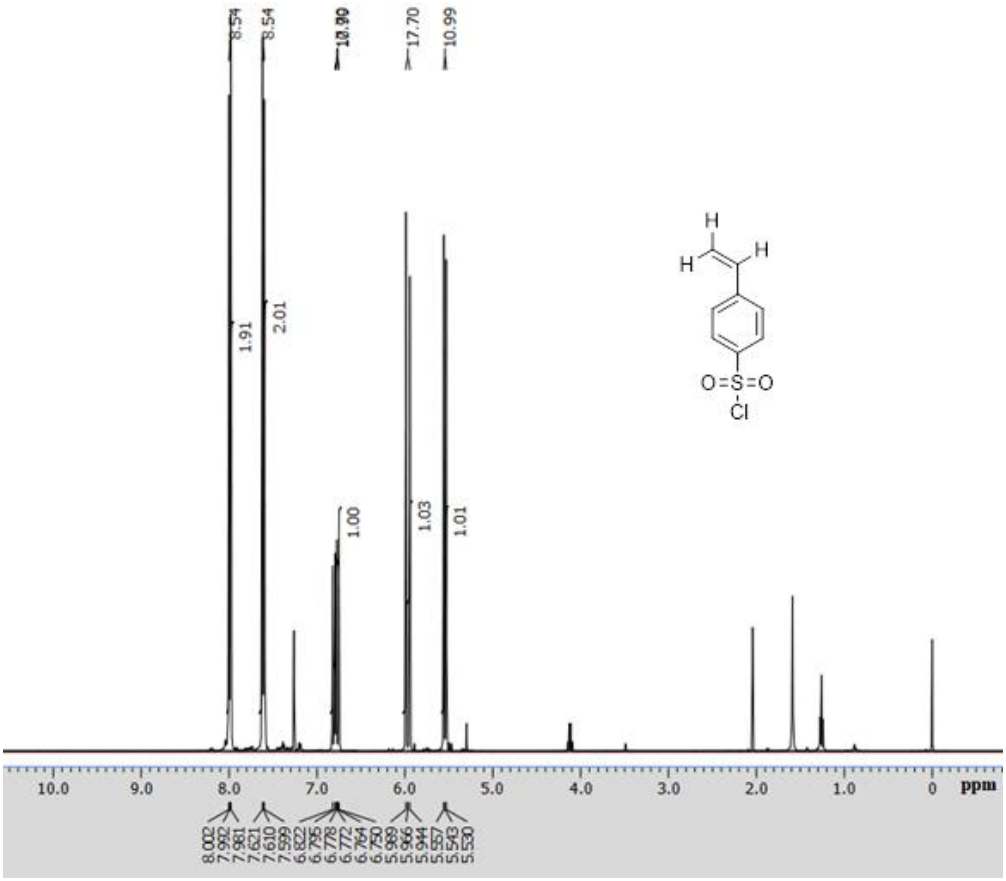

^{1}H NMR of *p*-styrenesulfonyl chloride (**SCl**) in $CDCl_3$

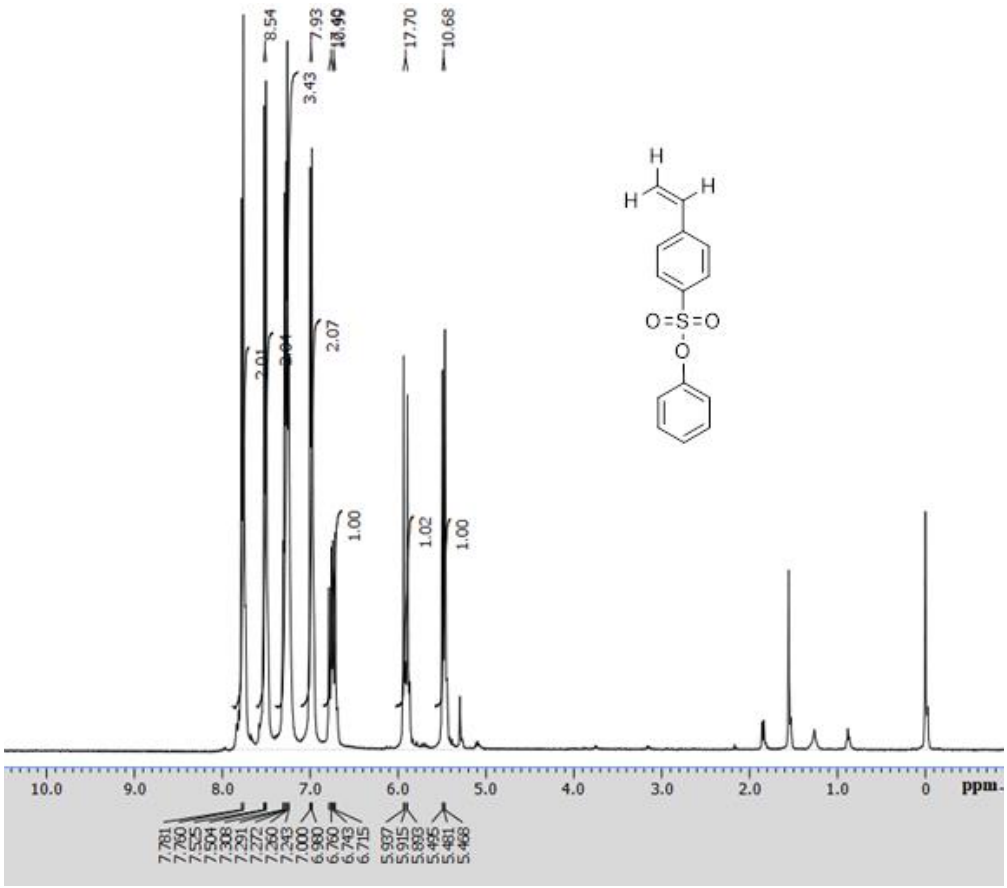

^{1}H NMR of *p*-phenyl styrenesulfonate (**S**) in $CDCl_3$

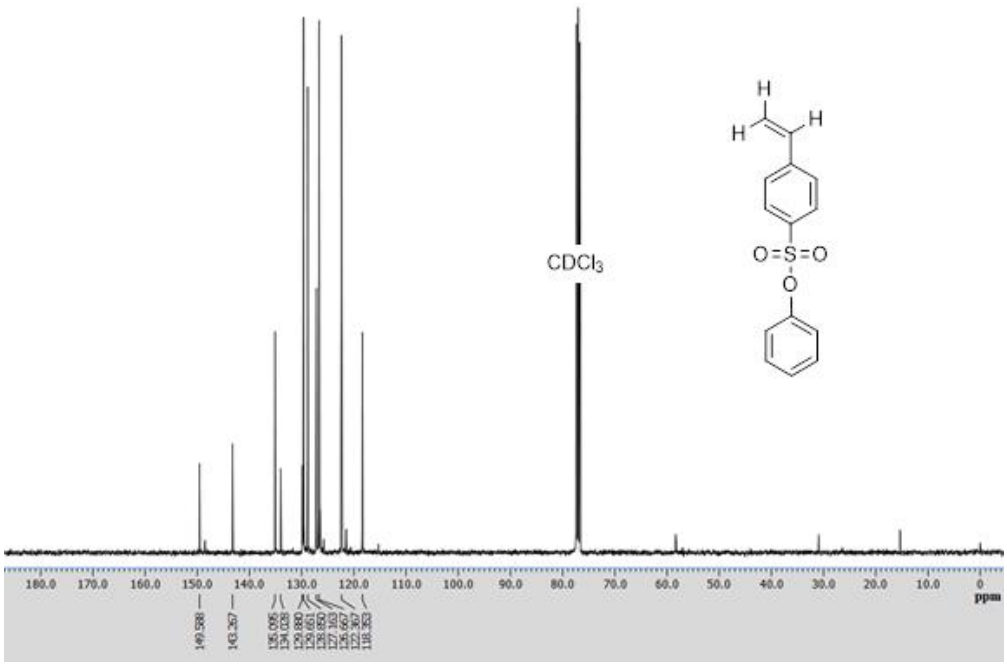

^{13}C NMR of *p*-phenyl styrenesulfonate (**S**) in $CDCl_3$

Appendix C

Supporting documents for CHAPTER IV

C.1 FT-IR spectra for core-corona polymer microsphere-supported sodium sulfonate 3 and the corresponding microsphere-supported catalyst 5

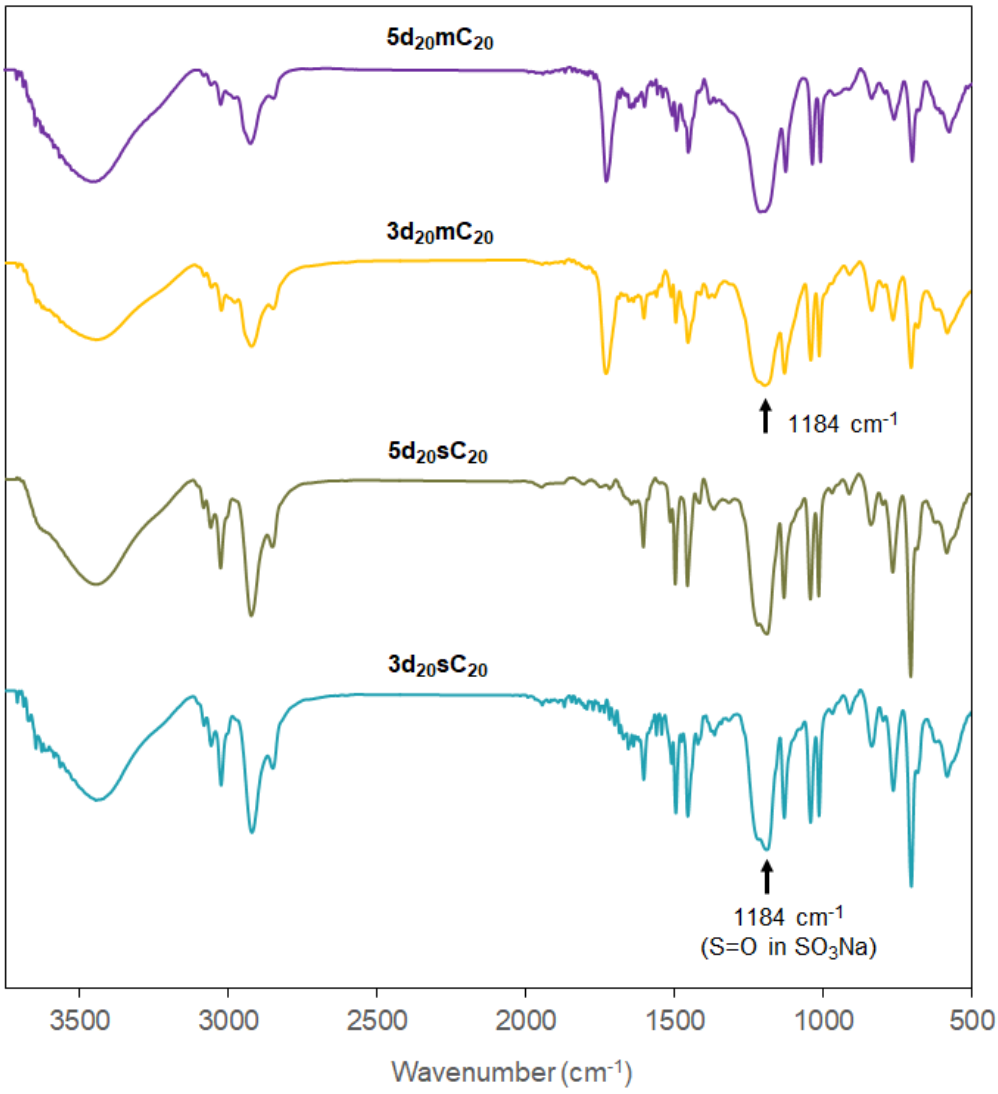

FT-IR spectra for entries 1, 2 in Table 4.1

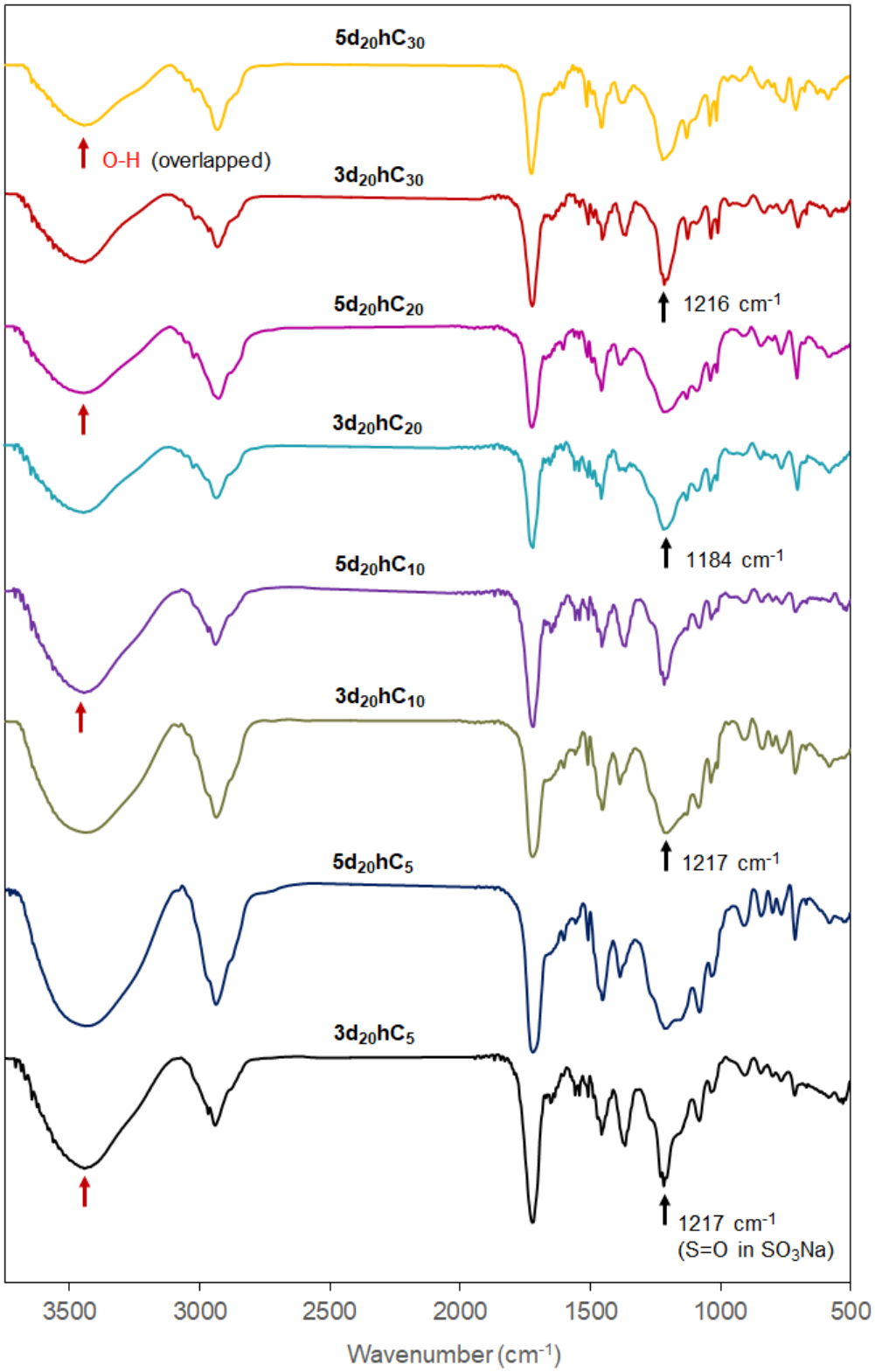

FT-IR spectra for entries 3-6 in **Table 4.1**

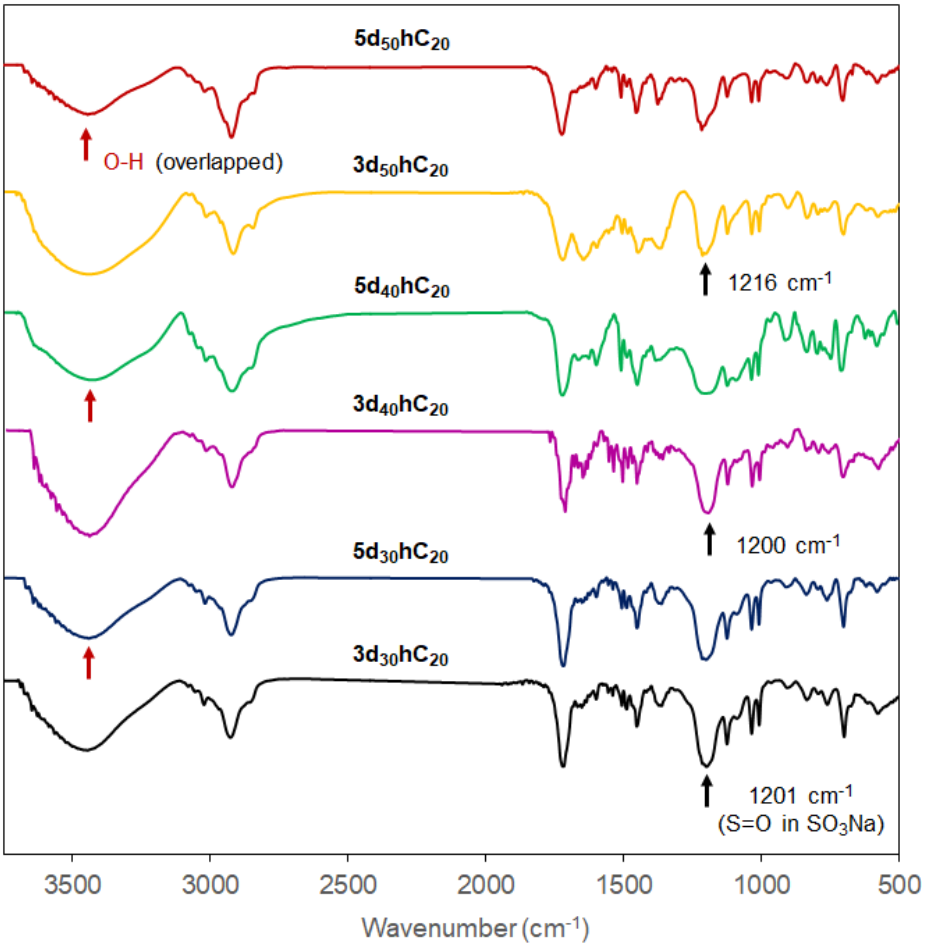

FT-IR spectra for entries 8-10 in **Table 4.1**

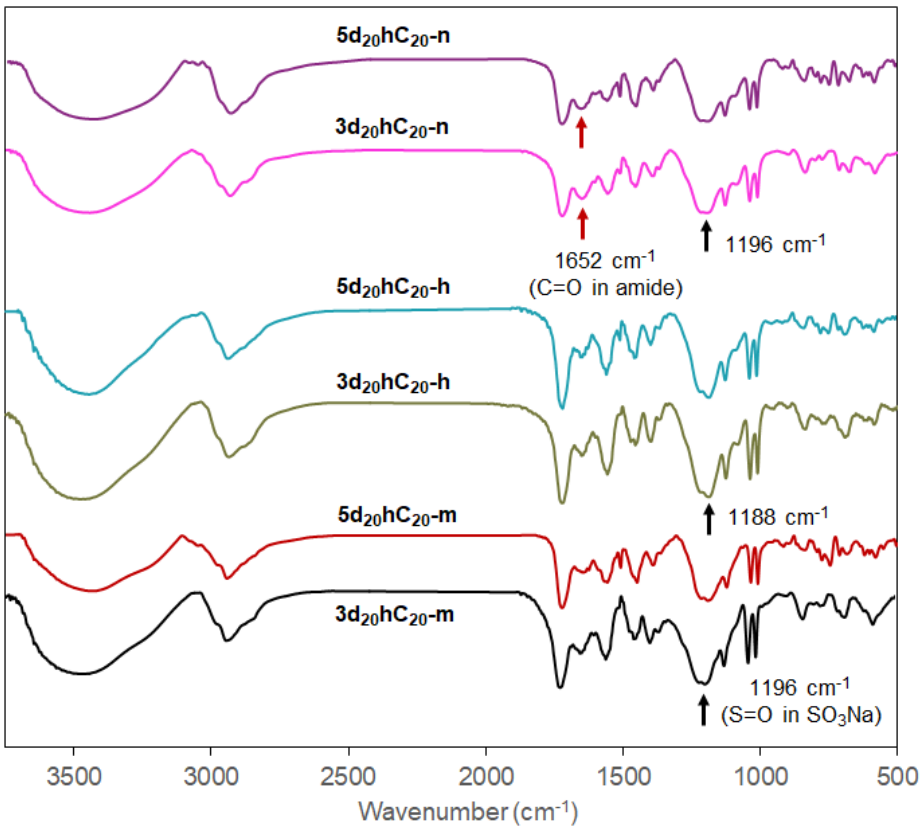

FT-IR spectra for entries 13-15 in **Table 4.1**

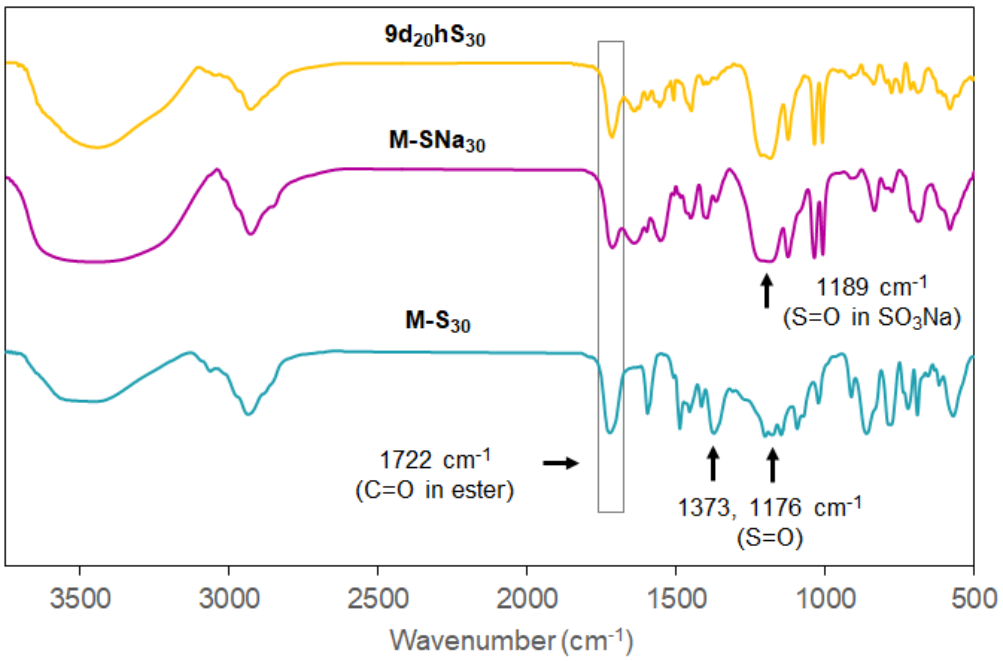

FT-IR spectra for **$9d_{20}sS_{30}$**

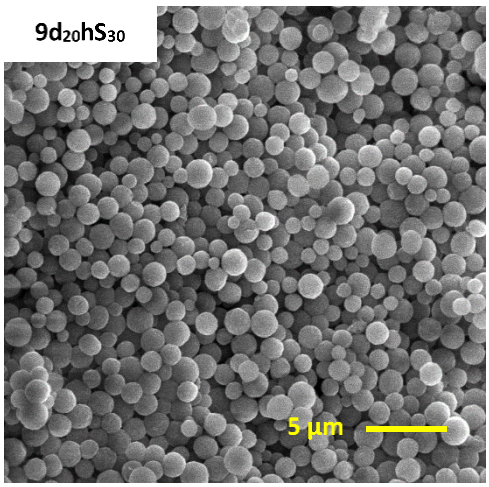

SEM image of **$9d_{20}hS_{30}$**

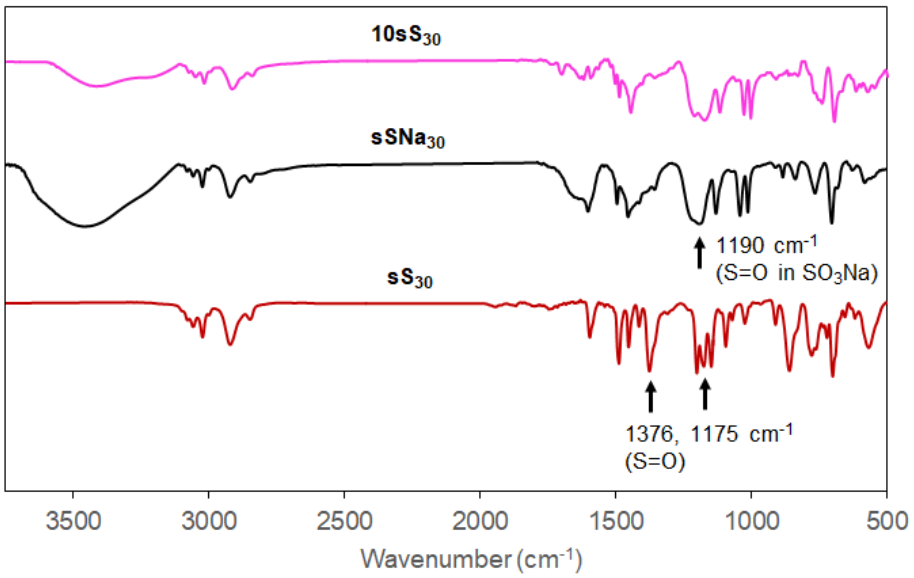

FT-IR spectra for **10sS$_{30}$**

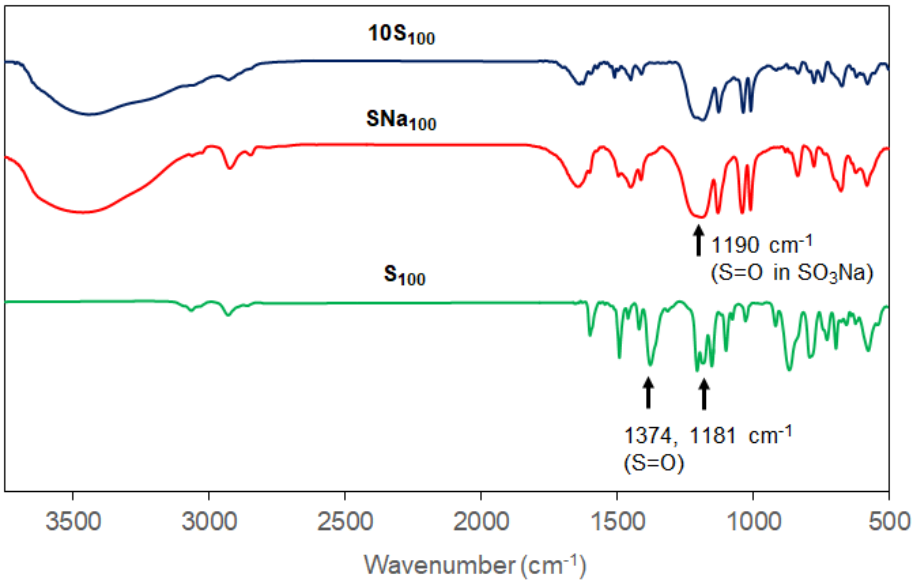

FT-IR spectra for **10S$_{100}$**

C.2 ^{1}H and ^{13}C NMR spectra

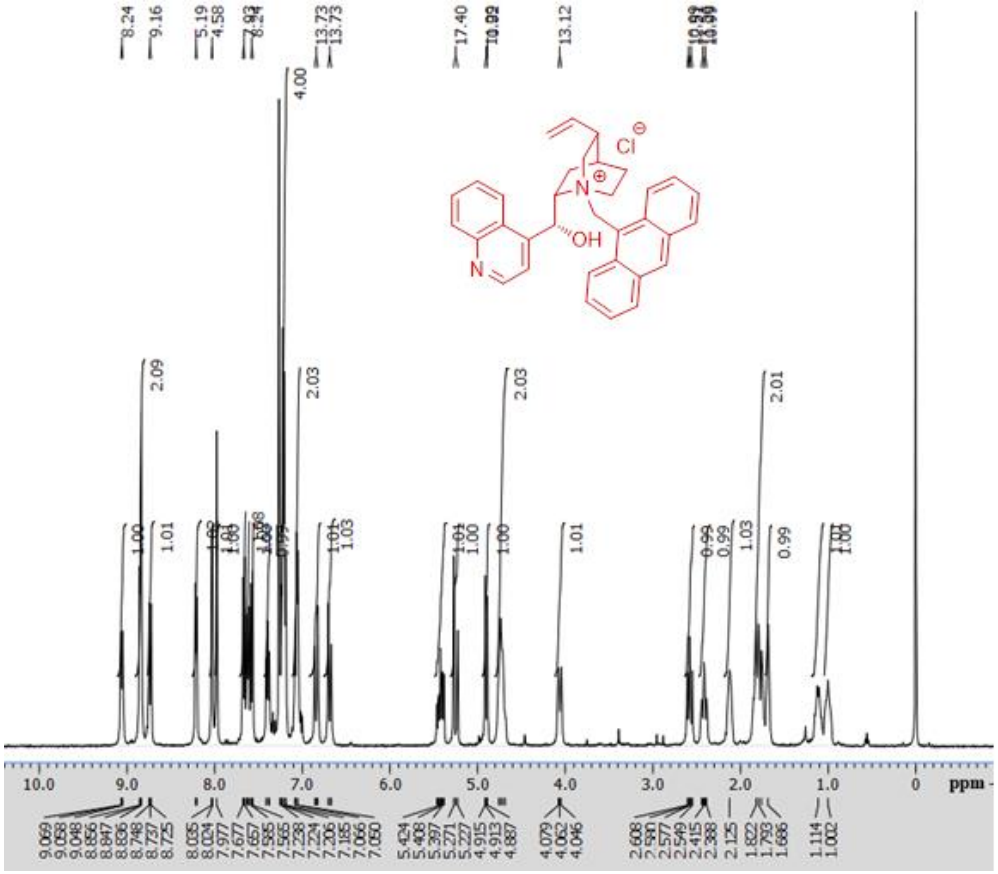

^{1}H NMR of **4** in $CDCl_3$

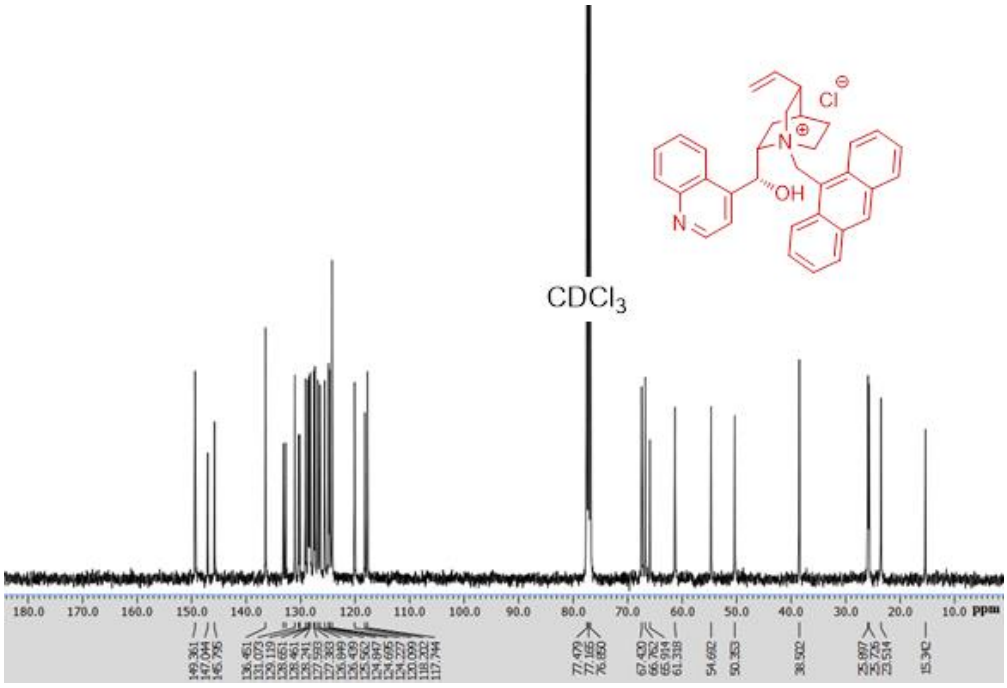

^{13}C NMR of **4** in $CDCl_3$

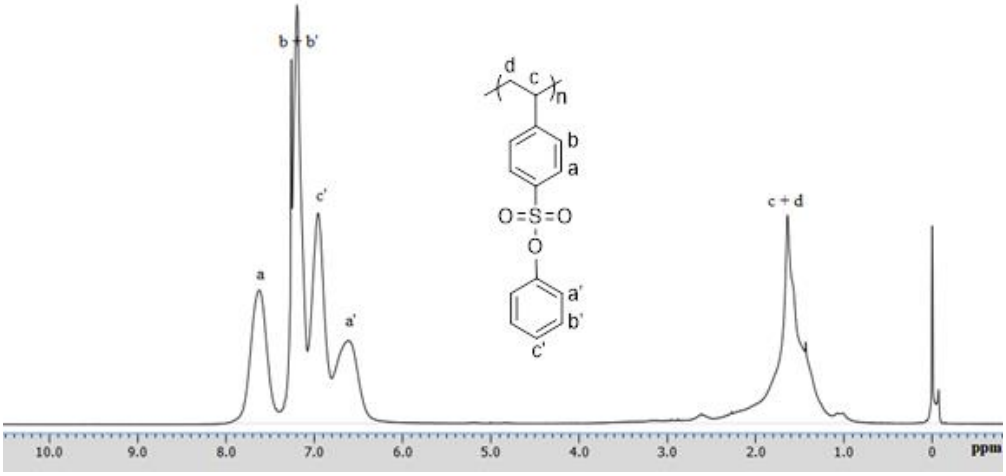

^{1}H NMR of **S_{100}** in $CDCl_3$

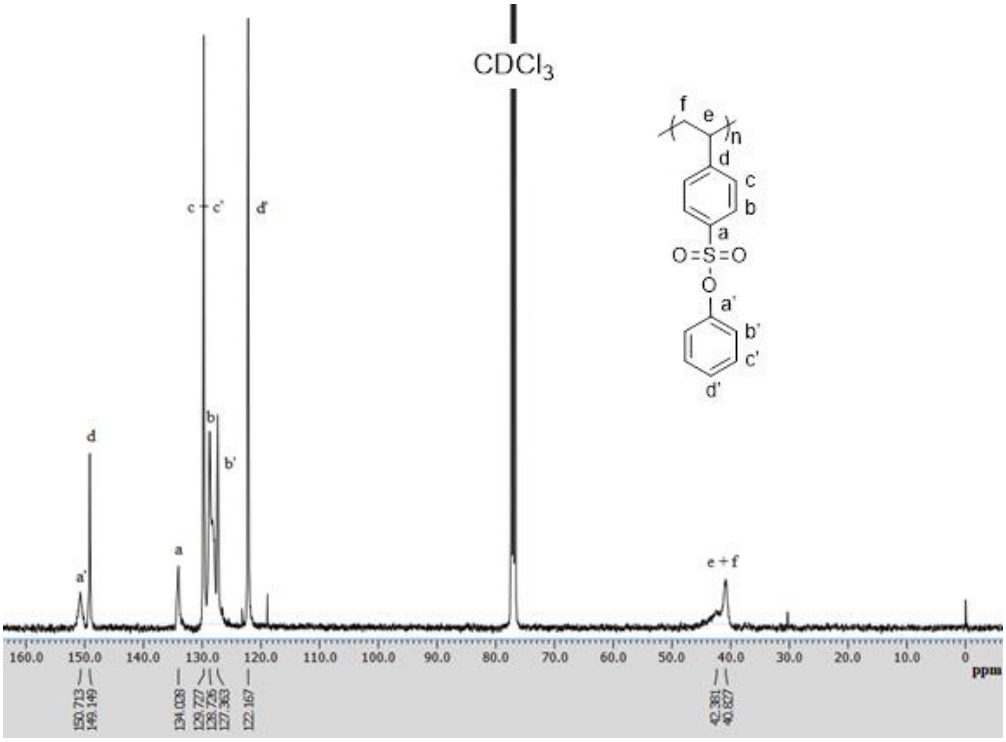

^{13}C NMR of **S_{100}** in $CDCl_3$

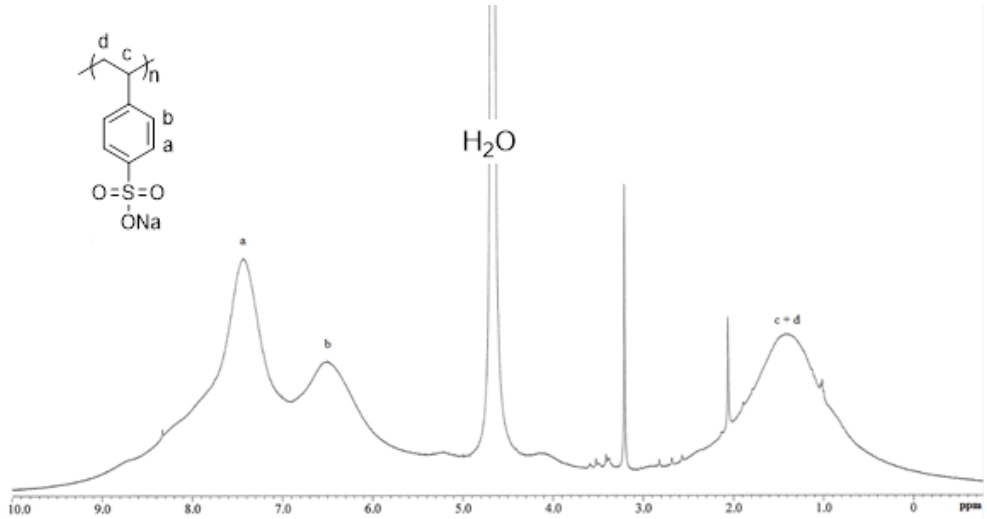

^{1}H NMR of **SNa$_{100}$** in D_2O

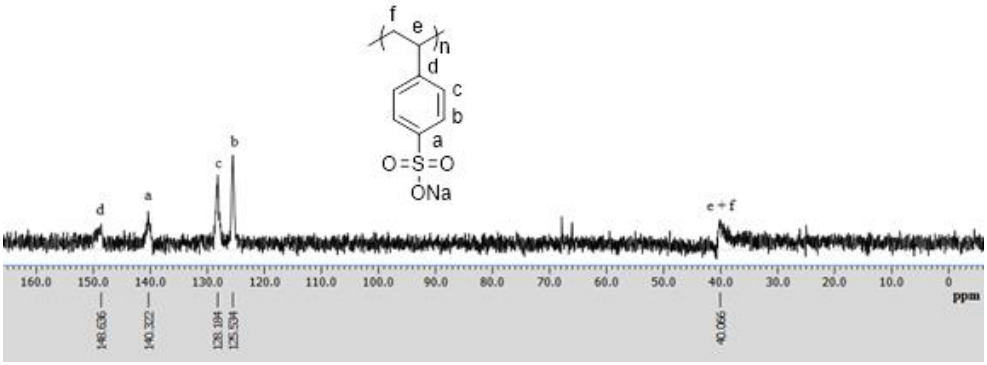

^{13}C NMR of **SNa$_{100}$** in D_2O

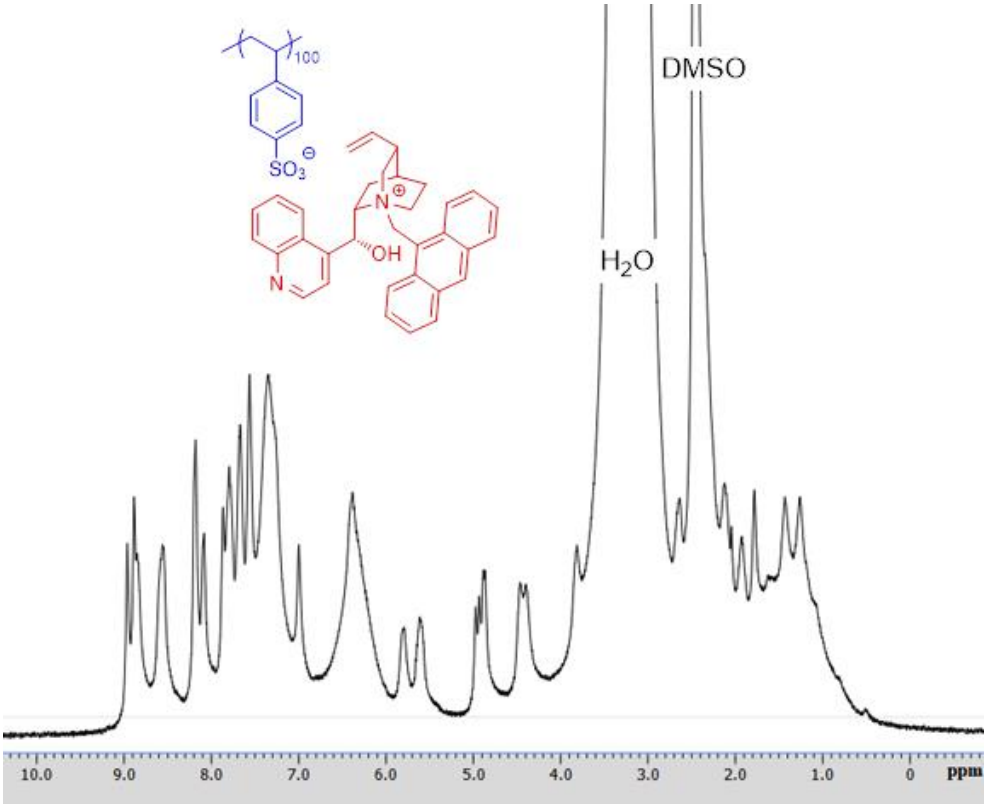

^{1}H NMR **10S$_{100}$** in DMSO-d_6

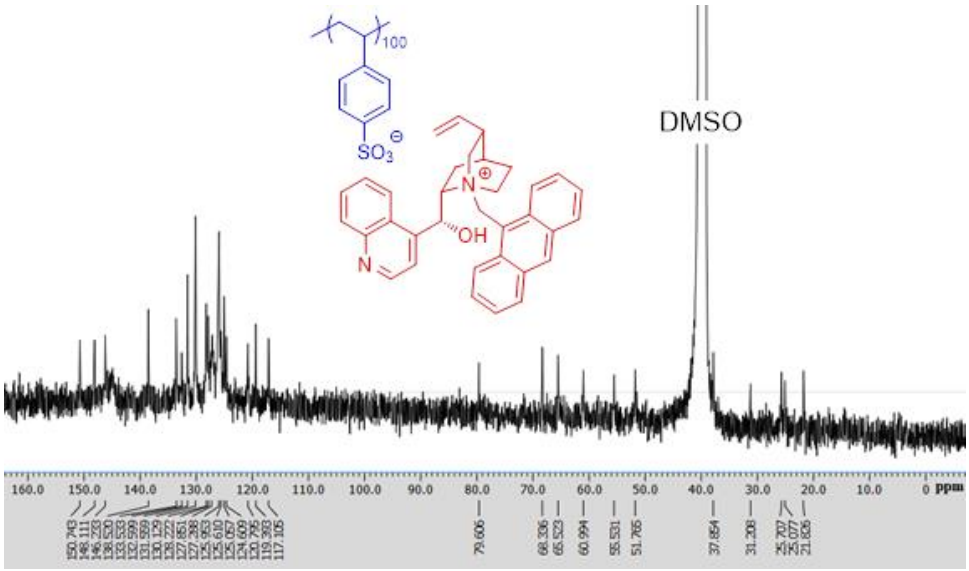

^{13}C NMR of **10S$_{100}$** in DMSO-d_6

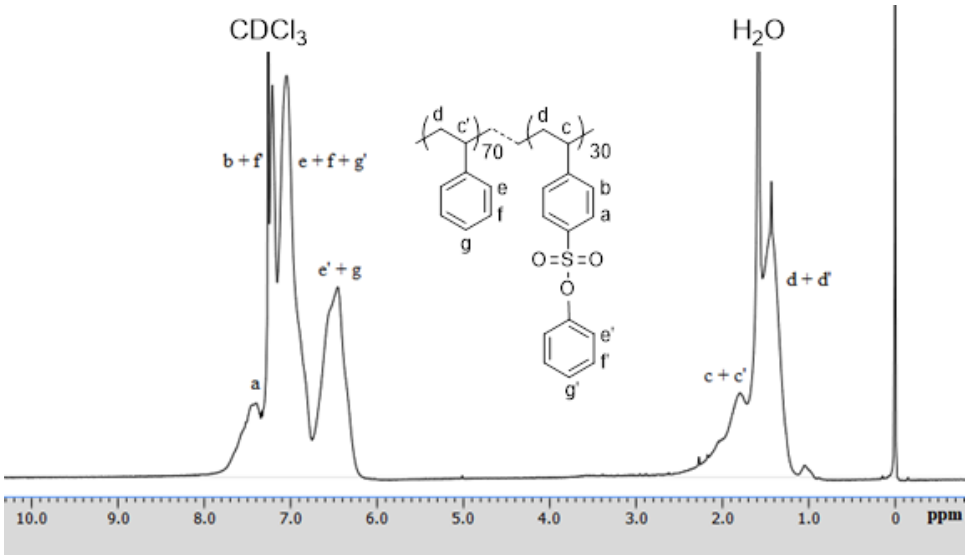

^{1}H NMR of **sS$_{30}$** in $CDCl_3$

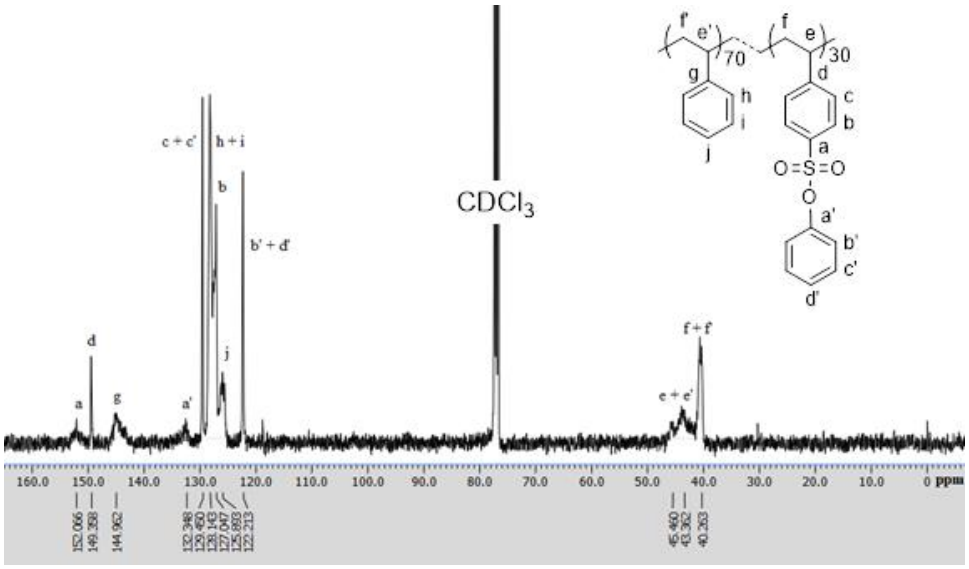

^{13}C NMR of **sS$_{30}$** in $CDCl_3$

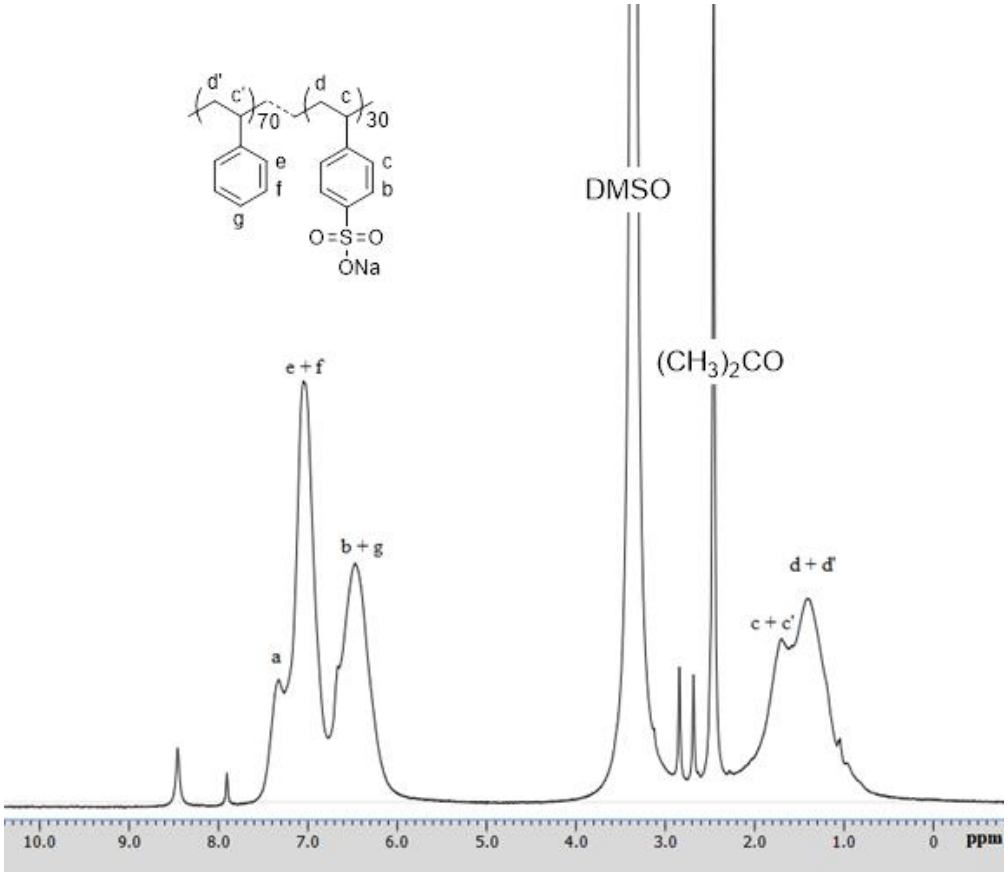

^{1}H NMR of **sSNa$_{30}$** in DMSO-d_6

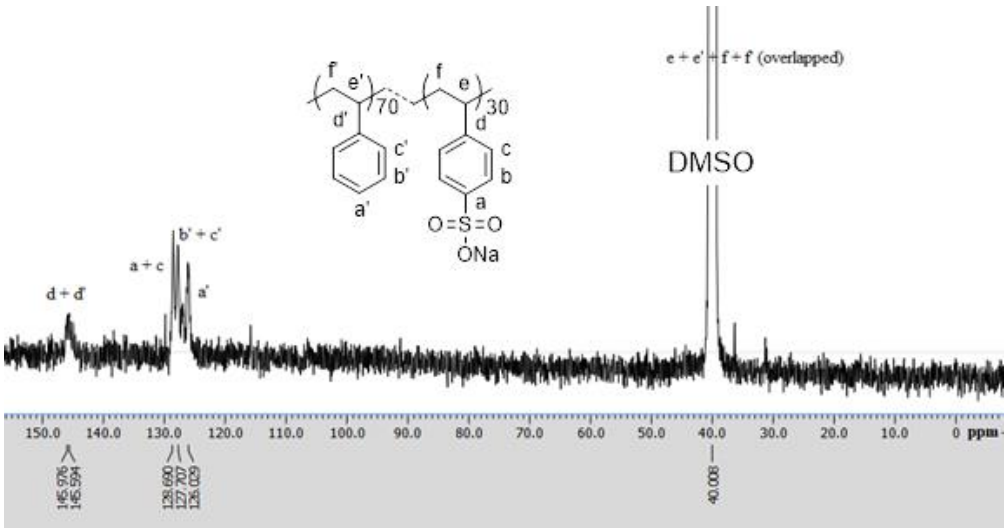

^{13}C NMR of **sSNa$_{30}$** in DMSO-d_6

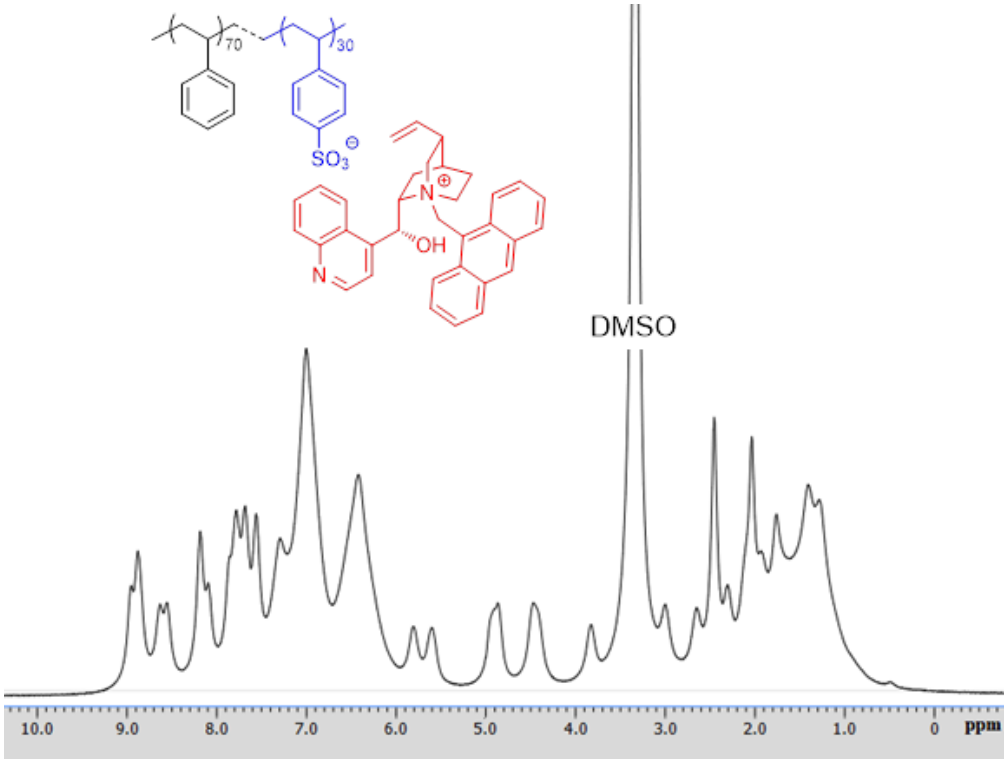

^{1}H NMR of **10sS$_{30}$** in DMSO-d_6

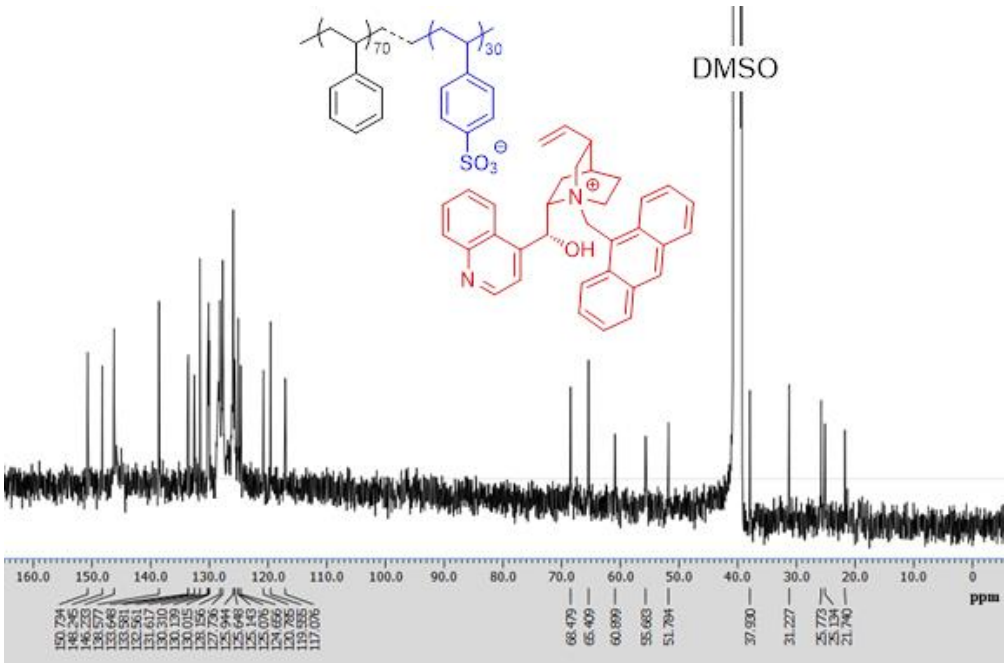

^{13}C NMR of **10sS$_{30}$** in DMSO-d_6

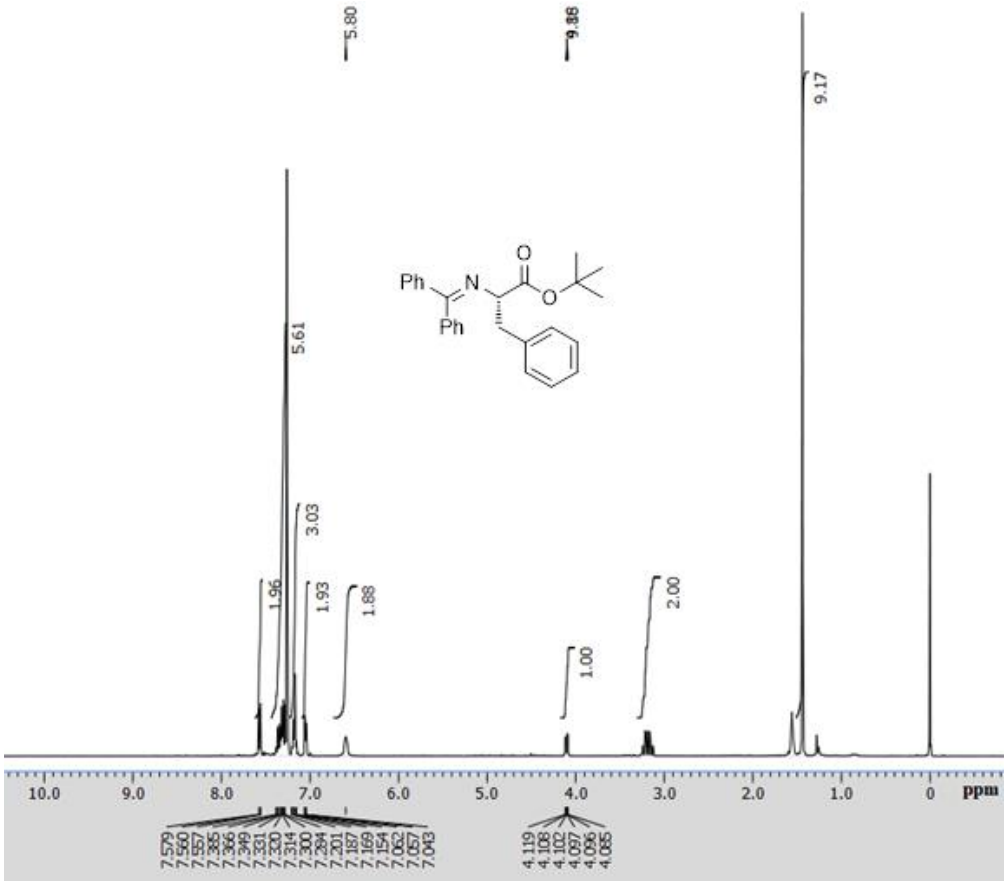

^{1}H NMR of **8a** in $CDCl_3$

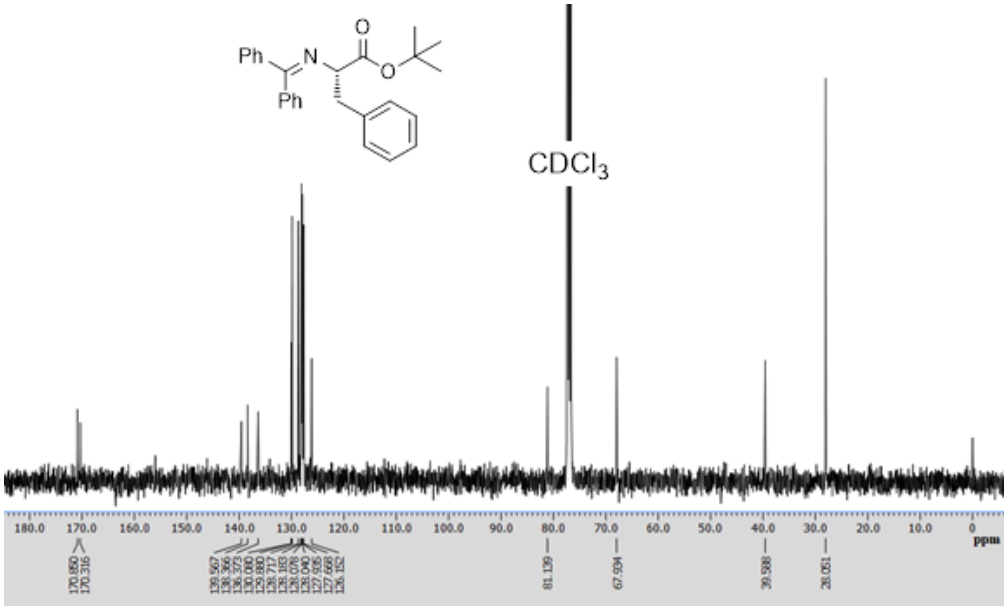

^{13}C NMR of **8a** in $CDCl_3$

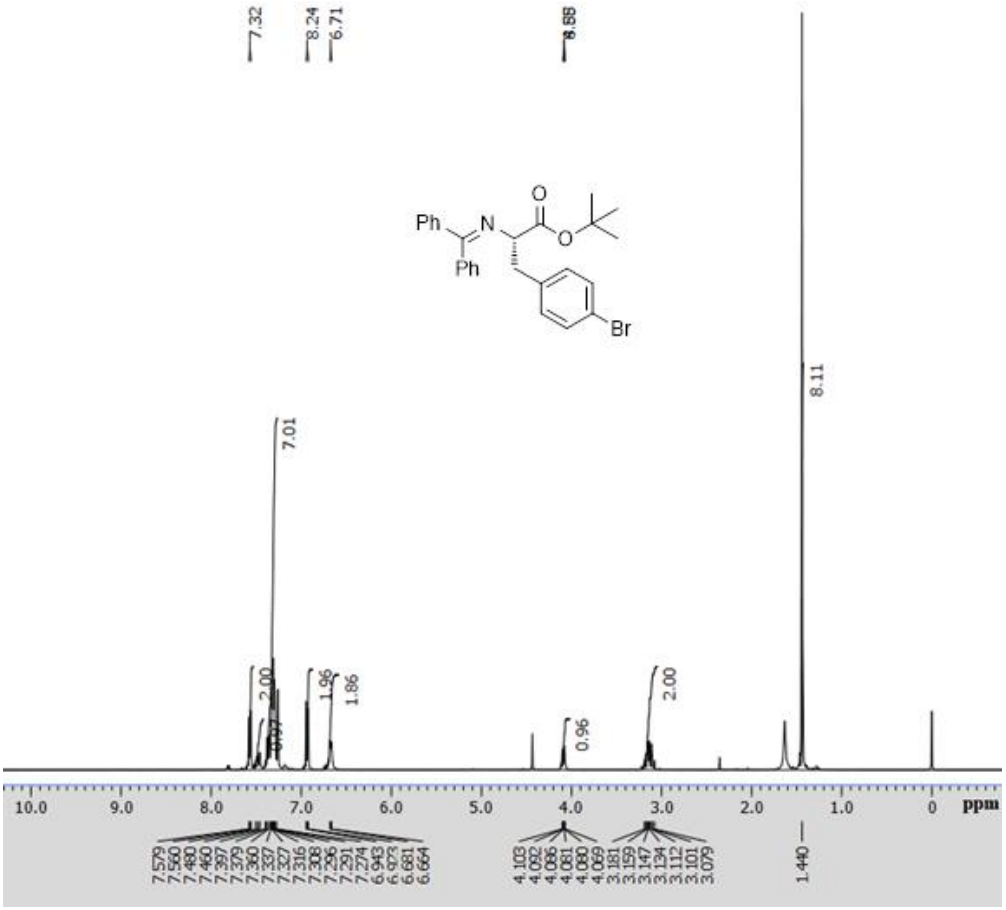

^{1}H NMR of **8b** in $CDCl_3$

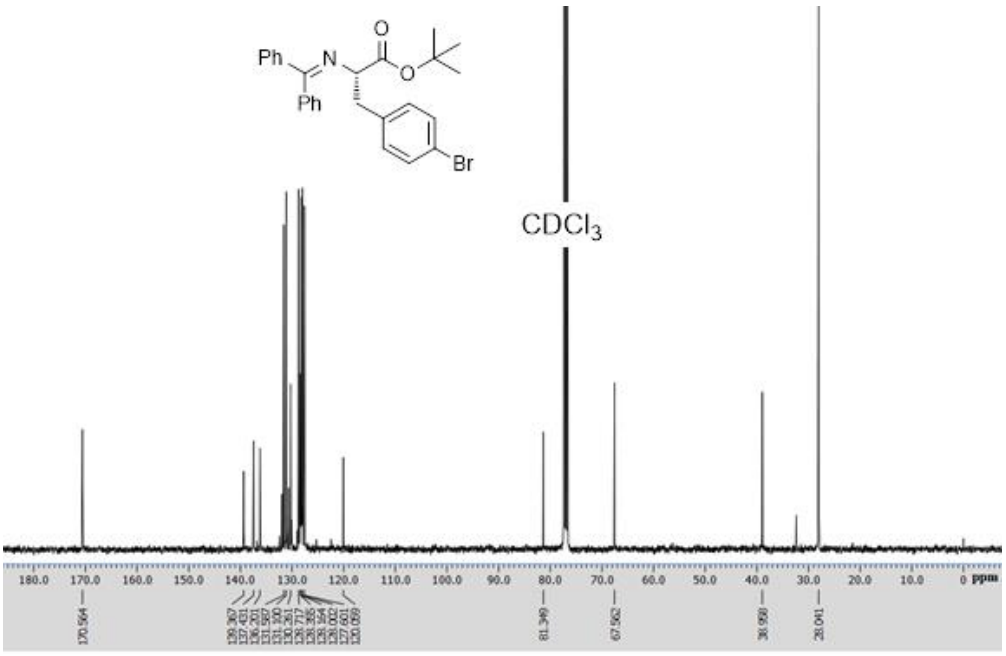

^{13}C NMR of **8b** in $CDCl_3$

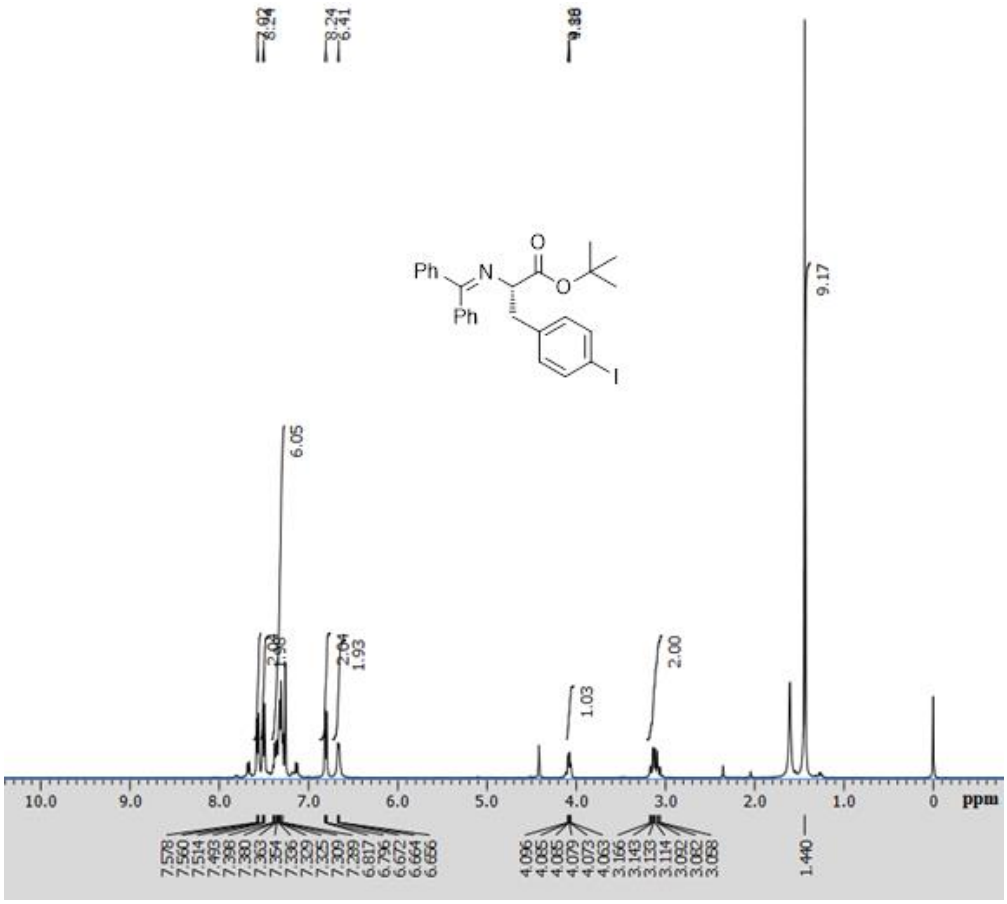

^{1}H NMR of **8c** in $CDCl_3$

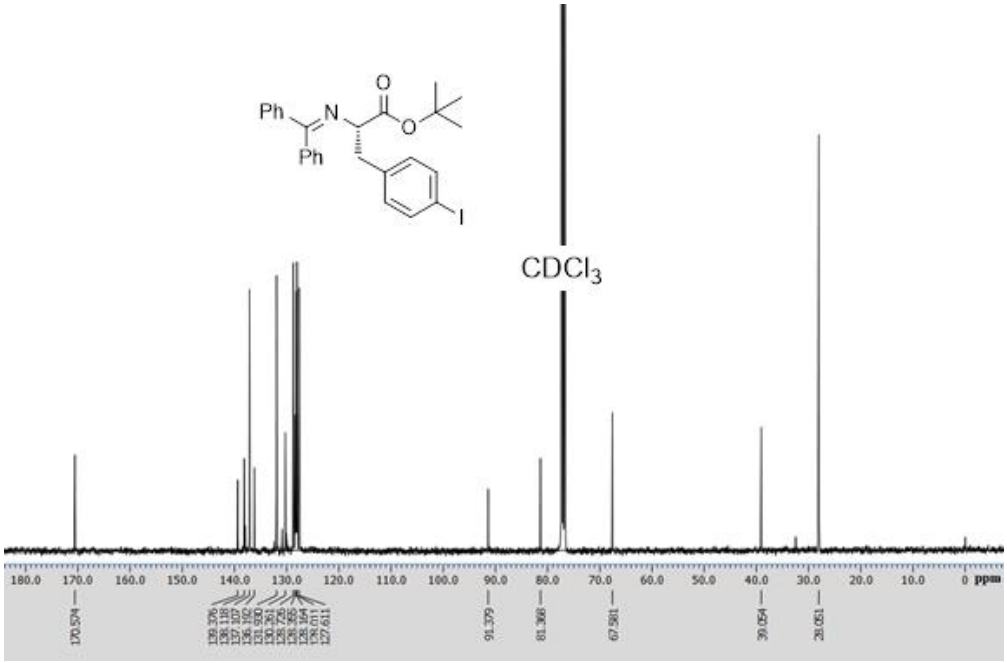

^{13}C NMR of **8c** in $CDCl_3$

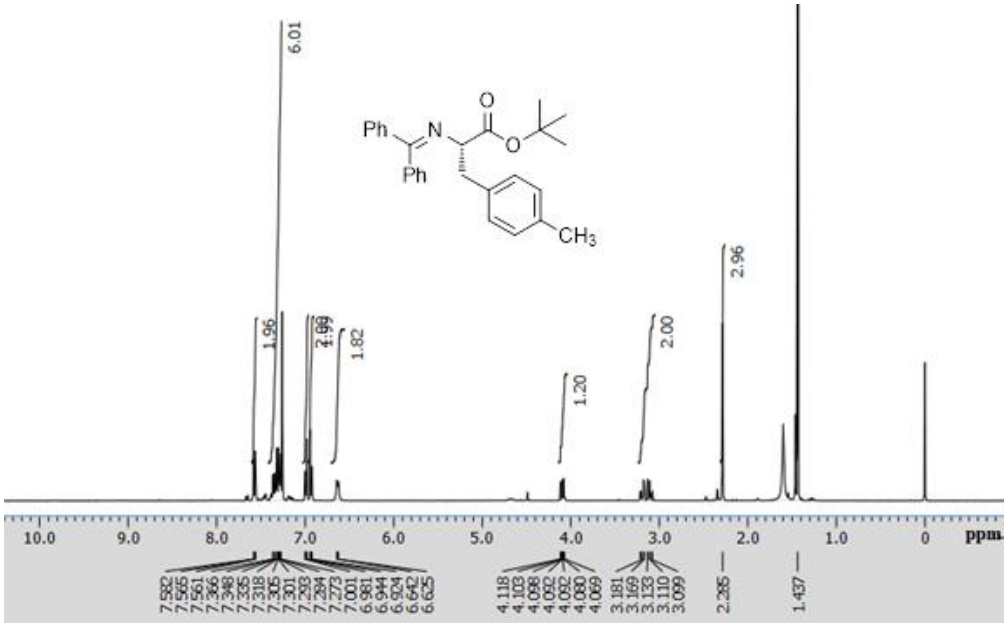

^{1}H NMR of **8d** in $CDCl_3$

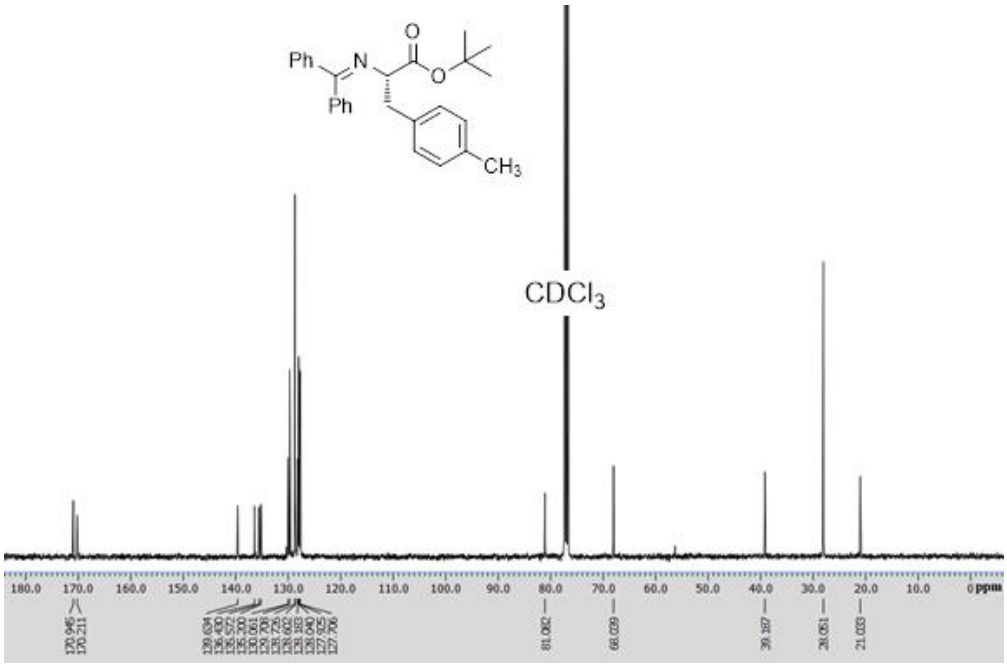

^{13}C NMR of **8d** in $CDCl_3$

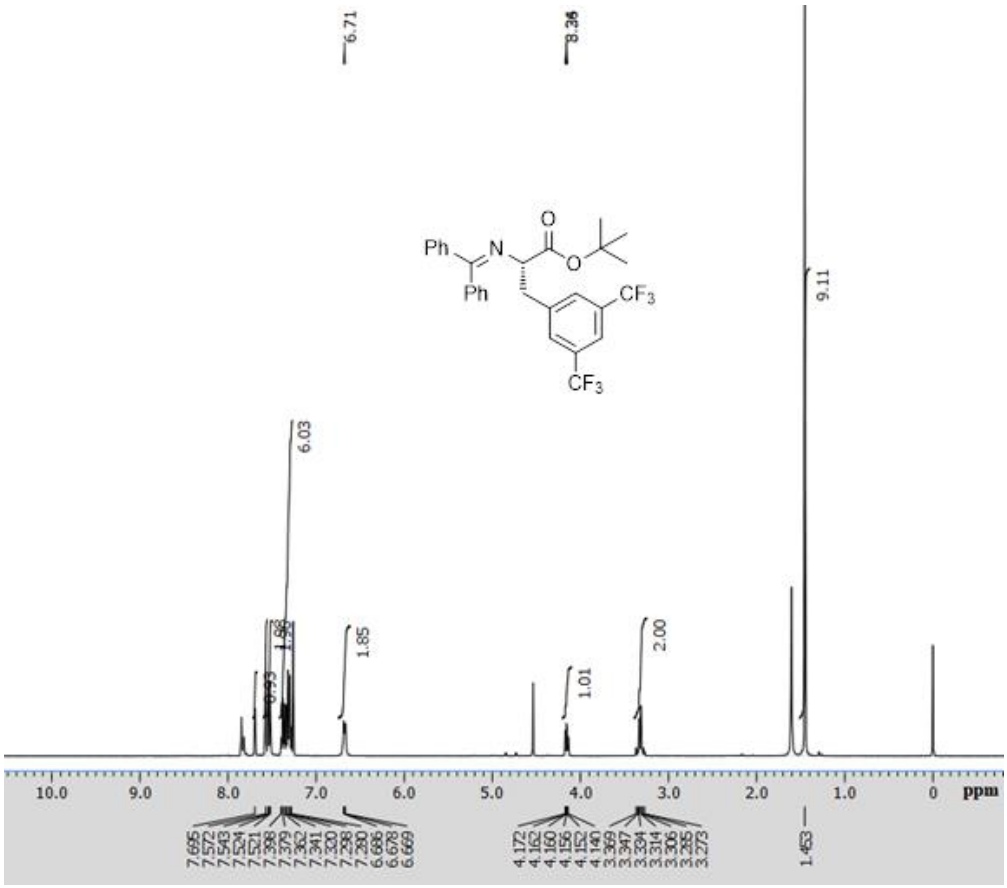

^{1}H NMR of **8e** in $CDCl_3$

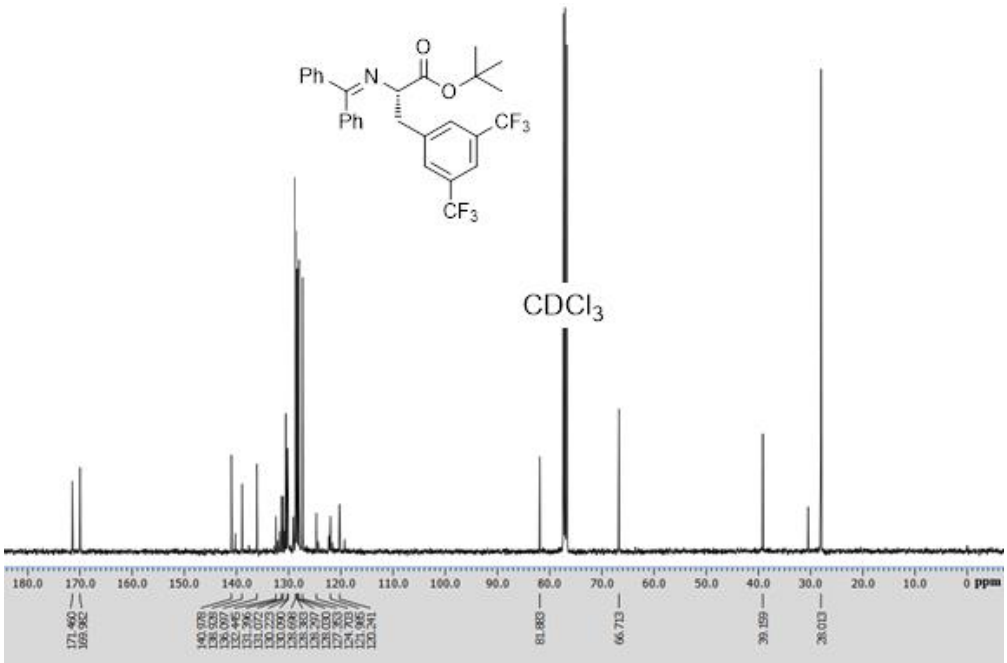

^{13}C NMR of **8e** in $CDCl_3$

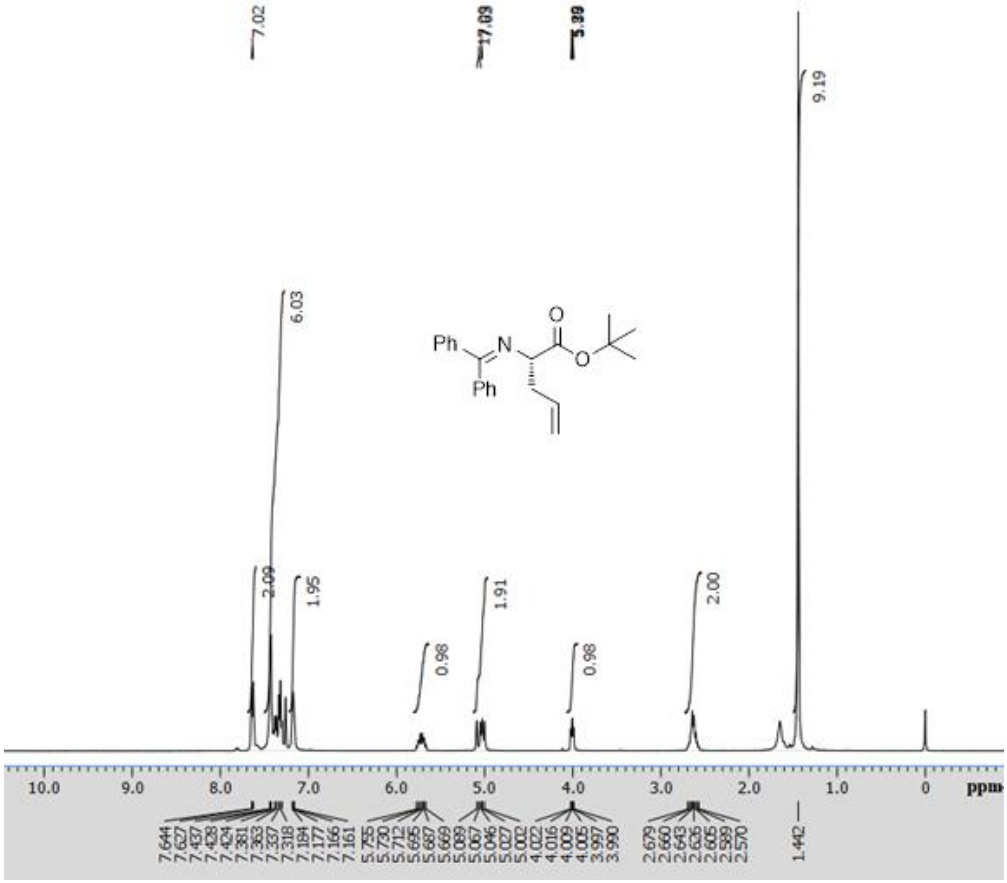

^{1}H NMR of **8f** in $CDCl_3$

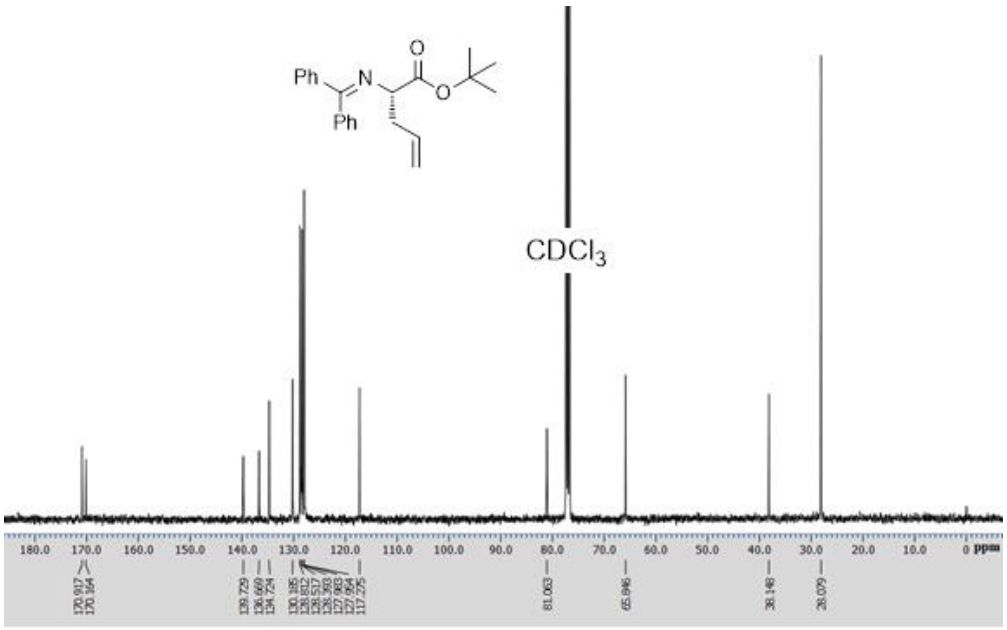

^{13}C NMR of **8f** in $CDCl_3$

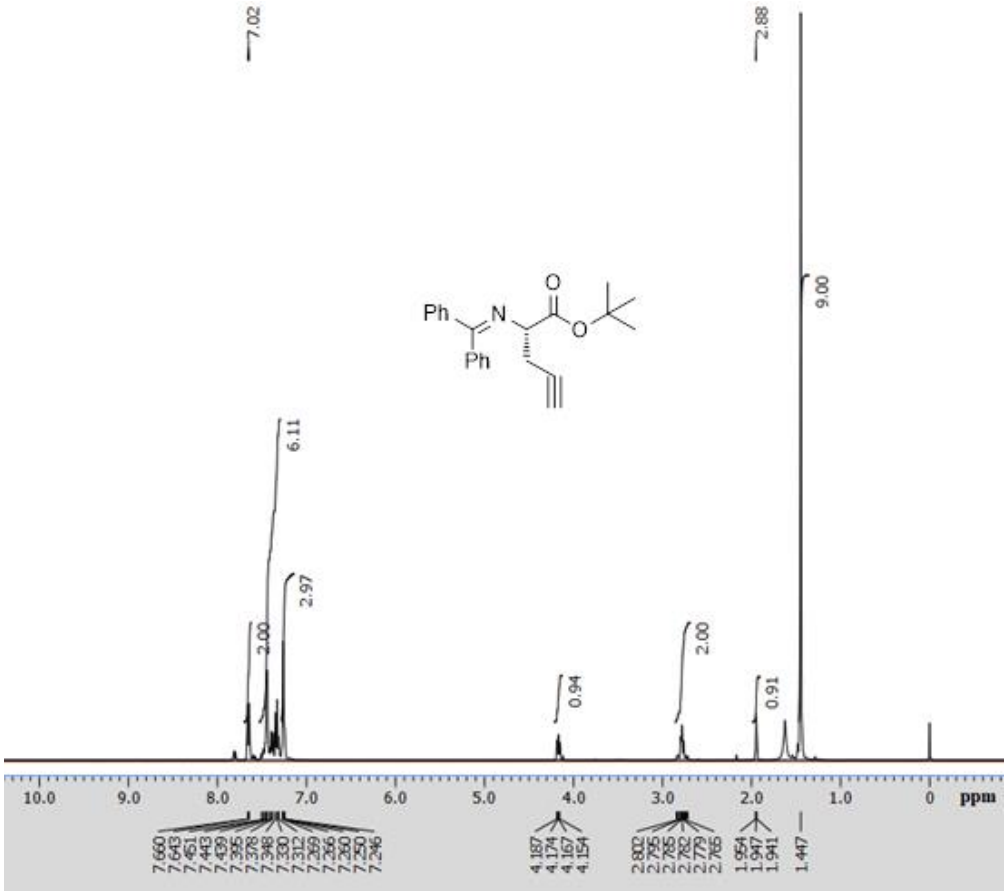

^{1}H NMR of **8g** in $CDCl_3$

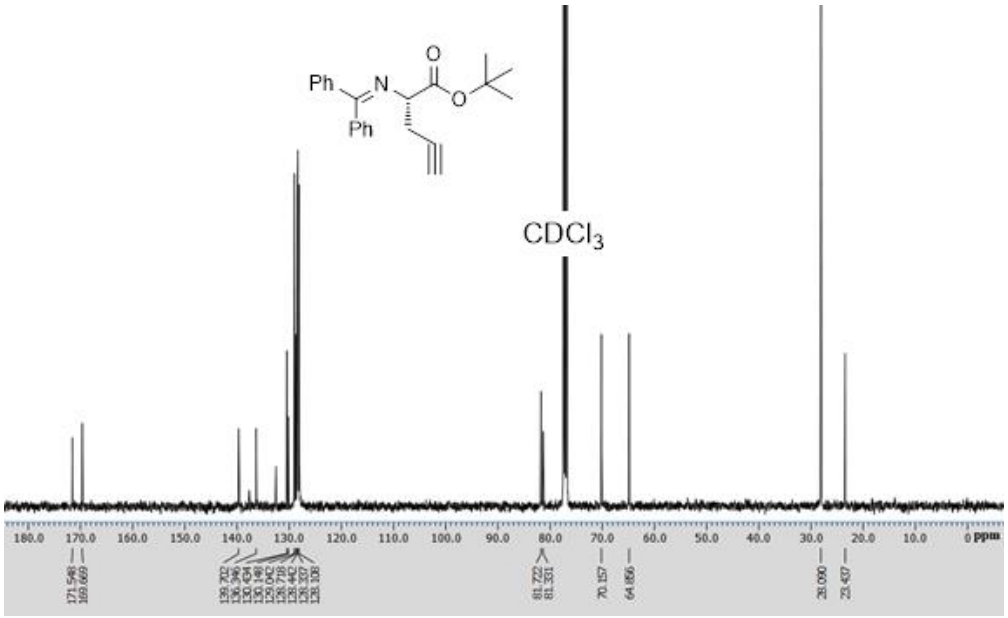

^{13}C NMR of **8g** in $CDCl_3$

C.3 HPLC chromatogram of asymmetric products

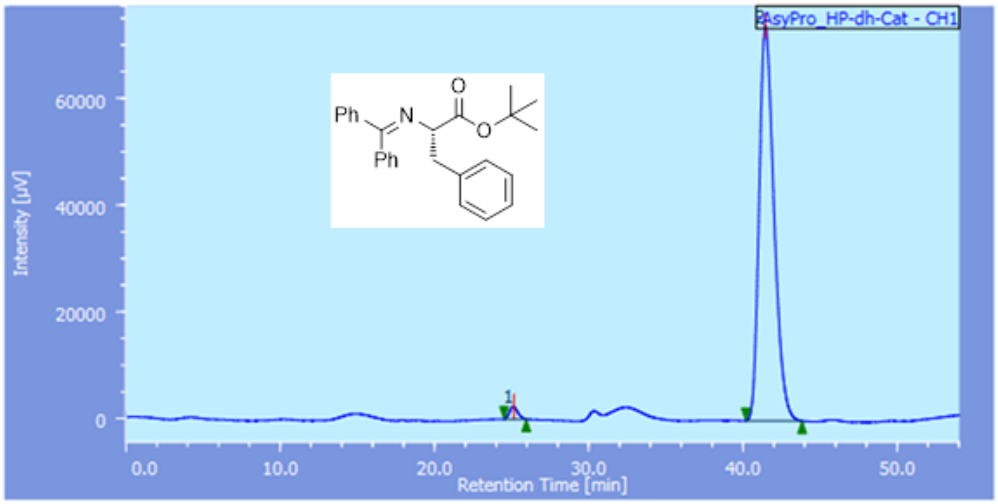

HPLC chromatogram of **8a**

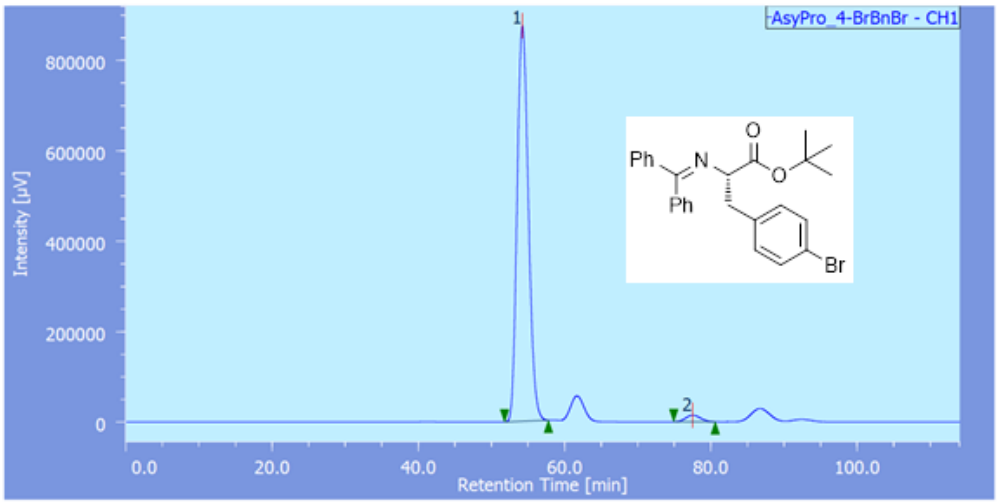

HPLC chromatogram of **8b**

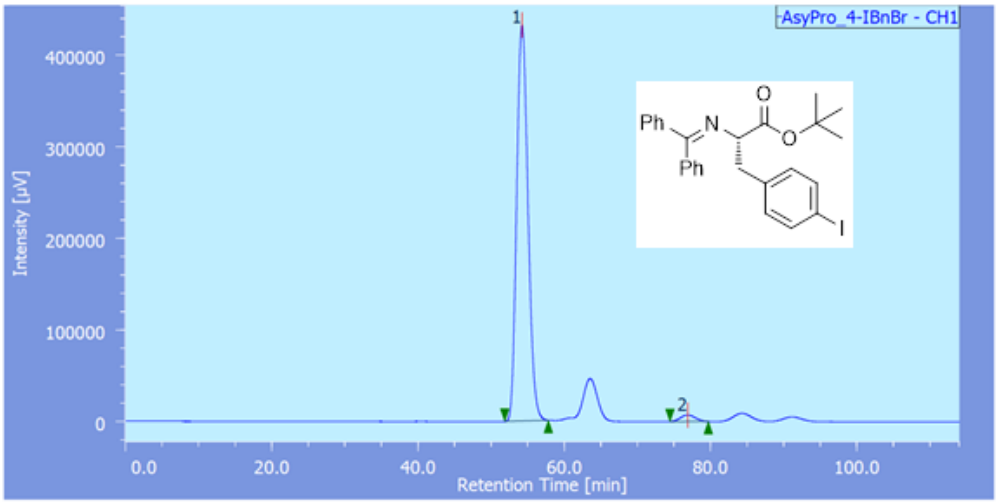

HPLC chromatogram of **8c**

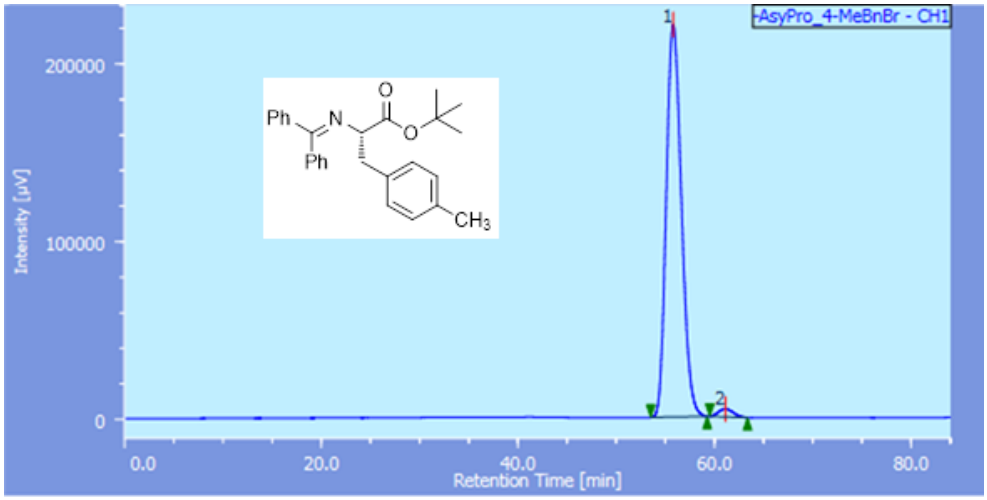

HPLC chromatogram of **8d**

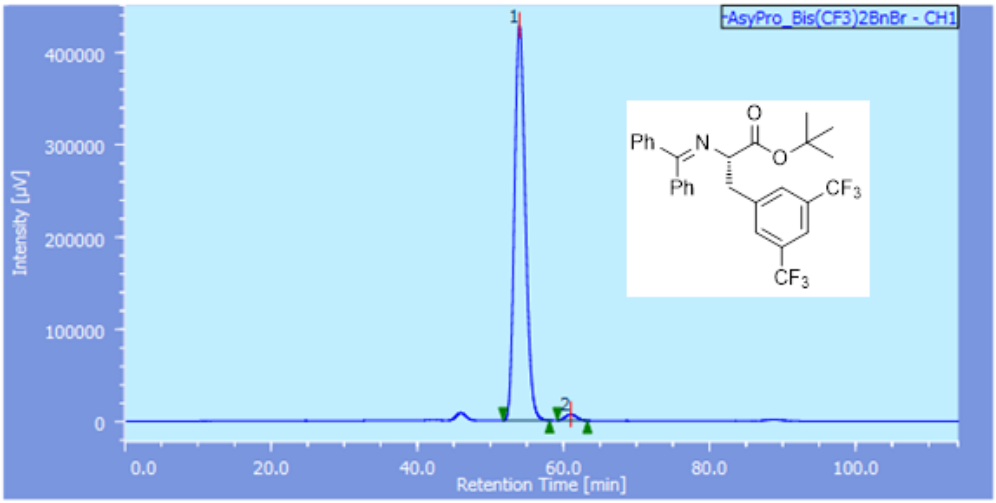

HPLC chromatogram of **8e**

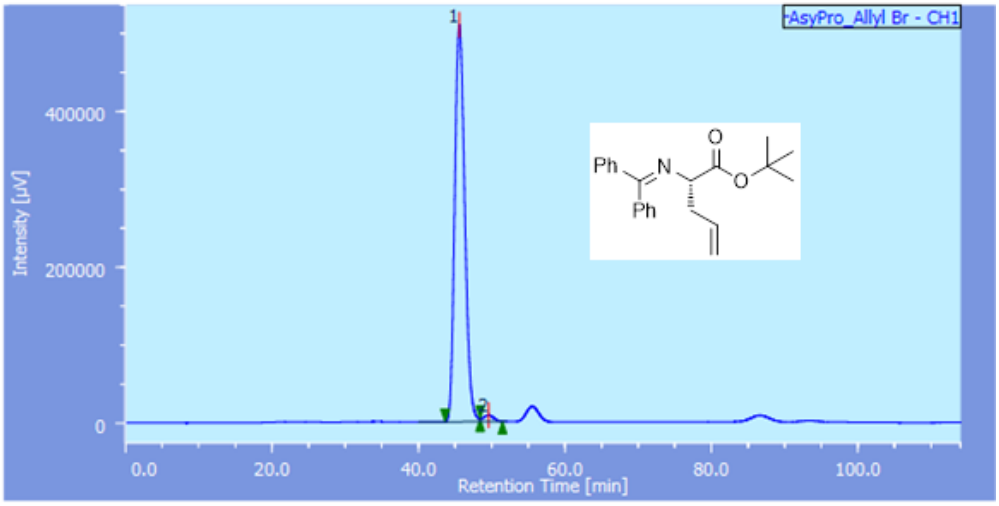

HPLC chromatogram of **8f**

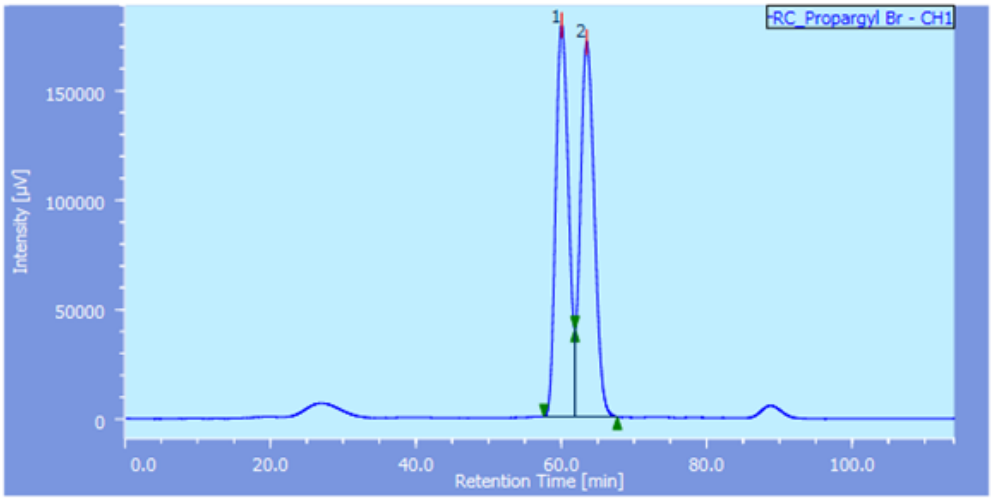

HPLC chromatogram of racemic mixture of **8g**

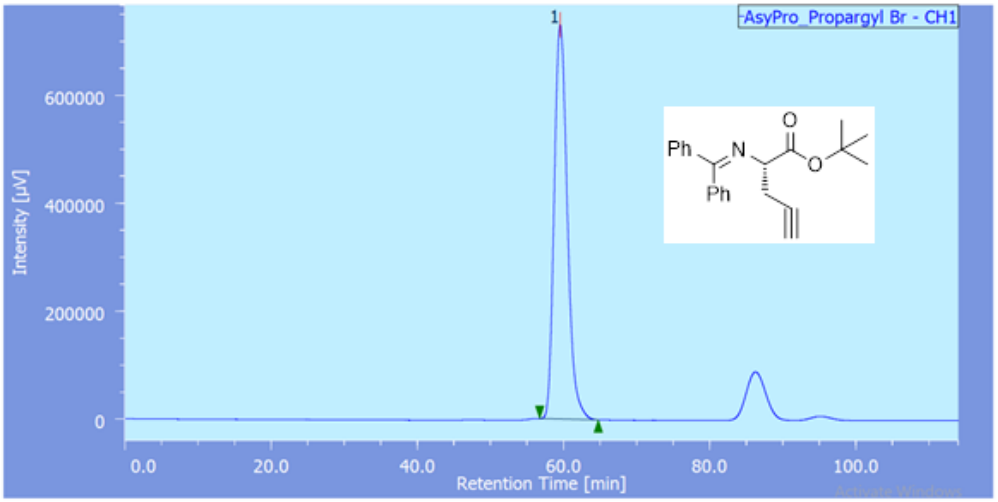

HPLC chromatogram of **8g**

C.4 FT-IR spectra and SEM image of reused catalyst $5d_{20}hC_{20}$

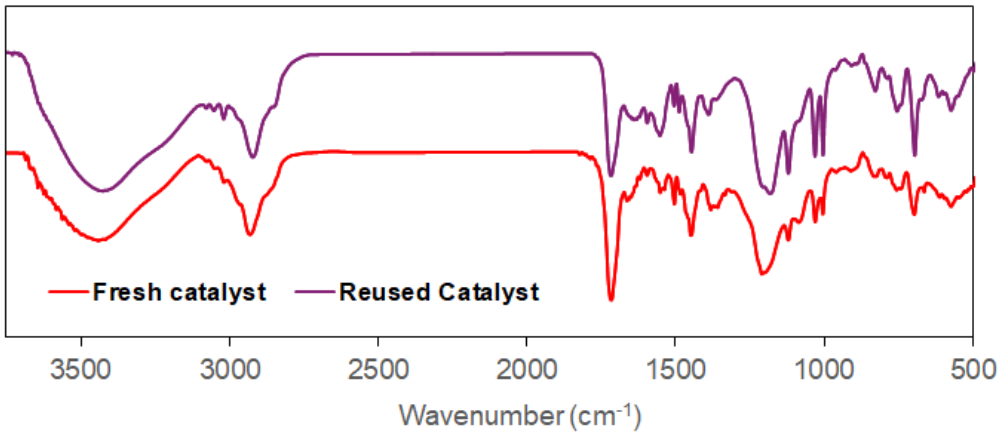

FT-IR spectra of the catalyst **$5d_{20}hC_{20}$**

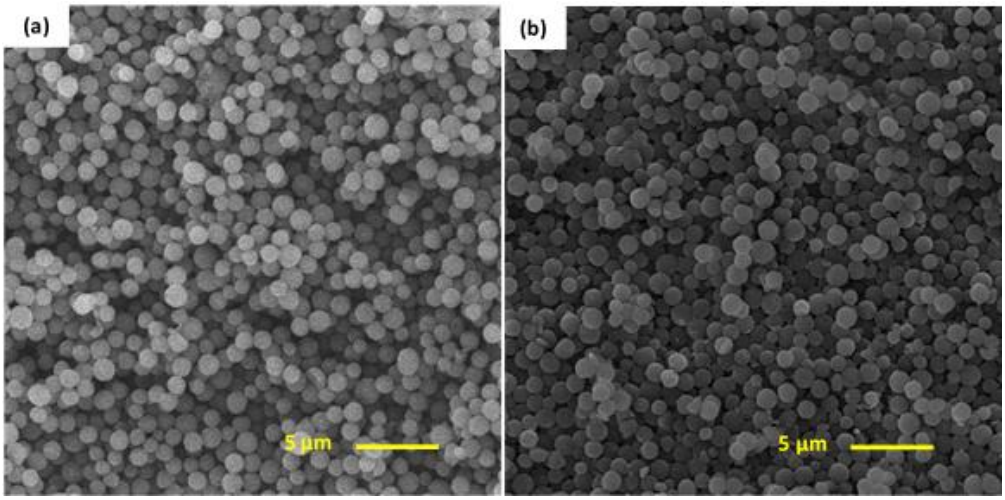

SEM images of the catalyst **$5d_{20}hC_{20}$**: Before reaction (a), and after reaction (b).

Appendix D

Supporting documents for CHAPTER V

D.1 FT-IR spectra for core-corona polymer microsphere-supported sodium sulfonate 3 and the corresponding microsphere-supported MacMillan catalyst 6

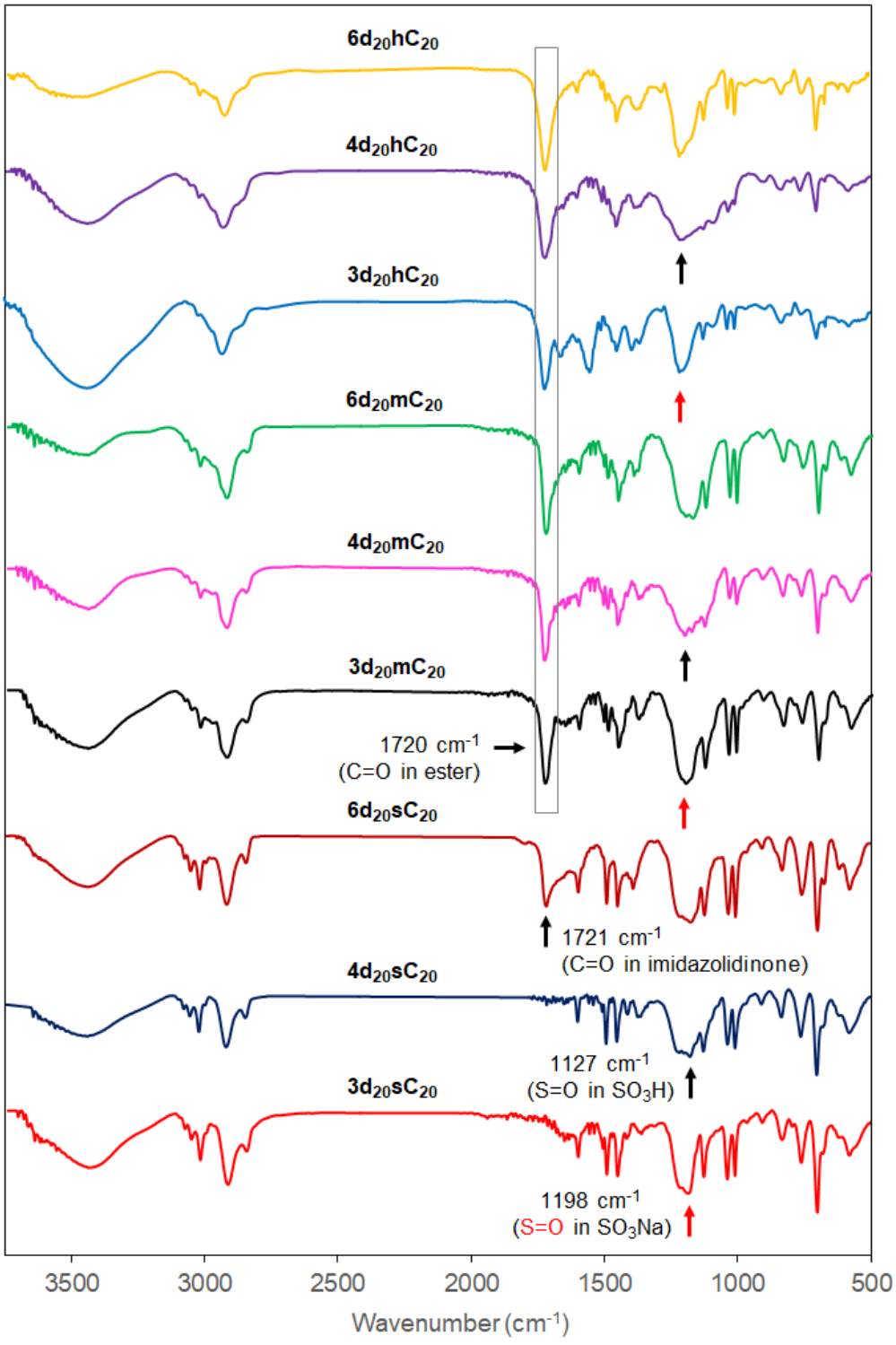

FT-IR spectra for entries 1-3 in **Table 5.3** and **Table 5.4**

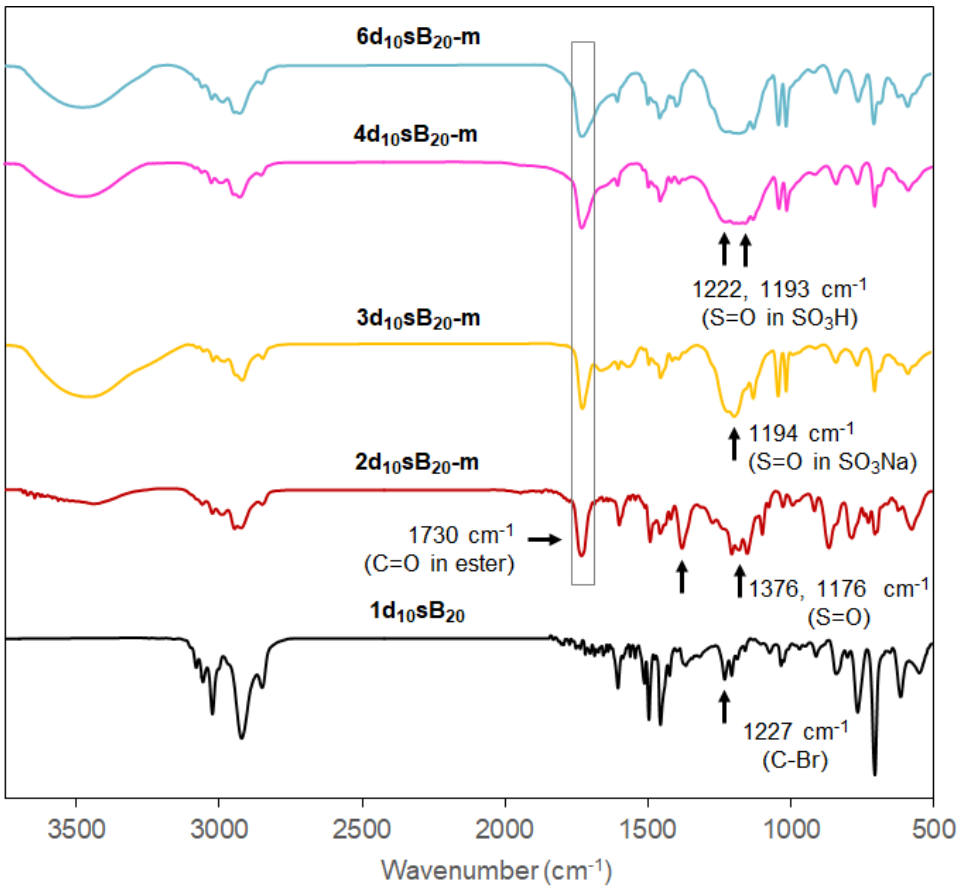

FT-IR spectra for **1d$_{10}$sB$_{20}$** and **6d$_{10}$sB$_{20}$-m**

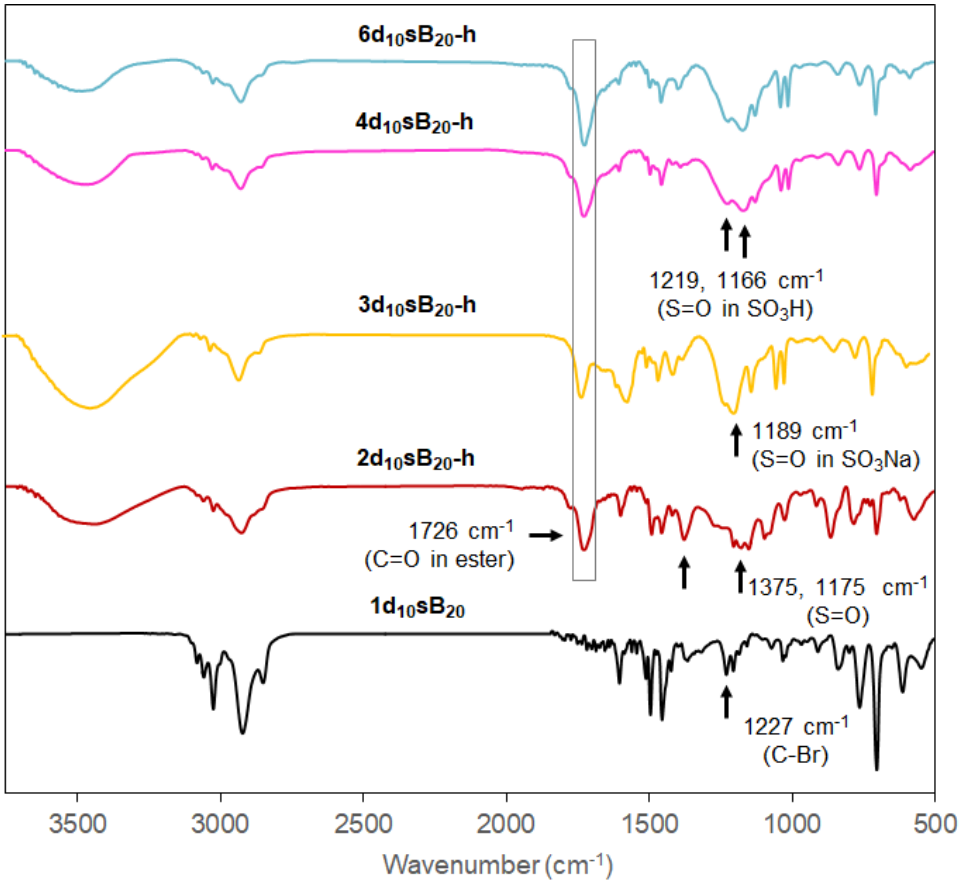

FT-IR spectra for **1d$_{10}$sB$_{20}$** and **6d$_{10}$sB$_{20}$-h**

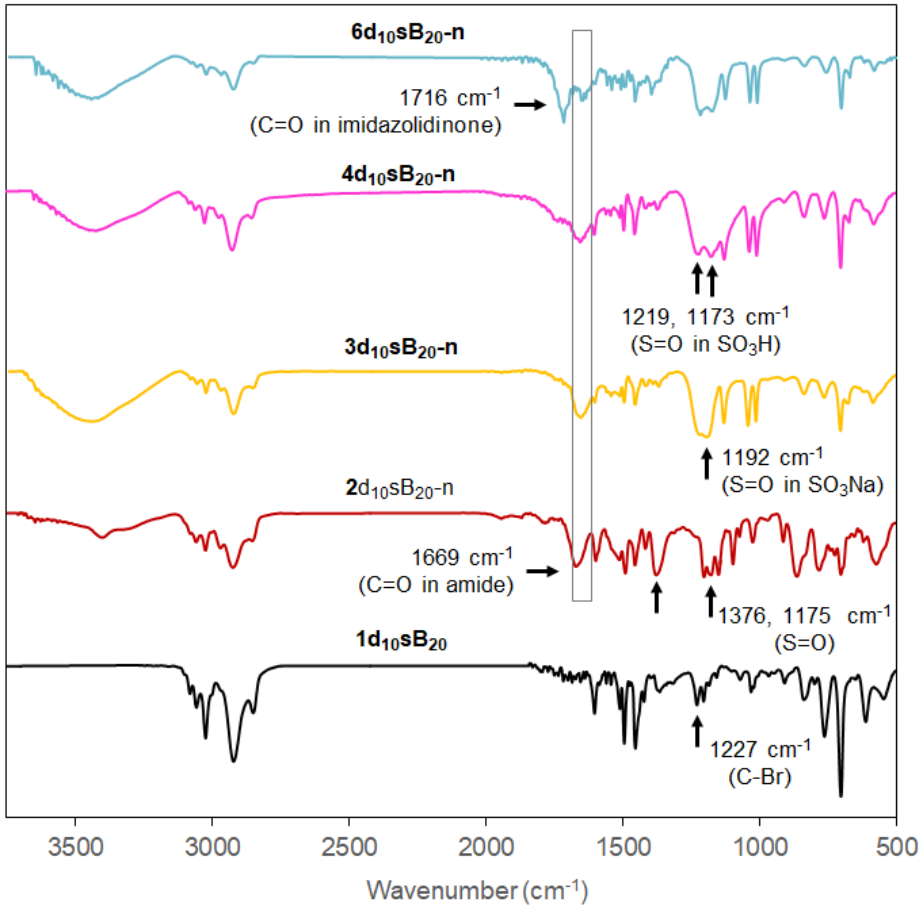

FT-IR spectra for **1d$_{10}$sB$_{20}$** and **6d$_{10}$sB$_{20}$-h**

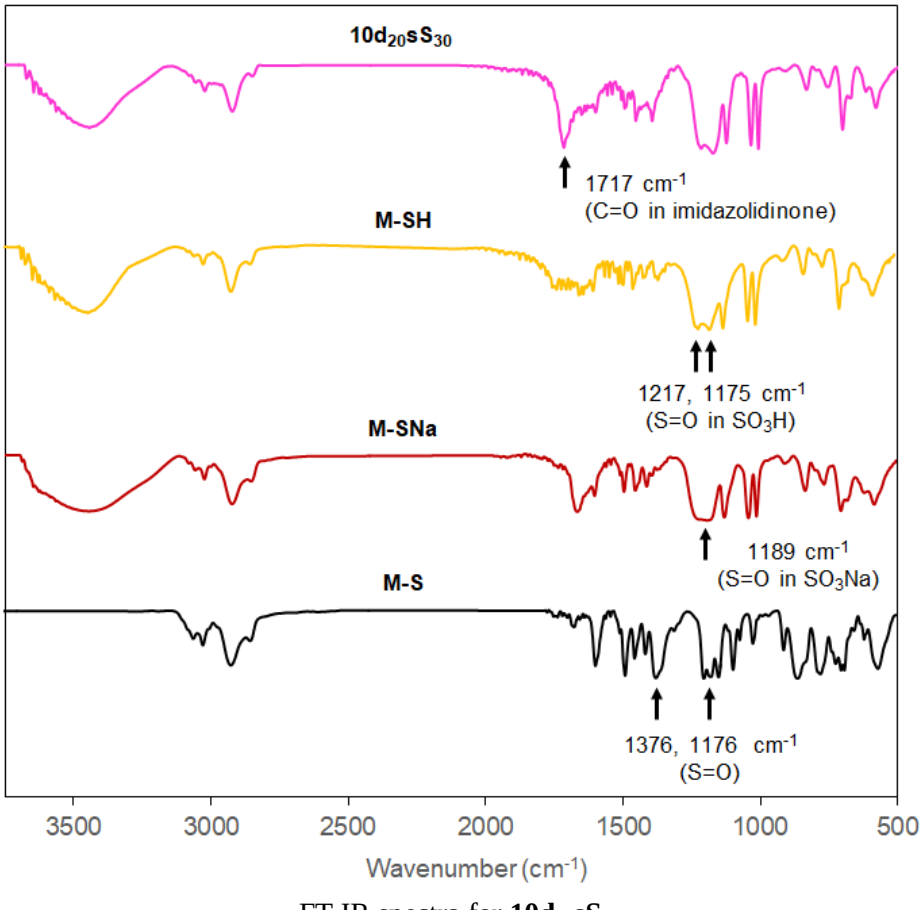

FT-IR spectra for **10d$_{10}$sS$_{30}$**

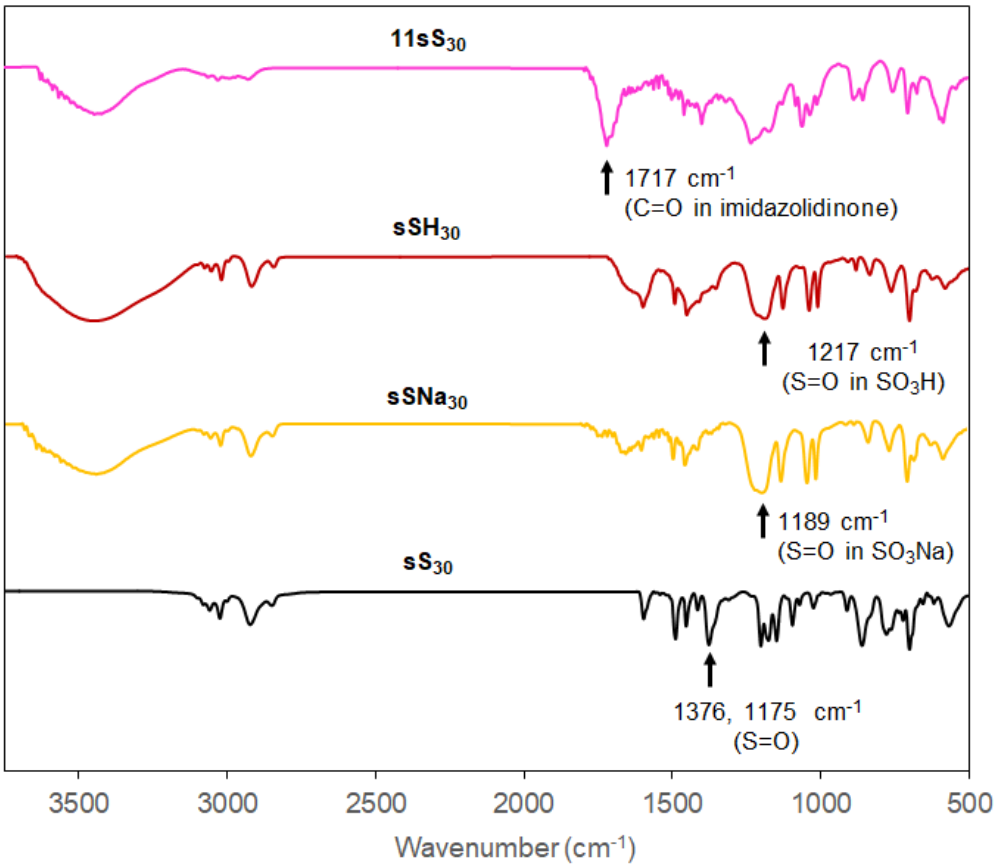

FT-IR spectra for **11sS$_{30}$**

D.2 SEM images of polymer microsphere 1 and the corresponding core-corona polymer microsphere 2

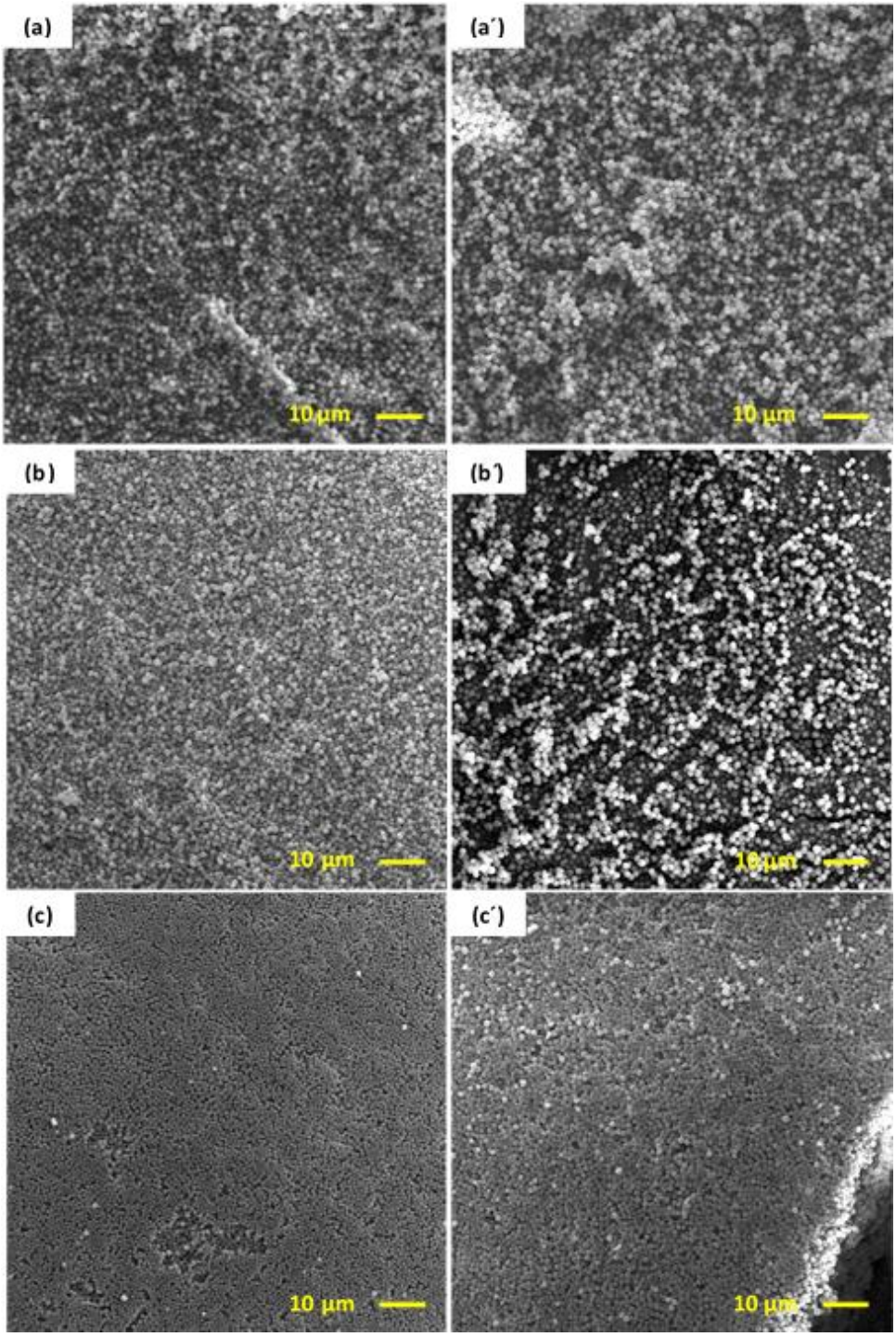

1d$_{20}$sC$_{20}$ (a), **2d$_{20}$sC$_{20}$** (a´), **1d$_{20}$mC$_{20}$** (b), **2d$_{20}$mC$_{20}$** (b´), **1d$_{20}$hC$_{20}$** (c), and **2d$_{20}$hC$_{20}$** (c´).

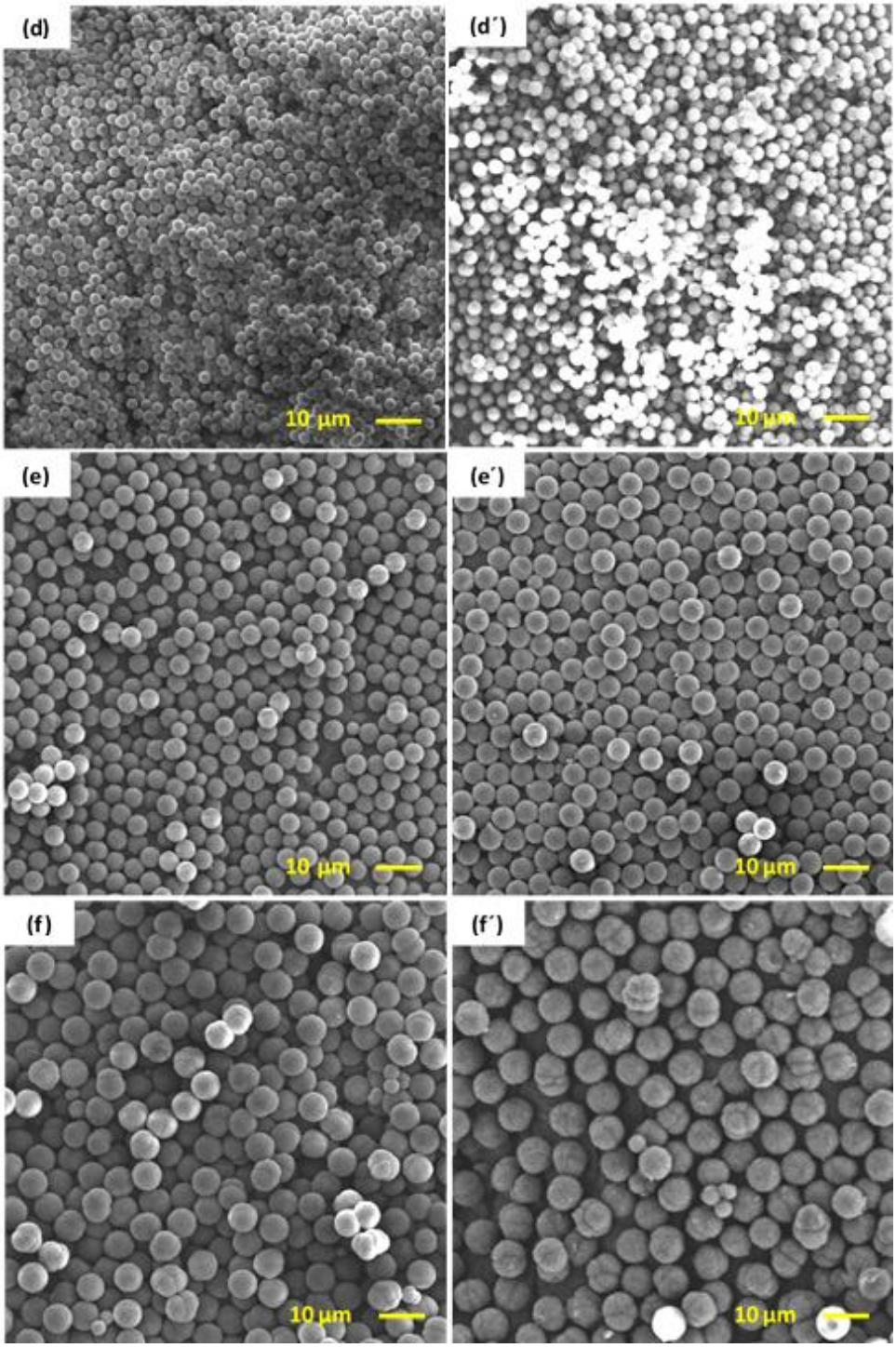

1d$_{20}$sC$_{20}$2 (d), **2d$_{20}$sC$_{20}$2** (d´), **1d$_{20}$sC$_{20}$4** (e), **2d$_{20}$sC$_{20}$4** (e´), **1d$_{20}$sC$_{20}$6** (f), and **2d$_{20}$sC$_{20}$6** (f´).

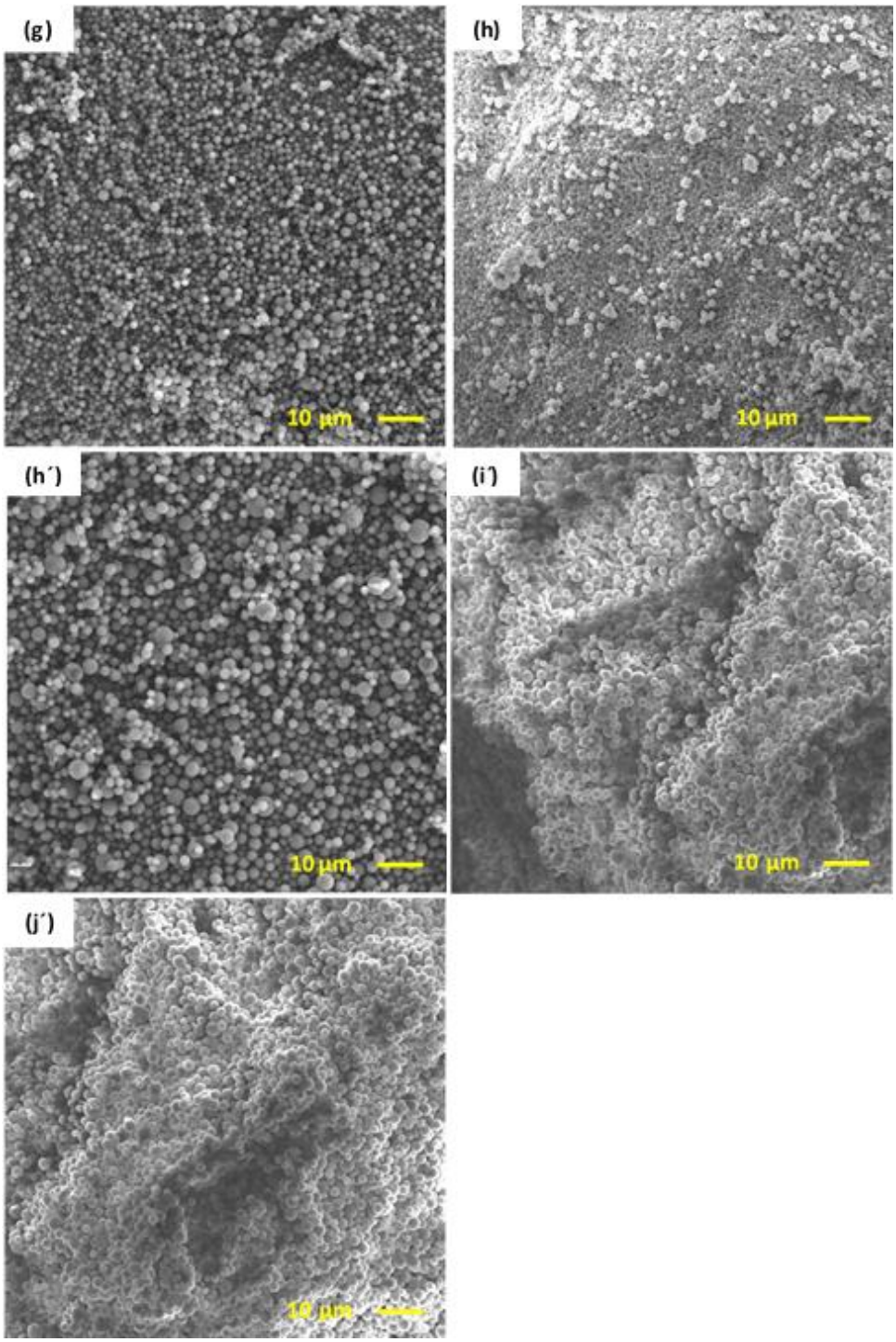

1d$_{10}$sM$_{10}$ (g), **1d$_{10}$sB$_{20}$** (h), **2d$_{10}$sB$_{20}$-50** (or 2d$_{10}$sB$_{20}$) (h´), **2d$_{10}$sB$_{20}$-200** (i´), and **2d$_{10}$sB$_{20}$-200** (j´).

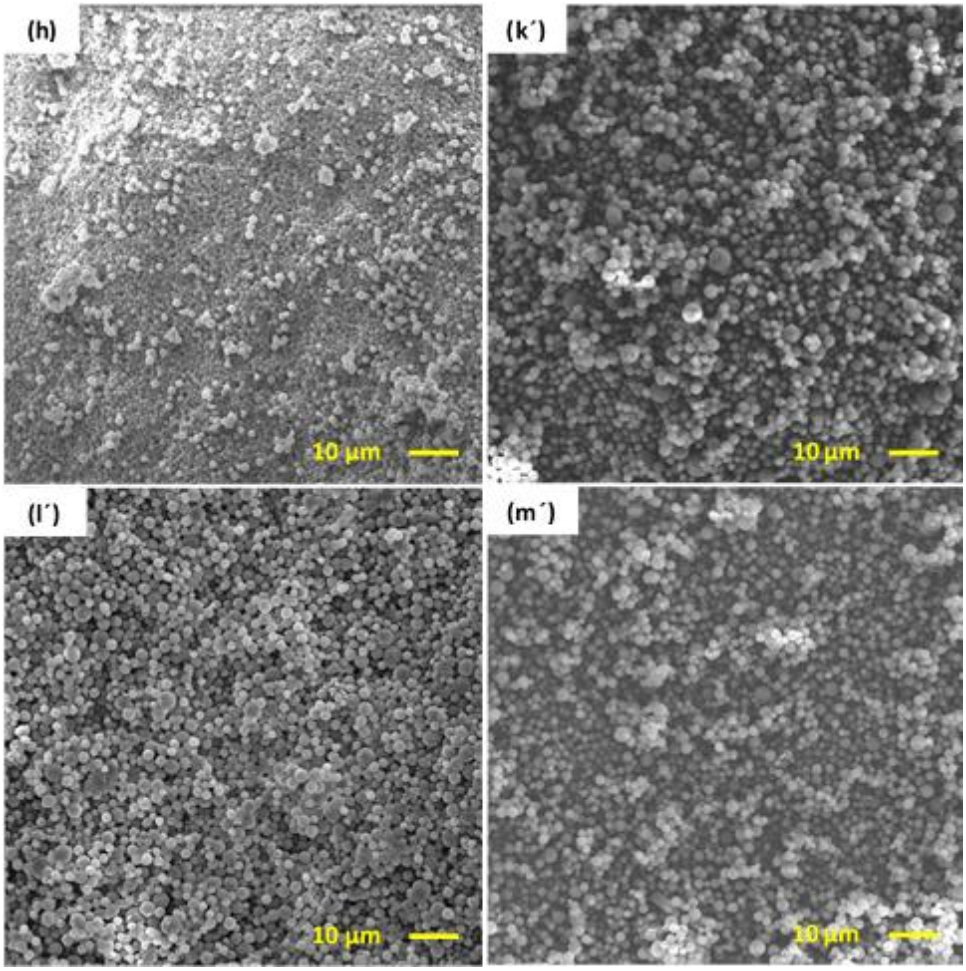

1d$_{10}$sB$_{20}$ (h), **2d$_{10}$sB$_{20}$-m** (k´), **2d$_{10}$sB$_{20}$-h** (l´), **and 2d$_{10}$sB$_{20}$-n** (m´).

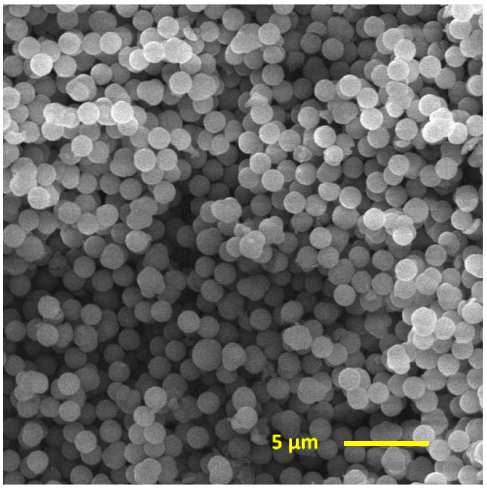

10d$_{20}$sS$_{30}$

D.3 ^{1}H and ^{13}C NMR spectra

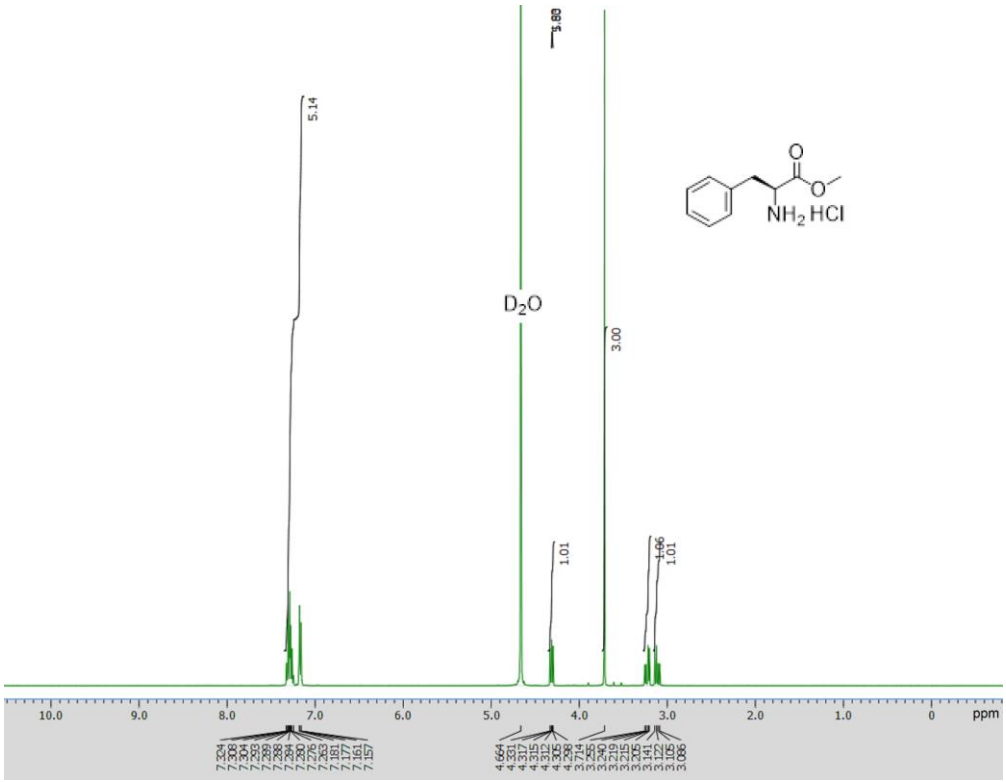

^{1}H NMR of **S1** in D_2O

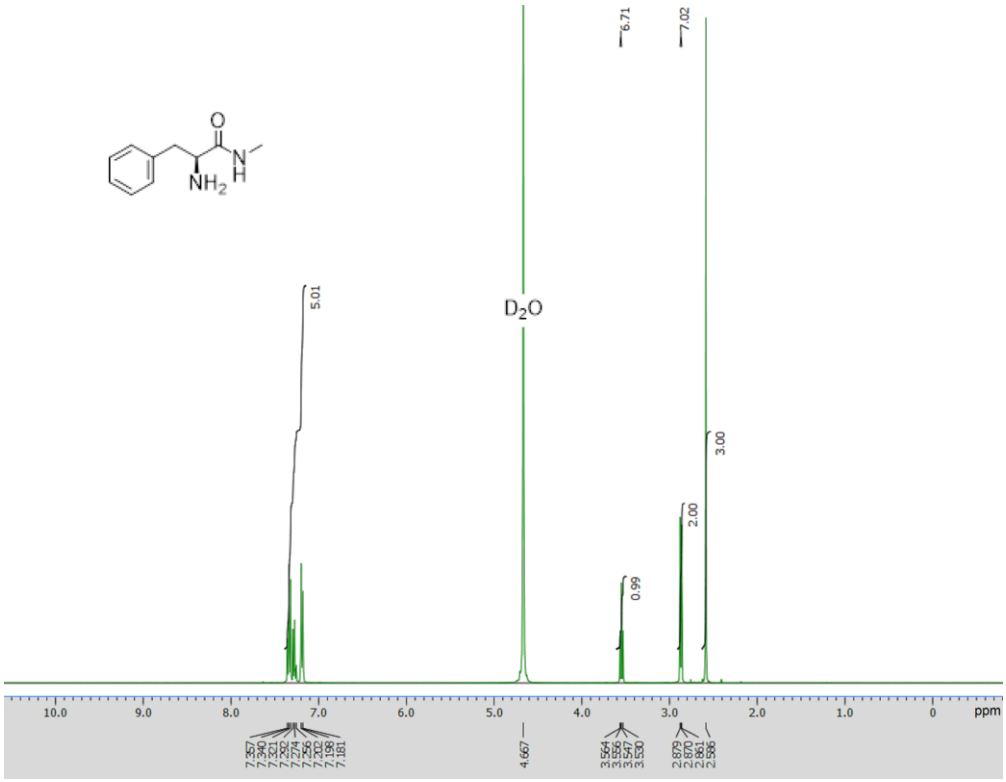

^{1}H NMR of **S2** in D_2O

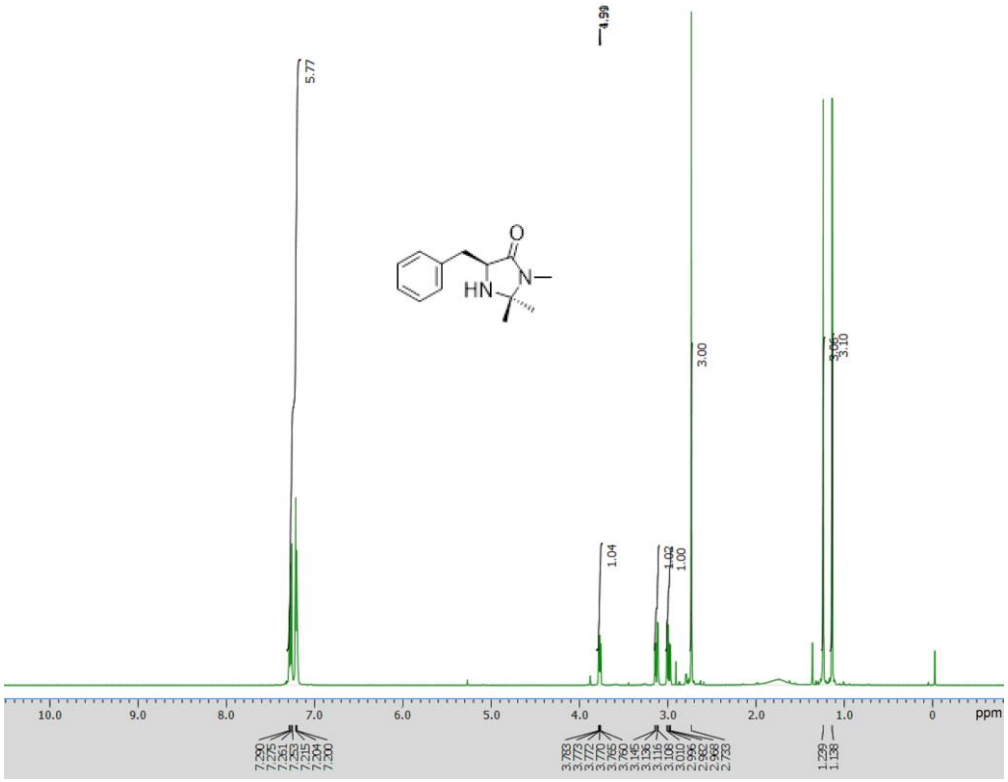

^{1}H NMR of MacMillan catalyst precursor **5** in $CDCl_3$

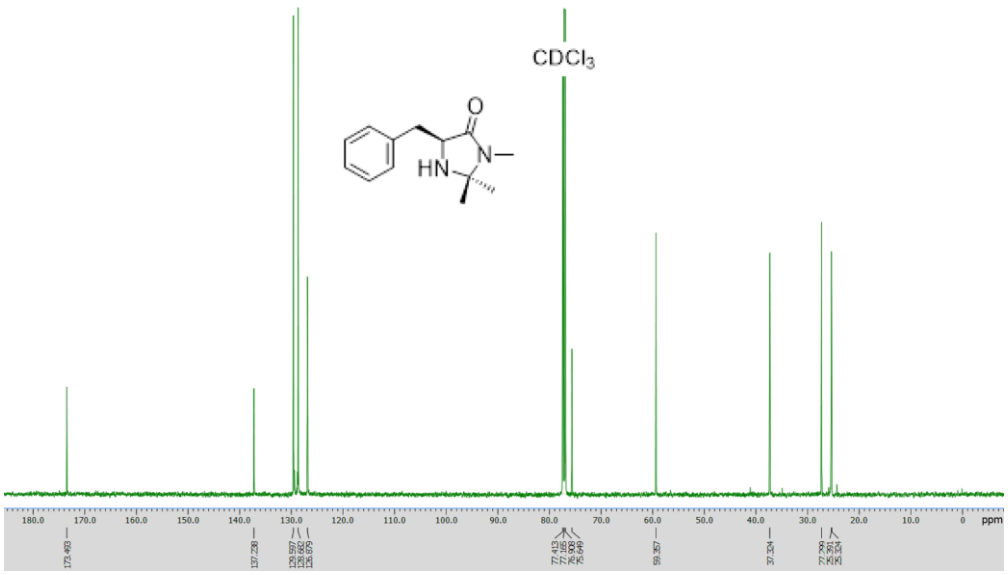

^{13}C NMR of MacMillan catalyst precursor **5** in $CDCl_3$

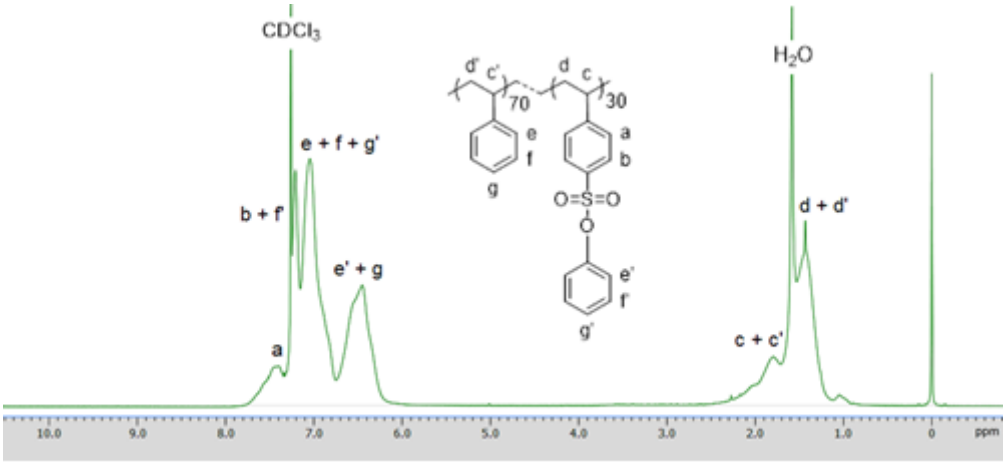

^{1}H NMR of **sS$_{30}$** in $CDCl_3$

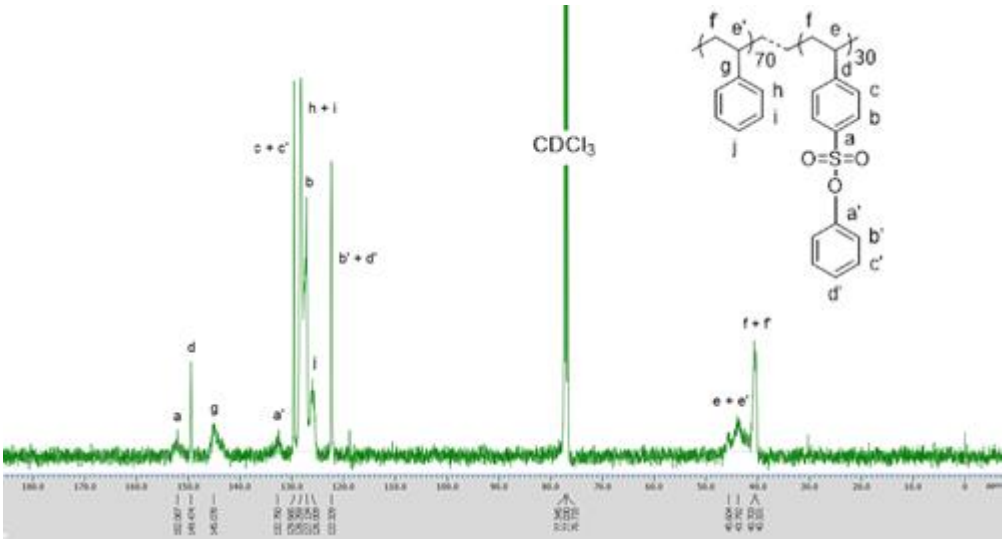

^{13}C NMR of **sS$_{30}$** in $CDCl_3$

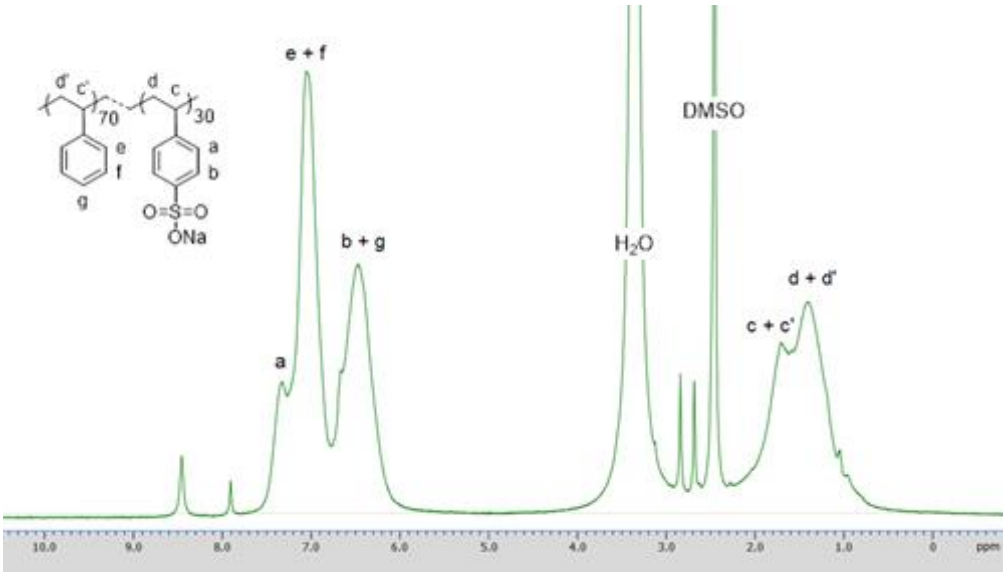

^{1}H NMR of **sSNa$_{30}$** in $CDCl_3$

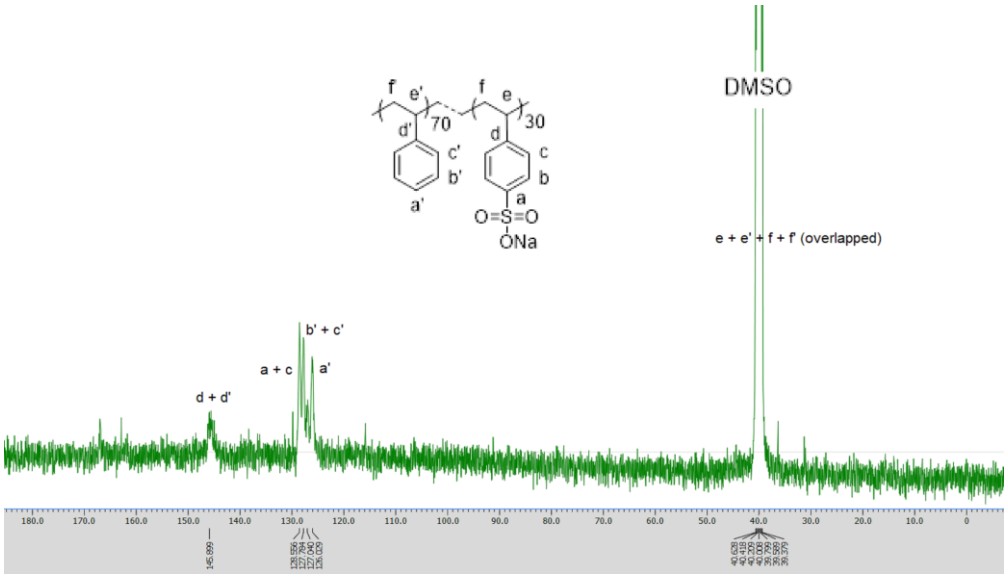

^{13}C NMR of **sSNa$_{30}$** in $CDCl_3$

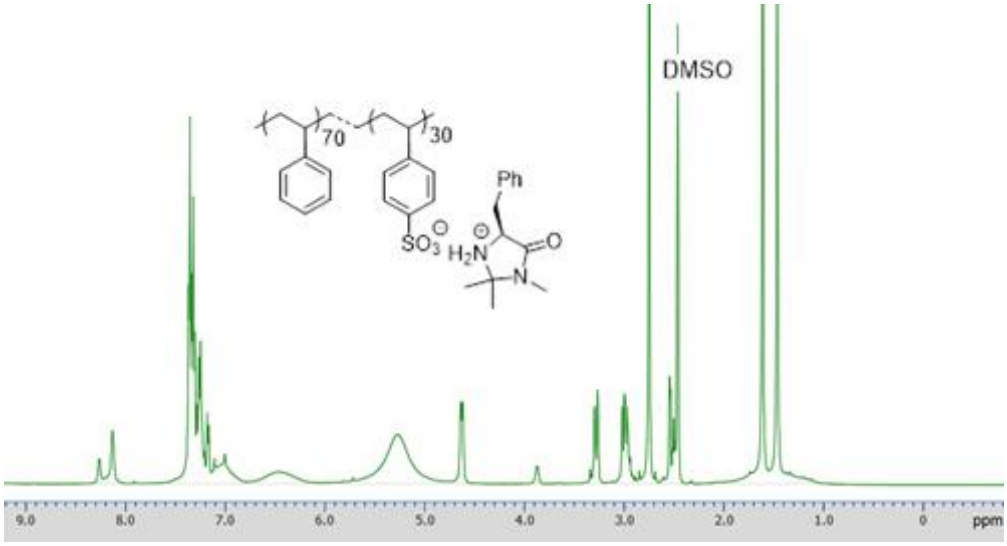

^{1}H NMR of **11sS$_{30}$** in DMSO-*d*$_6$

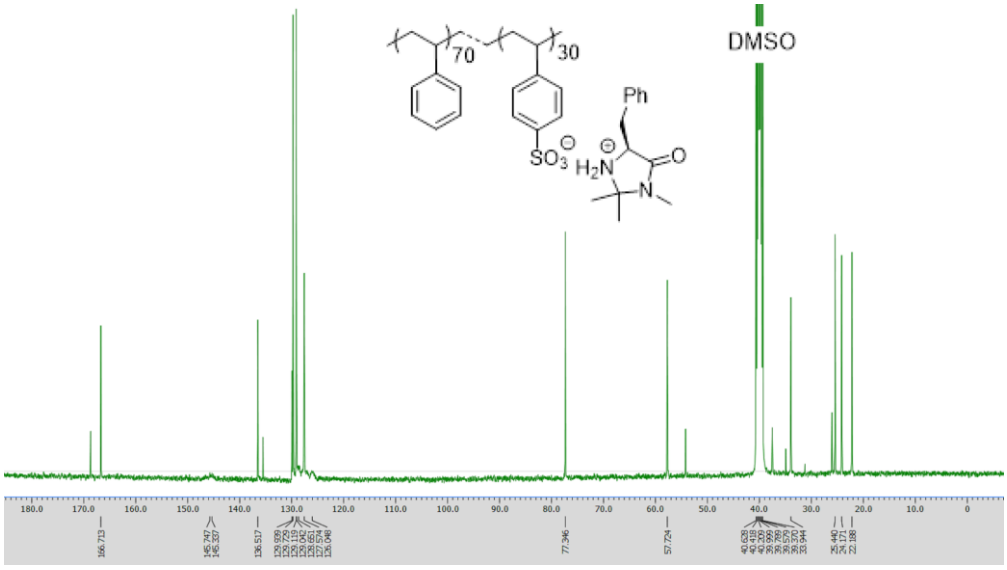

^{13}C NMR of **11sS$_{30}$** in DMSO-*d*$_6$

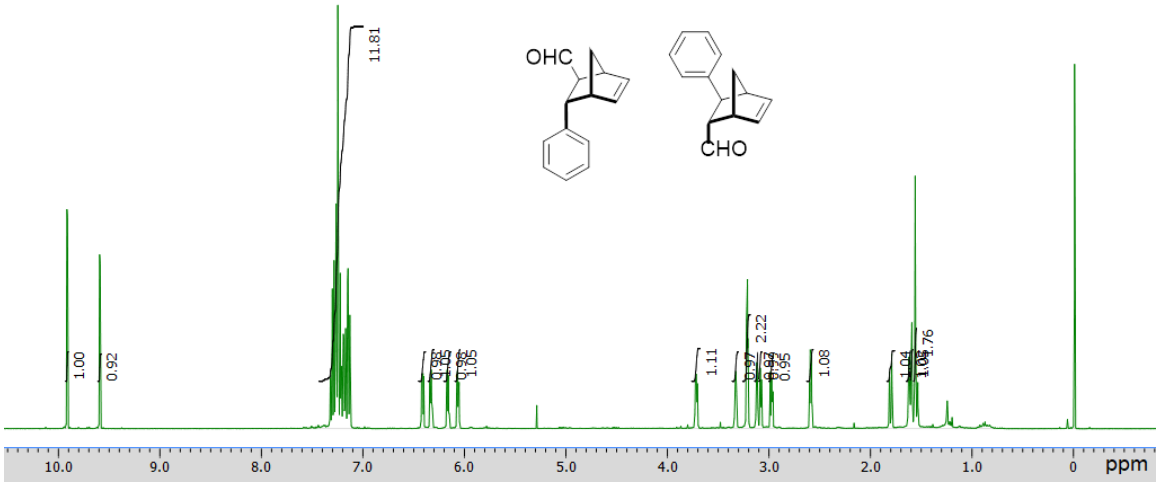

^{1}H NMR of **9** in $CDCl_3$

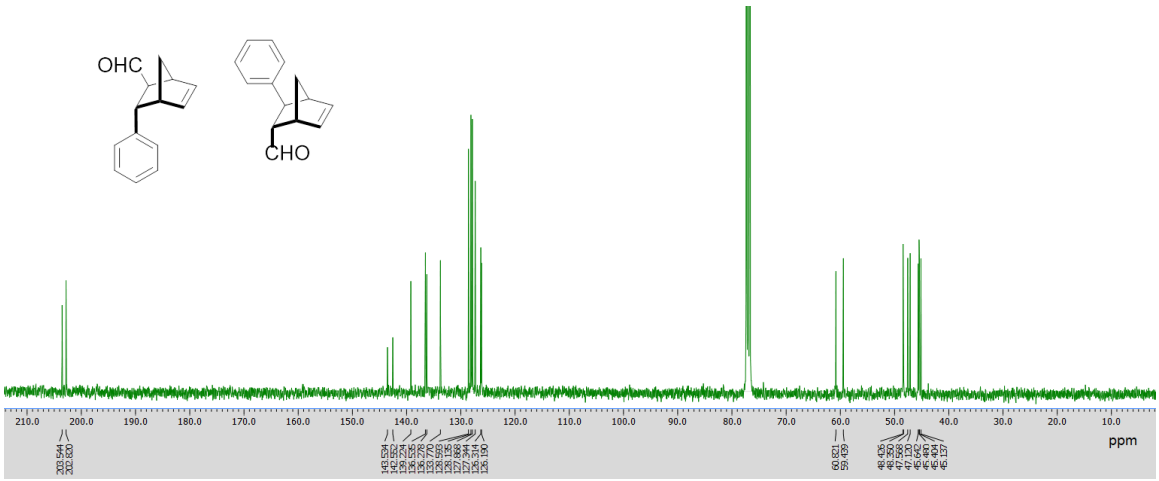

^{13}C NMR of **9** in $CDCl_3$

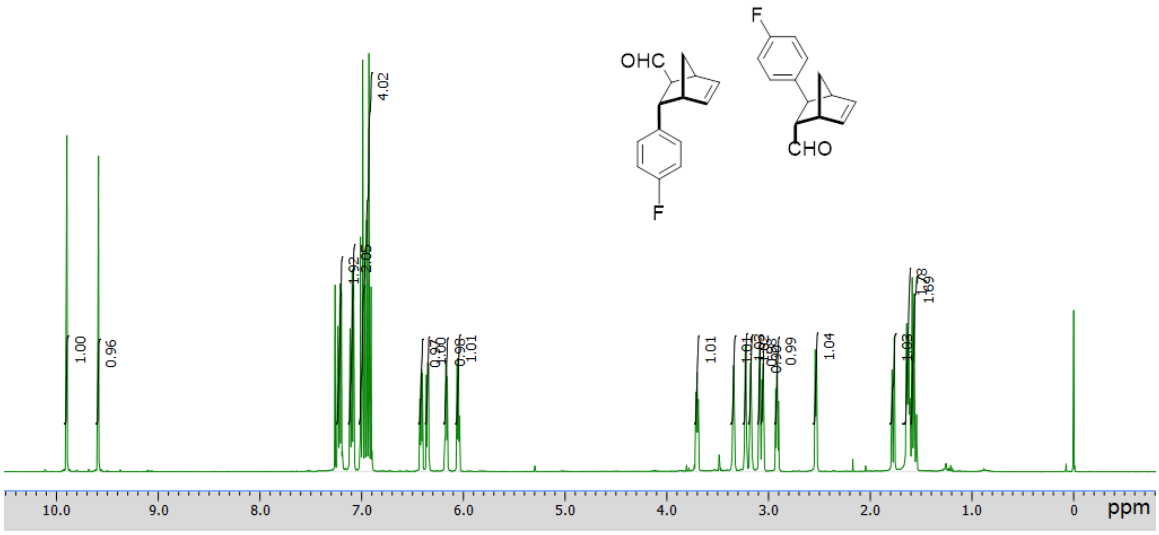

^{1}H NMR of **13** in $CDCl_3$

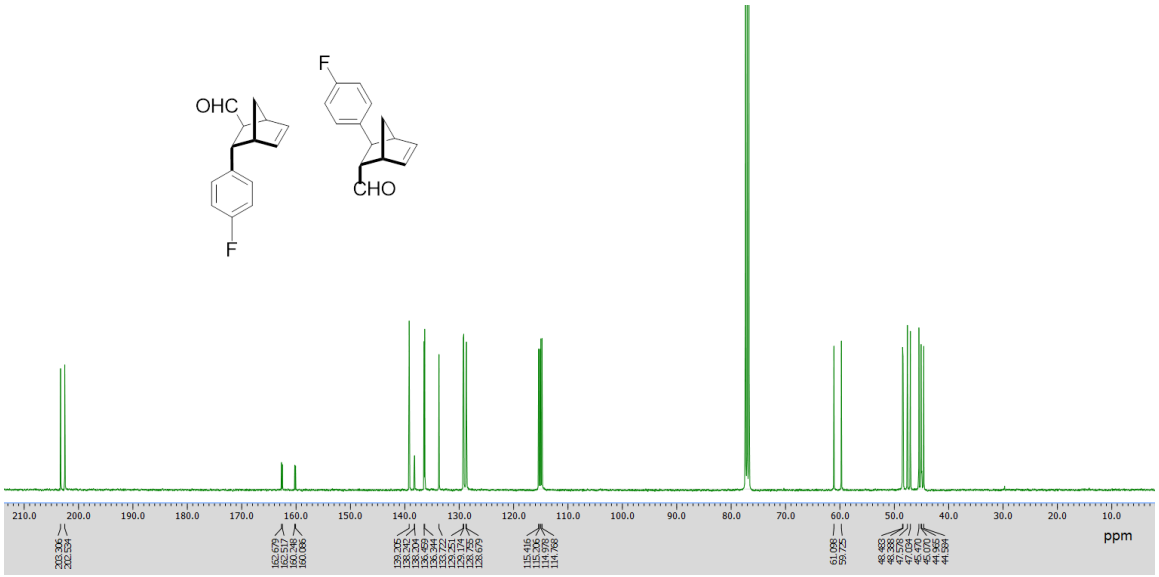

^{13}C NMR of **13** in $CDCl_3$

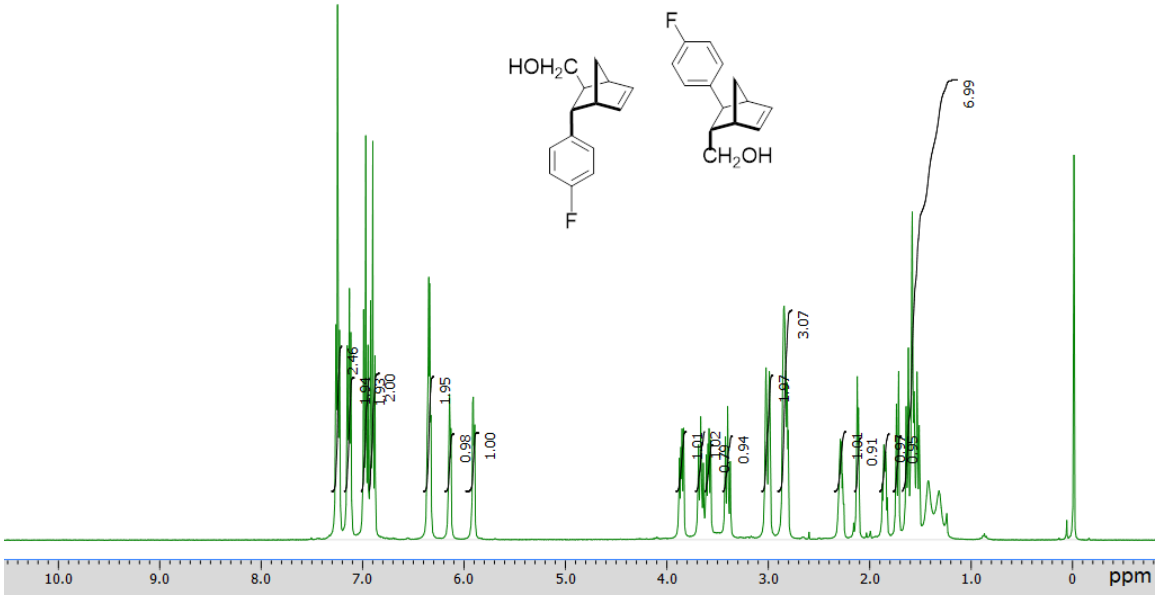

^{1}H NMR of **13** after reduction in $CDCl_3$

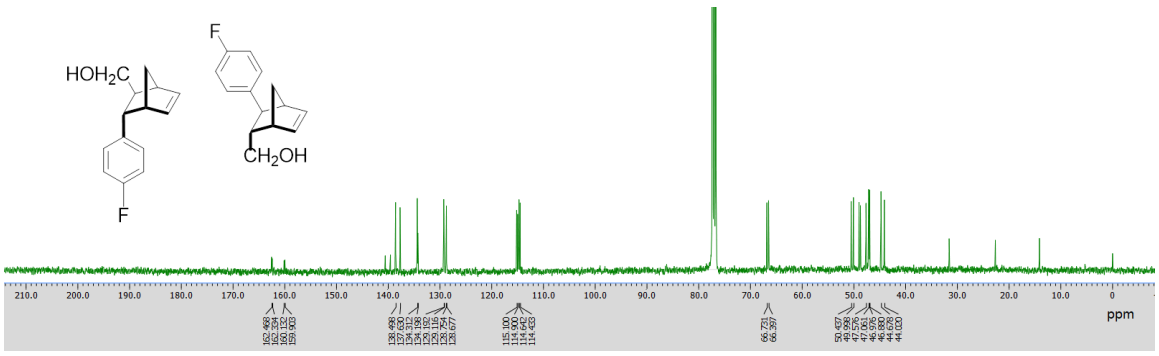

^{13}C NMR of **13** after reduction in $CDCl_3$

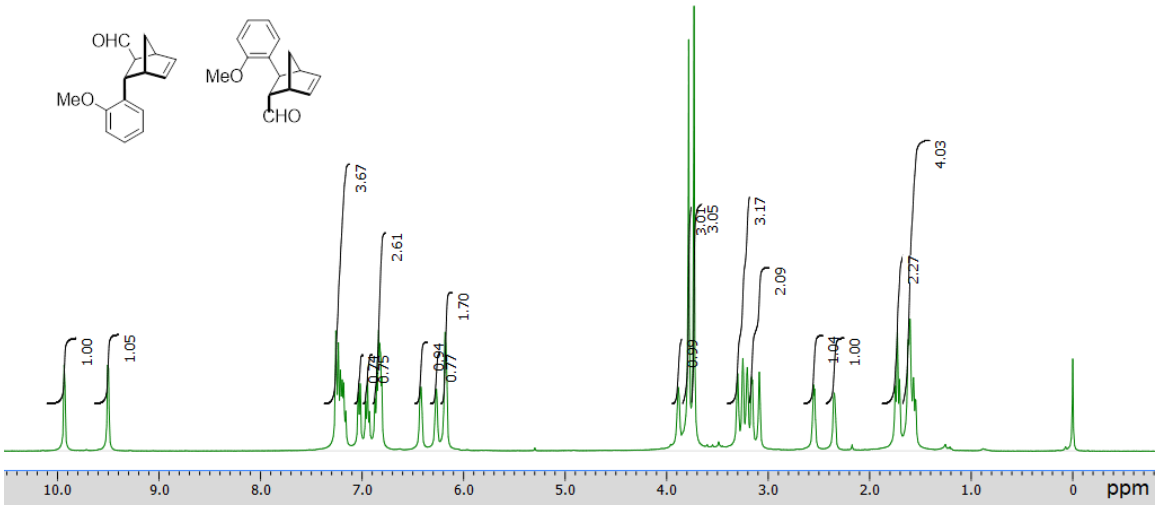

^{1}H NMR of **15** $CDCl_3$

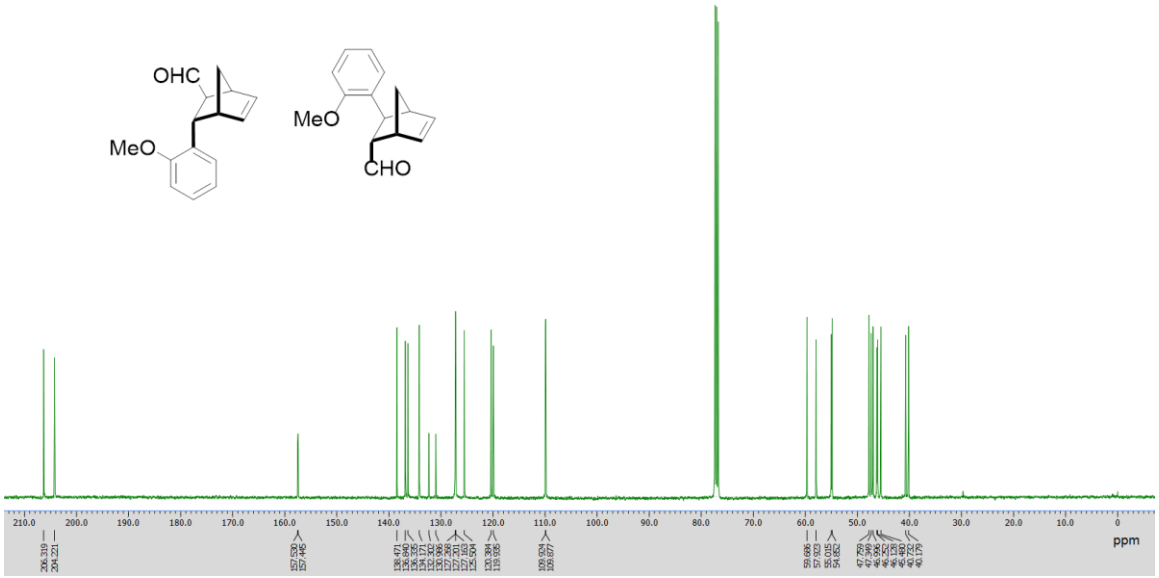

^{13}C NMR of **15** in $CDCl_3$

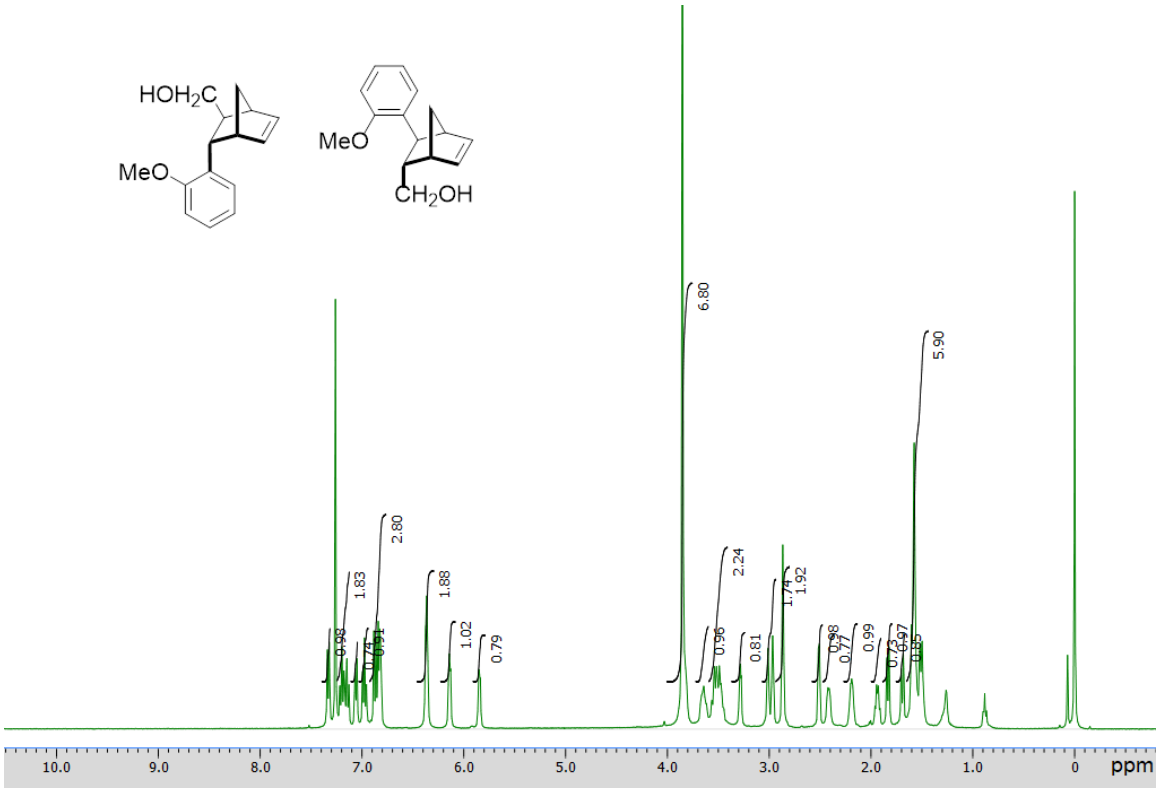

^{1}H NMR of **15** after reduction in $CDCl_3$

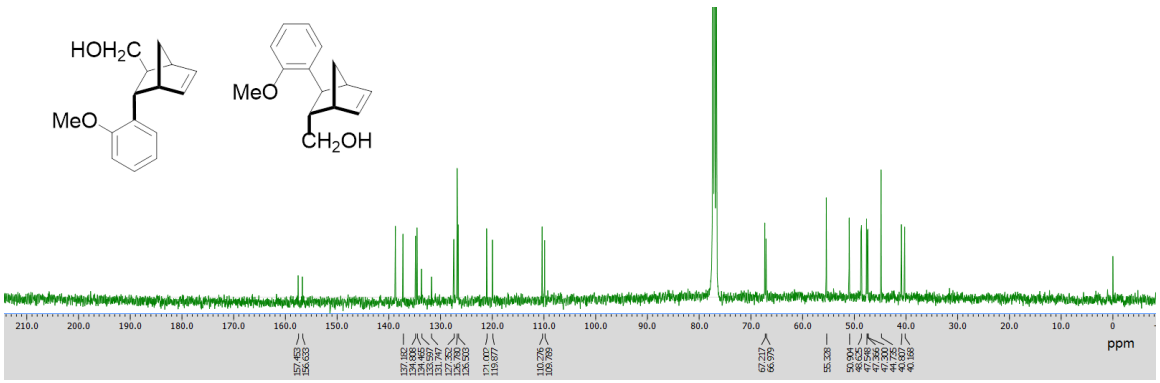

^{13}C NMR of **15** after reduction in $CDCl_3$

D.4 GC and HPLC chromatogram of Diels-Alder adducts

(a)

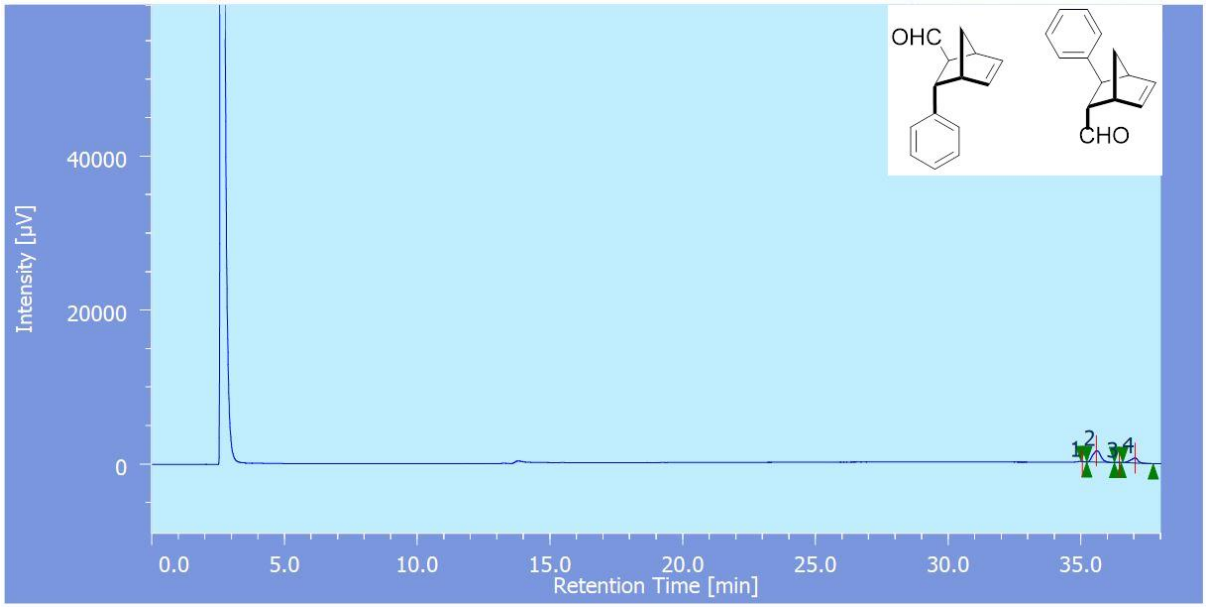

(b)

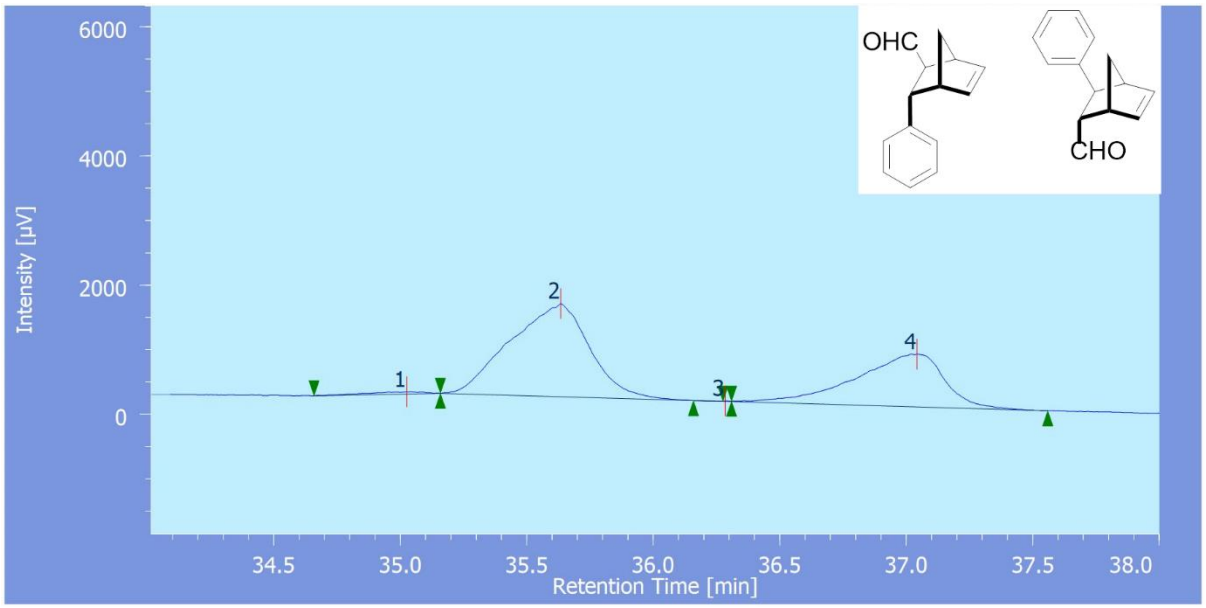

GC chromatogram of **9** (entry 8 in **Table 5.5**). (a) Full chromatogram. (b) Expanded chromatogram.

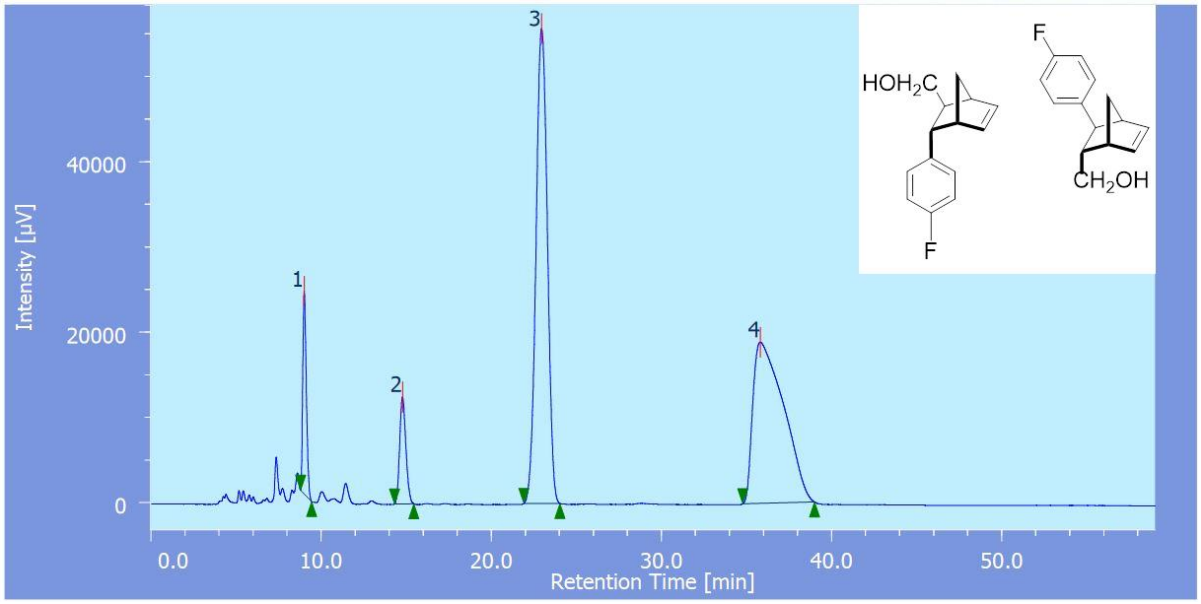

HPLC chromatogram of **13** after reduction

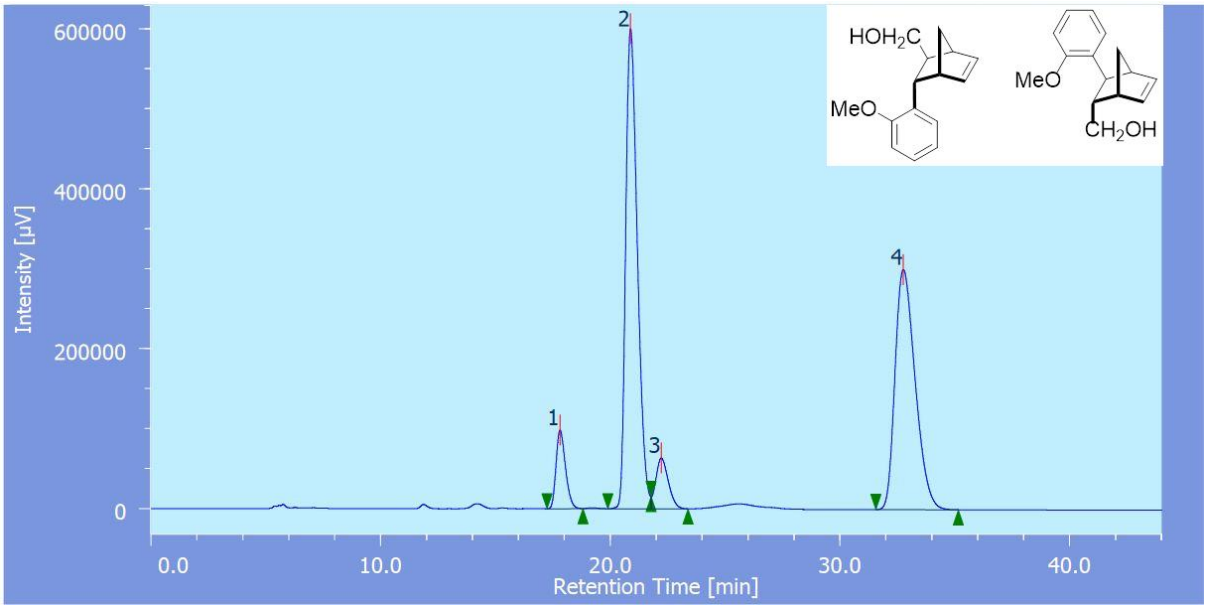

HPLC chromatogram of **15** after reduction

(a)

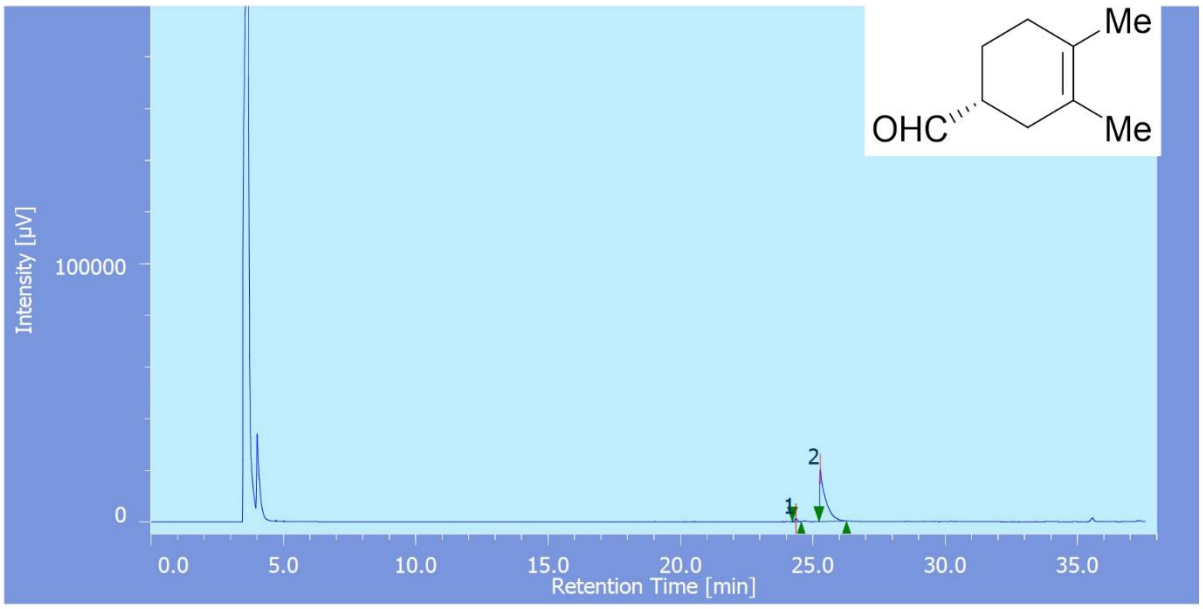

(b)

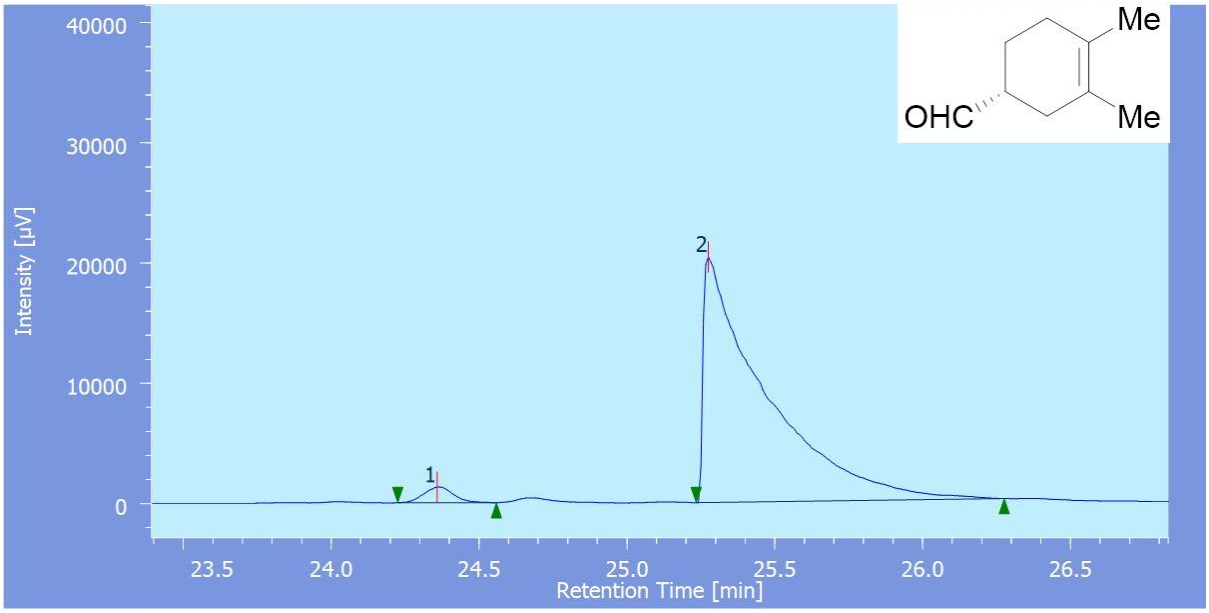

GC chromatogram of **19** (entry 4 in **Table 5.7**). (a) Full chromatogram. (b) Expanded chromatogram.

Acknowledgements

First and foremost, I would like to devote all the praises and obligations to the great gracious Almighty Allah for giving me the ability and patience for accomplishing this research work.

I would like to express my sincere gratitude to my supervisor Prof. Dr. Naoki Haraguchi for his continuous support during my PhD study. I have learnt from him how much a researcher can be preciseness which has inspired me during this study and admire his creativity and desire for chemistry. I like to thank my co-supervisor Prof. Dr. Shinichi Itsuno for his support during my PhD study. I am extremely grateful to Prof. Md. Abdus Salam, University of Dhaka, Bangladesh for advising me to join Prof. Haraguchi's group and for his suggestions during my stay in Japan. I am also grateful to my honorable thesis examiners Prof. Dr. Shinichi Itsuno and Prof. Dr. HidetoTsuji for reading my thesis and for their insightful comments on my thesis.

I would also like to express my heartiest regards and deepest sense of gratitude to my mentor and MSc's supervisor Professor Dr. Hasan Ahmad, Department of Chemistry, University of Rajshahi, Bangladesh for his scholastic guidance, valuable suggestions and cordial affection during my research work in Japan. My heartfelt thanks to my current and past lab mates for their continuous support during this PhD study. I would like to thank all the international, Japanese and Bangladeshi people I met during my study in Japan. I really had a great time with them. I would like to thank MEXT for the scholarship in my PhD study.

I express my special gratitude to my beloved mother, sisters, father in-law, mother in-law, brother in-law and all other family members for their encouragement, mental support, sacrifice and endless inspiration during the whole period of my study in Japan. Finally, I would like to express my heartfelt gratitude to my beloved wife Sharmin Jannat for his inexpressible love, caring and unlimited support. Thank you for being strong, patient and responsible in all the hard times when I was not available in Bangladesh for my family. Thank you for your encouragements and valuable advice throughout my study. You are not only a wonderful mother to my daughter Sabahat Jannat Odhora but also a magnetic wife.

Md. Wali Ullah Oli

Dedicated to My Beloved Wife

And

My Daughter Sabahat Jannat Odhora